A Collagen-GAG Matrix for the Growth of Intervertebral Disc Tissue

by

Dawn Hastreiter

Bachelor of Aerospace Engineering & Mechanics, Summa Cum Laude
University of Minnesota, 1995

Bachelor of Electrical Engineering, Summa Cum Laude
University of Minnesota, 1995

S.M. Aeronautics and Astronautics
Massachusetts Institute of Technology, 1997

SUBMITTED TO THE DEPARTMENT OF AERONAUTICS AND ASTRONAUTICS IN PARTIAL FULFILLMENT OF THE REQUIREMENTS FOR THE DEGREE OF

DOCTOR OF PHILOSOPHY IN AERONAUTICS AND ASTRONAUTICS AT THE MASSACHUSETTS INSTITUTE OF TECHNOLOGY

JUNE 2002

Signature of Author: _____
Department of Aeronautics and Astronautics
May 4, 2002

Certified by: _____
Myron Spector, Ph.D.
Professor of Orthopedic Surgery (Biomaterials)
Thesis Supervisor

Accepted by: _____
Wallace E. Vander Velde, Ph.D.
Professor of Aeronautics and Astronautics
Chair, Committee on Graduate Students

A Collagen-GAG Matrix for the Growth of Intervertebral Disc Tissue

by
Dawn Hastreiter

Submitted to the Department of Aeronautics and Astronautics on May 4, 2002
in Partial Fulfillment of the Requirements for the
Degree of Doctor of Philosophy in Aeronautics and Astronautics

Abstract

Intervertebral disc (IVD) degeneration and herniation is a significant problem, more so in the aviation field. The IVD also changes during spaceflight. Current treatments for IVD problems can have unfavorable long-term consequences. This thesis investigated a porous, biodegradable collagen-glycosaminoglycan (CG) matrix for the growth of IVD annulus fibrosus (AF) tissue *in vitro* in varied culture environments and in an *in vivo* experiment as an implant for defects in the AF.

Five experiments were performed. The *first* component involved the manufacture and characterization of the CG matrices used in the other studies. Additionally, type I, type II, and 50/50 type I/II CG matrices were made with nearly equal pore diameters, glycosaminoglycan content, and swelling ratios. *Second*, the capability of intervertebral disc cells to grow into the matrices was assessed by culturing AF explants on top of or between matrices. Cells were able to migrate up to 1 cm from the explant, implying that AF defects of this size could be filled with CG matrices. In the *third* experiment, explants and explant-matrix constructs were cultured in a rotating-wall bioreactor designed to simulate microgravity. Static culture served as a control. Bioreactor explants were more hydrated and had greater cellular proliferation. This experiment could serve as the ground control for a spaceflight experiment of AF explants. The *fourth* research component studied the effect of collagen composition on the proliferative and biosynthetic responses of AF cells seeded into CG matrices. Collagen content was varied by using the type I, type II, and type I/II CG matrices with matched characteristics mentioned above. Although the results indicated that the type II matrix performed slightly better, no major differences were seen among the matrix types. The *fifth* investigation was a canine *in vivo* study to assess the capability of the CG matrix constructs to aid in regeneration of AF tissue in surgically-created defects. No treatment was compared with implantation of unseeded and cell-seeded CG matrices. More tissue grew and more consistent hypercellularity was observed in defects with matrix implantation. From this research it has been shown that the matrix has potential for improving wound healing in the IVD.

Thesis Supervisor: Myron Spector, Ph.D.
Title: Professor of Orthopedic Surgery (Biomaterials)

Acknowledgements

I would like to acknowledge the aid and support of the following individuals:

From MIT:
Rosie Alegado
Ricardo Brau
Howie Breinan, Ph.D.
Jeannie Chao
Elliot Frank, Ph.D.
Toby Freyman, Ph.D.
Al Grodzinsky, Ph.D.
Brendan Harley
Allison Horst
Cyndi Lee, Ph.D.
Forgel O'Brien, Ph.D.
Patricia Reilly
Philip Seifert
Mark Spilker, Ph.D.
Alok Srivastava, Ph.D.
Donna Torres
Nicole Veilleux
Scott Vickers
Ioannis Yannas, Ph.D.
Laurence Young, Sc.D.

From Brigham and Women's Hospital:
Alper Comut, DDM, Ph.D.
Karim Eid, M.D.
Andreas Gomoll, M.D.
Debra Heath-Maki
Jean Henderson
Joyi Hsiao, DDM, Ph.D.
Huda Makhluf, Ph.D.
Hu-Ping Hsu, M.D.
Peggy Mills
Suichi Mizuno, Ph.D.
Stefan Meuller, M.D.
Martha Meaney-Murray, M.D.
Deb Leonard
Richard Ozuna, M.D.
Karen Rice
Thomas Schneider, M.D.
Sonya Shortkroff, Ph.D.
Myron Spector, Ph.D.
Sandra Taylor
Qi Wang
Xiuying Zhang, M.D.
Liqun Zou, M.D.

From Harvard Medical School:
David Brock, DDM
Elazar Edelman, M.D., Ph.D.
Kelvin Neu
Ravi Ranjan, M.D., Ph.D.

Table of Contents

List of Figures

List of Tables

Introduction

The Problem

Intervertebral disc (IVD) degeneration, leading to herniated discs and other disc disorders, accounts for a significant number of back debilitations per year in the general population. One to three percent of the population will have a disc herniation during their lifetimes (10). According to the 1988-90 National Hospital Discharge Survey (42), 250,000 adults per year were hospitalized for lumbar disc surgery, of which 185,000 were disc-related (laminectomy and discectomy), during that time period. Trends show that this number is increasing, and lumbar fusion is rising at an even faster rate (11, 42).

Description of the Intervertebral Disc

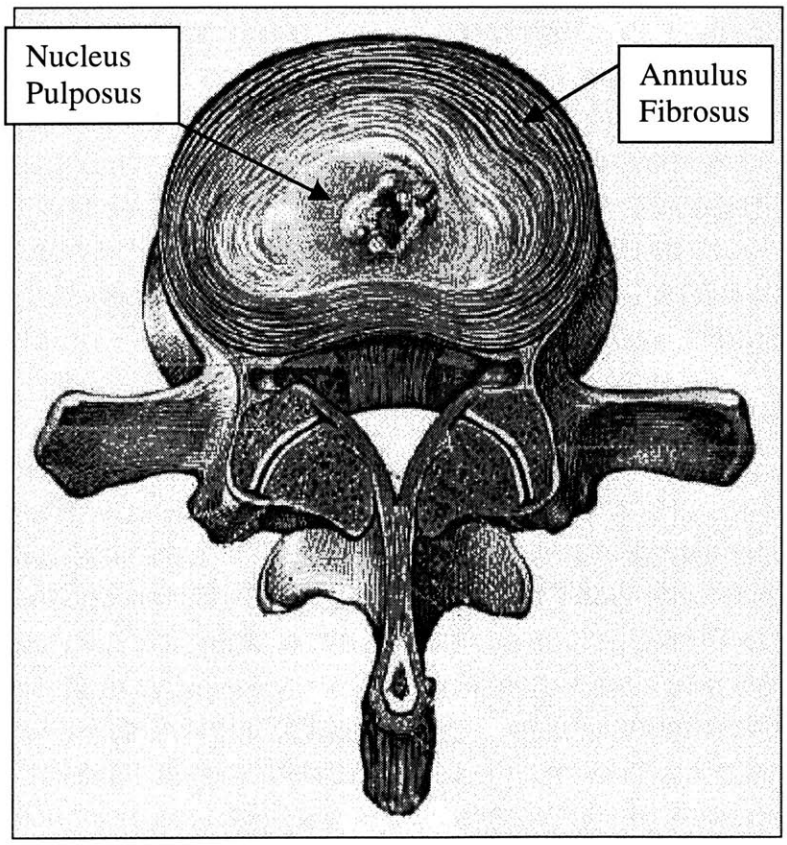

Figure 1. The Intervertebral Disc

A softer nucleus pulposus is surrounded by the lamellar sheets of collagen in the annulus fibrosus (Wheeless' Textbook of Orthopaedics) (2).

IVDs are fibrocartilage structures that separate the spinal vertebrae. A basic disc consists of hyaline cartilage end plates, the fibrocartilagenous annulus fibrosus (AF), and the inner nucleus pulposus (NP). Figure 1 displays a mid-height transverse section through a disc. The end plates enclose the annulus and nucleus between two vertebrae. The NP is a mass of hydrophilic glycosaminoglycans (mucopolysaccharides) and unstructured collagen. It is predominately composed of type II collagen in normal specimens and is gelatinous when young and more desiccated with increasing age (24, 53, 170, 189). The nucleus is responsible for withstanding the longitudinal, compressive forces on the spine. The AF is comprised primarily of types I and II collagen, with type I being more of a constituent in the outer portion (24, 53, 170, 189). The collagen fibers are layered in a series of annular sheets or lamellae. The orientation of the fibers within each sheet is 30-60° or 120-150° relative to the horizontal, and the orientation of the fibers in adjacent sheets alternates between these two angle ranges. The primary functions of the annulus are to allow the disc to withstand bending and torsional loads and to contain the nucleus under loading. Even as a result of a compressive forces on the spine, the orientation of the annulus fibers are such that they are always in tension (20).

The organization of the IVDs is highly specific due to complex and strenuous mechanical requirements placed on them by the spine. As a compressive spinal load is applied across an IVD, the force is absorbed mostly by the gelatinous NP. This action results in the generation of hydraulic pressure within the disc which is radiated in all directions. As the NP is squeezed, the annular fibers react by sliding over each other to form a more tightly packed arrangement. This restrains the disc circumference in spite of a reduction in disc width. The action results in the generation of large tensile stresses, which can be as high as 5 times the compressive load, within the lamellar fibers. The AF becomes very stiff, thereby preventing it from collapsing under the weight of the compressive load (20).

Disc Disorders

Disc herniation, depicted in Figure 2, occurs when the nucleus protrudes out of its normal space, erupting out through the AF or pushing the AF out of the normal disc space. Pain and motor loss result from compression of the spinal nerve roots by the herniated or bulged disc.

IVDs also undergo degeneration with aging. The disc spaces become narrower because the discs sink into the vertebral bodies. The degree of hydration and polysaccharide content of the nucleus pulposus decrease, and the collagen content increases. The cells of the disc, primarily chondrocytes, are still active but appear to produce incorrect matrix constituents.

Collagen Content

Immunohistochemical studies (170, 189) have shown that type I is in the normal outer annulus (OA) and the degenerative inner annulus (IA) and NP and type II is normally in the inner annulus and nucleus. A biochemical study (12) confirmed that type I collagen is produced at a higher rate in degenerated discs. Collagens account for 70% of the dry weight of the OA, but less than 20% of the dry weight of the NP in young people (24). Type I collagen decreases from 80% to 0 from the OA to NP. Type II collagen increases from 0 to 80% from the OA to NP (24). The nucleus contains collagen types II, VI, IX, and XI and the annulus contains collagen

types I, II, III, V, VI, IX (53), and type X (19). The amount of type II in the disc decreases with degeneration (171). Complete collagen turnover has been found to be theoretically 100 years in the canine and several decades in the rabbit based on experimental results.

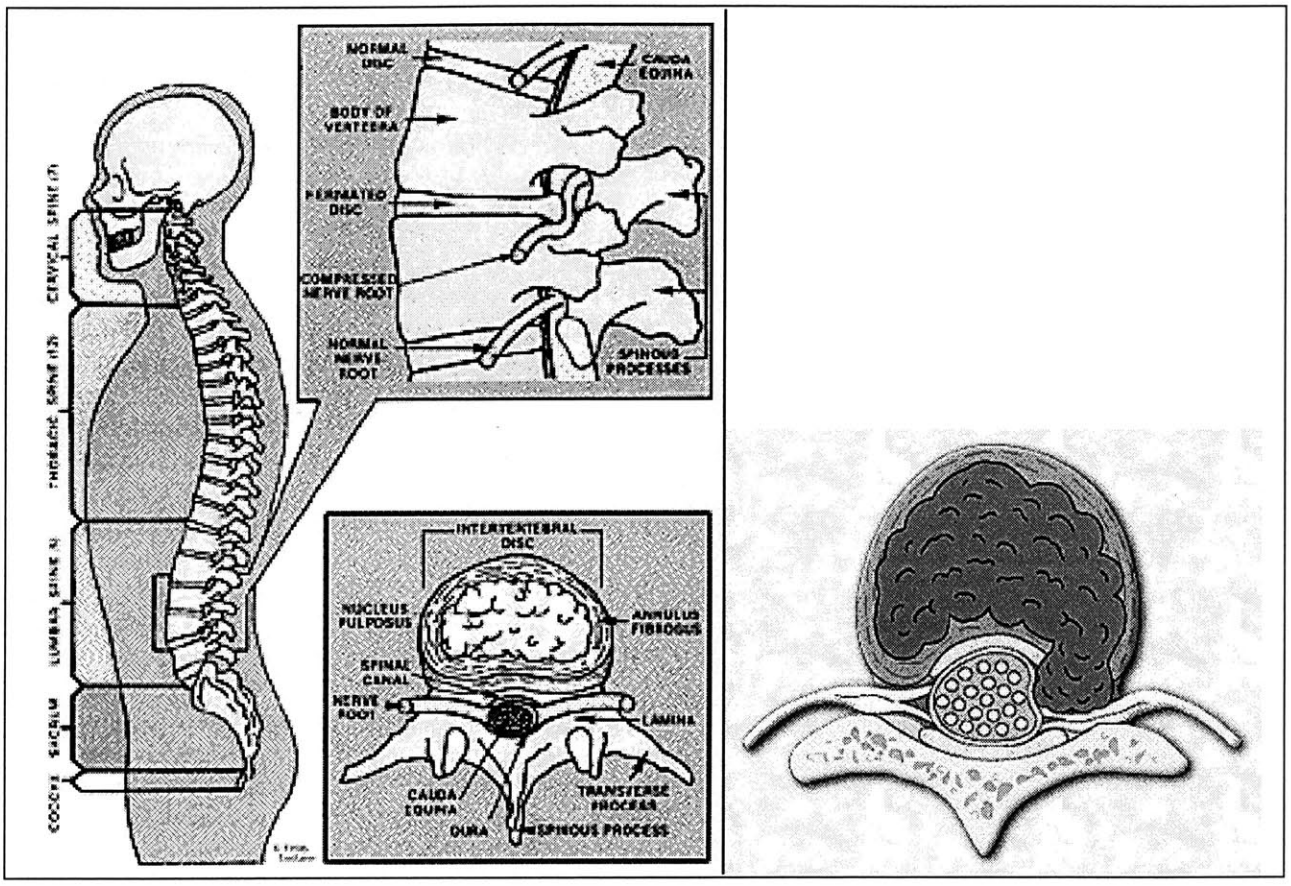

Figure 2. Spinal Anatomy and Intervertebral Disc Herniation

Left: Top: Lateral view of normal and herniated discs in the lumbar spine. Bottom: Transverse view through a normal disc. Right: Transverse view through a herniated disc. (Ludann Educational Services) (1)

Glycosaminoglycan (GAG) Content

The disc is richer is keratan sulphate than articular cartilage (99). The proteoglycan remodeling rate is over 3 years in man (193). In the canine, the mean GAG turnover time is 470 days. It is fastest in the OA and slowest in the NP. The turnover time in the IA is 260 days (223).

Properties of the Annulus Fibrosus

The annulus of IVDs is a rather unusual fibrocartilage structure. Unlike other fibrocartilages, it contains significant amounts of type II collagen. Immunohistochemical studies (170, 189) have shown that type I collagen is normally in the outer AF and the degenerative IA and NP and type II is normally in the IA and nucleus. Biochemical studies (5, 22) have discovered that approximately 35-60% of annulus collagen may be type II, with a decreasing gradient of type I and an increasing gradient of type II from OA to IA. It has also been found (22) that the amount of type I collagen increases significantly in the annulus with age and in degenerative spine conditions in regions where the mechanical stresses are highest.

The tensile strength of annulus is 15-50 kg/cm^2. The tensile strength of the longitudinal ligaments is 200 kg/cm^2. However, compressive loads of 20 kg/cm^2 can cause the disc to rupture because of the aforementioned property of the tensile loads of in the annulus to be several times greater than the compressive force applied to the disc. The tornsional strength of the disc is 40 kg/cm^2 (102). The normal compressive force on a lumbar disc is 3000 N (102).

The chemical make-up and hierarchical structure of the extracellular matrix of the annulus and nucleus, like other connective tissues, are maintained by the parenchymal cells of the disc. Incisional wounds and lesions through the deeper layers of the annulus fail to heal (87, 122, 127, 143, 193, 208). When reparative tissue does form in full thickness lesions through the annulus, it comprises fibrocartilage and osteophytic tissue that lacks the normal disc structure (87, 143, 144, 208). Rim lesions in sheep in five lumbar discs produced scar tissue in the OA and granulation tissue in the IA after one year. In some discs, propagation of the tear to the IA was present with no attempt at repair (55). Annular lesions are plugged in the outer part with fibrous tissue after 1-2 months and the inner part fails to close (87, 122, 208). Annular lesions in rabbits tend to calcify after one year (143, 144, 208). A study of different types of annular lesions made to the IVD showed that none have pressure-volume curves similar to control discs and that primary repair did not work (6).

In vitro studies of annulus tissue (32, 80) have revealed low biosynthetic and mitotic capability as opposed to other cell cultures. The low density and low mitotic activity of disc cells, in addition to the low degree of vascularity (193, 208), explain the limited healing potential of the AF (87, 122, 144). The absence of healing combined with the attempt of repair with fibrous tissue in injuries to the AF predisposes the disc to degenerative processes.

Cells of the Intervertebral Disc

Errington, et al. (52) believe "disc cells are distinctly different from articular chondrocytes, and their behavior cannot necessarily be directly extrapolated from that of articular cartilage chondrocytes." Below the terminology of several histological properties of the IVD is defined.

The IVD has a low cell density. It has often been observed that cell density is highest in the OA and endplate and declines as the center of the NP is approached (98, 155). Cell densities previously quoted for the normal annulus and NP are 9 and 4.3 x 10^3 cells/mm^3 (155). A more recent study of 41 autopsy specimens found densities of 4.0, 6.7, and 17 x 10^3 cells/mm^3 in the NP, IA, and OA, respectively (94).

That cells of the IVD have several morphologies has long been recognized. The generalization is often made that NP and IA cells resemble chondrocytes and OA cells are fibroblast-like. Other authors refer to the former as round and latter as elongated (52, 98). A recent study quantified that 96, 82, and 39% of cells in the human NP, IA, and OA were round (94).

Round disc cells in the IVD are often surrounded by a distinct round matrix containing levels and types of collagens and proteoglycans different from the rest of the extracellular matrix (84, 189). This area has been called the pericellular matrix (189, 221), pericellular capsule (52, 196), nest (221), territorial matrix (23, 53, 109), cell-associated matrix (33), lacuna (18, 84, 109, 116), pericellular lacuna (91, 182, 216), and cell halo (91, 216). In this work, it will be referred to as the pericellular matrix. Roberts, et al. (189) suggest that the formation of the rings in the pericellular matrix may result from movement of the cell confined within its capsule. The pericellular matrix contains significant amount of type IV collagen (171).

Groups of cells have been long reported in the IVD, especially in the NP (18, 109, 113, 155, 167, 189). The terminology of cell groups has been ambiguous. Clusters are usually defined as 3 or more cells (114). Clusters are also referred to as clumps (48, 116, 171), chondrons (171), groups (40), clones (171, 182, 216, 232), and nests (40). Weidner and Rice (232) defined chondrocyte cloning as multiple chondrocytes growing in small rounded groups or clusters sharply demarcated by a rim of adjacent fibrocartilage. They reported cloning in 79% of prolapse specimens and 65% of autopsy specimens. High numbers of cells per cluster have been reported: 15 (40), 21 (109). Coventry, et al. (40) report an increase in the number of clusters around middle age. Eckert and Decker reported the presence of round cells in clusters in the annuli of autopsy specimens (48). Recent work (115) suggests that clusters result from cell proliferation. Chondrocyte pairs, otherwise known as cell doublets (115), also show evidence of cell proliferation (115). For the purposes of this work, clusters and pairs of cells will be together termed grouped cells. A recent investigation concluded that 29, 13, and 5% of cells in the NP, IA, and OA, respectively, are in groups.

Necrosis means passive cell death caused by toxic external stimuli, while apoptosis is necessary and physiological cell death that is controlled by genes to maintain the homeostasis of an organism. Trout, et al. (221) defined necrotic cells by loss of membrane integrity, extensive vacuolization of organelles, and deposition of dense osmophilic masses in the cells. The disc has been found to have a high incidence of apoptotic cell death (84, 117, 186), which may be related to experienced stresses (145). Dead cells in the nucleus have been confirmed by other researchers (18, 53, 54, 91, 216, 221). That viable disc cell density in the NP decreases with age (221) may be caused by this (84). Trout, et al. (221) found that in the nucleus 2% of the cells are necrotic in fetal specimens whereas over 50% may be dead in adults. Their study also confirmed that the percentage of dead cells in the NP increased with age. Apoptosis of disc cells precedes neovascularization during disc formation and may thus cause it. The same study found that apoptosis is present in degenerated discs (151). Gruber, et al. (83) recently found that medium containing 20% FBS, 100 ng/mL PDGF, and 500 ng/mL IGF-1 significantly reduced apoptosis *in vitro*.

Stellate processes from IVD cells have been described. Errington, et al. (52) examined the cellular processes of disc cells extensively. Other researchers briefly mention these processes (189, 221). Stellate, secretory cells were reported in human NP near the endplates (113).

The Intervertebral Disc in Aerospace Medicine

IVD injuries are of particular relevance to space and aviation medicine. A higher incidence (per age group) of disc injuries than the normal population has long been recognized in aviation (11). The cause is two-fold: chronic exposure to vibration and excessive loading on the spine from high G forces (69, 142). Space medicine is another area where disc injury has been realized but has not been characterized as completely. Astronauts have suffered back pain in space and after return to Earth, and spinal lengthening has been noted. This may be associated with swelling of the IVDs due to lack of spinal loading, as has been seen in bed rest studies (131, 236). While these phenomena have been observed, few attempts have been made to correlate gross changes with events on the cellular level within the discs. Undoubtedly, the change in loading on the spine in microgravity alters the normal remodeling of the IVDs. Understanding alterations at the cellular level is key to recognizing any damage that may be inflicted upon astronauts and any possible therapies that could ameliorate the situation.

In-depth research on disc changes as a result of spaceflight has been limited. A major study (131) that was conducted with human subjects indicates that the gross changes are complete after a few days of bedrest or spaceflight. However, progressive changes are clearly occurring at the cellular level. After 5 weeks of bed rest, disc area returned to baseline within a few days of ambulation, but recovery took more than 6 weeks for bed rest of 17 weeks duration. This implies that disc changes are more critical for long-duration spaceflight. Notably, the only published data on human spaceflight subjects was from a short-duration mission which resulted in a rapid recovery, as might be expected. A major animal space-based study (158, 177) involved rats flown for two weeks on COSMOS 2044 in 1987. Many interesting morphologic and histological changes were observed. The weights of the discs were smaller and the collagen-to-proteoglycan ratios were higher in the flight group than the control group. Alterations in the collagen structure and orientation of the proteogylcans were observed as well. A subsequent COSMOS spaceflight study found similar changes in rat IVDs (59). Given these minuscule spaceflight data and the limited knowledge of causes of normal disc degeneration and disc regeneration capabilities, it is not yet possible to determine what these observed changes imply in the long-term for astronauts. The need for more information is compelling. One goal of the present research is to determine how the microgravity environment affects the cellular and tissue-level responses of the IVD through *in vitro*, ground-based studies.

Treatment

There are currently no satisfactory procedures for prosthetic replacement or regeneration of degenerated disc tissue. Laminectomy, the most limited surgical treatment that involves removal of any loose disc tissue and a bony plate covering the posterior aspect of an IVD, can only be performed in a limited number of cases. As many as 11% of laminectomies may have unfavorable outcomes (43). Discectomy, a surgical procedure in which loose and attached portions of the IVD are removed after laminectomy, can be successful in relieving radicular pain, usually for herniation. Approximately 200,000 discectomies are performed in the U.S. per year (88) at an average total cost of $29,000 per case (in 1988 dollars) (188). With aging or when portions of the IVD are removed, the disc loses height and its original load-sharing capacity

(159), and the vertebral column loses a specialized connective tissue whose function is to resist the compressive, rotational, and tensile stresses that are applied to it (102). Hanley and Shapiro (89) found a 98% incidence of reduced disc height following discectomy although the result was uncorrelated with outcome of the procedure. Another study has verified loss of disc height (225), which can lead to pain from facet joint syndrome (46) or stenosis of nerve root canals (41). Research (4, 26, 44, 70, 88, 89, 97, 122, 188, 204, 210, 230, 233) has shown that between 2-40% of patients have unsatisfactory long-term outcomes with discectomies although the results appear to be improving with time as surgical technique advances. Among the reasons for failure are: reherniation, scar tissue formation, and additional lumbar spine problems. Performing a revision discectomy only has a 50-62% success rate (70, 88, 191). A final resort for a "failed lumbar back" (due to aging or previous surgery) is fusion, in which at least two adjacent vertebrae are permanently connected with metal plates, rods, and/or bone cement. Fifty-one percent of lumbar fusions are due to intervertebral disc disorders (120). In 1990 figures, this amounts to 46,500 surgeries in the U.S. per year (218). While fusion of the involved joint can provide relief from symptoms in the short-term, 7-35% of patients have significant problems after spinal fusion (36, 70, 138). Studies show that fusion alters the biomechanics of the spine and causes increased stresses at the junction between fused and unfused segments (133, 180). A secondary surgery for fusion only has a 70% success rate (71).

IVD autografting and allografting is still highly experimental and the morphology of transferred discs is not normal (68, 121, 149, 150, 157, 172, 192). Autografts could complicate spinal pathology by creating trauma to an uninjured disc. Anatomical mismatch of donor tissue suggests that allografts will be unsuccessful. Artificial IVDs are still experimental (14, 15, 36, 51, 100, 118, 119, 125, 126, 139, 160, 198, 199, 224, 226, 235). Certain authors do not think such a device will be epidemiologically, anatomically, biomechanically, and psychosocially feasible (51). Autologous disc cell implantation is still highly experimental (85, 103) and requires a cell source (which may mean wounding an uninjured IVD).

A Possible Solution for Disc Degeneration

Research has shown that a significant number of degenerative disc diseases initiate by either a focal defect in the annulus or altered morphology of the nucleus (18, 197). These in turn lead to extrusion of NP material through the annulus (herniation). The realization that a majority of the annulus tissue is normal at the time of current surgical intervention and the demonstration that surgical techniques which alter spinal loading properties result in long-term pathological sequelae have led several investigators (14, 41, 74, 160, 199, 235) to suggest replacement of only the NP with artificial material. Such an approach would maintain disc height and compression resistance, two of the major factors that are necessary to prevent degeneration after surgery. Nucleus implants comprised of silicon are in initial clinical trials and proposed hydrogel implants could preserve fluid flow through the inner disc space (9, 14). A major impetus to such an approach is the lack of effective mechanisms for sealing the annulus gap after nucleotomy and artificial NP implantation. Extrusion of a nuclear implant would be an unfavorable outcome. AF tissue of IVDs has limited *in vivo* and *in vitro* healing potential (87, 122, 193). Suturing an annular lesion site has not been found to affect the outcome of a surgery.

One goal of the present research is to develop a mechanism for bridging an annulus defect and stimulating the intact tissue to regenerate across the defect. In essence, this is would be a mechanism of *in vivo* tissue engineering. The strategy to regenerate the AF tissue *in vivo,* instead of engineering the disc tissue *in vitro*, is based on the suppositions that a) physiological mechanical forces that serve as critical physical regulators of tissue formation cannot be simulated *in vitro*, and b) tissue formed *in vitro* would have to undergo remodeling *in vivo* once implanted in order to be incorporated into host tissue. By combining a mechanism of annular healing with a nuclear implant, such as a hydrogel, the problems that lead to a "failed back syndrome" could be avoided. The research presented examines a biodegradable matrix scaffold that can facilitate annular healing.

A Scaffold for Regeneration and Three-Dimensional Culture

IVD cells have been three-dimensionally cultured in alginate beads (28, 32, 33, 80, 86, 96, 129, 152, 153, 161, 194, 217), alginate gels (205), and agarose (80, 86, 152). While these systems have provided information about the behavior of these cells, they have limited usefulness as implants. A matrix for regeneration can serve several roles: structural support at the defect site, a barrier to growth of undesirable cells and tissue (inflammatory cells and scar tissue for example), a scaffold for cell migration and proliferation, and as a carrier or reservoir of cells or regulators (136). Investigations of articular chondrocyte-seeded scaffolds for repair of articular cartilage defects have been promising (35, 39, 60, 79, 169, 187). A variety of natural and synthetic materials have been employed: fibrin, collagen gels and collagen sponges, and polyglycolic and polylactic acids. The promising performance of collagen-glycosaminoglycan (CG) matrices in studies with articular chondrocytes (168, 169), meniscus (212, 213, 214), tendon (146, 147, 148, 202), dermis (242), and peripheral nerve (27, 50) have commended them for use in the present study.

Any implant used for regeneration of annulus must meet the following requirements: anti-immunogenicity, adherence to intact annulus tissue, ability to handle tensile stresses soon after implantation, capability for cell infiltration, and biodegradability. Collagen and glycosaminoglycans (GAGs) have been shown to be relatively weak antigens and their biocompatibility has been amply demonstrated (239). Adherence to intact annulus tissue is a surgical issue, and for the purposes of the present has been handled by simple suturing. Under the scope of this research, mechanical and swelling ratio testing of the CG matrices were used to assess implant material properties. The capability for cell infiltration was assessed by *in vitro* work; obviously though, pore diameter of the matrix must exceed that of the average annular cell diameter of approximately 11 μm (84). The biodegradability of the CG matrices is dependent upon their degree of cross-linking.

GAGs are negatively-charged, unbranched carbohydrates. Generally they are covalently linked to a protein core, thus forming a proteoglycan (110). GAGs are known to bind and modulate growth factors and cytokines, inhibit proteases, and be involved in adhesion, migration, proliferation, and differentiation of cells (110, 215).

Initial research by Schneider, et al. (201) in which CG matrices were seeded with adult canine annulus cells provided promising results. The study utilized the same experimental cell-seeding methodology as in the present research for testing two types of matrix: a collagen type I

matrix that was dehydrothermally cross-linked for 24 hours and a collagen type II CG matrix that was cross-linked by ultraviolet (UV) irradiation for 16 hours. Cylindrical disks of matrices were seeded with three million cells per matrix. Cell-seeded and unseeded matrices of each collagen type were cultured for 1, 7, and 14 days. The cell-seeded type I CG matrices contracted in diameter by approximately 43% by day 14. In contrast, the type II collagen matrices reduced in size by only 6%. No evident signs of degradation of either matrix were present during the course of the experiment. DNA in the type I matrix showed a 66% decrease between days 1 and 14 ($p < 0.001$). In contrast, in the type II matrix there was a significant loss of cells in the first week ($p = 0.0065$) but no significant change in cell number between 7 and 14 days; nor was there a significant difference in the DNA in the matrix between days 1 and 14. The amount of GAG produced by AF cells in the type I CG matrix did not change significantly over the 2-week course of the experiment. Cells in the type II collagen matrix showed a significantly higher amount of GAG, a 14-fold increase, after 14 days ($p = 0.019$). Cell morphology, in terms of being spherical or elongated, did not change appreciably in the type I matrix but the percentage of cells that were spherical increased in the type II matrices. Many cells in both matrix types stained intensely for α-smooth muscle actin, a protein often associated with contraction. Although differences in the behavior of the disc cells in the type I and II matrices were noted, a direct comparison between the type I and II matrix results cannot be made. As will be described later, the GAG content of the two matrix types was not similar. In addition, the matrix stiffnesses were not equal in part due to different cross-linking techniques.

Objectives

The presented research focuses on engineering a collagen-GAG matrix for the growth of intervertebral disc tissue. The matrix was used as a three-dimensional scaffold for *in vitro* IVD culture and as an *in vivo* annulus implant for annulotomies. The study of disc cell-matrix interactions was an important component of the research. Experiments aimed at determining the outgrowth properties of normal disc tissue, the affect of microgravity on disc tissue, and the development of an implant to facilitate annular regeneration accomplished this goal. The collagen content of the matrix and the culture conditions were independent variables assessed in the design of the CG matrix. The dependent variables that were measured were matrix contraction, cell proliferation, GAG production, and protein production.

The objectives of the present research follow. They are organized according to the specific experiments, which will be presented in detail later.

Experiment 1. Matrix Manufacturing and Evaluation of Matrix Properties

1) To develop a hybrid matrix comprised of collagen types I and II.
2) To approximately equalize the amount of GAG, pore size, and some measure of contractility for type I, II, and hybrid collagen CG matrices

Experiment 2. Explants in/on Matrices

1) To assess the capability of cells to migrate from annulus explants into three-dimensional CG matrices.
2) To compare 2-D and 3-D outgrowth from explants.
3) To determine the effect of 10 and 20% FBS mediums on contraction and outgrowth.

Experiment 3. Explants and Explant-Matrix Constructs Cultured in a Bioreactor

1) To assess the capability of cells to migrate from annulus explants into three-dimensional CG matrices in bioreactor culture.
2) To determine the change in proliferative and biosynthetic activity with time of cells in annulus fibrosus explants and explant-matrix constructs cultured in bioreactors.
3) To compare the degree of change in proliferative and biosynthetic activity of explant cells in bioreactors with those in static culture.

Experiment 4. Annulus Cells Seeded into CG Matrices

1) To determine the behavior of isolated annulus fibrosus cells seeded into CG matrices, reflected in matrix contraction, proliferative rate, and biosynthetic activity.
2) To determine the effect of the CG matrix collagen composition on annulus fibrosus cells seeded into matrices with approximately equal pore diameter, GAG content, and contraction potential.

Experiment 5. Animal Model of CG Matrix Implant

1) To determine the feasibility of the canine animal model for demonstration of the utility of a CG matrix annulus implant.
2) To compare the tissue formed at the implant site to normal tissue and tissue formed at a defect site that receives no implant.
3) To compare the regenerative capabilities of a cell-seeded matrix as opposed to an unseeded matrix.

Hypotheses

The hypotheses for the above objectives are outlined below, grouped according to the specific experiments.

Experiment 1. Matrix Manufacturing and Evaluation of Matrix Properties

1) A hybrid matrix comprised of type I and II collagen can be manufactured.

Experiment 2. Explants in/on Matrices

1) Cells will grow out of the explants into the matrix.
2) A higher FBS concentration medium will produce more cell outgrowth.

Experiment 3. Explants and Explant-Matrix Constructs Cultured in a Bioreactor

1) Annulus fibrosus cells in explants will undergo a phenotypic change with time, reflected by changes in proliferation and biosynthesis, while in culture.
2) More cells will migrate into the matrices from the explants in the bioreactor culture than in the static culture.

Experiment 4. Annulus Cells Seeded into CG Matrices

1) As compared to type I and type II collagen matrices, hybrid matrices composed of types I and II collagen will be more beneficial for annulus cells in terms of proliferative rate and biosynthetic activity.

Experiment 5. Animal Model of CG Matrix Implant

1) Tissue formed at an implant site will differ from tissue formed at a defect site that receives no implant.
2) More regenerative tissue will form in defects that receive a cell-seeded implant than in defects that receive an unseeded matrix.

Experiment 1: Manufacture and Characterization of Collagen-GAG Matrices

Introduction

Here is presented a brief review of past techniques for manufacture and characterization of the collagen-glycosaminoglycan (CG) matrices. How these techniques will be applied and modified to the present investigation is then discussed. The characterization goals of this investigation were to assess the glycosaminoglycan (GAG) content, pore size, and "ability to be contracted" of the CG matrices. Manufacturing goals were to develop a hybrid collagen types I and II matrix and normalization of the properties of the type I, II, and hybrid matrices.

General CG Matrix Types

The type I CG matrix employed in this investigation was originally designed for use as artificial skin (239, 240, 241, 243). As such, an optimal pore size for this matrix was determined and subsequently utilized. A certain volume of slurry, approximately 230 mL in a designed tray, was used to create this pore size. This slurry volume results in a characteristic matrix thickness, approximately 3-4 mm. Thus, matrix manufactured through this method is termed "skin protocol" matrix.

In working with articular chondrocytes and type I CG matrix, Breinan (21) reported that these cells prefer a smaller pore size in the matrix for optimal growth. He developed a matrix with a smaller pore size in the type I CG matrix by using a lower volume of slurry in the designated tray, approximately 160 mL. Lee (134) extended Breinan's work with articular chondrocytes but instead used 180 mL of type I slurry in the designated tray. This latter volume was adopted for the current investigation and is henceforth termed "cartilage protocol" type I matrix.

Cross-Linking

Cross-linking the CG matrix affects its strength, biocompatibility, resorption rate, and antigenicity (228). "Crosslinked collagen has a greater modulus of elasticity (Young's modulus), greater resistance to proteases and a lower degree of swelling than uncrosslinked collagen (227)." Common methods used to cross-link collagen structures are dehydrothermal treatment (DHT), ethanol immersion, ultraviolet light (UV), gluteraldehyde immersion, and treatment with 1-ethyl-3-(3-dimethyl aminoproply)carbodiimide (EDAC).

Dehydrothermal Treatment

DHT treatment cross-links through drastic dehydration which forms interchain peptide bonds between amino acid residues (240). It also covalently links the GAG to the collagen (238). DHT results in a decrease in the free amine group content and the water-binding capacity. It increases the tensile strength (181). Generally, all CG matrices fabricated in the MIT Fibers and Polymers Laboratory are cross-linked for by DHT for at least 24 hours.

Ethanol

Ethanol is known to be a cross-linking agent sometimes employed in general histological fixation. Ethanol immersion for CG matrices has been examined to a limited extent (202).

Ultraviolet Irradiation

UV cross-linking is achieved through covalent cross-links between free radicals on adjacent fibers which are formed during treatment (most likely aromatic amino acid residues like tyrosine and phenylalanine) (38, 228). UV cross-linking has been supported and studied in previous research (228, 229).

Gluteraldehyde

Gluteraldehyde is a well know histological fixative. Figure 3 displays the chemical equations for gluteraldehyde cross-linking. It has previously been studied as a cross-linking agent for CG matrices (101, 134, 202). There is evidence that the compound may be slightly cytotoxic (101).

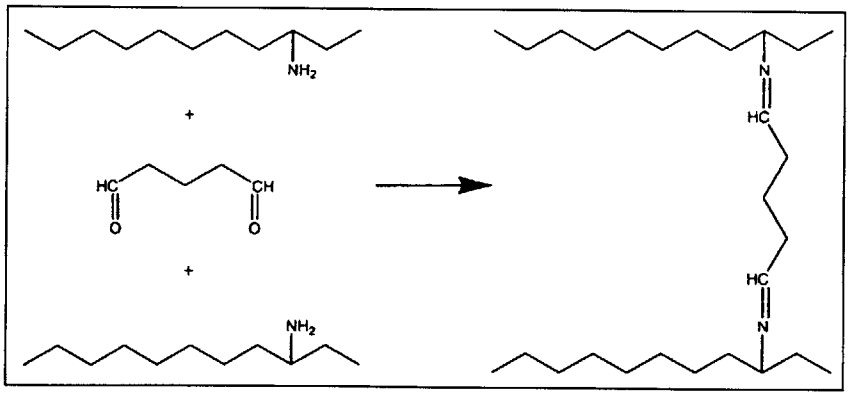

Figure 3. Chemical Equations Describing Gluteraldehyde Cross-Linking

1-ethyl-3-(3-dimethyl aminoproply)carbodiimide

EDAC is water-soluble Its unbound and excess chemicals are easily washed away because it is not incorporated into the amide cross-links that form. It forms collagen-collagen and collagen-GAG cross-links. During cross-linking, carboxylic groups of glutamic and aspartic acid residues are activated in the formation of amide bonds in the presence of lysine or hydroxylysine residues. N-hydroxysuccinimide (NHS) increases the rate and amount of cross-linking (78, 175), as shown in Figure 4. Olde Damink, et al. (175) found that little benefit is derived beyond 2 hours in the EDAC/NHS solution. These results were recently confirmed for the CG matrices (134).

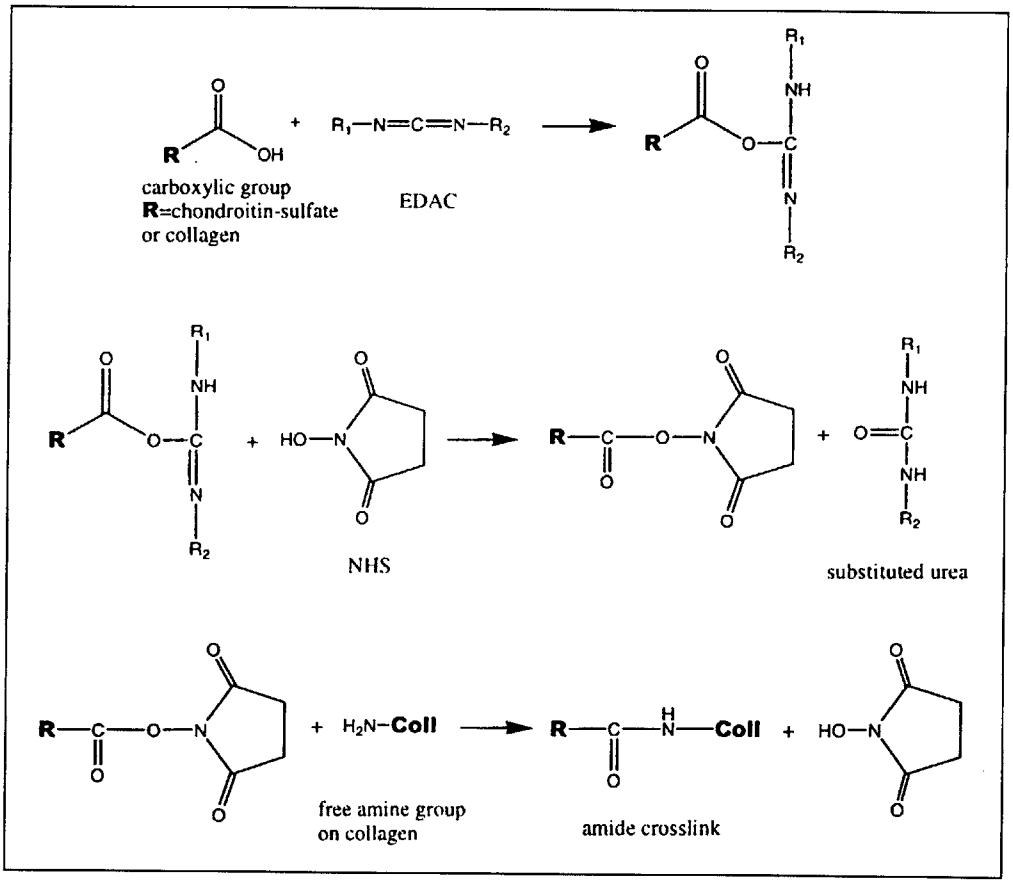

Figure 4. Attachment of GAG to Collagen by EDAC Cross-Linking

(Pieper, et al.) (181)

Comparison Studies and Assessment for Stiffness

Several studies have explored the mechanical properties and performance of the type I CG matrix with different cross-liking methods. One investigation (29, 30) compared the mechanical properties of the type I CG matrix at the macroscopic, light microscopic, and

electron microscopic levels. The strain data confirmed the similarity of the mechanical properties at all of these levels. The author felt that "the macroscopic mechanical behavior of the tissue analog can be interpreted as a statistical averaging of the mechanical behavior exhibited at the microscopic level" (29). It was also shown that 24 hours of gluteraldehyde treatment increased the tensile modulus of elasticity at failure by more than 60% as compared to DHT treatment alone (29). A recent study (202) determined the tensile modulus of elasticity for type I CG matrix sheets cross-linked by 24 hours of DHT treatment, 70% ethanol for 10 min., UV light for 12 hours, and gluteraldehyde immersion for 0.5-24 hours. The gluteraldehyde cross-linking for 24 hours and UV treatment for 12 hours were found to produce the greatest moduli. It was also determined that cells seeded into the matrix produced contraction of the matrix that was proportional (R^2 = 0.65) to the modulus of elasticity of the matrix. That is, stiffer matrices contracted less. Both of these investigations confirmed that the stress-strain curve for the matrix material follows the typical concave-up shape indicative of porous materials and soft tissues.

Another study (132) examined the effects of different cross-linking techniques on articular chondrocyte cell-seeded type I matrices. These were "skin protocol," 9 mm-diameter matrices all exposed to 24 hours of DHT. Techniques used were exposure to UV for 30 min. on each side (5 cm from a 258 nm source rated at 4510 $\mu W/cm^2$-note not the same source as in Experiments 1-3), immersion in 0.25% gluteraldehyde solution in 0.05 M acetic acid for 24 hours, and immersion in an EDAC solution for 2 hours. The compressive moduli of elasticity were 145 ± 23, 346, 369, and 1117 ± 109 (mean ± SEMs) for DHT only, UV, gluteraldehyde, and EDAC cross-linked matrices, respectively. (Note that these compressive moduli were three orders of magnitude less than the tensile modulus mentioned above for the same type of matrix.) The inverse of the swelling ratio was also correlated to the compressive stiffness. The authors found that the DHT and UV matrices contracted the most (60% reduction in diameter) while the EDAC matrices contracted the least (30% reduction in diameter) by 29 days. Cell-mediated contraction (CMC) decreased with increasing matrix stiffness. A inverse correlation was also seen between CMC normalized to DNA content and compressive modulus (R^2 = 0.69) and the inverse swelling ratio (R^2 = 0.98). After 29 days, the EDAC and gluteraldehyde matrices had DNA contents 20-40% higher than in the DHT and UV matrices.

Pore Analysis

A confocal microscopy analysis using the linear intercept method found an average pore size for the "skin protocol" type I matrix of approximately 150 μm (67). An SEM study determined the "skin protocol" type I matrix has a pore size of 205 ± 45 μm (107). A quantitative light microscopy analysis (21) using the linear intercept method revealed an average pore size of 83 μm for the type I matrix ("cartilage protocol") and statistics of 88 ± 14 μm (mean ± std. dev.) for the standard type II matrix. These pore sizes meet the requirement that pore size must exceed 11 μm. Louie (147) found coefficients of variation that ranged from 20-60% in the "skin protocol" matrix pore sizes.

Determination of Contractility of Matrix

The ability of cells to contract a matrix is difficult to assess prior to seeding cells into a matrix. This cellular contraction was previously shown to be correlated to the unseeded tensile and compressive stiffnesses (132, 202). More recently, it was shown that compressive stiffness 80-98% correlated with the inverse of the swelling ratio (134). Additionally, cell-mediated contraction by articular chondrocytes seeded into type I "skin protocol" matrices was found to be 70% correlated to compressive stiffness and 98% correlated to the inverse of the swelling ratio (134).

Swelling Ratio Testing

Denatured collagen behaves similar to ideal rubbers (244). Denatured collagen can be achieved by heating the collagen matrices above 80° C. The swelling ratio is a measure of the extent of cross-linking in randomly coiled polymer networks.

Normalization of Matrix Comprised of Different Collagen Types

While the work of Schneider, et al. (201) paved the way for the use of CG matrices for intervertebral disc (IVD) cells, the results of cell-seeding of the types I and II matrices were not directly comparable. The two matrix types had different amounts of GAG and the cross-linking techniques were dissimilar. In order to completely know what collagen type annulus cells prefer, these variables must be eliminated. This portion of the research essentially involves modifying the manufacturing techniques and assessing the properties of the matrix specimens to be used in Experiment 4. The primary aim is to normalize the GAG content, "ability to be contracted," and pore size of the type I, II, and hybrid matrices.

According to the past protocols and research, the GAG content of the standard type I and type II matrices were 8.7 ± 0.1% and 3.0 ± 0.1% of the total dry weight, respectively (21). Thus, it was felt that chondroitin sulfate would have to be added to the type II slurry to normalize the GAG content.

To match the "ability of the matrix to be contracted," it was decided to use swelling ratio testing due to the fact that it is technically easier to measure and it appeared in one study to be more closely related to cell-mediated contraction (134). A technically easier test was an important criteria because of the anticipated repetition of the test necessary for finding individual cross-linking times for the three types of matrices.

Methods

Collagen-GAG Matrix Synthesis

Type I Slurry

The type I CG scaffolds were coprecipitated from bovine tendon type I collagen (Integra Life Sciences, Plainsboro, NJ) and shark chondroitin-6-sulfate (CS) and converted into a highly porous membrane by freeze-drying (242, 244) (Appendix A). First, 3.6 g of the collagen was blended in 600 mL of 0.05 M acetic acid in a jacket-cooled blender (Eberbach Waring restaurant model blender, Ann Arbor, MI) at 4° C and 23,000 rpm for 1.5 hours. 120 mL of a 0.11 % (w/v in 0.05 M acetic acid) solution of chondroitin-6-sulfate (chondroitin sulfate C-4384 from shark cartilage, Sigma Chemical, St. Louis, MO) was added to the collagen solution over 15 min. using a peristaltic pump (Manostat cassette pump, Manostat, New York, NY). The slurry was then formed after blending at 4° C for an additional 1.5 hours. As measured by pH paper, the pH of the resulting slurry is approximately 3.5 (21). Slurry that was not to be precipitated into matrix immediately was stored in a refrigerator for up to two months. Slurry stored for more than one week was be reblended for 10-30 min. before use. Prior to placing the slurry in freezer pans, it was de-gassed by applying a vacuum pump (# 6K778B, Dayton Electric, Chicago, IL) to a 6 L sidearm flask for 30 min. until most bubbles were gone.

The type I slurry was placed in stainless steel tray with three 32 cm x 49 cm sections prior to freezing. For "skin protocol" matrix, one third of the slurry batch volume (approximately 230 mL) was placed in each section of this tray. For the "cartilage protocol" matrix, 180 mL of the slurry was placed in each section of the tray. Additionally, "double thickness" and "1/2 thickness" matrices were created for Experiment 2 for which 2/3 and 1/6, respectively, of the slurry batch volume was placed in each tray section. When adding the slurry to the tray, special care will be taken to avoid the formation of air bubbles.

Type II Slurry

Sigma Source

Prior to receiving commercial type II slurry from Geistlich Biomaterials, an attempt was made to manufacture type II slurry from native collagen. The collagen used was insoluble type II collagen from bovine Achilles tendon (# C-8886, Sigma Chemical, St. Louis, MO). This collagen was substituted for the type I collagen in the protocol above. For freezing, either the stainless steel tray mentioned above was used in the Virtis Genesis Freeze-Dryer (25LE, Virtis, Inc., Gardiner, NY) or a 9.5 cm-diameter stainless steel metal centrifuge tube was used in a freezing bath. The freezing bath consisted of heat transfer fluid (Heat Transfer Fluid XLT, PolyScience, Niles, IL) in a glass dessicator that was cooled with a liquid nitrogen coil system.

Geistlich Source

Type II collagen slurry was provided by Geistlich Biomaterials (Chondrocell slurry, Wolhusen, Switzerland). The slurry is manufactured through a proprietary process from porcine cartilage. Previous approaches for reconstituting this slurry into matrix (21) did not appear to produce the same results with Geistlich's current slurry. The method employed by Lee (134) (Appendix B) was adopted for primary attempts of matrix production. Briefly, the Geistlich slurry was centrifuged at 3500 rpm at room temperature for 5 min. to de-gas the slurry. Approximately 3.5 mL was added to each well of a 6-well plate (Falcon #08-772-1B, Fisher Scientific Co.). This volume of slurry was modified over the course of the investigation to determine how matrix thickness and pore size would be affected.

Additionally, GAG was added to the slurry to increase the % mass of GAG in order to match it to the type I matrix's GAG content. In this protocol (Appendix B), chondroitin-6-sulfate was added to the type II Geistlich slurry through high speed stirring with a stir bar. Then, the slurry was degassed as above. The slurry volume in the well-plates was altered to achieve the desired pore size (the same as the type I "cartilage protocol" pore size).

Hybrid Slurry

A hybrid slurry of types I and II collagen was formed by creating a solution of 50% type I slurry and 50% type II slurry (Appendix C). The type I slurry was produced by the methods stated above. The type II slurry was from Geistlich. Adding GAG to this slurry was also attempted by the stir bar stirring method. The hybrid slurry was centrifuged at 3500 rpm at room temperature for 5 min. to de-gas the slurry. Approximately 4 mL of the slurry was added to each well of a 6-well plate.

Freeze-Drying

The tray and well plates were placed in a freeze-dryer chamber (Virtis Genesis Freeze-Dryer 25LE, Virtis, Inc., Gardiner, NY) at a shelf temperature of -43° C (Appendix A). Well plates were initially frozen with their covers on to prevent formation of a skin. Slurry that was initially frozen in the liquid nitrogen cooling system was then transferred to the Virtis. The slurry was allowed to freeze for at least one hour in the Virtis (1.5 hours for the "double thickness" matrix). At this point, the cover was removed from any well plates. The vacuum pressure was then lowered to below 200 mtorr. Subsequently, the temperature was then raised to 0° C for sublimation. The freezing forms ice crystals which form the pores of the matrix. Following at least 12 hours of lyophilization (sublimating ice crystal under vacuum), the freezer chamber temperature was raised to 20° C. Pore size of the resulting matrix is dependent on the volume of slurry placed in the freezing vessel, the type of freezing vessel, and the temperature differential between the initial slurry and the freezing chamber. With regard to the latter, a higher temperature differential causes faster cooling resulting in more ice nucleation and smaller pores (107)).

Thickness

Prior to DHT cross-linking, the thickness of the matrices was measured in 6-10 random areas with a digital micrometer (CD-6"C, Mitutoyo).

Cross-Linking

DHT

All matrices were DHT cross-linked for at least 24 hours (unless otherwise stated assume 24 hours) (Appendix A). The matrix was first placed in open foil and often inside a sealed autoclave bag (for guaranteed sterility upon removal from the DHT oven). DHT cross-linking took place in a vacuum oven (Fisher Isotemp vacuum oven, Fisher Scientific, Medford, MA) for 24 hours at 105° C and 1 atm. Matrix was then stored in a dessicator until further cross-linking.

UV

Ultraviolet radiation was administered in a sterile vertical flow hood. The matrix was placed on foil 30 cm from a UV source (Philips Sterilamp #G10T5 1/2 L, $\lambda = 253.5$ nm), which is rated at 5.3 W for total output and 55.5 W/cm^2 at 1 m. All UV cross-liking in the present investigation was performed for 16 hours based on the results of Breinan (21). Matrix sheets were turned over halfway through the UV cross-linking time to expose each side to the same amount of radiation.

EDAC

EDAC cross-linking was performed for two hours at room temperature in a 5:2 solution of EDAC (#E7750, Sigma) to NHS (Appendix D). Solution amounts were based on 6 mmol EDAC/g collagen (175) and a 9 mm-diameter CG disc mass of 0.005 g. Excess EDAC was rinsed from the matrices with phosphate-buffered saline (Dulbecco's PBS; #14190-136, Life Technologies) and distilled water. Matrices were stored for up to 2 days in distilled water prior to use.

GAG Analysis

Matrices used for GAG analysis had either never been hydrated or were freeze-dried after having been hydrated (i.e., after EDAC cross-linking). The dry masses were obtained prior to digestion with papain (Appendix E). GAG was quantified using a modification of the dimethyl-methylene blue method (57) (Appendix F). Absorbance at 535 nm was determined with a spectrophotometer (LKB Biochrom Ultraspec). The amount of GAG was extrapolated from a

standard curve for shark chondroitin sulfate (chondroitin sulfate C-4384 from shark cartilage, Sigma Chemical, St. Louis, MO). The GAG in each matrix sample was divided by the mass to find the percent mass of GAG.

To assess whether EDAC cross-linking had any effect on the GAG content, samples from one type I matrix sheet were tested before and after 2 hours of EDAC cross-linking.

Matrix Pore Diameter Analysis

A quantitative pore diameter analysis based on a modification of the method of Breinan (21) was utilized (Appendix G). Dry matrix was fixed in 100% ethanol overnight. For each matrix batch examined, a horizontal and a vertical piece of matrix were embedded in glycol methacrylate (JB-4 embedding system, Polysciences, Inc., Warrington, PA) resin. These were sectioned at 5 μm (the horizontal piece was sectioned mid-thickness). Sections were stained with aniline blue. Images (5 from the horizontal section and 5 from the vertical section) were then captured from a light microscope (Olympus Vanox-T) connected to a digital camera (Olympus DP11) (Appendix H). The digital images were then edited to eliminate background artifacts. Pore size analysis was performed using the method of directed secants for the mean intercept length between the collagen elements that formed the walls of the matrix. A best-fit pore ellipse was calculated, and the pore diameter was taken to be the root mean square of the major and minor diameters of the ellipse multiplied by a 1.5 correction factor because pores are not sectioned through their maximums (72, 73, 222). The aspect ratio was considered to be the ratio of the major axis to the minor axis. Through this method, the porosity of the matrix could also be determined via simple thresholding methods. These values from the 10 sections were then averaged to determine the matrix characteristics.

The program requires an intercept to be 2 pixels thick in order to accept it as an intercept. To determine if results could be improved, images were tested with the "dilate" function applied to ascertain how much of a difference thicker lines made. The selection program also allows one to choose a circular area or a oval area for analysis. ANOVA was used to compare the results of these options on five images taken from separate slides of matrix # 23 (Appendix K).

Intra-observer variability was tested by analyzing several images twice and selecting a slightly different area of approximately the same size. Inter-observer variability was examined by having two separate researchers analyze seven images, each selecting as large an area as possible in the images.

Compression Stiffness Testing

Type I UV cross-linked matrices were tested for compressive stiffness (Appendix I) in order to compare with DHT cross-linking performed by another researcher (134). Matrices were hydrated in PBS and stored at 4° C for 24 hours prior to testing in order fully hydrate the specimens and remove air bubbles. The thickness of the specimen was measured with a micrometer (#263M, L.S. Starrett Co.) while hydrated in PBS. Discs were placed in a PBS-filled polymethylmethacrylate chamber mounted in the lower jaw of a Dynastat Mechanical Spectrometer (IMASS, Hingham, MA). A 50 g load cell (Sensotec, Cleveland, OH) fitted with a 9.5 mm-diameter polymethylmethacrylate cylindrical plunger was fixed in the upper jaw of the

Dynostat. Using computer controlled displacements, static compressive strains were applied in sequential increments of 1-5% up to a maximum of 40%. The displacement was held constant for 75 s to allow for stress relaxation and the equilibrium load was recorded at end of this time. These loads were converted to equilibrium stresses. The matrix compressive stiffness was computed as the slope of the best fit line of the resultant equilibrium stress-strain curve.

Strain testing was performed on type I "skin protocol" DHT and 16 hour UV cross-linked matrices. The matrices were dehydrothermally treated for 24 or 72 hours. Additionally, some were cross-linked by EDAC for 2 hours. These results were compared to those of a previous researcher (134).

Swelling Ratio

The swelling ratio (Appendix J) is inversely proportional to the cross-link density (227, 244). Samples were placed in a 90° C water bath for 2 min. to swell and denature the collagen. Unbound water was expelled from the matrices by placing them between them between sheets of filter paper and applying a 1 kg mass for 20 s. The wet mass (WM) was then immediately acquired. Samples were dehydrated in a DHT oven overnight at 110° C. The dry mass (DM) was recorded. The swelling ratio (227), defined as the inverse of the volume fraction of dry collagen (V_f), was calculated from the masses and densities of water (ρ_{water} = 1.00 g/cm^3) and collagen (ρ_{water} = 1.32 g/cm^3):

$$r = \frac{1}{V_f} = \frac{\left[\left(DM/\rho_c\right) + \left((WM - DM)/\rho_{water}\right)\right]}{DM/\rho_c}. \qquad \text{Equation 1}$$

EDAC and non-EDAC cross-linked "cartilage protocol" type I matrices were tested to make sure that swelling ratio testing revealed significant differences in cross-linking. Swelling ratio testing was performed on the type I, II, and hybrid matrices used for Experiment 4 as an approximate measure of the density of cross-links that are formed by the cross-linking methods mentioned above.

Statistics

Student's t-test was used for one-variable comparisons between 2 groups. ANOVA was used to compare the characteristics of the different matrix types with Bonferroni-Dunn post-hoc tests for individual comparisons.

Results

The parameters of manufacture and matrix characteristics are displayed for all matrix batches in Appendix K.

Matrix Manufacturing

Manufacture of the type II matrix with the Sigma collagen and freezing the Virtis produced a pore size that was macroscopically too large. Thus, freezing was attempted in a liquid nitrogen bath. Details of these trials are outlined in Appendix K. The temperature was very difficult to control by this method because the freezing vessel had to be lowered into the bath manually. Attempts at manufacture by this method were abandoned when Geistlich slurry became available.

Cross-Linking

UV

After 16 hours of UV cross-linking, the matrix sheets often had a yellow hue. This form of cross-linking was very advantageous because the sheets were also sterilized by the technique. The matrices physically behaved stiffer after cross-linking as assessed by difficulty in cutting discs.

EDAC

The first step in EDAC cross-linking is hydration of the matrices in distilled water alone in order to swell the matrices for EDAC cross-linking. Generally, air bubbles in the matrix were forced out by compression with a forceps at this stage. It was noted that a few hybrid and type II matrices would remain deformed by this act so removable of bubbles was not practiced in the practical application of EDAC cross-linking. It was also noticed, that upon initial water hydration, the hybrid matrices would permanently decrease in diameter.

EDAC cross-linked discs clearly had greater stiffness as assessed by ability to compress them with a forceps.

GAG Content

The GAG content of the matrices is displayed in Table 1. The type I "skin protocol" matrix had 7.9 ± 1.2% (mean ± standard deviation) mass of GAG in the matrix. The "cartilage protocol" matrix had a slightly lower GAG content of 6.9 ± 1.4%. The GAG percentage increased to 10.1 ± 0.9% when only 1/6 slurry batch was used per pan section ("1/2 thickness"). (Note that all of the "1/2 thickness" matrix was manufactured from one slurry batch so the high GAG content could be an anomaly of this batch.) The type I matrix tested for GAG content before and after 2 hours of EDAC cross-linking (matrix 120, Appendix K) had % mass of GAG of 7.89 ± 0.70 after DHT only and 7.99 ± 0.38 after EDAC cross-linking.

The Geistlich slurry matrix had a GAG content of 1.2% mass, lower the previous reported value for prior batches of slurry (21). Adding CS to the type II slurry increased the % mass of GAG in the resulting matrix (Figure 5). By extrapolating on a linear regression, 0.0105

g was deemed an effective amount of CS to add to 20 mL of the type II slurry in order to match the type I matrix % mass of GAG of approximately 7%. Note that some of the data points in Figure 5 were added after 0.0105 g CS was designated the final additive. At an addition rate of 0.0105 g CS/20 mL type II slurry, the resulting % mass of GAG had a high standard deviation but an average value of 6.7 (Figure 5 and Table 1).

Table 1. Overall Characteristics for the Different Types of Matrix

Data is presented as mean ± standard deviation. CS = chondroitin sulfate. Swelling ratio here is presented after 2 hours of EDAC cross-linking. Shaded matrices are those used in Experiment 4.

Matrix Type	Volume	Freezing Tray	GAG Content (% mass)	Thickness (mm)	Pore Diameter (μm)	Pore Aspect Ratio	Porosity (%)	Swelling Ratio
I	1/6 slurry batch (1/2 thickness)	1/3 pan section	10.1 ± 0.9	2.0 ± 0.7	170 (small n)	1.42	87	
I	180 mL (cartilage protocol)	1/3 pan section	6.9 ± 1.4	2.9 ± 0.4	236 ± 59	1.3 ± 0.3	93 ± 2	5.9 ± 0.6
I	1/3 slurry batch (skin protocol)	1/3 pan section	7.9 ± 1.2	3.6 ± 0.7	271 ± 35	1.3 ± 0.3	91 ± 3	
II	3.5 mL	6-well plate well	1.2 (small n)	2.5 ± 0.5	125 ± 42	1.1 ± 0.1	89 ± 2	4.4 ± 0.5[1]
II + 0.0105 mg CS/20 mL	4 mL	6-well plate well	6.7 ± 2.2	2.8 ± 0.6	202 ± 51	1.1 ± 0.1	91 ± 2	5.6 ± 0.8
hybrid (50% I/50% II)	4 mL	6-well plate well	5.0 ± 1.5	2.5 ± 0.4	228 ± 52	1.2 ± 0.1	92 ± 2	6.0 ± 1.0

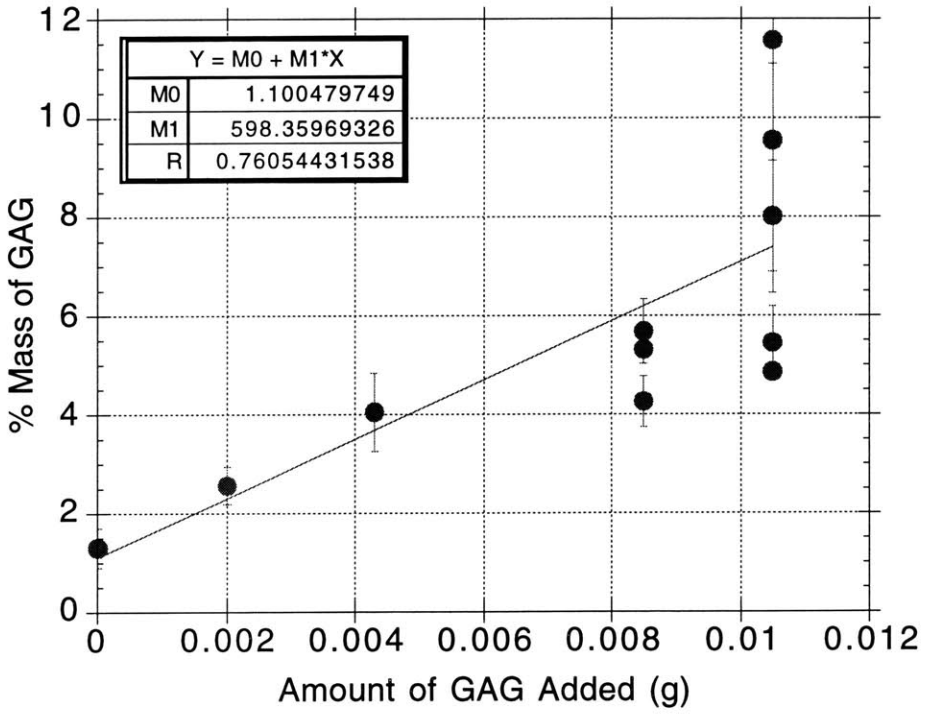

Figure 5. Percent Mass of GAG in the Resulting Matrix vs. Amount of GAG (CS) Added to 20 mL of Type II Collagen-GAG Slurry

Compared to the other matrix types, the hybrid matrix had a lower GAG content of 5.0 ± 1.5%. Hybrid matrix batches were made with 0.0085 g CS/20 mL type II slurry and 0.0105 g CS/20 mL type II slurry added (matrix 119 and 125; Appendix K) which resulted in GAG contents of 6.14 ± 0.03 and 6.17 ± 1.27% mass, respectively. However, when GAG was added to the hybrid slurry, the resulting matrix had a pore size that was too large to match the type I and II matrices. As pore size was deemed a more important parameter to closely match, addition of GAG to the hybrid slurry was abandoned.

Pore Characterization

Pore sizes for the main matrix types are presented in Table 1. In general pores from vertical section images were slightly smaller than pores from horizontal sections. Vertical matrix sections displayed a gradient in pore size from top to bottom, with bottom pores being smaller, and larger pore presenting at the top of the matrices.

The analysis parameter of "dilation" did not significantly affect the pore diameter, aspect ratio, or porosity ($p > 0.14$; ANOVA). Thus, this option was not used for analysis of the matrices. Whether a circle or oval selection was used in the analysis also did not affect the outcome parameters ($p > 0.2$; ANOVA) significantly, but the average pore diameter and aspect ratio was slightly higher with oval selections. Resultantly, oval selections were employed for matrix analysis because a larger number of pores could be contained by an oval. Often it was observed that the larger the physical area analyzed, the larger the resulting pore diameter. Intra- and inter-observer variabilities in pore size analysis each ranged as high as 20% for the same image.

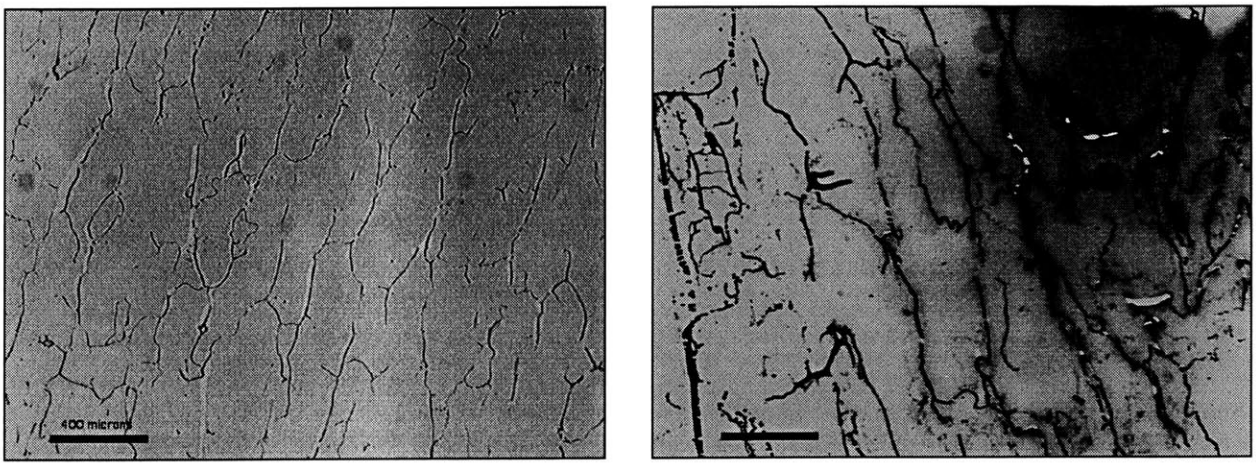

Figure 6. Images of Type I "Skin Protocol" Matrix

Sections prepared by JB-4 embedding and 5 μm sectioning. Left image displays horizontal section and right image is vertical section. Scale bar = 400 μm. The blotches are staining artifacts that were removed prior to image analysis. Note the strikingly oriented pores.

The type I "skin protocol" matrix had a pore diameter of 271 ± 35 μm (mean ± standard deviation) (Figure 6 and Table 1). The "cartilage protocol" type I matrix had a pore diameter of 236 ± 59 μm. With this matrix thickness, the variation of pore size with distance from the

bottom of the freezing pan became evident (Figure 7). Pores closer to the bottom of the pan were smaller, and the top of the matrix had very large pores. This effect became more exaggerated when the "1/2 thickness" matrix was produced (Figure 8). The type I matrix had very oriented pores no matter what the thickness of the matrix. For instance, the aspect ratio for the "skin protocol" and "cartilage protocol" type I matrices were 1.3 ± 0.3.

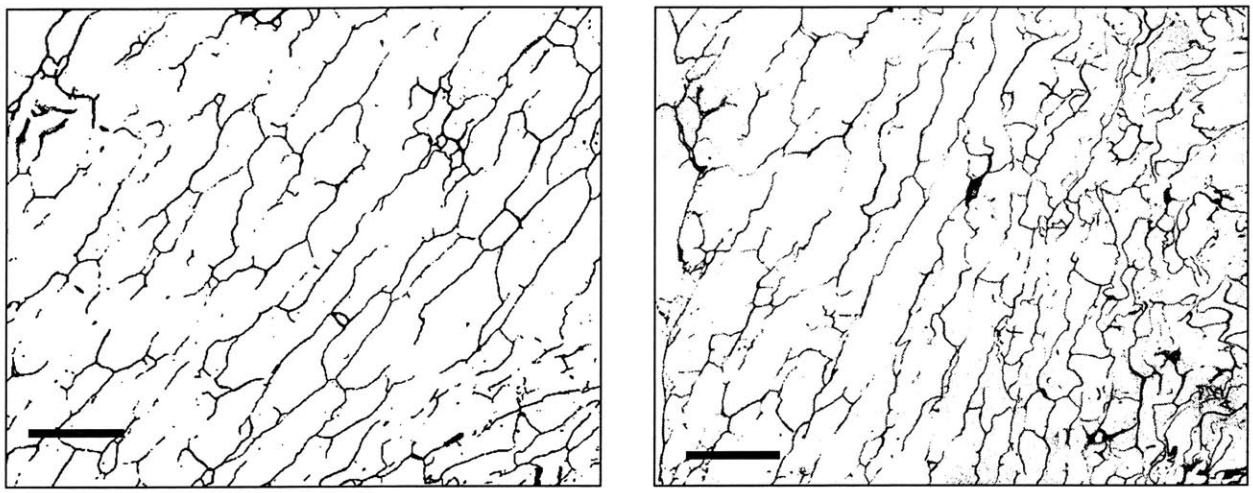

Figure 7. Images of Type I "Cartilage Protocol" Matrix

Sections prepared by JB-4 embedding and 5 μm sectioning. These images have also been edited for artifacts and thresholded. The left image displays a horizontal section and the right image is a vertical section. Scale bar = 400 μm. Note the strikingly oriented pores. The right image demonstrates the variation of pore size through the thickness of the matrix. The right side of the right image is from a level that was closer to the bottom of the matrix.

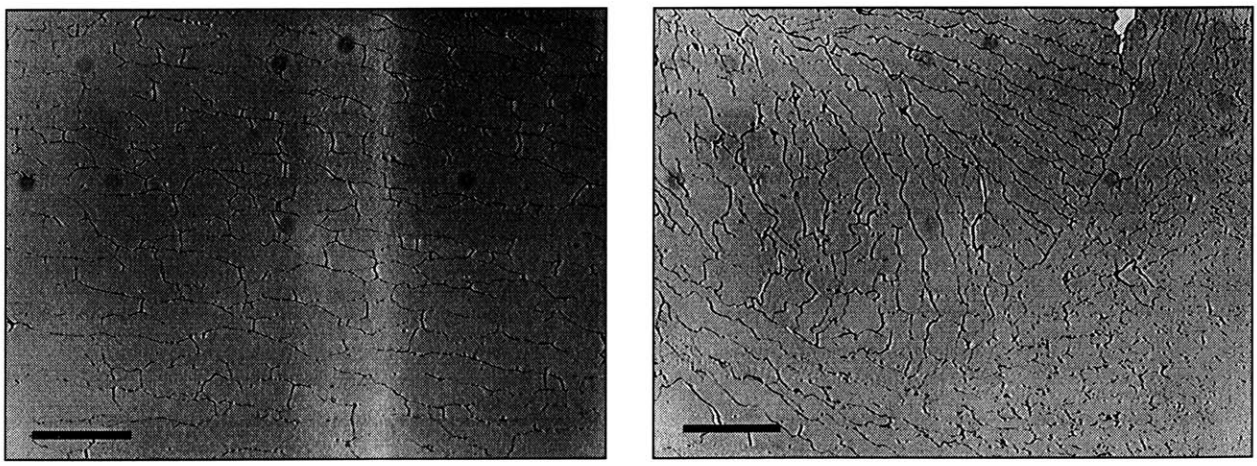

Figure 8. Images of Type I "1/2 Thickness" Matrix

Sections prepared by JB-4 embedding and 5 μm sectioning. The left image displays a horizontal section and the right image is a vertical section. Scale bar = 400 μm. The blotches are staining artifacts that were removed prior to image analysis. Note the strikingly oriented pores.

The Geistlich type II slurry alone produced a matrix with a pore size approximately half of that for type I slurry (Figure 9; Table 1). When GAG was added to the slurry the pore size increased. This seemed somewhat proportional to the amount of GAG added as the pores size was 164 ± 45 μm with 0.0085 g CS/20 mL type II slurry (matrix 109; Appendix K) and 202 ± 51 μm with 0.0105 g CS/20 mL type II slurry (Figure 10; Table 1). The pore structure was less oriented, as evidenced by the pore aspect ratio for the type II matrices being 1.1 ± 0.1. The type II matrix was noted to have thicker pore walls than the type I matrix. This was evidenced by the slight decrease in porosity for the type II matrices (Table 1) compared to the type I matrices.

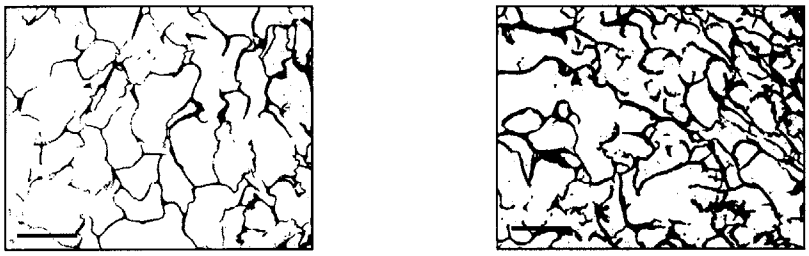

Figure 9. Images of Type II Matrix

Sections prepared by JB-4 embedding and 5 μm sectioning. These images have also been edited for artifacts and thresholded. The left image displays a horizontal section and the right image is a vertical section. Scale bar = 200 μm. Images have been reduced so that magnification is the same as on the above images. This matrix was manufactured with 4.5 mL of type II slurry per 6-well plate well. Note the less oriented pore structure and the greater wall thickness compared to type I matrices.

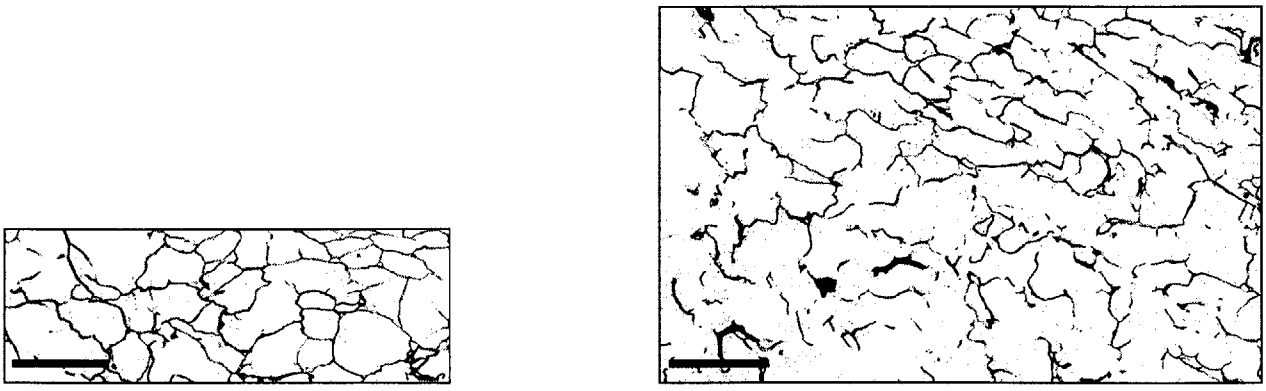

Figure 10. Images of Type II Matrix with Chondroitin Sulfate Added

Sections prepared by JB-4 embedding and 5 μm sectioning. These images have also been edited for artifacts and thresholded. The left image displays a horizontal section and the right image is a vertical section. Scale bar = 400 μm. This matrix was manufactured by mixing the type II slurry with 0.0105 g chondroitin sulfate per 20 mL. Note the less oriented pore structure and the greater wall thickness compared to type I matrices.

As might be expected, the pore characteristics (pore size, aspect ratio, porosity) of the hybrid matrix were often in between those of the type I and type II matrices. As mentioned above, hybrid matrix batches were made with 0.0085 g CS/20 mL type II slurry and 0.0105 g

CS/20 mL type II slurry added (matrices 119 and 125, respectively; Appendix K) which resulted in pore sizes of 264 ± 35 μm and 285 ± 43 μm, respectively. Here again is demonstrated the property that addition of GAG increases the pore size. These latter pore sizes were too large to match those of the type I and II matrices to be used for Experiment 4. Thus, the pore size of the pure 50% type I slurry/50% type II slurry matrix was 228 ± 52 μm (Figure 11).

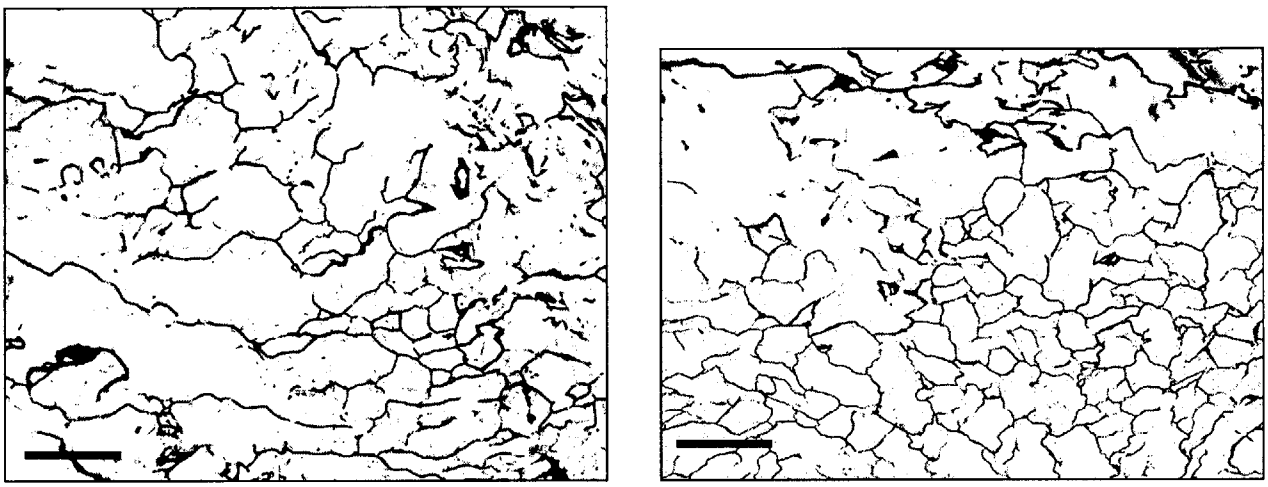

Figure 11. Images of Hybrid Matrix

Sections prepared by JB-4 embedding and 5 μm sectioning. These images have also been edited for artifacts and thresholded. The left image displays a horizontal section and the right image is a vertical section. Scale bar = 400 μm. Note the less oriented pore structure and the greater wall thickness compared to type I matrices. These images also demonstrate the great variability in pore sizes and structure present in all the matrix types. The top of the right image displays some of larger pores seen on the top of the matrices.

Compressive Stiffness Testing

Table 2. Compressive Stiffness Results for Type I "Skin Protocol" Matrix

Results are presented as mean ± standard error of the mean. Cross-linking methods were additive to the same matrix.

Cross-Linking Method			Compressive Stiffness (Pa)
DHT (hours)	UV (hours)	EDAC (hours)	
24			145 ± 23 (n = 6)[2]
24	16		298 ± 29 (n = 12)
24		2	1140 ± 85 (n = 10)[3]
24	16	2	919 ± 117 (n = 6)
72	16	2	863 ± 98 (n = 5)

Strain testing of the type I "skin protocol" matrix produced the results shown in Table 2. The addition of EDAC cross-linking produced a three-fold increase in compressive stiffness. ANOVA revealed no significant difference between any of the EDAC cross-linked groups. For

this reason, DHT cross-linking for only 24 hours was maintained and performing UV cross-linking prior to EDAC cross-linking was abandoned.

Swelling Ratio

A significant difference was found between the swelling ratios of the type I "cartilage protocol" matrix that was cross-linked by DHT (8.9 ± 1.8) only vs. an additional 2 hours of EDAC cross-linking (5.9 ± 0.6) ($p < 0.0001$; Student's t-test). As can be seen in Table 1, the swelling ratios for the three types of matrix used in Experiment 4 ranged from 5.6-6.0 after 2 hours of EDAC cross-linking. In addition, some testing was performed on the type II matrix with no GAG added. This matrix had a swelling ratio of 4.4 ± 0.5 after 2 hours of EDAC cross-linking, but it should be noted that 4 mm-diameter discs were used instead of the usual 9-mm diameter.

Matrix Types Comparison

Table 1 displays the average characteristics (shaded) of the three matrix types for which standardization of all parameters except collagen type was attempted. The three matrices that had the closest parameters are labeled I (cartilage protocol), II + chondroitin sulfate, and the hybrid in this table. The thickness of the hybrid matrix was significantly less than those of the other two matrix types ($p < 0.001$; Bonferroni-Dunn). The GAG content of the hybrid was also significantly less than that of the other two matrix types ($p < 0.02$; Bonferroni-Dunn). The pore diameter was not different among the three matrices ($p = 0.26$; ANOVA). The significant difference in GAG was knowingly allowed in order to have the pore sizes match. The swelling ratios were not significantly different ($p = 0.46$; ANOVA).

Discussion

Matrix Manufacturing

The results demonstrate the type I and type II slurries can be modified from previous protocols. This is the first report of the manufacture of a collagen types I and II hybrid matrix. The Geistlich slurry has clearly changed since previous batches were received because the older protocol for the slurry (21) was unsuccessful and the GAG content has decreased slightly from 3% to 1.2% mass.

Creation of a type II slurry using Sigma type II collagen was halted when commercial slurry became available. The primary difficulty in manufacture of the former was lack of a constant temperature freezing environment that would freeze lower than -43° C. Based on the results of the liquid nitrogen bath, the ideal freeze-dryer air temperature for creation of a type II slurry in this way is likely somewhere between -70° C and -50° C. Another issue in production

of matrix by this method is finding a pure source of type II collagen. Sigma has not tested # C-8886 Sigma type II collagen for purity.

Cross-Linking

UV cross-linking was a very convenient technique because the matrix was sterilized in the process and could be stored long-term afterwards. Qualitatively, EDAC produced a stiffer matrix but it had to be used within 2 days.

GAG Content

The GAG content of the type I matrices was similar to the 8.7% reported by Brian (21). Based on the amount of GAG added during manufacture of the type I matrix, the theoretical percentage should be 8.6% mass. That the actual averages were less than this for the "skin protocol" and "cartilage protocol" matrices may be due to incomplete mixing or cross-linking of the GAG to the matrix.

GAG was successfully added to the type II slurry although a large variability was noted between matrix samples. Results could likely be improved if a higher speed mixing system was employed.

Pore Characteristics

During freezing, the CG precipitate is forced into a matrix around growing ice crystals. Ice nucleation is the process by which pores are created in the matrix. In general, the faster the cooling process, the more ice nuclei are activated before solidification is complete. The more nuclei the smaller the pores will be. Thus, a larger differential between the slurry temperature and the freezing temperature causes faster cooling.

Consistent throughout the matrices (no matter what type) was the observation that the pores varied throughout the thickness of the matrix. Larger pores were found on top and smaller pores on the bottom. This is likely due to the fact that the air temperature in the freezer dryer is about 20° C warmer than the shelf temperature when it is set at -43° C. Since pore size is related to the temperature differential during the freezing process (initial slurry temperature and freezing temperature), these findings are explained by the different temperature differentials experienced by the top the slurry exposed to the air temperature and the bottom of the slurry exposed to the pan temperature. In short, the bottom of the matrix freezes faster and more ice nucleation occurs (107). That pore diameter decreases with decreasing volume is likely a function of the quicker formation of ice crystals in the slurry.

The observation that examination of a larger area of matrix results in a larger average pore diameter has been seen by another researcher (107). It may be related to selection bias when the observer must choose small area of analysis.

The pore sizes for the type I matrix in this investigation are much larger than those reported by Breinan (21) (83 μm for the 160 mL volume in the pan section). There are several reasons for this discrepancy. Breinan used 160 mL vs. the 180 mL used presently. Greater

volume in the same vessel produces a larger pore size. The microscope camera for acquiring digital images for analysis has been upgraded and allows for a greater area to be displayed in each image. In general, pore size is larger when a greater area is used. As mentioned above, this could be due to a selection bias (i.e., the observer will choose matrix sections that appear to fit many pores in the image => pores with smaller diameter). Also, Breinan filled in all open walls for the pores. This will provide nice, rounded pores for analysis, but the matrix is not a closed pore system. Filling in the walls artificially decreases the pore size. Finally, Breinan did not use the 1.5 correction factor that is employed presently. Taking these factors into consideration, it is likely that pore size for the type I "cartilage protocol" matrix is only slightly larger than that designed by Breinan. This opinion is based on the facts that the volume was 20 mL more and the difference between the "cartilage protocol" and "skin protocol" matrices used presently (~50 mL difference) was only 40 μm.

Note that the pure type II slurry from Geistlich produced a matrix with a pore diameter of 125 μm with the present fabrication methods and pore characterization analysis. Breinan (21) had a medium pore size for his type II matrix of 88 μm using his pore characterization analysis, similar in pore diameter to his type I "cartilage protocol" matrix. Given that the present "cartilage protocol" matrix is 236 μm, a pore diameter of 125 μm is likely about half of what Breinan used as a medium pore size. Breinan also noted no significant differences in the biosynthesis of articular chondrocytes that were seeded into a large range (50-250 μm) of matrix pore diameters.

Other researchers have documented pore sizes similar to those found in the present investigation. Irving found pores of 205 ± 45 μm for type I slurry frozen at -40° C using linear intercept analysis and scanning electron microscope images. Through similar methods, Flynn (58) achieved a pore size of 150 μm. Chen (31) and Wong (237) used the linear intercept method on embedded sections of "skin protocol" type I matrix. Chen found a pore diameter of 145 μm. Wong reported major and minor pore axis diameters of 260 and 160 μm, respectively. None of these previous researchers used the 1.5 correction factor. For comparison to the pore size reported in the present investigation, their pore size become 217-308 μm with the correction factor.

In the present study, pore diameter was found to increase with addition of GAG to the slurry for both type II and hybrid matrices.

Compressive Stiffness Testing

Initially, it was thought that combining cross-linking techniques would increase the mechanical stiffness. The results showed this not to be the case. Even adding 48 hours of extra DHT cross-linking and 16 hours of UV cross-linking to 2 hours of EDAC cross-linking did not improve the compressive stiffness. Thus, at present the strongest cross-linking protocol is 24 hours of DHT followed by 2 hours of EDAC cross-linking.

Swelling Ratio

While the swelling ratios between the three types of matrix cross-linked similarly were statistically similar, it cannot be stated explicitly from this that their compressive stiffnesses would be the same. Although there is a correlation between swelling ratio and compressive

stiffness, it is not 100%. However, swelling ratio does give some indication of the ability of the matrix to be contracted by cells (134).

The swelling ratios reported here are higher than seen in a previous study (134) of "skin protocol" type I matrix cross-linked for 2 hours by EDAC. In that study, the swelling ratio of the aforementioned matrix was 3.2, approximately half that seen in this study. This difference could be explained by minor changes in the technique, different types of matrix, or inter-observer variability. As such, it may be recommended that if swelling ratios are to be compared, it is advisable to perform the tests simultaneously as was done in this study.

GAG content will affect the swelling ratio. More GAG in a matrix will make it swell more, thus increasing the swelling ratio. However, more GAG in a matrix that has been DHT and EDAC cross-linking will also increase the amount of cross-linking, thus lowering the swelling ratio.

Matrix Types Comparison

The type I, type II + GAG, and hybrid matrices had similar pore diameters and swelling ratios. The latter would be an indication at the amount of cross-linking, and therefore the ability to be contracted was similar. The hybrid matrix was not quite as thick as the other two matrices, but this not considered to be a fundamental matrix property that would affect cell proliferation or biosynthesis. The GAG content of the hybrid was lower at 5% compared to the 6.7-6.9% mass in the other two matrices. The hybrid matrices were also noted to shrink slightly upon hydration. Whether this was due to the decreased GAG content is unclear. Matrices with more GAG will swell more, but the type I and II matrices did not swell more than their original diameter on average.

Acknowledgements

This study was supported by the Brigham Orthopedic Foundation and the Harvard/MIT Training Program in Biomaterials (1 T32-DE07311) (DH). The authors gratefully acknowledge use of the facilities of the Fibers and Polymers Laboratory at MIT under the supervision of Professor Yannas for fabrication of the collagen matrices. Integra Life Sciences supplied the type I collagen. Geistlich Biomaterials provided the type II collagen slurry.

Experiment 2: Intervertebral Disc Explants Cultured in/on Collagen-GAG Matrices

Introduction

The regenerative capabilities of the intervertebral disc (IVD) are not fully known. Important aspects of healing in other connective tissues are the proliferation of parenchymal cells and their migration into the transitional reticular collagen stromal network. These processes will also be determinants of IVD cell infiltration of exogenous matrices implemented for tissue engineering. The objective of this study was to investigate the capability of cells to grow out of the annulus fibrosus into a three-dimensional (3-D) scaffold *in vitro*.

Explants are small pieces of tissue that contain both cells and the normal extracellular matrix of a tissue. The explant model for study of the intervertebral disc has been used previously (16, 80, 108, 219). Compared to other tissues, organ culture of the disc is less traumatic to the tissue because under normal conditions the disc is relatively avascular (193, 208). Indeed, the annulus fibrosis relies almost entirely on diffusive transport for nutrients (193). The well-characterized and strong collagen architecture of the annulus suggests that it is able to withstand long-term culture. Explant outgrowth is also a preferred method for obtaining cells from viable human IVD tissue because surgical specimens yield so little tissue (80). For purposes of the present research, explant studies model the capability of cells from intact tissue to penetrate the matrix.

Explants were placed on top of matrices and between two matrix sections. The investigation of annulus explants surrounded by a collagen-glycosaminoglycan (CG) matrix has several purposes: 1) it helps develop a better understanding of the behavior of annulus fibrosus cells migrating from the tissue into a CG matrix at a defect site, and 2) the study perfects the static control portion of Experiment 3. Explants were also placed in 2-D culture as outgrowth controls.

Intervertebral Disc Annulus Culture Medium

Several types of medium have been employed for basic cell culture of annulus cells. For base medium researchers have used MEM with Earle's salts (80), Ham's F-12 (153), DMEM (96, 104, 195), and DMEM/F-12 (32, 104). Ichimura (104) compared DMEM and Ham's F-12 and found that DMEM produced significantly better results. DMEM/F-12 has been employed for use in articular cartilage often (21, 134). Most researchers (32, 96, 104, 153, 195, 206) have employed medium containing 10% fetal bovine serum (FBS). However, Johnson (114) used 20% FBS for the first 5 days of culture after digestion to cause rapid attachment. Gruber (80) developed the following medium for annulus specifically after trying many combinations: MEM with Earle's salts, 1% L-glutamine, 1% nonessential amino acids, 1% penicillin/streptomycin, 1% fungizone, and 20% FBS. Addition of ascorbic acid to this medium did not change the results. In the present study, explants and explant-matrix constructs were also cultured in 10% and 20% fetal bovine serum (FBS) medium types to evaluate the advantages of a higher serum

concentration medium for annulus explants. Based on previous research, it was hypothesized that a 20% FBS medium would result in more cells outside of the explant.

Methods

Tissue Acquisition and Formation of Explants

The lumbar spine from L1 to L6 was sterilely resected from 6 canines (2-7 years old) (Appendix L). Each spine was placed in phosphate buffered saline (Dulbecco's PBS; #14190-136, Life Technologies) supplemented with 2% penicillin (100 U/mL)/streptomycin (100 mg/mL; #15070-063, Life Technologies) and 1% fungizone (2.5 mg/mL, #15295-017, Life Technologies) at 4° C until dissection. Generally dissection began within 2 hours of resection of the spine. The IVDs were dissected from the spines (Figure 12). The ligaments and nucleus pulposus were removed from each IVD. The IVDs were then bisected along their thickness to make thinner explants, generally 2-3 mm thick. A 5 mm-diameter dermal punch (Keyes #33-25) and hammer were used to cut the explants. It was noted which disc each explant arose from.

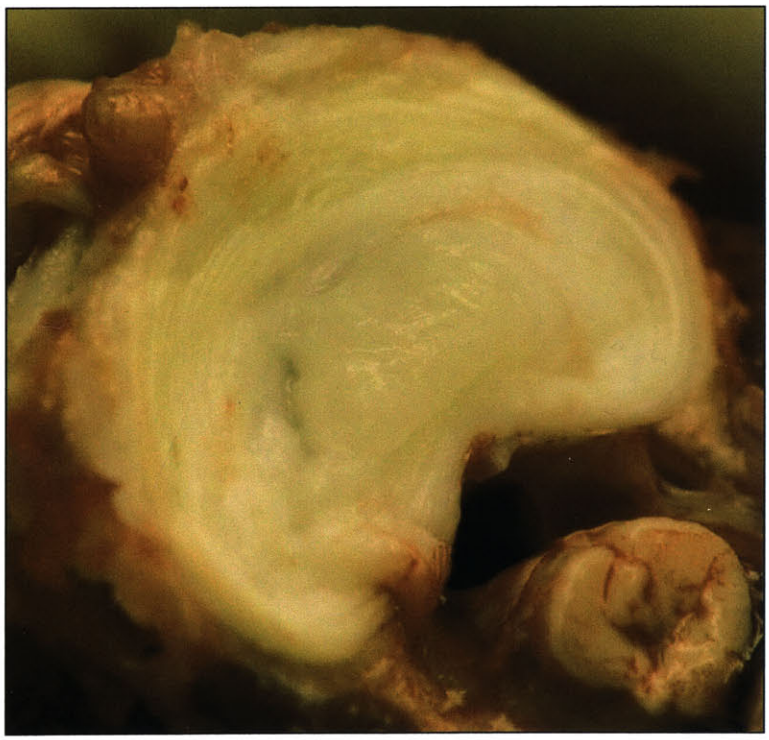

Figure 12. Canine Lumbar Intervertebral Disc

The IVD has been separated from one vertebral body. The severed spinal cord in the lower right corner.

Culture Conditions

10% and 20% FBS medium types were used in this experiment. The 10% FBS medium consisted of DMEM/F12 (#11320-033, Life Technologies) supplemented with 2% penicillin/streptomycin (#15070-063, Life Technologies), 1% fungizone (2.5 mg/mL, #15295-017, Life Technologies), 0.025 g/L of L-ascorbic acid phosphate (magnesium salt n-Hydrate, #D13-12061, Wako Chemicals USA, Inc.), 10% FBS (Austrailian Fetal Bovine Serum, #SH30084.03, Hyclone Laboratories), and 1% L-glutamine (#25030-081, Life Technologies) (Appendix M). Based on the results of Gruber (80), the 20% FBS medium consisted of MEM with Earle's salts (#11090073, Life Technologies), 1% L-glutamine, 1% nonessential amino acids (#9304, Irvine Scientific), 2% penicillin/streptomycin, 1% fungizone, and 20% FBS. Enough medium was added to reach the top of the explant (approximately 1 ml) or explant-matrix construct (approximately 3 ml). Medium was changed every 2-3 days (Appendix N). Culture took place in an incubator at 37° C in an atmosphere of 5% CO_2 and 95% humidity.

Type I CG Matrix

The type I CG matrix was produced by freeze-drying a coprecipitate of type I collagen from bovine tendon and chondroitin 6-sulfate from shark cartilage. The procedure is outlined in Experiment 1 and Appendix A. For this experiment, "skin protocol," "double thickness," and "1/2 thickness" matrices were manufactured. The matrices were dehydrothermally treated in a vacuum oven for 24 hours (in an autoclave bag) and additionally cross-linked by ultraviolet radiation for 16 hours[4]. For the latter, the matrix was placed on foil 30 cm from a UV source (Philips Sterilamp #G10T5 1/2 L, λ = 253.5 nm), which is rated at 5.3 W for total output and 55.5 W/cm^2 at 1 m. Matrix sheets were turned over halfway through the UV cross-linking time to expose each side to the same amount of radiation.

The "skin protocol" and "1/2 thickness" matrices had the characteristics shown in Table 3 based on findings in Experiment 1. The characteristics of the "double thickness" matrix were not specifically quantified but it was observed that the thickness was nearly twice that of the "skin protocol" matrix. The pores were also very, very large.

Table 3. Characteristics for the Main Matrix Types in Experiment 2

Data is presented as mean ± standard deviation. GAG = glycosaminoglycan

Type I Matrix	Freezing Tray	GAG Content (% mass)	Thickness (mm)	Pore Diameter (μm)	Pore Aspect Ratio	Porosity (%)
1/6 slurry batch (1/2 thickness)	1/3 pan section	10.1 ± 0.9	2.0 ± 0.7	170 (small n)	1.42	87
1/3 slurry batch (skin protocol)	1/3 pan section	7.9 ± 1.2	3.6 ± 0.7	271 ± 35	1.3 ± 0.3	91 ± 3

Squares of 2.5 x 2.5 cm were cut from the matrix sheets with a scalpel. This size was selected because it was that maximum that could fit in the 3.5 cm-diameter wells of the 6-well plates (Falcon 08-772-1B, Fisher Scientific Company).

2-D Culture

15-32 explants from 6 canines were centered in 6-well plates for 2-D culture (Figure 13). 105 (n = 6 canines) and 43 (n = 4 canines) explants received the 10% and 20% FBS medium types, respectively. The area of attachment of the 2-D explants was evaluated by placing a 1 mm measurement grid under the culture dishes under an inverted microscope within the first few days. 14-37 2-D explants were sacrificed at 2, 4, 6, and 8 weeks. Upon sacrifice, the wet mass was measured for 103 of the explants.

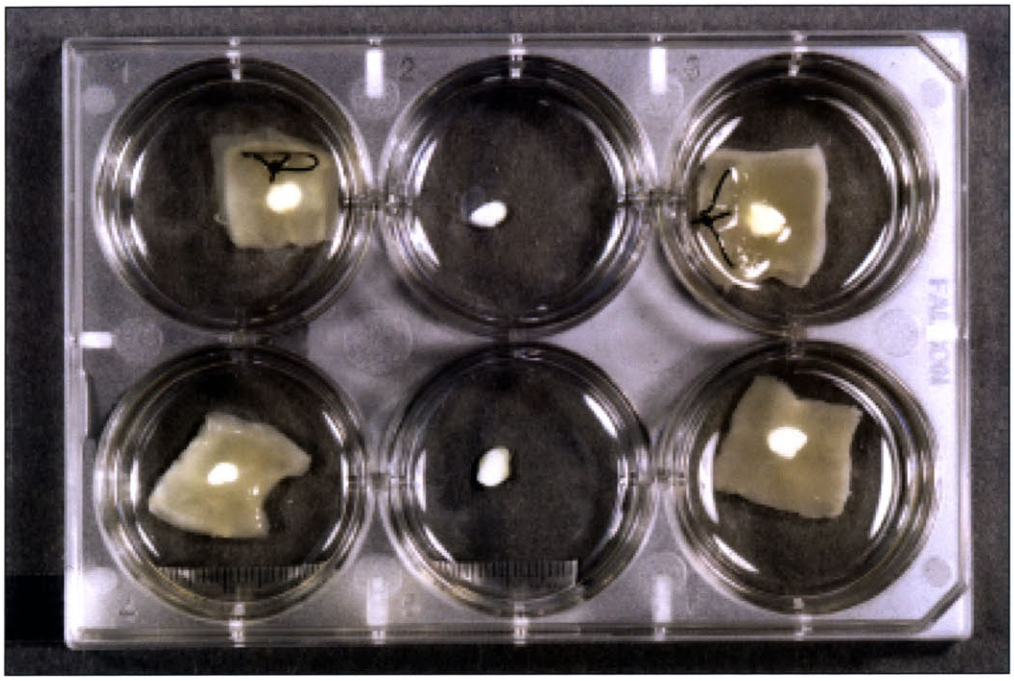

Figure 13. Well Plate Section Displaying Culture Method

The middle wells demonstrate 2-D culture. Wells in the upper corners display culture of "1/2 thickness" matrix sandwiches. Wells in the lower corners demonstrate explants on top of matrices. These samples are after two months in culture. More yellow areas of the matrix indicate cell outgrowth, as confirmed by microscopy. Note that the matrix contraction was not uniform. Matrices originally just fit into the wells.

The outgrowth of cells from the 2-D explants was evaluated by inverted microscopy every other day for the first 2 weeks of culture and every week thereafter. Outgrowth was reflected in the increased number of cells surrounding the explant and the increasing distance to which the cells had migrated. It was scored on a semi-quantitative scale:

0, represented no cells outside the explant,
1, represented 1-100 cells,
2, reflected 100-1000 cells,
3 and 4, corresponding to the increasing exponential range, and
5, represented greater than 100,000 cells and confluence in the well-plate.

3-D Culture

Explants on Top of Matrices

19-32 explants each from 4 canines were placed on top of 2.5 x 2.5 cm squares of "skin protocol" matrix (Figure 13 and Figure 14b). These explant-matrix constructs were then placed in 6-well plates. The explants were allowed to adhere to the matrices for 10-15 min. prior to addition of any medium. 64 and 45 explant-matrix constructs received the 10% and 20% medium types, respectively. 13-25 3-D constructs were sacrificed at 2, 4, 6, and 8 weeks. 20 and 16 matrix squares without explants were also cultured in the 10% and 20% FBS medium types, respectively.

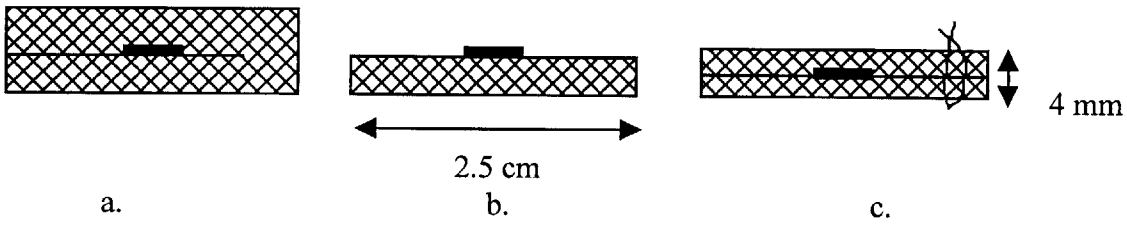

Figure 14. Type of Explant-Matrix Constructs

a. "Double thickness" matrix sandwich. b. Explant on top of "skin protocol" matrix. c. "1/2 thickness" matrix sandwich.

"Double-Thickness" Matrix Sandwiches

A slit was made in the 2.5 cm x 2.5 cm squares midway through the thickness and 50% into the square to form a sandwich (Figure 14a). Explants from 2 canines were placed into the center of the matrix via the slit, and these explant-matrix constructs were then placed in 6-well plates. The explants were allowed to adhere to the matrices for 10-15 min. prior to addition of 10% FBS medium. The 3-D constructs were sacrificed at 2, 4, 6, and 8 weeks.

"1/2 Thickness" Matrix Sandwiches

Two 2.5 cm x 2.5 cm squares of "1/2 thickness" type I CG matrix were sutured together at one end (Perma-Hand Silk Suture, straight needle, taper point, ST-1, black braided, 3-0; #K852H, Owens & Minor) (Figure 14c). Explants from 4 canines were placed in the middle of

the two halves of these sandwiches. These explant-matrix constructs were then placed in 6-well plates (Figure 13). The explants were allowed to adhere to the matrices for 10-15 min. prior to addition of the 10% or 20% FBS medium types. The 3-D constructs were sacrificed at 2, 4, 6, and 8 weeks.

Matrix Dimensional Measurements

Matrix dimensions were measured within 1-3 hours of medium addition and then every week. As dimensions did not change equally, the mid-length dimensions in two orthogonal directions were measured with a ruler (#72909, Electron Microscopy Sciences). Cross-sectional area of the matrix constructs was calculated to determine contraction of the scaffold. Initial wet areas were compared. Subsequent areas were compared normalized to the initial wet area. Cell-mediated contraction was calculated by:

$$\frac{\text{Average Control Area} - \text{Construct Area}}{\text{Initial Dry Area}} x100\%. \qquad \text{Equation 2}$$

Histology

After sacrifice, constructs and explants were placed in 10% neutral buffered formalin (10% buffered formalin phosphate; #SF100-20, Fisher Scientific Co.) for at least 2 days. Specimens were manually dehydrated (Appendix O), bisected through the explant, and half embedded in paraffin and half in glycol methacrylate resin (JB-4 embedding system, Polysciences, Inc., Warrington, PA; Appendix P). 5 μm microtomed paraffin sections were stained with H & E (Appendix Q). The following parameters were assessed under light microscopy (Olympus Vanox-T): cell morphology (round or elongated), cell location, and cell proliferation. Outgrowth from the 3-D constructs was reflected in the increased number of cells surrounding the explant and the increasing distance to which the cells had migrated.

Statistics

ANOVA was used to assess whether the area of attachment of the explants and wet mass at sacrifice was significantly different among canines, disc level, sacrifice time, and FBS medium type. Student's t-test was used to determine whether there was a difference in outgrowth time between the two FBS medium types. Correlations of outgrowth time with disc level and canine were determined with ANOVA. Differences in cell outgrowth score with FBS medium type were assessed with Student's t-tests for the individual times. Spearman rank correlation was employed to discover the relationship of culture time with cell outgrowth score from the 2-D explants. The relationship of cross-sectional area with FBS medium type and whether the matrix was part of an explant construct or not was assessed with ANOVA. Bonferroni-Dunn post-hoc tests and Student's t-tests were used for single variable comparisons. The relationship of cell-mediated contraction to FBS medium type and culture time was tested with ANOVA.

Results

2-D Explants

The 2-D explants adhered to the culture dishes usually within 1-4 days. The area of attachment to the culture dishes was 15 ± 2 mm^2 (mean ± standard deviation; n = 138). This parameter was not significantly different among sacrifice times, between the two FBS culture mediums, among disc levels, or among canines. The explants often became oval in shape after initial formation as a round 5 mm-diameter explant.

The 2-D explants had an average wet mass of 44 ± 14 mg (n = 95) at sacrifice. This parameter was significantly different among the 6 canines ($p = 0.0011$; ANOVA) with two of the canines having explants with lower masses. The wet mass did not vary with disc level. It was however correlated to FBS medium type ($p = 0.02$; ANOVA) and sacrifice time ($p = 0.007$; ANOVA), as shown in Figure 15. In general, wet mass decreased with time in culture. This effect was more pronounced in the 20% FBS medium type. However, it should be noted that the wet masses of the explants in the 20% FBS medium were already lower than those in the 10% FBS medium at 2 weeks so the differences in FBS medium type may be due to the differences in wet masses among the canines.

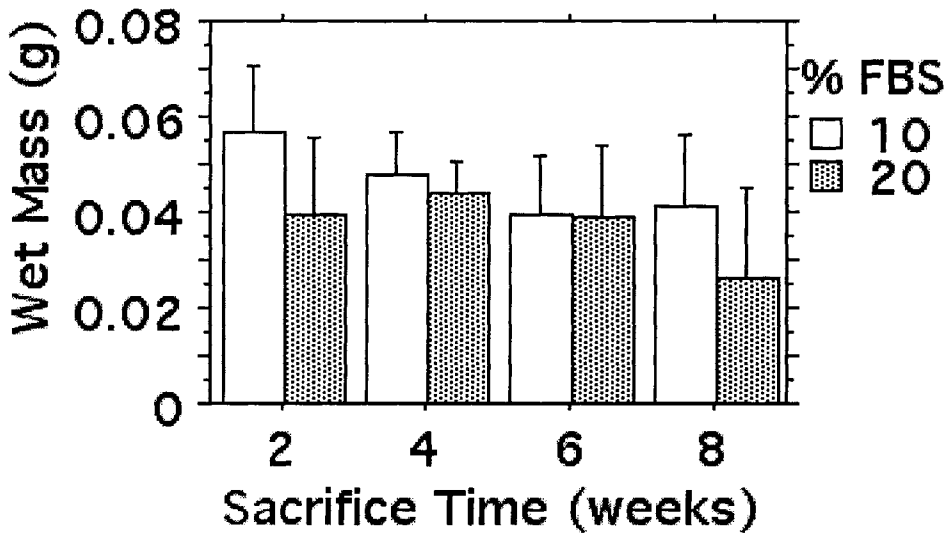

Figure 15. Wet Mass vs. Sacrifice Time for the Different FBS Medium Types

Error bars represent standard deviations. n = 10-28 at 10% FBS and n = 4-5 at 20% FBS. Wet mass was significantly different among the sacrifice times and FBS medium types.

Cell outgrowth from the explants in 2-D culture in the 10% (n = 104 explants from 6 canines) and 20% FBS (n = 43 explants from 4 canines) medium types occurred after 9.7 ± 2.9 and 7.7 ± 2.6 days, respectively ($p < 0.0002$; Student's t-test). Outgrowth time was not related to disc level. Explants from certain canines did have faster outgrowth ($p < 0.0001$; ANOVA). Exponential outgrowth appear to occur after initial outgrowth. Cell outgrowth score increased with time in culture ($p < 0.0001$, Spearman rank correlation; Figure 16). The explants in the

20% FBS medium had significantly more cell outgrowth onto the culture dishes ($p < 0.034$; Student's t-tests; Figure 16) at all but 3 culture times (3, 4, and 8 weeks). Time to confluence in the culture dishes varied from 3 to 8 weeks.

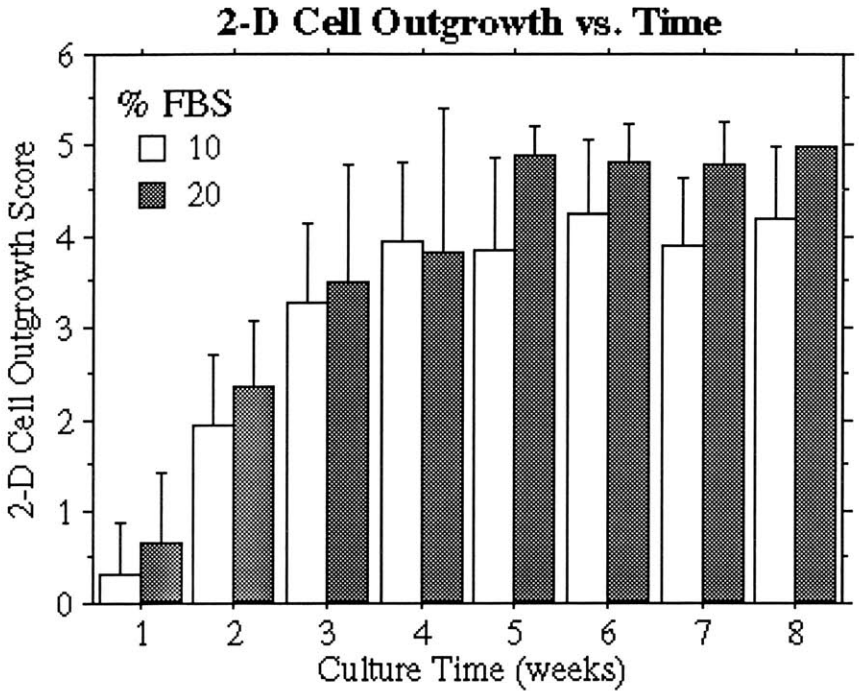

Figure 16. Cell Outgrowth from Explants in 2-D Culture

Error bars represent the standard deviation. *n* decreased from 148 at 1 week to 14 at 8 weeks. Outgrowth in the 10% FBS medium was significantly less than that in 20% FBS medium at all times except 3, 4, and 8 weeks.

Histological evaluation revealed the development of a multiple layer of cells on the surface of the tissue samples by two weeks.

Explants on Top of Matrices

The initial wet cross-sectional area measurements (as a percentage of the initial dry area) of the matrices were significantly different ($p < 0.008$; ANOVA) for the two medium types with values being 11% and 6% less in the 20% FBS medium for the controls and explant-matrix constructs, respectively ($n = 64$ in 10% and 45 in 20% FBS medium types from 4 canines; Table 4). In addition, the initial wet cross-sectional areas were different between the controls and explant-matrix constructs ($p < 0.01$; ANOVA) with explant constructs being 11% and 6% less in the 10% and 20% FBS medium types, respectively (Table 4). The explant-matrix constructs cultured in both FBS medium types decreased in cross-sectional area proportional to time in culture ($p < 0.0001$; ANOVA), and matrices in the 20% FBS medium contracted more ($p < 0.0074$; ANOVA). The constructs in both medium types decreased in cross-sectional area significantly more than matrix controls ($p < 0.041$; Student's t-tests). By 8 weeks, controls had

contracted to approximately 75% of their initial wet area whereas the explant-matrix constructs had contracted to approximately 50%. These findings are seen in Figure 17. Cell-mediated contraction increased during culture time ($p < 0.0001$; ANOVA; Figure 18). Constructs placed in the 10% FBS medium type had more cell-mediated contraction overall ($p = 0.002$), but, unlike constructs in the 20% FBS medium type, cells did most of the contracting within 1 week.

Table 4. Initial Matrix Wet Cross-Sectional Areas

Values are expressed as a percentage of the initial dry areas. Matrices in the different FBS medium types were significantly different ($p < 0.0078$ for controls and explant constructs). Controls were significantly different from explant constructs ($p < 0.001$ for 10% FBS medium; $p < 0.01$ for 20% FBS medium).

FBS Medium Type	Type of Matrix	
	Control	Explant Construct
10%	90 ± 12%	79 ± 10%
20%	79 ± 5%	73 ± 9%

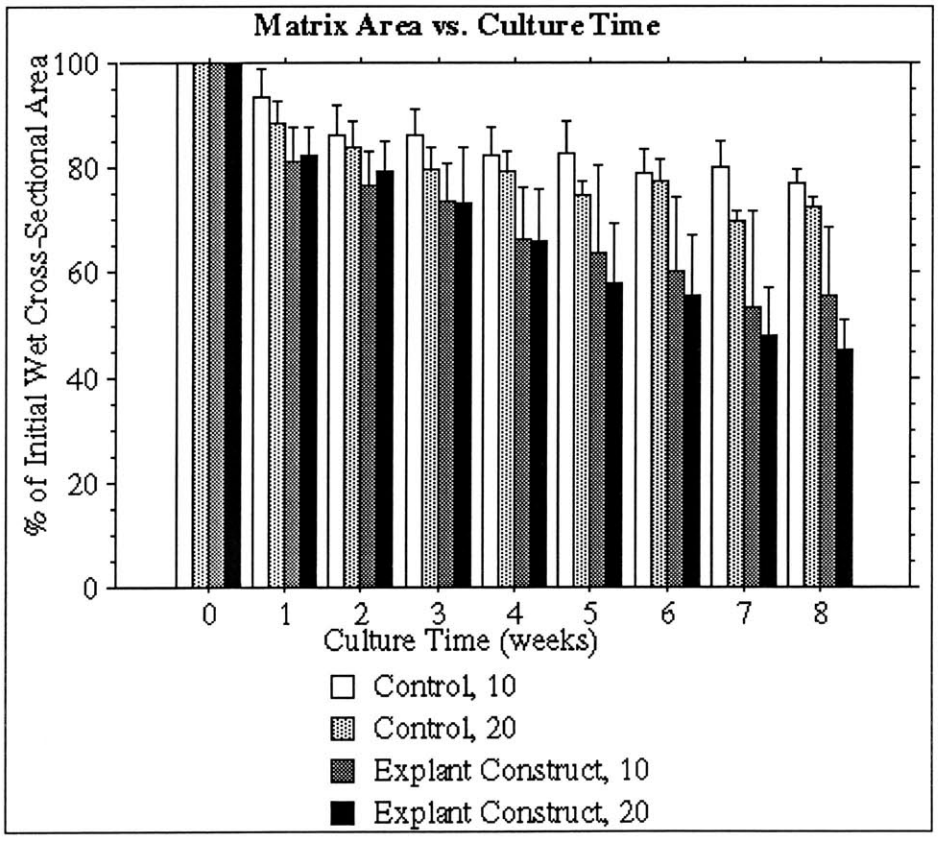

Figure 17. Contraction for Matrices with Explants on Top

Error bars represent standard deviations. n = 3-20 per time point for controls, and n = 5-64 per time point for explant-matrix constructs. All matrices decreased in cross-sectional area during time in culture ($p < 0.0001$; ANOVA). Controls contracted significantly less ($p < 0.041$; Students t-tests) than the matrix-explant constructs. Matrices in the 20% FBS medium contracted more ($p < 0.0074$; ANOVA).

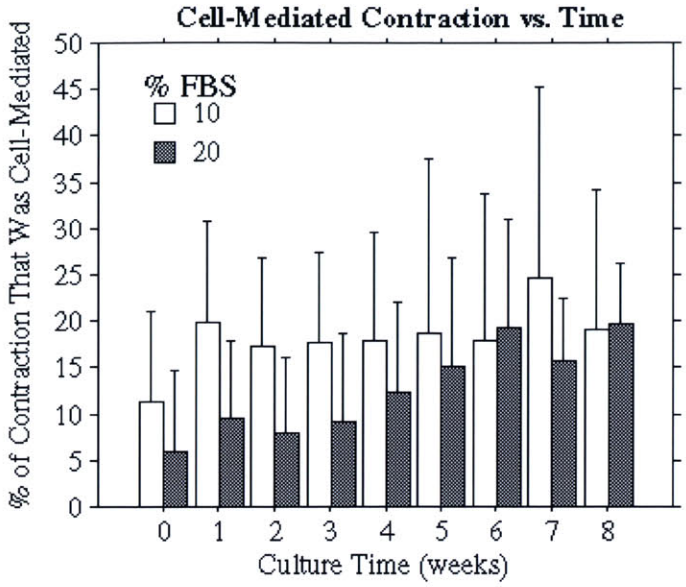

Figure 18. Cell-Mediated Contraction vs. Culture Time

Error bars represent standard deviation. *n* decreased from 108 at time 0 to 12 at 8 weeks. There was a significant effect of culture time ($p < 0.0001$; ANOVA) and FBS concentration ($p = 0.002$; ANOVA) on cell-mediated contraction.

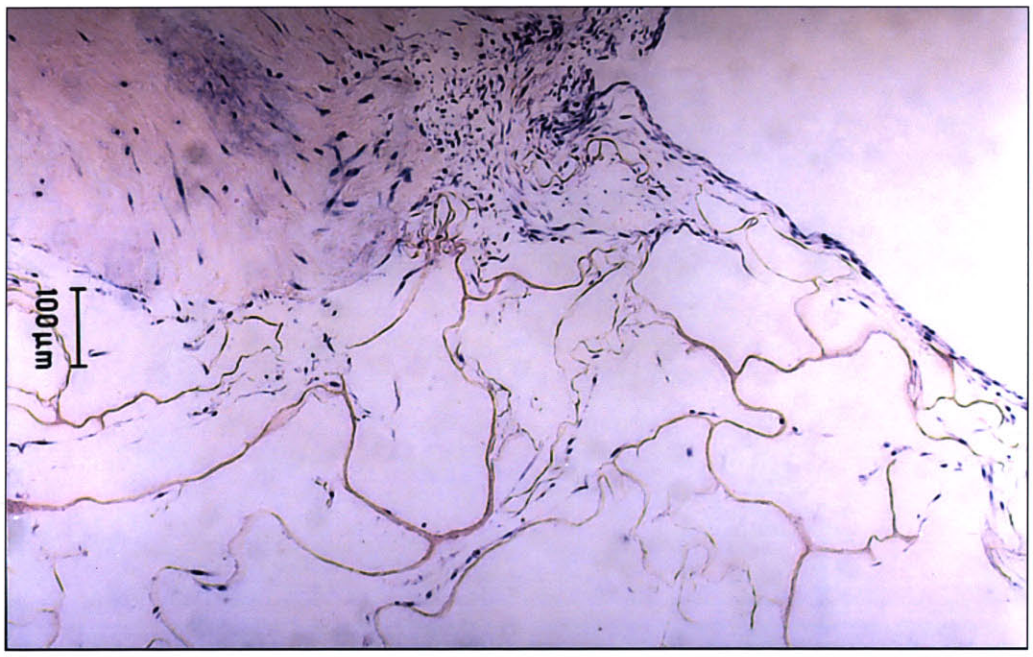

Figure 19. An Explant Cultured on Top of a CG Matrix

The micrograph is from a 6-week time point. The explant is located in the upper left corner. Note the large build up of cells on the right side of the explant, the layer of cells on top of the matrix, and the infiltration of cells into the matrix.

Histological results from the explants on top of matrices revealed that cell migration occurred within the CG scaffolds and inside the explants (Figure 19). Cell migration to the bottom of the matrices was found by 4 weeks. In some cases, horizontal cell migration to the edge of the matrix was macroscopically apparent in those constructs sacrificed at 8 weeks. Microscopically, this development was identified before 8 weeks time (1 cm in some cases). Evaluation of the explants revealed the development of a multiple layer of cells on the surface of the explant by two weeks, similar to that present on the 2-D explants.

"Double Thickness" Matrix Sandwiches

These matrices contracted approximately 10% upon hydration, approximately 10% less than the matrices with explants on top in the 10% FBS medium type. For the explants from the two canines in which this matrix was employed, constructs contracted by approximately 20% after 6-8 weeks. Histological analysis revealed that few cells were migrating into the matrix. It was felt to be due to the very large pore size, and this type of matrix-explant construct was abandoned for use after the two canines.

"1/2 Thickness" Matrix Sandwiches

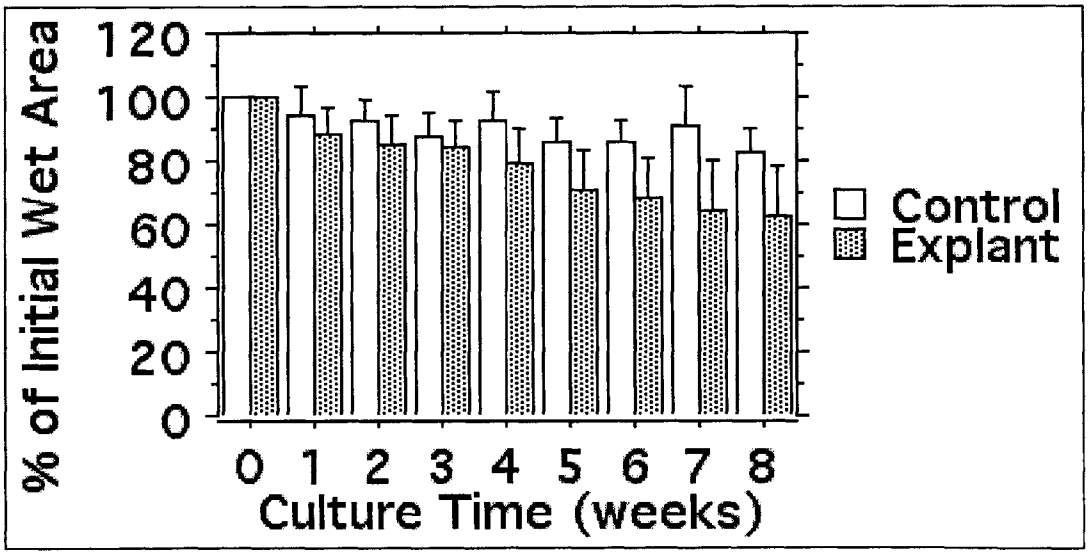

Figure 20. Contraction Profiles for Matrix Sandwiches Made from Half-Thickness Matrix

Error bars represent standard deviations. n = 5-23 per time point for controls, and n = 9-60 per time point for explant-matrix constructs. Time 0 represents the initial measurement after 1-3 hours of hydration in medium. The controls contracted significantly different from the matrix-explant constructs.

The matrix contracted 30-35% within 1-3 hours of hydration. Controls contracted an additional 20% while the matrix-explant constructs contracted by another 40% over time in culture (Figure 20). Culture time was a significant factor ($p < 0.0001$, ANOVA), and the explant

constructs contracted more than the controls ($p < 0.0001$, ANOVA). Figure 21 shows a matrix sandwich for which the bottom layer has contracted more than the top layer. An example of extreme cell-mediated contraction of the matrix sandwiches is displayed in Figure 22.

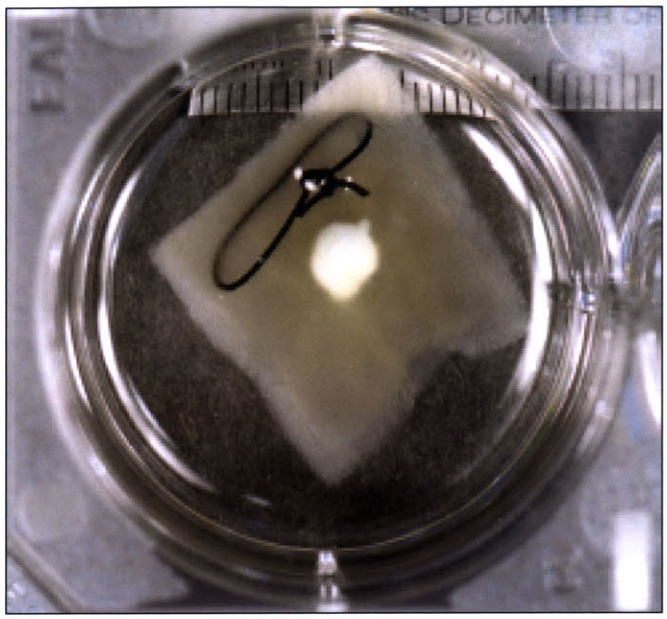

Figure 21. A Matrix Sandwich in Which the Bottom Layer Has Contracted More Than the Top Layer

This sample was in culture for 2 months. The well is 3.5 cm in diameter.

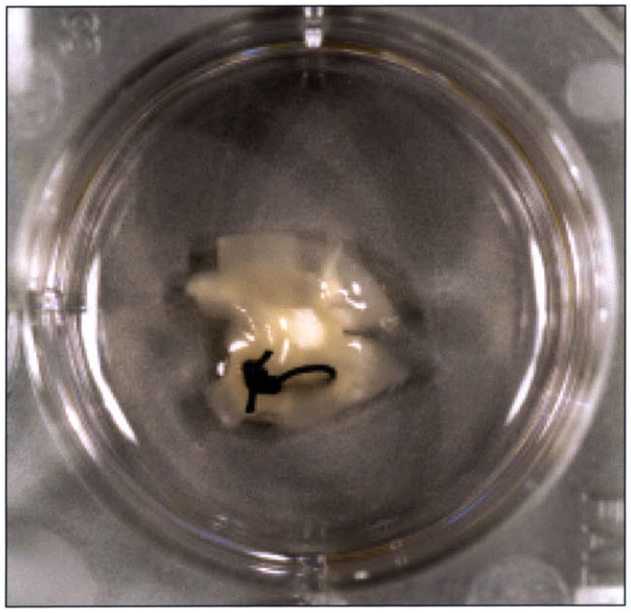

Figure 22. An Example of a Matrix Sandwich Displaying Extreme Cell-Mediated Contraction

The sandwich shown is after 6 weeks in culture. The well is 3.5 cm in diameter.

Discussion

Significant disc cell migration from explants of annulus occurred in 2-D and 3-D culture. This is the first report of cell migration from annulus tissue into CG matrices. The cells that grew out came from two possible sources: proliferation of cells on the surface of the explants and migration of cells near the surface out of the explant. Cells were able to migrate into an adjacent CG scaffold, and results were improved with the lower pore size matrices.

Significant differences in time to outgrowth and amount of outgrowth in 2-D culture and contraction in 3-D culture were found between the 10 and 20% FBS medium types. It should be noted that the FBS concentration was not a pure variable in this study. The medium types and additives were different to compare the standard IVD medium employed in the Brigham and Women's Orthopedic Research Laboratory to that developed by Gruber (80). Thus, the comparison is more appropriately called a comparison of two medium types, one of which has 10% FBS and another which has 20% FBS. However, to simplify the discussion, these will be termed the 10 and 20% FBS medium types.

The wet mass of the 2-D explants decreased with time. This may be the result of several processes: loss of glycosaminoglycan (GAG) in the explants or degradation of the extracellular matrix of the explant by the cells or culture environment. Although it may be an effect of *in vitro* culture alone, such a process may take place when an IVD is wounded. It is interesting that the average area of attachment was only 15 mm^2 while a 5 mm diameter has an area of 25 mm^2. This parameter was not measured until the explant had attached. It suggests that within those few days, the explants may have degraded substantially or that the change in shape of the explants (change in aspect ratio) affected the area significantly. The change in shape is likely caused by lamellae being oriented similarly in a curved direction. When the explant is removed from its normal architecture, the lamellae are no longer locked into a curved orientation. Often, it became apparent macroscopically that the lamellae straightened.

Cell outgrowth from the explants was affected by the FBS medium type. Explants in 20% FBS medium grew out on average 2 days earlier and had more outgrowth as culture time progressed. This suggests that certain regulators in the medium, most likely growth factors present in FBS, can influence cell proliferation. Such a finding may be advantageous for the tissue engineering of annulus fibrosus.

The multiple layers of cells that appeared on the outside of the explant have been observed in other studies. Within our own laboratory, the phenomenon (1-4 cells thick) was observed with human nucleus explants (93).

An unexpected finding was the difference in matrix contraction initially for the two medium types. The result suggests that matrix contraction is influenced by mediators in medium. Given that the most significant difference between the two medium types was the FBS concentration, perhaps a component of FBS is a major influence on medium-mediated contracted. For this reason, pre-wetting matrices in medium for use in explant constructs or cell-seeding studies is ill-advised. That the explant-matrix constructs contracted more initially than the controls is not unexpected. The explants were wet when placed on the dry matrices. During the adherence process the area of the matrix that became wet as a result adhered to the explant. Thus, a center area of the matrix already was fixed in a contracted state.

The effect of the medium type on matrix contraction was further established as culture progressed. Matrices in the 20% FBS medium type contracted more. This event was not caused by medium effect on cell proliferation or contractile ability alone because the controls in the two

medium types continued to be different over time. Cell-mediated contraction of the matrices was evident by the significant differences in cross-sectional area between the controls and the explant-matrix constructs over time. Most of the cell-mediated contraction for the explant-matrix constructs in the 10% FBS medium type occurred during the first week. Given the 2-D results, cells in the 20% FBS medium may have spent more metabolic energy proliferating instead of contracting the matrix. However, by 6-weeks, the amount of cell-mediated contraction between the two medium types was nearly the same. Thompson, et al. (219) have shown that the proliferative and biosynthetic potential of canine annulus explants is better in 20% FBS than other pure growth factors like platelet-derived growth factor, epidermal growth factor, fibroblast growth factor, and transforming growth factor β.

Interestingly, there appeared to be an effect of pore size on degree of initial contraction. The "double thickness," "skin protocol," and "1/2 thickness" matrix constructs contracted 10%, 21%, and 35%, respectively, upon initial hydration. This observation is clouded somewhat by the fact that the "skin protocol" matrices were not used as sandwiches, but overall, smaller pore matrices that were 16 hour UV cross-linked contracted more upon hydration. Some part of this could be due to more matrix becoming attached to the explant during the adherence phase.

The question finally arises as to which medium type is better. The 20% FBS medium produced more and faster proliferation but the matrices contracted more. 20% FBS medium, as some have suggested to be optimal for annulus cell culture (80), is then advocated for 2-D culture, especially passaging of annulus cells, in order to improve culture results. Although the results between the two medium types here may not directly apply to cell-seeded matrices, the fact the controls contracted more in 20% FBS medium is concerning. 20% FBS medium is then not advocated for matrix culture of annulus explants or cells because of the additional contraction of the matrix. Contraction of matrices to be implanted for tissue engineering is undesirable as an implant would pull away from and become smaller than the defect site. In the future, explant culture of the IVD could be employed to produce cells from human discectomy samples that could later be used to effect repairs via autologous chondrocyte replacement procedures or cell-seeded matrices for tissue engineering. In order to effect faster outgrowth of cells from these specimens, the following conditions could be used: higher concentrations of FBS in the medium as shown in this study, growth factors, or enzymatic treatment of the explants (185).

That annulus cells have the capability for proliferation and migration suggests that conditions might be found to favor these processes *in vivo* to enhance wound healing. The results also help to explain the ability, albeit limited, of annulus to form scar tissue over several months in that significant cellular migration was found over a two-month time period *in vitro*. This study is the first time IVD explants have been used in conjunction with CG matrices. The ability of cells to migrate into the CG matrix commends its use an a scaffold for tissue regeneration of the annulus. If an annular gap is bridged with a matrix scaffold, annulus cells have the capability to migrate into it for up to 1 cm.

Acknowledgements

This study was supported by the Brigham Orthopedic Foundation, the Harvard Center for Engineering in Medicine Bioengineering Discovery Fund, the North American Spine Society, and the Harvard/MIT Training Program in Biomaterials (1 T32-DEO7311) (DH). The authors

gratefully acknowledge use of the facilities of the Fibers and Polymers Laboratory at MIT under the supervision of Professor Yannas for the fabrication of the collagen-GAG matrices. Dr. Ray Connelly of the New England Medical Center Surgical Research Center and Dr. Contrares at the Harvard Institutes of Medicine are also thanked for providing the canine specimens. Integra Life Sciences supplied the type I collagen.

Experiment 3: Intervertebral Disc Explants and Explant-Matrix Constructs Cultured in a Bioreactor

Introduction

The intervertebral disc (IVD) is known to change during spaceflight. To study this tissue under simulated microgravity, canine lumbar intervertebral disc annulus explants were cultured in a bioreactor designed for such purposes. For the first time, a collagen-glycosaminoglycan (CG) matrix was employed to surround the explants in order to prevent migration of cells out of the explant and to explore tissue engineering in this scaffold.

The primary purpose of culturing matrix sandwiches in bioreactors was to determine the effect of simulated microgravity on IVD annulus fibrosus tissue. It was felt necessary to enclose tissue explants in matrix to prevent permanent cell migration from the explant, as has been seen by other researchers (95, 154). An additional outcome of this study was a trial of how the CG matrix would perform in an environment with a higher flow rate, an approximation of the more rigorous demands of the *in vivo* state. Explants, explants enclosed in matrix sandwiches, and empty matrix controls were cultured in bioreactors for up to 6 weeks. Equivalent specimens were cultured simultaneously under static conditions.

Bioreactors

Annulus tissue receives nutrients through direct diffusion and fluid flow from the interstitial fluid (193). Stationary culture does not approximate the mass transport conditions present *in vivo*. One culturing system that can simulate enhanced mass transport while exerting minimal shear forces is the bioreactor. The effects of the bioreactor culturing environment on intervertebral disc explants were explored in the present research. The primary purpose of culturing explants in a bioreactor was to determine the effect of simulated microgravity on disc tissue. It was expected that the increased mass transfer would cause enhanced tissue growth within the matrices. This would be a significant enhancement in the development of a implant for IVD annulus defects.

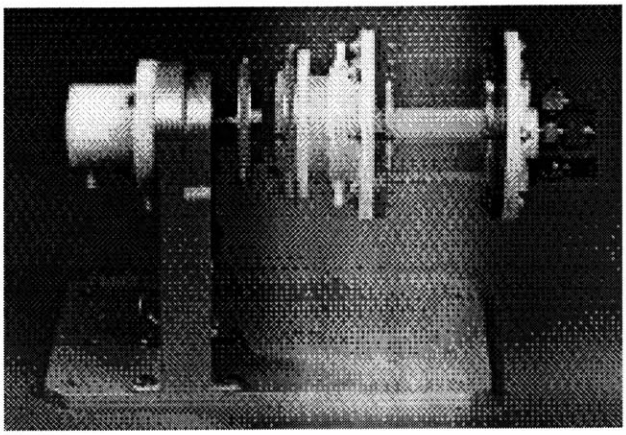

Figure 23. NASA-Designed Synthecon Bioreactor

(NASA) (3)

Rotating-wall bioreactors (Figure 23), which randomize the gravity vector, have been investigated by other researchers as culture environments for simulating microgravity (37, 47, 56, 62, 76, 211) and tissue engineering. Spaceflight data has

revealed the similarity of the system to microgravity conditions (62, 178). Bioreactors have the unique property of allowing for suspension of cultured substrates while reducing the shear stress applied, and they have demonstrated success in the culture of explants (47, 95, 124, 154) and matrix/gel constructs (65, 66, 154). One study (154) of bioreactor-cultured explants from another tissue revealed that explant cells were lost to the medium, a finding verified by other researchers (95), but some returned to the explant. This migration into the medium was inhibited by enclosing the explants in a collagen or agarose gel. The collagen gel significantly inhibited and the agarose gel completely prevented cell migration from the explant. Since certain normal *in vivo* states have conditions similar to bioreactor culture (i.e., higher fluid flow), several researchers have only been able to duplicate conditions in the body by using bioreactors (8, 17, 34, 47, 75, 77, 105, 111, 112, 124, 141, 154, 173). The bioreactors increase cell-matrix interactions. Still other investigators (13, 45) have found that bioreactor culture of chondrocytes with and without matrix scaffolds may provide biologic materials for implantation into cartilage defects. One researcher (65, 66) determined that the increased mass transport rates of gases and nutrients that are provided by a rotating-wall vessel enhance the proliferation and biosynthesis rates of cell-matrix constructs by more than 50% as compared to static culture. In terms of tissue generation, the bioreactor system has been shown to produce the greatest growth compared to other increased mass transport devices such as spinner flasks (64). Chondrocyte-matrix constructs were even cultured in bioreactors on Mir (65). It was found that, compared to earth-based bioreactor culture, the Mir bioreactor constructs were more spherical, smaller, and mechanically inferior.

Another reason to investigate the growth of explant-matrix constructs in bioreactors is in preparation for a spaceflight experiment. Neither IVD cells or explants of any tissue have ever been flown in space. Culturing an explant instead of just cells alone may be a preferred model to determine the influence of altered environments on a tissue. Explants allow for communication between cells and for the extracellular matrix to be used as a possible cellular metabolite. Moreover, a matrix scaffold may be necessary for effective culture of an explant so it has some potential for three-dimensional growth and to prevent cell migration into the medium.

Methods

Experimental Plan

Explants and explant-matrix constructs from three canines each (n = 75 5 mm diameter explants per canine), as well as matrix controls, were cultured in a Synthecon bioreactor (Cylindrical Rotary Cell Culture Systems, 250 mL; Synthecon, Inc.) and under static conditions. Time points of sacrifice were 0, 2, 4, and 6 weeks. Sacrificed explants and constructs were evaluated by mass and volume measurements, by histology, and for glycosaminoglycan (GAG) and DNA content. Bioreactor medium was sampled to determine the number of cells in the medium.

Type I CG Matrix

The type I collagen-glycosaminoglycan (CG) matrix was produced by freeze-drying a coprecipitate of type I collagen from bovine tendon and chondroitin 6-sulfate from shark cartilage. The procedure is outlined in Experiment 1 and Appendix A. For this experiment, "skin protocol" matrix was manufactured (matrices 1, 3, 4, 6-8, 42, and 44 for explant constructs and matrix 43 for controls from Appendix K). The matrices were dehydrothermally treated in a vacuum oven for 24 hours (in an autoclave bag) and additionally cross-linked by ultraviolet radiation for 16 hours[5]. For the latter, the matrix was placed on foil 30 cm from a UV source (Philips Sterilamp #G10T5 1/2 L, λ = 253.5 nm), which is rated at 5.3 W for total output and 55.5 W/cm^2 at 1 m. Matrix sheets were turned over halfway through the UV cross-linking time to expose each side to the same amount of radiation. This matrix had a GAG content of 7.9 ± 1.2% mass, thickness of 3.6 ± 0.7 mm, pore diameter of 271 ± 35 μm, pore aspect ratio of 1.3 ± 0.3, porosity of 91 ± 3, and compressive stiffness of 298 ± 29 Pa (see Experiment 1). 9 mm-diameter discs were punched from the matrix sheets with a dermal punch (Barron Vacuum Trephine, 9 mm, #K20-2062, Katena Products, Inc.).

Tissue Acquisition, Formation of Explants, and Specimen Preparation

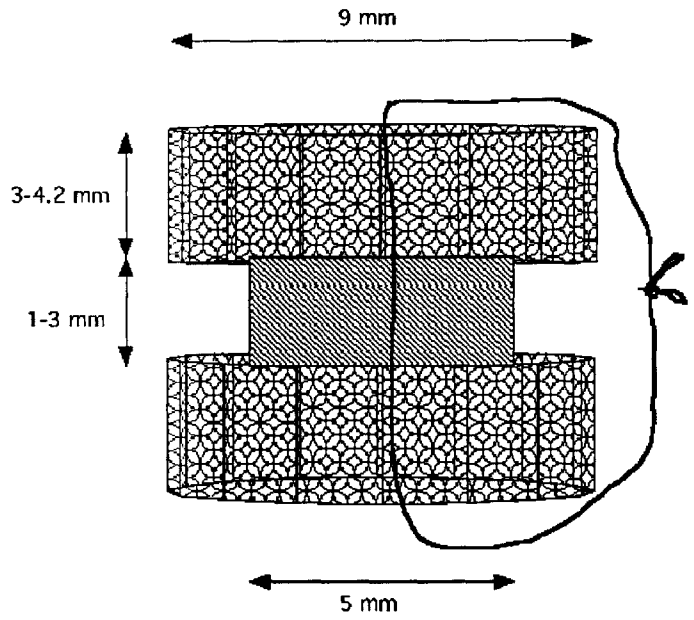

Figure 24. Explant-Matrix Construct Used in the Bioreactor Experiment

The explant is in the middle and is surrounded by two 9-mm diameter matrix discs. These are all sutured together.

The lumbar spine from L2 to L7 was sterilely resected from 6 canines (2-7 years old) (Appendix L) 1.2 ± 0.6 hours after sacrifice. Each spine was placed in phosphate buffered saline (Dulbecco's PBS; #14190-136, Life Technologies) supplemented with 2% penicillin (100

U/mL)/streptomycin (#15070-063; Life Technologies, Inc.) and 1% fungizone (2.5 mg/mL, #15295-017, Life Technologies) at 4° C until dissection. Generally dissection began within 2 hours of resection of the spine. The IVDs were dissected from the spines (Figure 12). The ligaments and nucleus pulposi were removed from each IVD. The IVDs were then bisected along their thickness to make thinner explants, generally 2-3 mm thick. A 5 mm-diameter dermal punch (Keyes #33-25) and hammer were used to cut 75 explants for each canine.

Explants from three of the canines were cultured in the bioreactor and static culture freely. Explants from the other three canines were formed into matrix constructs and cultured in those environments. The explants formed into matrix constructs were placed between two 9 mm CG discs. A suture (Perma-Hand Silk Suture, straight needle, taper point, ST-1, black braided, 3-0; #K852H, Owens & Minor) was used to hold the construct together (Figure 24). The suture was not bound tightly as this created bunching of the matrices on the knot side. Control constructs consisted of two matrix disc sutured together. Matrix constructs were allowed to adhere for 10-15 min. before being placed in any medium.

Cell Culture

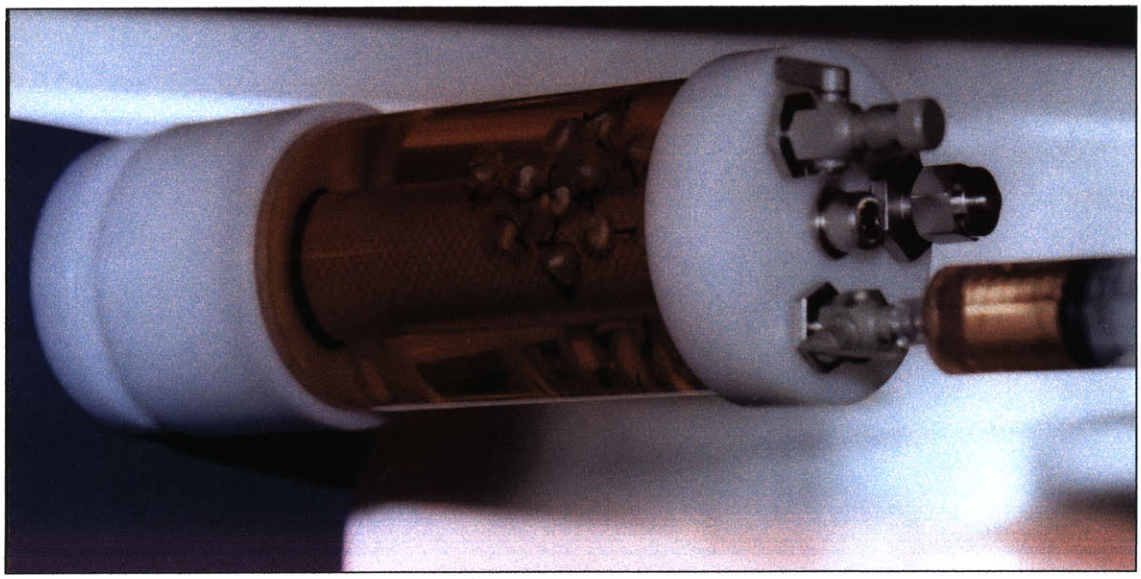

Figure 25. Synthecon Bioreactor with Explant-Matrix Constructs Inside.

The bioreactor is at a very low rotation rate in the picture to allow for photography, thus explaining the fact that some constructs are not suspended.

Nine specimens from each canine were sacrificed immediately, that is, after formation of the constructs or after cutting the explants. Explants were placed in culture on average 6.9 ± 1.3 hours after canine sacrifice. In the bioreactor (Figure 25) and static culture each initially, 33 specimens were placed for each canine or control matrix-construct. Static specimens were cultured in 6-well plates (Falcon #08-772-1B, Fisher Scientific Co.) where each well was coated with 2 mL of 4% agarose (m/v; Seaplaque agarose; #50100, FMC BioProducts) (Appendix R). Explant-matrix constructs in static culture were maintained on their sides at all times to prevent gravity from causing more cells to migrate into one matrix disc more than the other. Static and

bioreactor culture took place in an incubator at 37° C in an atmosphere of 5% CO_2 and 95% humidity.

As this was a explant-matrix construct experiment, a 10% FBS medium was employed based on the results of Experiment 2. The culture medium consisted of Dulbecco's modified eagle medium/nutrient mixture-F12 (#11320-033; Life Technologies, Inc.) supplemented with 2% penicillin/streptomycin, 1% fungizone, 0.025 g/L of L-ascorbic acid phosphate (magnesium salt n-hydrate; #D13-12061, Wako Chemicals USA, Inc.), 10% FBS (Austrailian Fetal Bovine Serum, #SH30084.03, Hyclone Laboratories, Inc.), and 1% L-glutamine (#25030-081, Life Technologies, Inc.) (Appendix M). (All percentages are by volume.)

The Synthecon bioreactor held 250 mL of medium. Half of the medium was replaced every other day (Appendix S). On most days 5 mL of medium was first removed and a hemocytometer cell count (Appendix U) was taken to determine how many cells were present in the medium (scaled up to 250 mL based on 5 mL count). On sacrifice days, all 250 mL of medium was removed. Culture, sampling, and medium change procedures were those described by other researchers (183, 203). Bioreactor specimens were maintained in the settling regime described by Freed and Vunjak-Novakovic (63). The rotation speed of the bioreactor was altered such that a majority of the constructs appeared to be suspended in the medium.

In static culture, enough medium was added to reach the top of the explant (4-5 mL initially and 3 mL thereafter) or explant-matrix construct (6 mL initially and 5 mL thereafter). Medium was changed every 2 days (Appendix N). The well plates were changed every 2 weeks because of breakdown of the agarose.

Mass and Dimensional Measurements at Sacrifice

In static and bioreactor culture each, nine explants or explant-matrix constructs were sacrificed at 2 and 4 weeks. Ten to fifteen each were sacrificed for both culture environments at 6 weeks. At sacrifice, they were washed 3 X 10 min. in sterile PBS. 2-3 in every group were allocated for histology. The others were used for quantitative measurements. For these that were constructs, the explant was separated from the matrix discs with a scalpel.

The dimensional measurements of the explants were taken with an analog micrometer (Mitutoyo #505-633-50). The thickness was measured as well as both diameters of the areal cross-section. The matrices were measured hydrated in PBS in 6-well plates coated with agarose. A diameter template was placed under the well plate to measure the diameter. If the two orthogonal diameters appeared greater than 10% different, both diameters were measured. The thickness was measured with an analog micrometer. The volume was calculated from the thickness and cross-sectional areas (from the diameters). The aspect ratio was calculated from the diameters.

The explants and matrices were then placed on filter paper to remove standing water. They were weighed (wet mass) and frozen at -20° C. The explants and matrices were lyophilized in a freeze dryer (Labconco 4.5) (Appendix T) to remove water. They were then weighed again (dry mass). The percent hydration was then calculated by

$$\%\ \text{hydration} = \left(1 - \frac{\text{dry mass}}{\text{wet mass}}\right) x100\%. \qquad \text{Equation 3}$$

The explants and matrices were digested in papain (Sigma #P3125; Appendix E) prior to biochemical analysis.

Biochemical Analyses

After digestion in papain, an aliquot of the sample solution in a 2 mL Hoechst dye 3328 (Polyscience Inc.)/buffer solution was measured by a fluorometer (model TKO 100, λ_{ex}=365 nm, λ_{em}=460 nm, Hoefer Scientific Instruments, San Francisco, CA) (Appendix V). The DNA content was extrapolated from a standard curve of calf thymus DNA (Sigma #D3664). The mean DNA content of the control matrices for both culture environments at each time point was subtracted from the DNA content of the matrices containing cells at the corresponding time points and culture environments. This was then divided by the explant or matrix mass because of changing dry masses in this experiment. In addition, a separate analysis was performed to compare constructs to free explants. In this case, the DNA of the two matrices (normalized by control matrix DNA) surrounding the explant was added to the explant's DNA to result in a total DNA quantity.

GAG content of the digested explants and matrices was assessed by a modification of the dimethyl-methylene blue method (57). Absorbance at 535 nm was determined with a spectrophotometer (LKB Biochrom Ultraspec 4050, Pharmacia, Piscataway, NJ) (Appendix F). The amount of GAG was extrapolated from a standard curve for shark chondroitin sulfate (C-4384, Sigma) in distilled water. The GAG content was expressed as a percentage of the dry mass because of changing dry masses in this experiment.

Histology

Explant-matrix constructs were not separated for histology. After sacrifice, constructs and explants were placed in 10% neutral buffered formalin (10% buffered formalin phosphate SF100-20, Fisher Scientific Co.) for at least 2 days. Specimens were manually dehydrated (Appendix O), bisected through the explant, and half embedded in paraffin and half in glycol methacrylate resin (JB-4 embedding system, Polysciences, Inc., Warrington, PA; Appendix P). 5 μm microtomed JB-4 sections were stained with H & E (Appendix Q). The following parameters were assessed under light microscopy (Olympus Vanox-T): cell morphology (round or elongated), cell location, and cell proliferation. Outgrowth from the explants was reflected in the increased number of cells surrounding the explant and the increasing distance to which the cells had migrated into the matrix. Cell layers were also noted for the free explants.

Statistics

For the explants and matrices, multi- and single variable ANOVA were used to assess the effects of sacrifice time, culture environment, canine, and whether the explant was part of a matrix-explant construct or not on dry mass, % hydration, aspect ratio, volume, % mass of DNA, change in % mass of DNA, and % mass of GAG. Bonferroni-Dunn post-hoc tests were utilized for selected analyses. Linear regression was used to assess correlations between volume and masses and percent hydration and % mass GAG. Student's t-test was used to compare cells in the bioreactor medium. Multi-variable ANOVA was utilized to determine how culture time, whether the explant was part of a construct, and culture environment affected the total DNA.

Results

Free Explants

Bioreactor Culture

In the bioreactor, 4.1 ± 3.6 x 10^6 cells (average ± standard deviation) were present in the medium at each medium change. The value did not appear to depend on time in culture. The average rotation speed needed in the bioreactor for suspension of the explants was 31.9 ± 2.3 rpm. Aggregated cells were sometimes visible growing in the medium and on the inside ends of the bioreactor. Explants from 2 of the 3 canines stuck together in the bioreactor after 7-10 days. They were separated at each sacrifice time.

Dry Mass

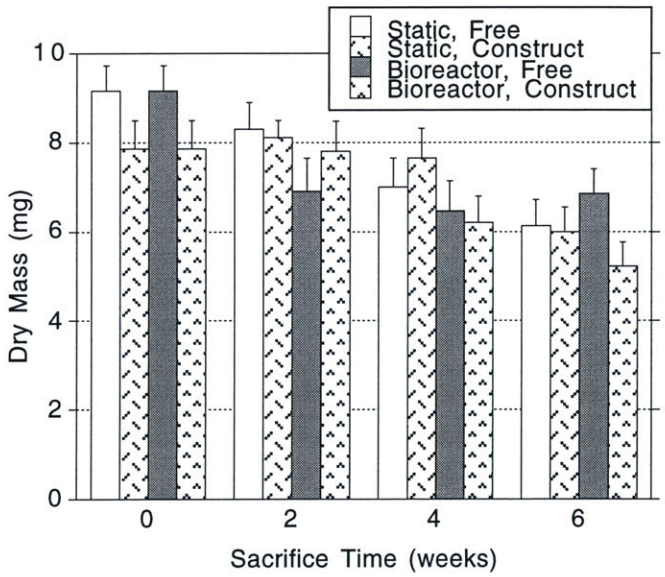

Figure 26. Dry Mass vs. Sacrifice Time for the Explants

Error bars represent standard errors. n = 16-35 for each group per time point. Free and construct in the legend refer to whether the explant was part of a matrix-explant construct or not. Time in culture significantly affected the dry mass but culture environment and whether the explant was part of a matrix-explant construct did not.

The dry mass of the explants decreased significantly with time in culture from 8.6 ± 2.9 mg initially to 6.1 ± 3.3 mg after 6 weeks ($p < 0.0001$; ANOVA) (Figure 26). Culture environment and whether the explant was part of an explant-matrix construct or not did not influence the decrease in dry mass over time in culture ($p > 0.20$; ANOVA). However, the initial dry mass for construct explants was significantly less than that of the free explants ($p = 0.032$;

ANOVA). This was likely due to an initial significant difference among the tissue from the different canines ($p = 0.012$; ANOVA).

Percent Hydration

The percent hydration of the explants changed significantly with time in culture ($p < 0.0001$; ANOVA) (Figure 27). In general, this parameter decreased with time in culture, except for the explants in constructs in the bioreactor. In fact, the average percent hydration for the construct explants in the bioreactor was higher than baseline at 2 and 4 weeks. Explants in bioreactor culture in general had a higher percent hydration ($p = 0.0019$; ANOVA). Construct explants also had a higher percent hydration ($p = 0.0153$; ANOVA).

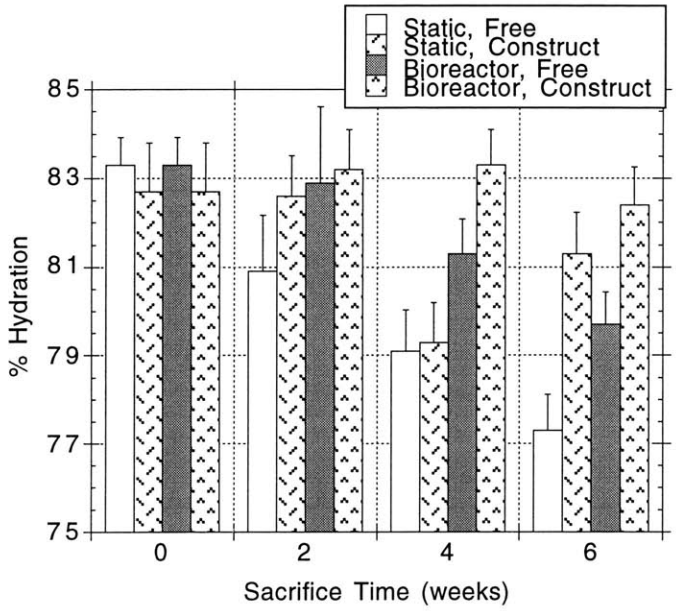

Figure 27. Percent Hydration vs. Sacrifice Time for the Explants

Error bars represent standard errors. n = 16-35 for each group per time point. Percent hydration was calculated from the wet and dry masses. Free and construct in the legend refer to whether the explant was part of a matrix-explant construct or not. Time in culture, culture environment, and whether the explant was part of a construct significantly affected the percent hydration.

Aspect Ratio

The aspect ratio of the explants increased significantly with time in culture from 1.12 ± 0.08 initially to 1.27 ± 0.22 after 6 weeks ($p < 0.0001$; ANOVA) (Figure 28). Culture environment significantly influenced the change in aspect ratio ($p = 0.0044$; ANOVA) with explants in static culture having greater aspect ratios at 4 and 6 weeks. Whether the explant was part of an explant-matrix construct or not did not significantly influence the increase in aspect ratio over time in culture ($p > 0.06$; ANOVA). Note, as seen in Figure 28, the aspect ratio was not 1 initially even though round explants were punched.

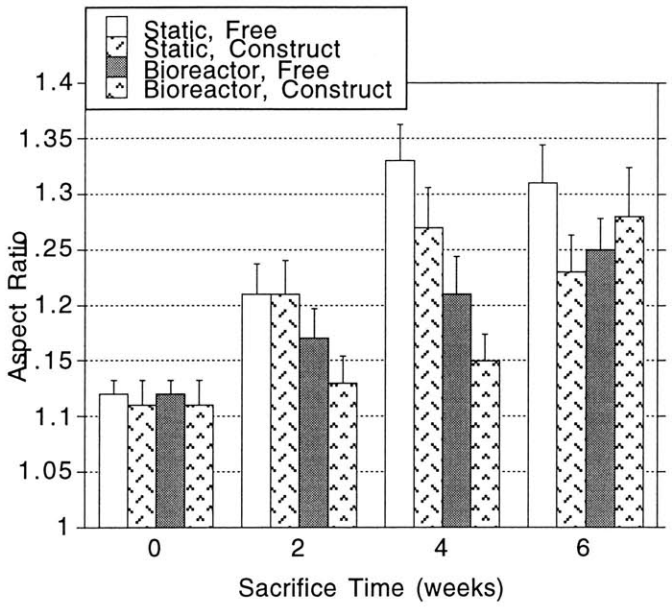

Figure 28. Aspect Ratio vs. Sacrifice Time for the Explants

Error bars represent standard errors. n = 19-45 for each group per time point. Aspect ratio was calculated from the orthogonal diameters of the explants. Free and construct in the legend refer to whether the explant was part of a matrix-explant construct or not. Time in culture and culture environment significantly affected the aspect ratio but whether the explant was part of a matrix-explant construct did not.

Volume

The volume of the explants decreased significantly with time in culture from 55 ± 14 mm^3 initially to 35 ± 16 mm^3 after 6 weeks ($p < 0.0001$; ANOVA) (Figure 29). Culture environment did not significantly influence volume ($p = 0.69$; ANOVA). Whether the explant was part of an explant-matrix construct or not in general did not significantly influence the decrease in volume over time in culture with the exceptions of: construct explants having a greater volume at 2 weeks ($p = 0.04$; ANOVA), construct explants in static culture have a greater volume at 4 weeks ($p = 0.0499$; ANOVA), and free explants having a greater volume in the bioreactor at 6 weeks ($p = 0.038$; ANOVA). Volume was correlated with dry mass ($R^2 = 0.54$; linear regression) and wet mass ($R^2 = 0.83$; linear regression).

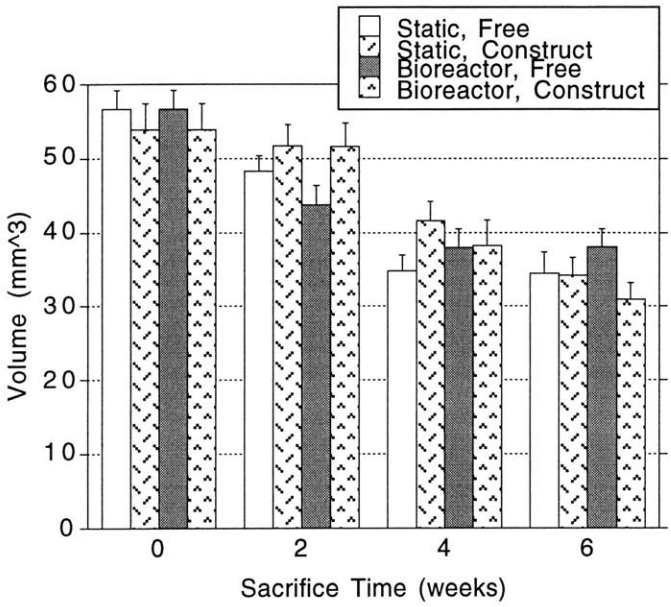

Figure 29. Volume vs. Sacrifice Time for the Explants

Error bars represent standard errors. n = 19-45 for each group per time point. Free and construct in the legend refer to whether the explant was part of a matrix-explant construct or not. Volume significantly decreased with time in culture. Culture environment significantly affected the volume in only a few cases but whether the explant was part of a matrix-explant construct did not.

DNA

DNA analysis was performed based on the percentage of dry mass of DNA due to the changing dry masses of the explants over time. The % mass of DNA was significantly different with time in culture ($p < 0.0001$; ANOVA), culture environment ($p = 0.002$; ANOVA), and whether the explant was part of a construct or not ($p = 0.006$; ANOVA) (Figure 30). In all cases, the % mass of DNA increased during culture time. Explants in the bioreactor environment had higher values for this parameter. Unexpectedly, explants that were part of a construct had less DNA as a percentage of the dry mass. This could be explained by the fact that the original samples for the construct and non-construct explants were significantly different for this parameter ($p = 0.01$; Student's t-test) as the tissue came from different sets of canines.

Thus, an additional analysis was performed for which the average percentage of mass that was DNA at time = 0 for the construct and non-construct explants was subtracted from values for the latter time points in order to determine changes in the % of dry mass that was DNA. This analysis yielded dramatically different results (Figure 31). Time in culture ($p < 0.0001$; ANOVA) and culture environment ($p < 0.0023$; ANOVA) still significantly affected the parameter in the manner stated above; however whether the explant was part of construct or not was no longer a significant factor. It becomes clear from Figure 31 that there was a large increase in the percent mass that was DNA from t = 0 to 2 weeks, and this parameter decreased thereafter for construct explants.

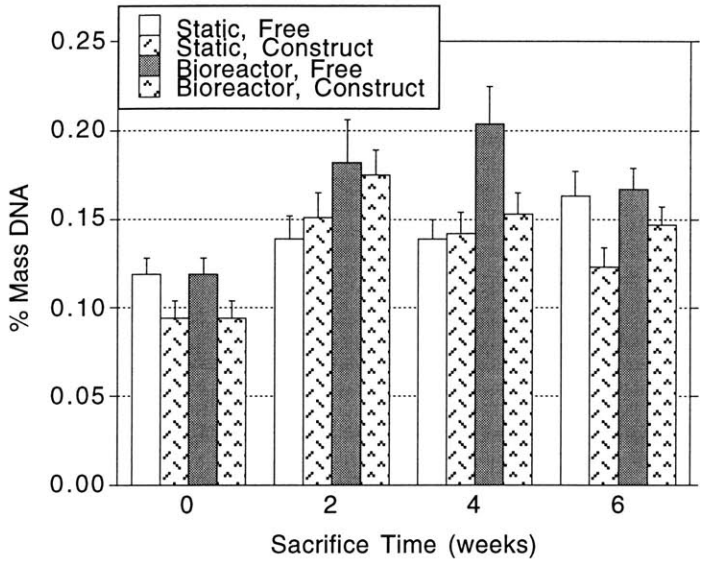

Figure 30. Percent of Dry Mass that is DNA vs. Sacrifice Time for the Explants

Error bars represent standard errors. n = 16-35 for each group per time point. Free and construct in the legend refer to whether the explant was part of a matrix-explant construct or not. This parameter was significantly affected by time in culture, culture environment, and whether the explant was part of a matrix-explant construct or not ($p \leq 0.006$).

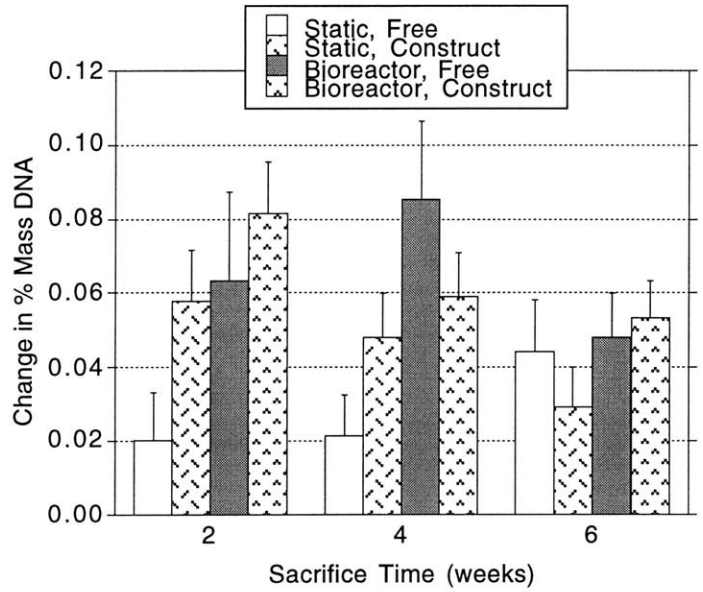

Figure 31. Change in Percent of Dry Mass that is DNA vs. Sacrifice Time for the Explants

Error bars represent standard errors. n = 16-35 for each group per time point. The change in percent of mass that was DNA was relative to time = 0. Free and construct in the legend refer to whether the explant was part of a matrix-explant construct or not. Results are presented as change from average t = 0 values for each group. This parameter was significantly affected by time in culture and culture environment but not whether the explant was part of a matrix-explant construct.

GAG

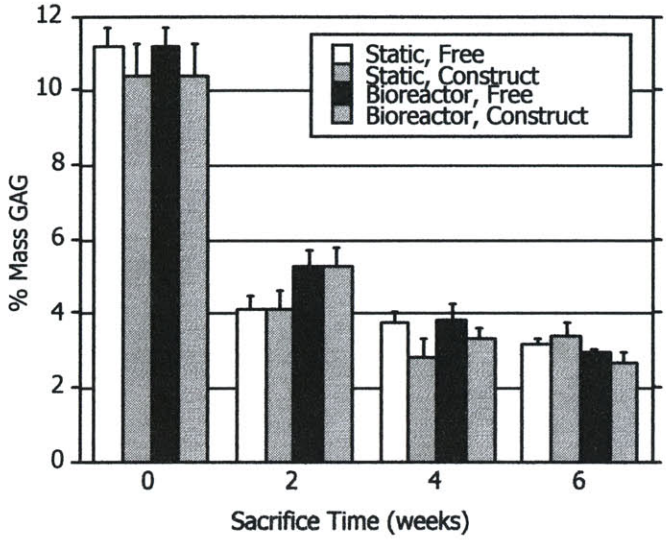

Figure 32. Percent of Dry Mass that is GAG vs. Sacrifice Time for the Explants

Error bars represent standard errors. n = 16-35 for each group per time point. Free and construct in the legend refer to whether the explant was part of a matrix-explant construct or not. This parameter was generally significantly affected only by time in culture ($p < 0.0001$).

GAG analysis was performed based on the percentage of dry mass of GAG due the changing dry masses of the explants over time. The % mass of GAG was significantly different with time in culture ($p < 0.0001$; ANOVA). Culture environment only affected the parameter at 2 weeks with explants in the bioreactor retaining more GAG at this time point ($p = 0.0124$; ANOVA). Whether the explant was part of a construct or not did not affect the % mass of GAG ($p = 0.09$; ANOVA) (Figure 32). In all cases, the % mass of GAG decreased during culture time. The percent hydration of the explants did not appear to be correlated to the % mass of GAG.

Matrix Constructs

At 6 weeks, it was sometimes difficult to cleanly separate the matrices from the explants. This is shown in Figure 33 where it is difficult to distinguish the edges of the matrix. The explant is the whiter material in the middle.

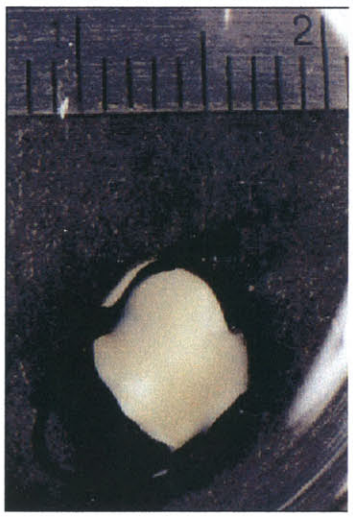

Figure 33. Explant-Matrix Construct from Static Culture After 6 Weeks

Bioreactor Culture

In the bioreactor, $1.5 \pm 1.8 \times 10^6$ cells (average ± standard deviation) were present in the medium at each medium change.

The value did appear to increase with time in culture. The average rotation speed needed in the bioreactor for suspension of the explants was 19.0 ± 1.4 rpm. By 4 weeks, the constructs stuck together in the bioreactor. They were separated at the sacrifice times. In general, the matrices were severely degraded in the bioreactor at 6 weeks. In some cases, the matrices for a specific explant were entirely gone.

Dry Mass

The dry mass of the matrices decreased significantly with time in culture from 3.2 ± 0.5 mg at time 0 to 1.7 ± 0.7 mg at 6 weeks ($p < 0.0001$; ANOVA) (Figure 34). Culture environment and whether the matrix was part of a construct only affected the dry mass at the 6 week time point, with construct matrices in the bioreactor having the least mass. The explant construct matrices in the bioreactor had significantly less mass than the control matrices in the bioreactor ($p = 0.0036$; ANOVA) and the explant constructs in static culture ($p < 0.0001$; ANOVA).

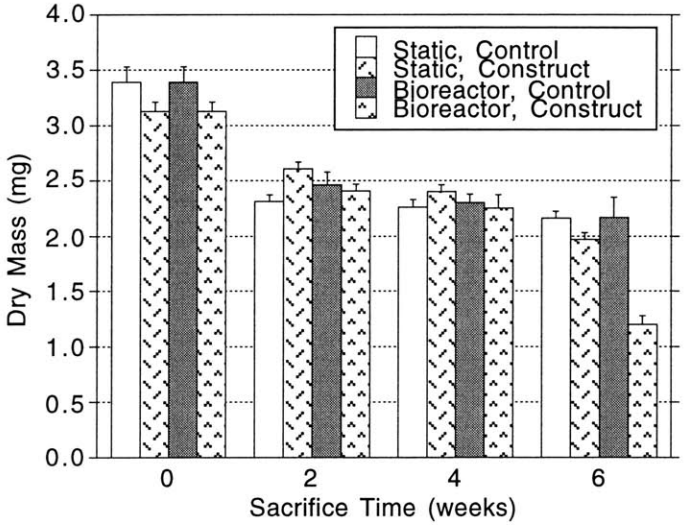

Figure 34. Dry Mass vs. Sacrifice Time for the Matrices

Error bars represent standard errors. n = 4-22 and n = 37-71 for each control and construct group, respectively, per time point. Control and construct in the legend refer to whether or not an explant was attached to the matrix. Time in culture significantly affected the dry mass but culture environment and whether an explant was attached generally did not.

Volume

Matrix volume for those attached to explants decreased from 213 mm^3 at t = 0 to 29 mm^3 at 6 weeks, with values on average being less for bioreactor samples. Control matrix volume changed from 268 mm^3 at t = 0 to 95 mm^3 at 6 weeks. Clearly time in culture affected volume ($p < 0.0001$; ANOVA) (Figure 35). Culture environment was only a significant influence at 4 and 6 weeks for the explant constructs ($p < 0.0001$; ANOVA) and at 6 weeks for the controls ($p = 0.0182$; ANOVA). For these cases, explant construct matrices had less volume in the bioreactor;

however, at 6 weeks the controls had a higher volume in the bioreactor. Whether an explant was attached to the matrix significantly affected the volume, with explant construct matrices having decreased volume in general ($p < 0.0001$; ANOVA). Even initially this was true. Volume was correlated with dry mass ($R^2 = 0.55$; linear regression) and wet mass ($R^2 = 0.745$; linear regression).

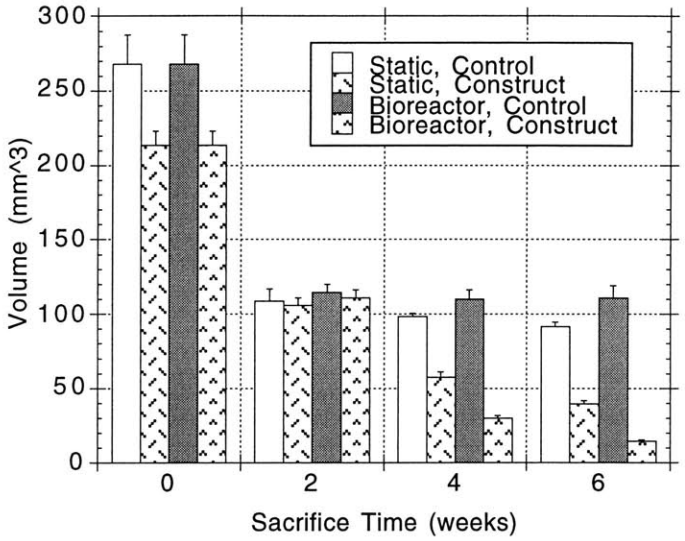

Figure 35. Volume vs. Sacrifice Time for the Matrices

Error bars represent standard errors. n = 4-22 and n = 38-68 for each control and construct group, respectively, per time point. Control and construct in the legend refer to whether or not an explant was attached to the matrix. Volume significantly decreased with time in culture. Culture environment significantly affected the volume in only a few cases and explant construct matrices in general had less volume.

DNA

DNA analysis was performed based on the percentage of dry mass of DNA due to the changing dry masses of the matrices over time. In addition, this value for control matrices was subtracted from the values for the construct matrices to assess explant/cell-associated changes. This normalized % mass of DNA was significantly different with time in culture ($p < 0.0001$; ANOVA) and culture environment ($p < 0.0001$; ANOVA) (Figure 36). In all cases, the normalized % mass of DNA increased during culture time. Matrices in the bioreactor environment had higher values for this parameter.

GAG

GAG analysis was performed based on the percentage of dry mass of GAG due the changing dry masses of the matrix over time. This parameter could not be normalized for the

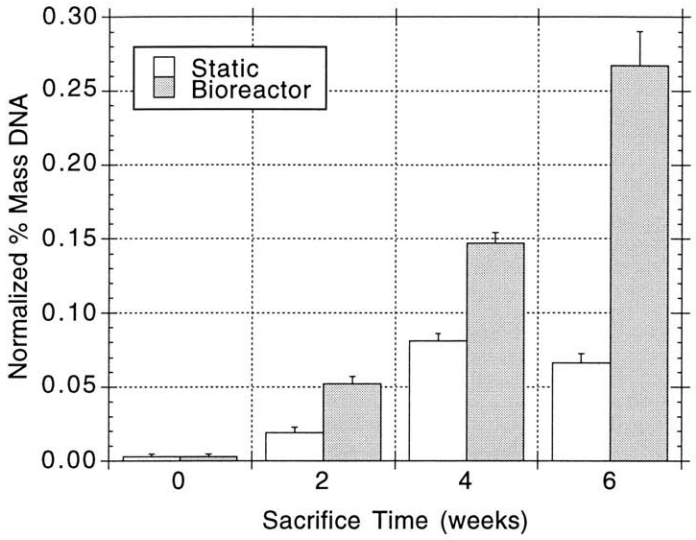

Figure 36. Normalized Percent of Dry Mass That is DNA vs. Sacrifice Time for the Explant Construct Matrices

Error bars represent standard errors. n = 42-70 for each group per time point. The percent of dry mass that was DNA for the controls was subtracted from that of the construct matrices to achieve the normalization in this plot. DNA content of the explant constructs significantly increased with time in culture and more so for matrices in the bioreactor.

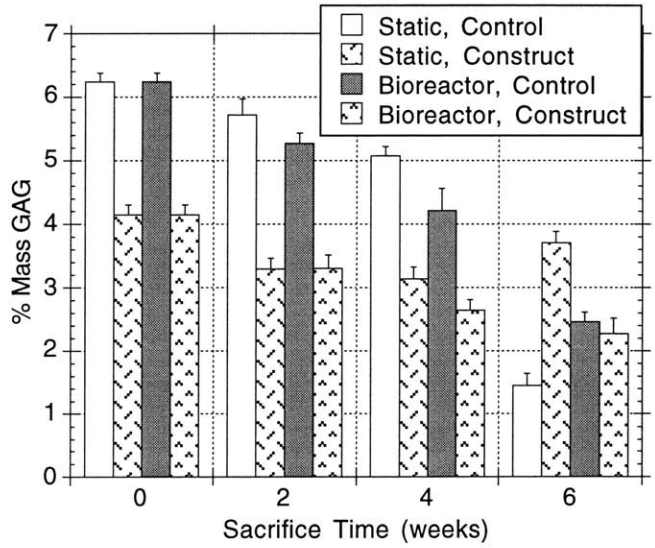

Figure 37. Percent of Dry Mass That is GAG vs. Sacrifice Time for the Matrices

Error bars represent standard errors. n = 4-22 and n = 37-69 for each control and construct group, respectively, per time point. Control and construct in the legend refer to whether or not an explant was attached to the matrix. GAG content significantly decreased with time in culture.

amount of GAG in the controls because the GAG in the control matrices was higher initially. It should be noted that the GAG in the control matrices decreased with time in culture ($p < 0.0001$; ANOVA) but was not significantly dependent on culture environment. The % mass of GAG of the explant construct matrices was significantly different with time in culture ($p < 0.0001$; ANOVA) and culture environment ($p = 0.0009$; ANOVA) (Figure 37). In all cases, the % mass of GAG decreased during culture time; however static culture matrices a had higher values compared to bioreactor-cultured matrices as culture time increased.

Histology

Figure 38 displays a micrograph of an explant-matrix construct from the bioreactor after 6 weeks (Appendix P). A significant amount of new matrix was produced by the specimens in the bioreactor.

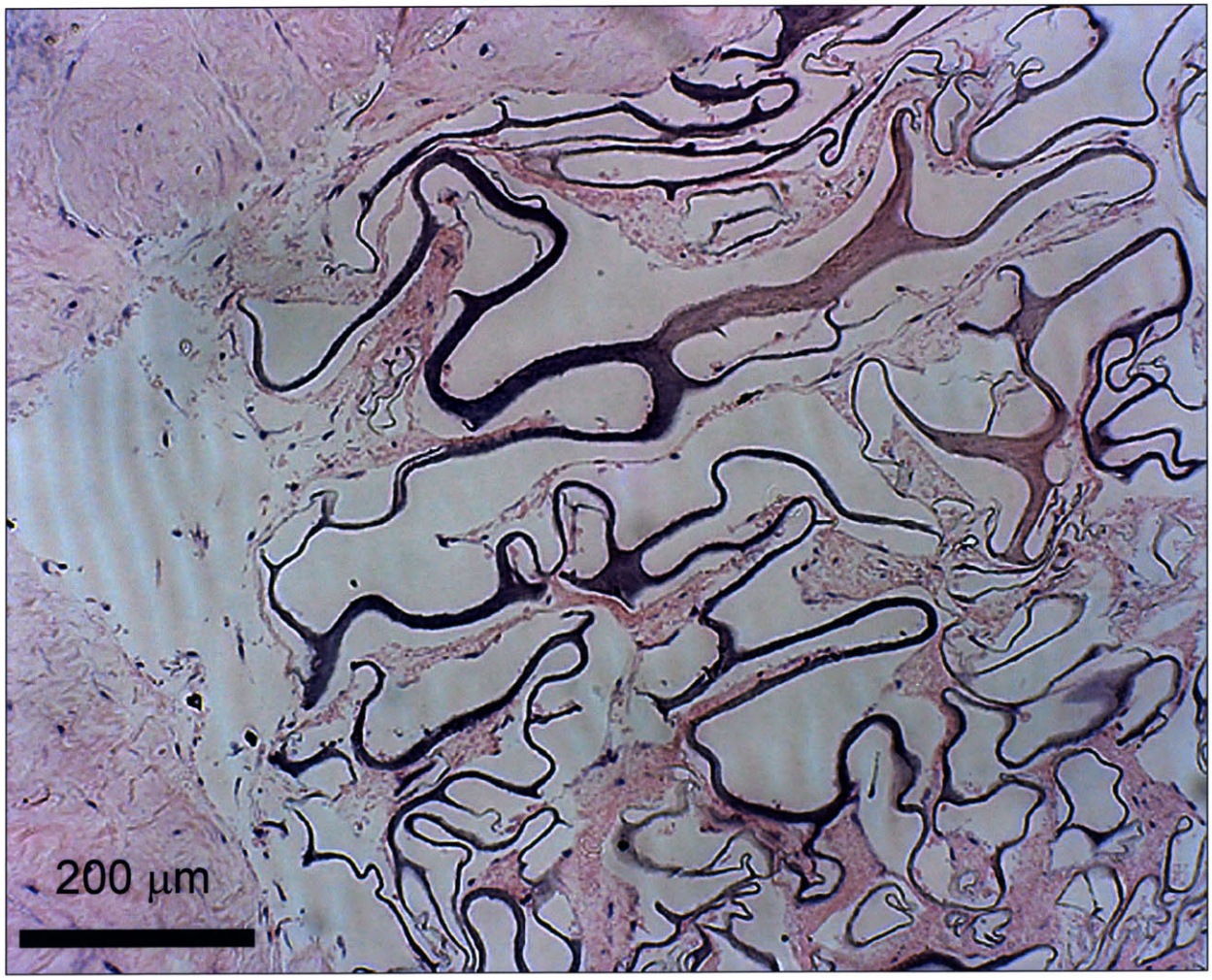

Figure 38. Explant Matrix Construct from the Bioreactor at 6 Weeks

The left corners show the explant. The bluer structure on the right is original matrix. The intervening tissue is newly formed matrix by the cells that have migrated out of the explant.

Comparison Between Free and Construct Results

Significantly more cells were in the bioreactor medium when the explants were free ($p < 0.0001$; Student's t-test).

Figure 39 displays the combined DNA results. For constructs, the DNA of the explant has been combined with that of the two matrices surrounding it. This has been compared with the DNA content of the free explants. Sacrifice time was a significant factor in the total amount of DNA ($p = 0.0004$; ANOVA). This was mostly due to increases in DNA content at 2 and 4 weeks and then a general decrease at 6 weeks. Whether the explant was part of a construct or not was only a significant factor of the total DNA at 2 and 4 weeks ($p < 0.025$; ANOVA). Culture environment did not significantly influence the total DNA ($p = 0.0713$; ANOVA).

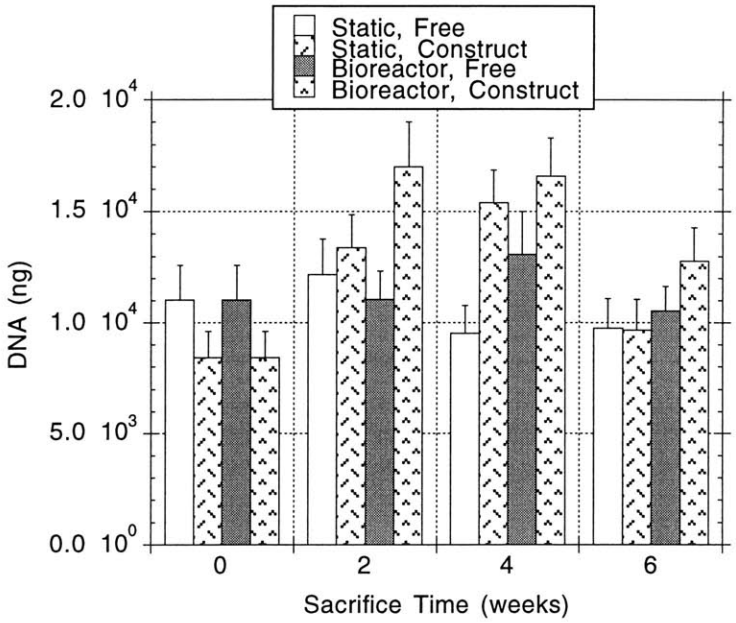

Figure 39. Total DNA vs. Sacrifice Time for the Explants and Explant Constructs

Error bars represent standard errors. n = 16-35 for each group per time point. The total DNA was that in the explants and two surrounding matrices for the construct explants. Total DNA was affects by time in culture and whether the explant was part of a construct or not.

Discussion

Explants

The explants used in this study decreased their dry mass as culture time progressed. This could be due to loss of extracellular matrix proteins (loss of architectural constrainment) or cellular (due to altered environment) or culture environment degradation of the tissue. The former is supported by the substantial loss in GAG in the explants after initial culture (Figure

32). That the original aspect ratio of explants was greater than 1 is likely caused by lamellae being oriented similarly in a curved direction in the normal IVD. When the explant is removed from its normal architecture, the lamellae are no longer locked into a curved orientation. Often, it became apparent macroscopically that the lamellae straightened. These aspect ratio findings were also observed in Experiment 2. The decreased aspect ratio of explants in the bioreactor compared to those in static culture may be due to greater hydration in these explants.

The percent hydration of the construct explants in the bioreactor did not decrease as substantially as that of explants in the other groups. It was also higher than baseline at 2 and 4 weeks. Often GAG content is associated with hydration of a tissue. A strong correlation was not found between loss of GAG and decreased hydration for any group in this study. The fact that the bioreactor construct explant % mass of GAG decreased with time in culture but the percent hydration did not leads one to believe that the simulated microgravity environment was increasing/maintaining the hydration. The free bioreactor explants were also more hydrated than the ones in static culture. Human IVDs are known to swell during bed rest and spaceflight (131). Thus, one could hypothesize that the greater hydration in the bioreactor is due to gravity unloading. The mechanism for how the water content is increased/maintained in the setting of decreasing GAG content is unclear. Since aggregated GAGs are more likely to maintain complexed water, it is possible that more of the GAG in the bioreactor specimens was aggregated.

More cells were present in the medium of the bioreactor when the explants were free. This could be caused by the free explants proliferating more; however only at the 4 week time point was there more DNA in the free explants in the bioreactor (Figure 31). Alternatively, the explants could have produced the same number of cells, but the cells emitted from the explants were contained by the matrix for the explant-matrix constructs. This is supported by the fact that the number of cells in the bioreactor medium when constructs were inside increased with time as the matrices degraded or became infiltrated with many cells. In general, the annulus explants did not lose cells in the bioreactor to the same extent as has been reported by other researchers (95, 154). This could be due to a more organized and stiffer extracellular architecture present in the IVD annulus. Interestingly, the explants of all groups increased their DNA contents. Perhaps this implies a proliferative response in the tissue being removed from its native environment. Increasing cell layers have also been observed in nucleus pulposus explants culture *in vitro* (93).

Matrix Constructs

The UV cross-linked matrices employed in this study degraded during time in culture, as evidenced by the decrease in dry mass of the controls. This decrease could in part be due to the loss in GAG content (Figure 37). The explants or cells in the matrix also likely contributed to the degradation. These matrices did not sustain long term culture well in the bioreactor when cultured with explants. The average dry mass of the construct matrices in the bioreactor at 6 weeks was much less than that in static culture. Many of the major changes in the matrix-explant constructs in the bioreactor from 4 to 6 weeks were likely due to severe degradation of the matrix during this time period. Since the bioreactor has been shown by some to better model the *in vivo* environment than static culture (8, 17, 34, 47, 75, 77, 105, 111, 112, 124, 141, 154, 173), it might be the case that the matrices would degrade severely by 6 weeks if implanted in an IVD. Complete *in vivo* degradation of the CG matrices by cells has been documented by 3-4 months (21, 134, 147) and often occurs faster than corresponding *in vitro* culture. If a 16 hr. UV cross-

linked matrix is to be used for bioreactor culture, culture for only up to 4 weeks is recommended. It is not expected that a 16 hr. UV cross-linked matrix would last much longer than 6 weeks *in vivo*. Results may be improved with cross-linking the CG matrices with 1-ethyl-3-(3-dimethyl aminoproply)carbodiimide (EDAC) (175).

That the control matrices had a greater volume initially is not surprising. As in Experiment 2, binding of the explant to the matrix can contract that portion of the matrix which is bound. The significant difference in volume in the construct matrices at 4 and 6 weeks compared to the control matrices (Figure 35) suggests cell-mediated contraction, as was seen in Experiment 2. Cell-mediated contraction could be both from degradation of the matrix by cells or by cells physically pulling on the matrix. The ability of cells to contract CG matrices has been reported by numerous researchers (101, 132, 202) and studied quantitatively (67). Contraction of cell-seeded CG matrices has even been reported for IVD canine annulus cells (201). It has been suggested that matrix contraction is related to expression of contractile proteins, such as α-smooth muscle actin (93, 201).

Cells were able to migrate into the matrices from the explants. That annulus cells have the capability for proliferation and migration suggests that conditions might be found to favor these processes *in vivo* to enhance wound healing. The results also help to explain the ability, albeit limited, of annulus to form scar tissue over several months in that significant cellular proliferation and migration was found *in vitro*.

The % mass of GAG decreased with time for both the control and construct matrices. Why the control matrices had a higher GAG content initially is unclear. While it is true that a different matrix sheet was used for the controls, the matrix sheet was produced from the same slurry batch as half of the matrix used for the constructs. It is interesting that at 6 weeks, the construct matrices in static culture had the most GAG of any group (Figure 37) and it was more than the same group's average at 4 weeks. This would imply that the cells in these matrices were producing GAG. Two possibilities exist as to why this was not observed in the bioreactor construct matrices. 1) Cells in the bioreactor matrices had a higher DNA content. Perhaps they were devoting more metabolic energy to proliferation instead of biosynthesis. 2) It is possible that cells in the bioreactor construct matrices were producing GAG but the increased fluid flow environment of the bioreactor caused newly produced proteins to leach out into the medium.

The combined matrix and explant DNA results (Figure 39) show that more cells were retained/produced in the explants in the bioreactor. Enclosure by a matrix increased the number of cells in a construct in the bioreactor at all times. This was only true for static culture at 2 and 4 weeks. It should be noted that DNA here is changing in a setting of decreasing mass of the matrices and explants.

Simulated Microgravity Culture

Bioreactor culture of the annulus explants produced some interesting results. Most impressive was the increased amount of DNA in the matrices in the bioreactor compared to those in static culture. This has implications for tissue engineering of the IVD annulus. It shows that the bioreactor may be a better environment for *in vitro* engineering of tissue or as a model system for what might happen if a matrix is implanted *in vivo*. This opinion is shared by other researchers investigating the Synthecon bioreactors for tissue engineering of articular cartilage (61, 63, 64, 65, 66).

Still, bioreactor culture has some complications compared to static culture. It was often observed that the explants or constructs would become stuck together in the bioreactor. This finding has been observed by several outside researchers but is often not reported in the literature. The clumping can confound results by having cells from different explants or constructs grow into each other.

These results show that IVD explants can be cultured in a bioreactor that simulates microgravity. This study could serve as a ground control for a future spaceflight experiment of annulus explants. While a CG matrix did produce better DNA results, improving the degradation characteristics of the matrix is necessary for tissue engineering purposes in bioreactors.

Acknowledgements

This study was supported by the Brigham Orthopedic Foundation, the Harvard Center for Engineering in Medicine Bioengineering Discovery Fund, the North American Spine Society, and the Harvard/MIT Training Program in Biomaterials (1 T32-DEO7311) (DH). The authors gratefully acknowledge use of the facilities of the Fibers and Polymers Laboratory at MIT under the supervision of Professor Yannas for the fabrication of the collagen-GAG matrices. Dr. Ray Connelly of the New England Medical Center Surgical Research Center is also thanked for providing the canine specimens. Integra Life Sciences supplied the type I collagen.

Experiment 4: Intervertebral Disc Cells Seeded into Collagen-GAG Matrices of Different Collagen Types

Introduction

Matrix collagens may be insoluble regulators of cell function, as has been demonstrated for articular cartilage (184). Towards the design of a matrix scaffold for regeneration of intervertebral disc (IVD) annulus tissue, it is necessary to determine the appropriate constituency of the matrix. For this reason, the results of cell-seeding of matrices comprised of type I collagen, type II collagen, and both types I and II collagen were compared. The glycosaminoglycan (GAG) content, pore diameter, and the ability of the matrix to be contracted were the same for all three matrix types, as assessed in Experiment 1. Annulus cell-seeded matrices, of 9 mm diameter, were cultured up to 4 weeks. Favorable results include minimal matrix contraction, the greatest number of cells in the matrix over time, the greatest amount of GAG in the matrix over time, the greatest amount of GAG production, and the greatest amount of protein production.

As stated previously, the intervertebral disc annulus fibrosus is a mixture of collagen types I and II (170, 189). In the spirit of the tissue engineering maxim of isomorphous replacement, would it not be logical to conclude that disc cells would prefer a matrix comprised of both collagen types? Perhaps having integrin attachments to both collagen types would promote the production of both collagens and other extracellular matrix proteins normal to the IVD annulus more effectively. Thus, it was hypothesized that the hybrid matrix comprised of collagen types I and II would yield the most favorable results in this experiment.

Three-Dimensional Culture of IVD Cells

Three-dimensional culture of IVD cells has been attempted previously. Gruber, et al. (80) seeded explant-derived disc cells into alginate and agarose. They found that the cells assumed a round shape and formed multicelled colonies. The cells seemed to lie in a lacunar space. Intervertebral disc cells have been cultured in alginate beads (28, 32, 33, 80, 86, 96, 129, 152, 153, 161, 194, 217), alginate gels (205), and agarose (80, 86, 152). Setton, et al. found a distribution of collagen I and II expression similar to the *in vivo* situation when cells were cultured in alginate gels (205). IVD cells have also been cultured in synthetic matrix scaffolds (166, 207).

More recently, annulus cells have been seeded into CG matrices. Rong, et al. (190) examined the nature of proteoglycans produced by passage 4 annulus cells in monolayer and 3-D culture in the type I "skin protocol" matrices. In this case, the matrices were dehydrothermally (DHT) cross-linked for 72 hours, ultraviolet (UV) cross-linked for 16 hours, and 1-ethyl-3-(3-dimethyl aminoproply)carbodiimide (EDAC) cross-linked for 2 hours. 9 mm discs were seeded with 2 million cells each. Results showed that the cells in CG matrices produced a greater percentage of aggregated proteoglycans than cells in monolayer culture after one week in culture

and that the percentage of aggregated proteoglycans was similar to native tissue. The cells in the matrix tended to predominate along the outside of the matrix after one week but more cells were inside the matrix after 4 weeks. Multiple cell layers were seen on the outside of the matrices. The authors also describe cells in the interior pores as being suspended by cell processes and extracellular matrix.

Comparison of Type I and Type II CG Matrices

A study by Schneider, et al. (201) utilized the same experimental cell-seeding methodology as in the present research for testing two types of matrix with IVD annulus cells: a collagen type I matrix that was DHT cross-linked for 24 hours and a collagen type II CG matrix that was cross-linked by UV irradiation for 16 hours. Cylindrical disks of matrices were seeded with three million cells per matrix. Cell-seeded and unseeded matrices of each collagen type were cultured for 1, 7, and 14 days. The cell-seeded type I CG matrices contracted in diameter approximately 43% by day 14. In contrast, the type II collagen matrices reduced in size by only 6%. No evident signs of degradation of either matrix were present during the course of the experiment. DNA in the type I matrix showed a 66% decrease between days 1 and 14 ($p < 0.001$). In contrast, in the type II matrix there was a significant loss of cells in the first week ($p = 0.0065$) but no significant change in cell number between 7 and 14 days; nor was there a significant difference in the DNA in the matrix between days 1 and 14. The amount of GAG produced by annulus fibrosus cells in the type I CG matrix did not change significantly over the 2-week course of the experiment. Cells in the type II collagen matrix showed a significantly higher amount of GAG, a 14-fold increase, after 14 days ($p = 0.019$). Cell morphology (spherical or elongated) did not change appreciably in the type I matrix but the percentage of cells that were spherical increased in the type II matrices. Many cells in both matrix types stained intensely for α-smooth muscle actin, a protein associated with contraction. Although differences in the behavior of the disc cells in the type I and II matrices were noted, a direct comparison between the type I and II matrix results cannot be made. The GAG content of the two matrix types was not similar. In addition, the matrix stiffnesses were not equal in part due to different cross-linking techniques.

Such comparisons have also been performed using articular cartilage chondrocytes (135). However, here again, GAG content, matrix stiffness, and seeding conditions were not normalized. A study was also performed with bovine meniscus cells comparing type I and type II matrices (164). These were matrices fabricated via methods described by Breinan (21). In this case, the matrices were cross-linking similarly with 24 hr. DHT and UV irradiation for 16 hours. The seeded (using 9×10^5 cells per 9 mm-diameter matrix) type I matrices contracted by 50% after 3 weeks with minimal contraction of the type II matrices.

Seeding Methods

Three methods of seeding of matrices have been documented: static (pipette or drop method), dynamic (agitation, stir flask, spinner flask), and bioreactor. Several previous users of cell-seeded matrices employed the static drop method where the cells are pipetted onto the matrix (21, 101, 202). Other research has determined that dynamic (25) or bioreactor seeding are

often preferable to static seeding. Burg, et al. (25) showed that cells seeded and cultured in spinner flasks into polyglycolide matrices had the greatest metabolic activity and cell distribution compared to static seeding and culture in other environments; however, DNA content was not measured in this study. Pre-wetting the matrices prior to seeding has long been practiced. Numerous investigators have pre-wet the matrices with medium (25).

Methods

Experimental Plan

Annulus cells were acquired from 6 canines. For each canine, these cells were seeded into 12 9 mm-diameter matrices of each of the three matrix types. Four matrices (1 for histology and 3 for biochemical/radiolabeling analysis) of each matrix type per canine were sacrificed at 2, 15, and 29 days. 27 unseeded matrices for each matrix type were cultured as controls. Nine (2 for histology and 7 for biochemical/radiolabeling analysis) of these were sacrificed at 2, 15, and 29 days. Sacrificed matrices were evaluated by mass and dimensional measurements, by histology, for GAG and DNA content, and by radiolabeling with sulfate and proline.

CG Matrix

Type I Collagen Matrix

The type I collagen-glycosaminoglycan (CG) matrix was produced by freeze-drying a coprecipitate of type I collagen from bovine tendon (Integra Life Sciences) and chondroitin 6-sulfate from shark cartilage (chondroitin sulfate C-4384 from shark cartilage, Sigma Chemical, St. Louis, MO). The procedure is outlined in Experiment 1 and Appendix A. For this experiment, "cartilage protocol" matrix was manufactured (matrix 124 from Appendix K).

Type II Collagen Matrix

Type II collagen slurry was provided by Geistlich Biomaterials (Chondrocell slurry, Wolhusen, Switzerland). The slurry is manufactured through a proprietary process from porcine cartilage. Chondroitin-6-sulfate at a level of 0.0105 g/20 mL slurry was added to the type II Geistlich slurry ("GAG and pore size matched," Appendix B). The slurry was centrifuged at 3500 rpm at room temperature for 5 min. for degassing. Approximately 4 mL was added to each well of a 6-well plate (Falcon 08-772-1B, Fisher Scientific Co.). The slurry was then freeze-dried as for the type I collagen matrix (Appendix A). (Matrices 129-130 from Appendix K were used in this study.)

Hybrid Collagen Matrix

A hybrid slurry of types I and II collagen was formed by creating a solution of 50% type I slurry and 50% type II slurry (Appendix C). The type I slurry was produced by the methods stated above (Appendix A). The type II slurry was from Geistlich. No additional GAG was added because the pore size became too large if this was done. The hybrid slurry was centrifuged at 3500 rpm at room temperature for 5 min. to de-gas the slurry. Approximately 4 mL of the slurry was added to each well of a 6-well plate. The slurry was then freeze-dried as for the type I collagen matrix (Appendix A). (Matrix 131 from Appendix K was used in this study.)

Cross-Linking and Comparison of the Characteristics of the Matrix Types

The matrices were dehydrothermally treated in a vacuum oven for 24 hours (without an autoclave bag) and additionally cross-linked by EDAC for 2 hours (Appendix D). 9 mm-diameter discs were punched from the matrix sheets with a dermal punch (Barron Vacuum Trephine, 9 mm, #K20-2062, Katena Products, Inc.).

The matrices in this experiment had the parameters shown in Table 5. The thickness of the hybrid matrix was significantly less than those of the other two matrix types ($p < 0.001$; Bonferroni-Dunn). The GAG content of the hybrid was also significantly less than that of the other two matrix types ($p < 0.02$; Bonferroni-Dunn). The pore diameter was not different among the three matrices ($p = 0.26$; ANOVA). The significant difference in GAG was knowingly allowed in order to have the pore sizes match. The swelling ratios, as a measure of the ability of the matrix to be contracted, were not significantly different ($p = 0.46$; ANOVA). It was noted that the type II and hybrid matrices had a slightly larger wall thickness than the type I matrix.

Table 5. Characteristics for the Matrix Types Used

Data is presented as mean ± standard deviation. CS = chondroitin sulfate. Swelling ratio here is presented after 2 hours of EDAC cross-linking.

Matrix Type	Volume	Freezing Tray	GAG Content (% mass)	Thickness (mm)	Pore Diameter (μm)	Pore Aspect Ratio	Porosity (%)	Swelling Ratio
I	180 mL (cartilage protocol)	1/3 pan section	6.9 ± 1.4	2.9 ± 0.4	236 ± 59	1.3 ± 0.3	93 ± 2	5.9 ± 0.6
II + 0.0105 mg CS/20 mL	4 mL	6-well plate well	6.7 ± 2.2	2.8 ± 0.6	202 ± 51	1.1 ± 0.1	91 ± 2	5.6 ± 0.8
hybrid (50% I/50% II)	4 mL	6-well plate well	5.0 ± 1.5	2.5 ± 0.4	228 ± 52	1.2 ± 0.1	92 ± 2	6.0 ± 1.0

Tissue Acquisition and Digestion

The lumbar spine from L2 to L7 was sterilely resected from 6 canines (2-7 years old) (Appendix L) 1.3 ± 0.4 hours after sacrifice. Each spine was placed in phosphate buffered saline (Dulbecco's PBS; #14190-136, Life Technologies) supplemented with 1% antibiotic-antimycotic solution (Gibco-BRL No. 15240-096, Life Technologies) at 4° C until dissection. Dissection began 4.4 ± 1.3 hours after canine sacrifice. The IVDs were dissected from the spines (Figure

12). The ligaments and nucleus pulposi were removed from each IVD. The annulus tissue was then cut into small pieces with a scalpel, approximately 2 mm^3.

The tissue was then digested after rinsing with PBS. The annulus pieces from 5 discs were placed in 100 mL of trypsin (0.05%)/EDTA (0.53 mM) (#25300-062, Life Technologies) for 2 hours on a shaker in an incubator at 37° C in an atmosphere of 5% CO_2 and 95% humidity. The tissue was placed in the trypsin 5.7 ± 1.7 hours after canine sacrifice. After washing with PBS, the tissue was digested for 3 hours in a 100 mL solution of 99 mL of DMEM/F12 medium (#11320-033, Life Technologies), 1 mL of antibiotic-antimycotic solution, and 0.2 g of collagenase (type IA, #C9891, Sigma) on a shaker in an incubator. The solution was then filtered through sterile 70 μm cell strainers to remove undigested tissue. The cells were washed in cell culture medium (described below) and counted (Appendix U).

Passaging and Storage

For proliferation of cells in tissue culture flasks, a 20% FBS medium was used based on the results of Experiment 2. The medium consisted of DMEM/F12 medium supplemented with 1% antibiotic-antimycotic solution (Gibco-BRL No. 15240-096, Life Technologies), 0.025 g/L of L-ascorbic acid phosphate (magnesium salt n-hydrate; #D13-12061), 20% FBS (Austrailian fetal bovine serum; #SH30084.03, Hyclone Laboratories), and 1% L-glutamine (#25030-081, Life Technologies, Inc.) (Appendix M). (All percentages are by volume.) The newly digested cells were plated in 75 cm^2 tissue culture flasks (0.2 μm vented caps, canted neck; #10-126-11, Fisher Scientific Co.) at a density of 2 $x10^6$ cells/flask. Cells removed after the first confluence were considered passage 1 (P1) cells. The cells were grown up to P3 (Appendix W) with a plating density of 0.75 $x10^6$ cells/75 cm^2 tissue culture flask between passages. They were then frozen at -70° C (Appendix X) for storage until use. When unthawed (Appendix Z) approximately 1 week prior to seeding, the cells were plated in 75 cm^2 tissue culture flasks at a density of 1 $x10^6$ cells/flask. The number of cells unfrozen for the experiment was based on the lowest flask cell yield and a unfreezing yield of 60%. These plating densities were chosen based on previous experience with densities of 0.75 million cells/flask (201) and the observations that approximately 50% of the digested cells die after being plated and approximately 25% of the unfrozen cells die after being plated. P4 cells were used for cell seeding. Work by Gruber, et al. has shown that there is no statistical difference in IVD annulus cell phenotype after 4 passages in 2-D and 3-D culture (81).

Cell Seeding

A pilot study (Appendix Y) was performed that compared the drop method of seeding to spinner flask seeding with a goal of seeding with 2 million cells per 9 mm-diameter CG disc. The drop method resulted a 67% higher DNA count than the spinner flask method; although, the drop method produced a slightly higher variance. The decreased efficiency of seeding by spinner flask method at this seeding rate has been demonstrated by another researcher (134). Due to the increased efficiency, the pipette method was chosen for seeding.

The goal was to seed the 9 mm-diameter matrix discs with 2 million cells each (Appendix AA). The matrices had been cross-linked with EDAC 1 day prior to seeding and were stored in

distilled water. One hour prior to seeding, the hydrated matrices were placed in an incubator at 37° C. They were not pre-wet with medium based on the results of Experiment 2. The P4 annulus cells were suspended at a density of 50 million cells/mL after counting with a hemocytometer twice (Appendix U). Dead cells were counted to determine cell viability. Under sterile conditions, the hydrated matrices were dried for approximately 5 min. on sterile filter paper (Fisherbrand P8; #09-795J, Fisher Scientific Co.) and placed in 6-well plates (Falcon #08-772-1B, Fisher Scientific Co.) with wells coated with 2 mL of 4% agarose (m/w; Appendix R). 20 µl of the cell suspension was then pipetted onto one surface of all of the matrices. After 10 min., the matrices were flipped over an additional 20 µl of cell suspension was added to this opposite surface. The matrices were placed in an incubator for 2 hours. Then, 0.5 mL of 10% FBS medium (see below) was added to each well. After another 4 hours (6 hours after initial seeding), another 2.5 ml of medium was added to each well.

Culture of Cell-Seeded Matrices

Culture of the cell-seeded matrices took place in an incubator at 37° C in an atmosphere of 5% CO_2 and 95% humidity. Based on the results of Experiment 2 and a pilot seeding study with human annulus cells (Appendix BB), a 10% FBS medium was employed because of matrix contraction concerns. The culture medium consisted of DMEM/F12 medium supplemented with 1% antibiotic-antimycotic solution, 0.025 g/L of L-ascorbic acid phosphate, 10% FBS, and 1% L-glutamine (Appendix M). Medium was changed every 2 days and 3 mL was added to each well. The well plates were changed every 2 weeks because of breakdown of the agarose.

Radiolabeling with ^{3}H and ^{35}S

Twenty-four hours prior to sacrifice (after 1, 14, and 28 days in culture), three discs of each matrix type for each canine and 7 controls for each matrix type were radiolabeled with tritiated proline (^{3}H) (proline, L-[2,3,4,5-^{3}H]; #NET483, Perkin Elmer or #TRK534, Amersham Pharmacia Biotech, Inc.) and radioactive sulfate (^{35}S) (#NET041H, Perkin Elmer) (Appendix CC) (128). This was to determine the biosynthetic rate of protein (mostly collagen) and GAG, respectively. The radiolabeling medium contained 10 µCi/mL of each isotope. Single- and double-labeled medium was allocated for scintillation counting calibration. Radiolabeling was performed for 24 hours. The discs were then washed 5 x 15 min. in PBS supplemented with 0.8 mM Na_2SO_4 (anhydrous sodium sulfate; S421-1, Fisher Scientific Co.) and 1.0 mM proline (P-8449, Sigma). Some of the final wash solution was taken for scintillation counting.

The discs were frozen at -20° C. The matrices were then lyophilized in a freeze dryer (Labcondo 4.5) (Appendix T) to remove water and subsequently weighed (dry mass). The matrices were digested in papain (Sigma #P3125; Appendix E) prior to biochemical analyses and scintillation counting.

Dimensional Measurements

Measurements of the diameter of the matrices were taken at 6 hours and 1, 2, 3, 4, 5, 6, 7, 9, 12, 14, 15, 18, 21, 24, 28, and 29 days after seeding. A diameter template was placed under the 6-well plates coated with agarose to measure the diameter. If the two orthogonal diameters appeared greater than 10% different, both diameters were measured. Specimens were not measured after radiolabeling. The aspect ratio was calculated from the diameters. Since often two different diameters were measured, the effective diameter was calculated as the root mean square of these two diameters:

$$d_{eff} = \sqrt{\frac{d_1^2 + d_2^2}{2}}. \qquad \text{Equation 4}$$

Cell-mediated contraction was calculated by subtracting the seeded disc effective diameter from the average control matrix effective diameter for that matrix type at that time point and dividing by the original diameter of the matrices, 9 mm:

$$\frac{\text{Average Control } d_{eff} - \text{Seeded } d_{eff}}{\text{Initial Dry diameter}} x100\%. \qquad \text{Equation 5}$$

For those discs allocated for biochemical analysis, the cell-mediated contraction for the day prior to sacrifice was divided by the DNA content to yield a measure of cell-mediated contraction normalized by the number of cells available to cause contraction.

Specimens allocated for histology (one disc per matrix type per canine per time point for seeded and 2 per matrix type per time point for controls) also had their hydrated thickness measured with an analog micrometer (Mitutoyo 505-633-50) at sacrifice time. The volume was calculated from the thickness and cross-sectional areas (from the diameters).

Biochemical Analyses

After digestion in papain, an aliquot of the sample solution in a 2 mL Hoechst dye 3328 (Polyscience Inc.)/buffer solution was measured by a fluorometer (model TKO 100, λ_{ex}=365 nm, λ_{em}=460 nm, Hoefer Scientific Instruments, San Francisco, CA) (Appendix V). The DNA content was extrapolated from a standard curve of calf thymus DNA (Sigma #D3664). The mean DNA content of the control matrices at each time point was subtracted from the DNA content of the cell-seeded matrices for the corresponding time points and matrix types.

GAG content of the digested matrices was assessed by a modification of the dimethyl-methylene blue method (57). Absorbance at 535 nm was determined with a spectrophotometer (LKB Biochrom Ultraspec 4050, Pharmacia, Piscataway, NJ) (Appendix F). The amount of GAG was extrapolated from a standard curve for shark chondroitin sulfate (C-4384, Sigma) in distilled water. The mean GAG content of the control matrices at each time point was subtracted from the GAG content of the cell-seeded matrices for the corresponding time points and matrix types.

Scintillation Counting

For the matrix samples, 100 μL of sample digest was combined with 4 mL of scintillation fluid (ScintiVerse II; FI-09-0797, Fisher Scientific Co.) and counted in a liquid scintillation counter (Packard Tri-Carb 4640; Packard Instrument Co.). For the calibration medium, 20 μL of medium was used and the counts were multiplied by 5 to match the sample volume of the matrices. Scintillation vials were counted for 1 min. each. The counts per minute from the single- and double-labeled calibration medium was used to determine spillover between the ^{3}H and ^{35}S channels (Appendix DD). The mean counts per minute of the control matrices at each time point was subtracted from the counts per minute of the cell-seeded matrices for the corresponding time points and matrix types. The counts per minute were converted to nanomoles of incorporated proline and sulfate by determining the fraction incorporated and using the known concentrations of cold proline and sulfate in DMEM/F12 medium (Appendix DD). The nanomoles incorporated was divided by the radiolabeling time (24 hours) and DNA content for normalization.

Histology

One disc per matrix type per canine per time point for seeded and 2 discs per matrix type per time point for controls were sacrificed at 2, 15, and 29 days for histology. The matrices were examined macroscopically and for firmness with a forceps. Matrices were placed in 10% neutral buffered formalin (10% buffered formalin phosphate; SF100-20, Fischer Scientific Co.) for at least 2 days. Specimens were manually dehydrated (Appendix O), bisected through the explant, and half embedded in paraffin and half in glycol methacrylate (JB-4 embedding system, Polysciences, Inc., Warrington, PA) resin (Appendix P). 5 μm microtomed JB-4 sections were stained with H & E (Appendix Q). The following parameters were assessed under light microscopy (Olympus Vanox-T): cell morphology (round or elongated), cell location, and cell layers around the disc.

Statistics

Multi- and single variable ANOVA were used to assess the effects of sacrifice time, seeding status (if applicable), and matrix type on dry mass, aspect ratio, effective diameter, cell-mediated contraction, volume, normalized DNA, % mass GAG, GAG content, sulfate incorporation, and proline incorporation. Bonferroni-Dunn post-hoc tests were utilized for selected analyses. Linear regression was used to assess the correlation between volume and effective diameter.

Results

Cells Prior to Seeding

The average digestion yield from the annulus tissue of 5 lumbar IVDs was $6.6 \pm 2.1 \times 10^6$ (mean ± standard deviation) cells (minimum = 2.6×10^6 cells). Attempts at digesting the tissue for longer amounts of time yielded poor results. Following the plating densities described above for digested, passaged, and thawed cells, the average 75 cm^2 flask yield was $1.1 \pm 0.5 \times 10^7$ cells. The lowest yield was 5.0×10^6 cells/flask. The average time to confluence was 7 ± 2 days with time to confluence decreasing with passage number. Cell yield per flask did not appear to depend on the passage stage or time to confluence. The viability after thawing was 85 ± 35%. The cell viability at seeding was 92 ± 4%. The cells had a fibroblast-like appearance in 2-D culture and produced not an insignificant amount of matrix in the 20% FBS medium.

Culture Observations of the Matrices

The hybrid matrices shrank slightly upon hydration prior to EDAC cross-linking, as has been described in Experiment 1. Many more dead cells were observed in the medium of the seeded hybrid matrices in the first two days after seeding. However, the amount of cells in the medium within a few days after seeding was much less than previous experience with UV cross-linked cell-seeded matrices (Appendix BB).

The matrices taken for histology were quite firm by 4 weeks for all matrix types. It was difficult to compress them with a forceps.

Dry Mass

The dry mass of the matrices increased with culture time for the seeded matrices ($p < 0.0001$; ANOVA). There was also a significant difference among the matrix types for this parameter ($p < 0.0001$; ANOVA). In order of increasing dry mass beyond baseline, the performance of the matrices was hybrid, type I, and type II (Figure 40). The control matrices in general decreased in dry mass with time in culture ($p = 0.0224$; ANOVA). Thus, the controls had significantly less mass than the seeded matrices ($p < 0.0001$; ANOVA).

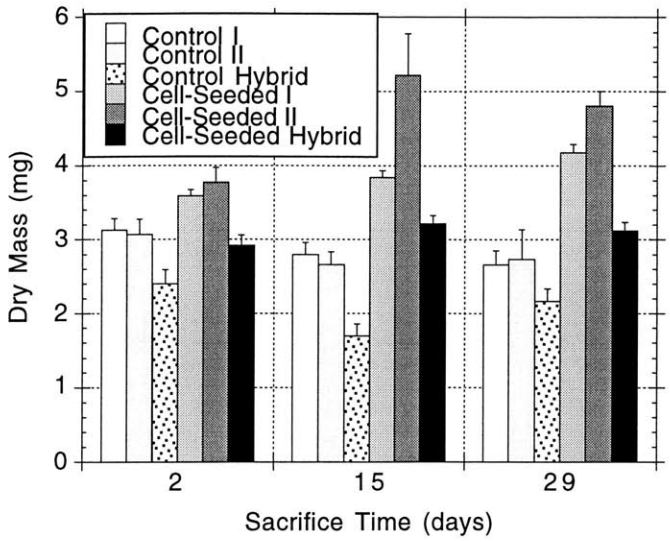

Figure 40. Dry Mass vs. Culture Time

Error bars represent the standard error of the mean. n = 17-18 and n = 7 for each matrix type for the seeded and unseed matrices, respectively.

Matrix Contraction

Figure 41, Figure 42, and Figure 43 show images of matrices of different collagen types and their contraction with time. Approximately 38% of the matrices in this study had an aspect ratio greater than 1 (not shown in a plot). Aspect ratio of the matrices increased with time in culture ($p < 0.0001$; ANOVA) from 1.04 ± 0.15 at 6 hours to 1.15 ± 0.17 at 29 days for all the matrices. The type II matrix had a significantly lower aspect ratio ($p < 0.0001$; ANOVA). The control matrices had lower aspect ratios ($p < 0.0001$; ANOVA), and most of the change in this parameter for the seeded matrices occurred during the last 2 weeks in culture.

The effective diameter, the root mean square of orthogonal diameters, of the matrices over time is shown in Figure 44. Note that at the 6 hour time point, the effective diameter of the hybrid matrix was significantly less than that of the other two matrix types ($p < 0.0001$; Bonferroni-Dunn). The hybrid matrices were approximately 8 mm at this time while the type I and type II matrices were 8.7 and 8.6 mm, respectively. The control matrices for all collagen types generally maintained their original diameters over the 4 weeks. Although the hybrid matrices contracted more initially, the type I collagen matrices reached the same degree of contraction around 2 weeks, with seeded matrices for both being approximately 6 mm after 4 weeks. The seeded type II matrices had an effective diameter near 7.3 mm at 4 weeks.

Cell-mediated contraction, the percentage change in effective diameter due to the presence of cells in the matrix, is displayed in Figure 45. It increased with time in culture ($p < 0.0001$; ANOVA). Cell mediated contraction was significantly different among the matrix types ($p < 0.0001$; ANOVA). In order of increasing cell mediated contraction, the performance of the matrices was type II, hybrid, and type I. Cell-mediated contraction normalized to DNA content is displayed in Figure 46. Cells in the type I and hybrid matrices were able to contract the matrix

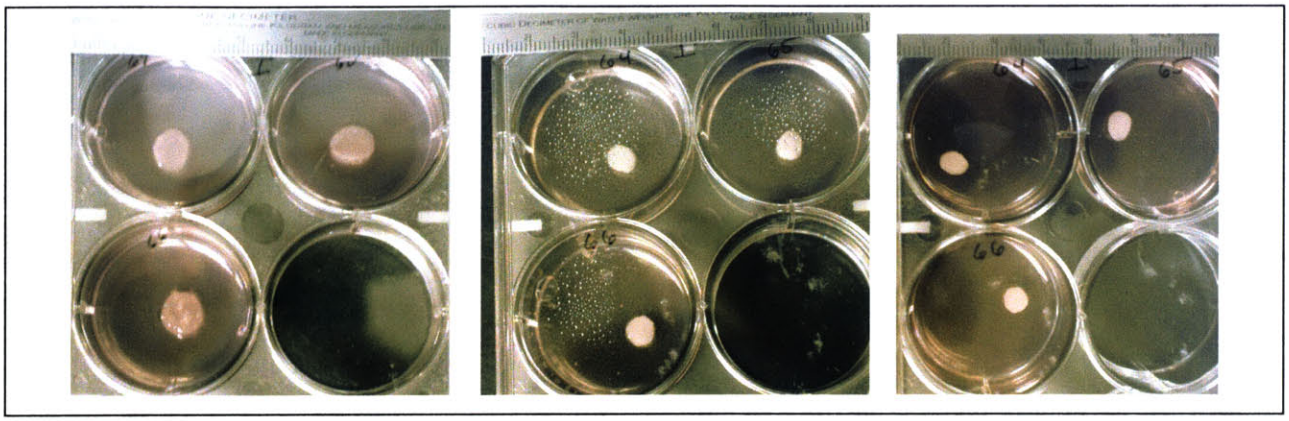

Figure 41. Cell-Seeded Type I Collagen Matrices.

Left-most picture is 6 hours after seeding. Middle picture is 2 weeks after seeding. Right image is 4 weeks after seeding.

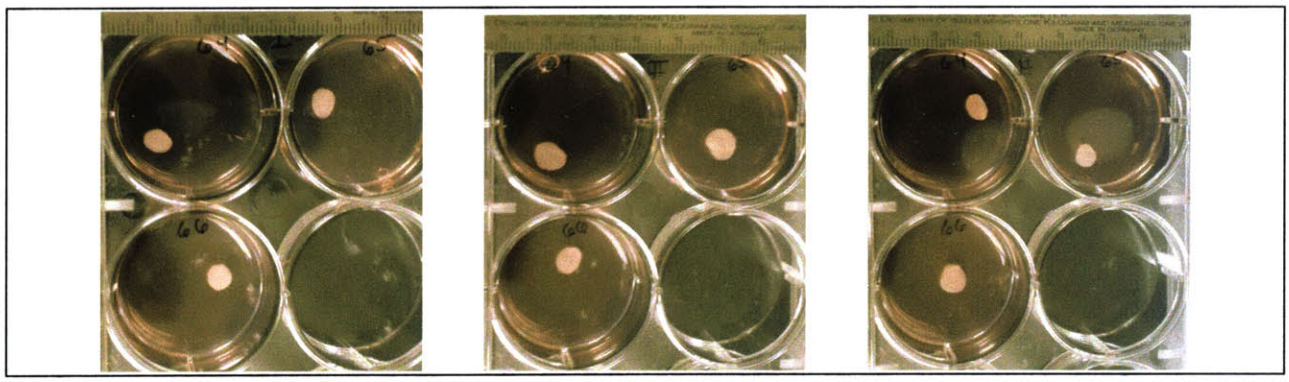

Figure 42. Cell-Seeded Matrices of the Different Collagen Types after 4 Weeks.

From left to right, the images are of type I, type II, and hybrid matrices.

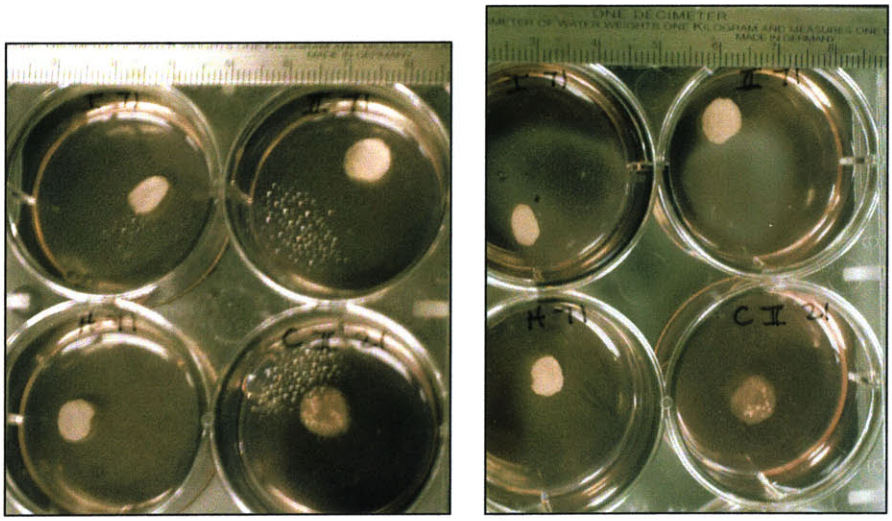

Figure 43. Matrices of Various Collagen Types.

Left image is from 2 weeks post seeding and the right image is from 1 month after seeding. Starting in the upper left-hand corner and moving clockwise, the matrices are: cell-seeded type I, cell-seeded type II, type II unseeded control, and cell-seeded hybrid.

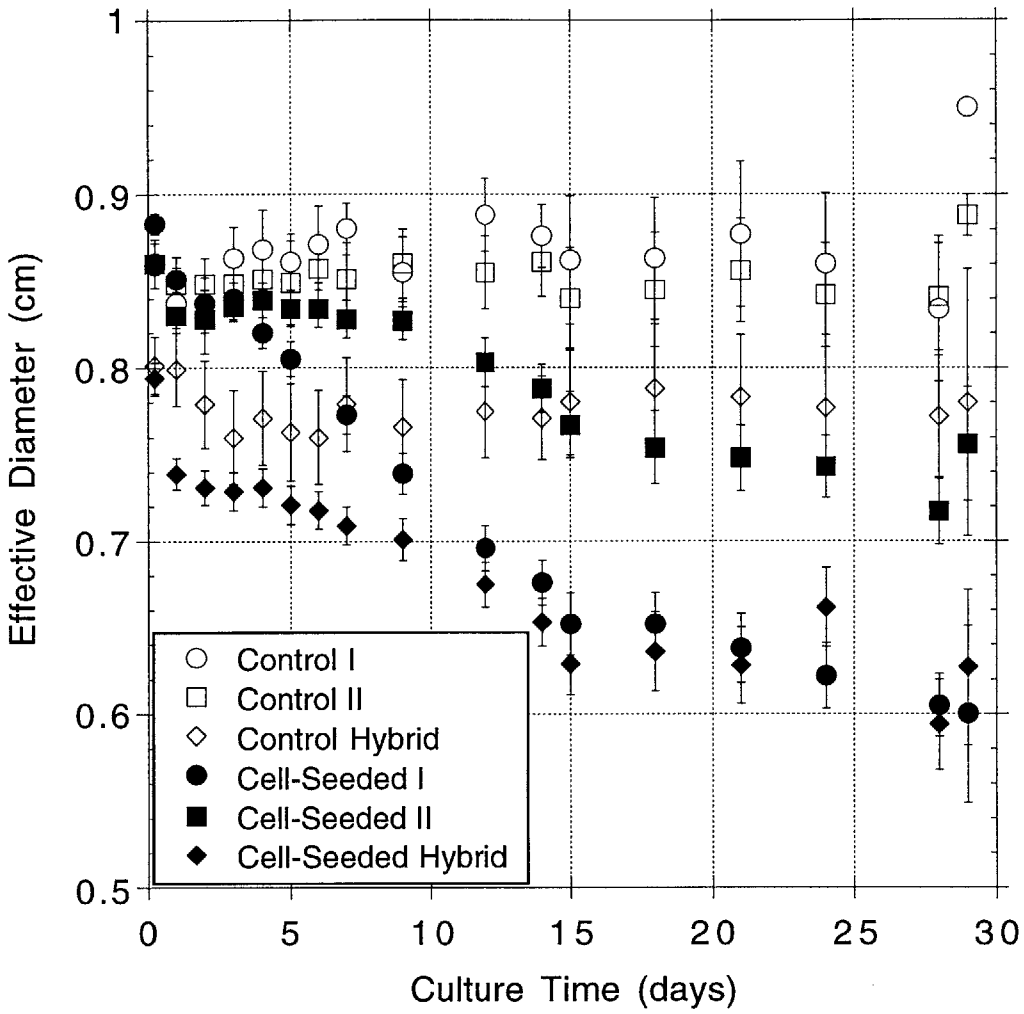

Figure 44. Effective Diameter vs. Culture Time

Error bars represent the standard error of the mean. Effective diameter was the root mean square diameter of two orthogonal diameters of the matrix. *n* decreased from 72 to 6 per matrix type for the seeded contructs. *n* decreased from 25-27 to 1-3 per matrix type for the unseeded controls. The control matrices did not contract much beyond their initial diameters. The hybrid matrix had an initial diameter that was significantly smaller than that of the other two matrix types. The seeded type II matrices contracted the least of the seeded matrices.

more easily. The difference in this parameter among the matrices types was significant at 15 and 29 days ($p < 0.026$; ANOVA).

Interestingly, Figure 44 and Figure 45 demonstrate that the dynamics of cell contraction changed over time. Around the 1 week time point, there was some plateauing of contraction or expansion of the matrix diameter. From 1-2 weeks, contraction in the seeded matrices was nearly linear. Cell-mediated contraction began to plateau again after 3 weeks.

As the contraction of the matrices is actually a volume contraction, the volume of the matrices sacrificed for histology was measured (Figure 47). Notably the volume of the seeded hybrid matrices did not change much with time in culture. The volume of the seeded type II matrices did not change substantially until 29 days whereas the seeded type I matrices exhibited

a steady contraction. For the seeded matrices, volume was significantly different with time in culture ($p < 0.0001$; ANOVA) and matrix type ($p < 0.0001$; ANOVA). Volume was somewhat correlated with effective diameter ($R^2 = 0.61$, $p < 0.0001$; linear regression).

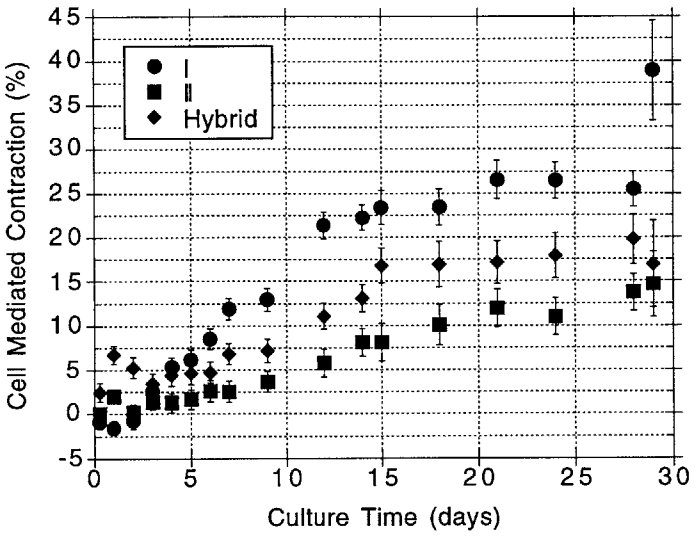

Figure 45. Cell-Mediated Contraction vs. Culture Time for the Cell-Seeded Matrices

Error bars represent the standard error of the mean. *n* decreased from 72 to 6 per matrix type during culture time. Cell-mediated contraction was calculated by subtracting the control matrix percent contraction from the seeded matrix percent contraciton. The type II collagen matrix had the least cell-mediated contraciton while the type I collagen matrix had the most.

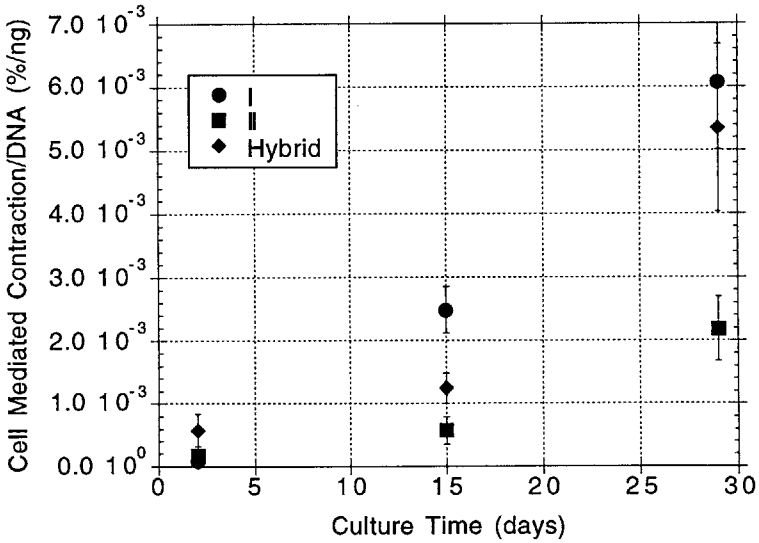

Figure 46. Cell-Mediated Contraction Normalized by DNA vs. Culture Time

Error bars represent the standard error of the mean. $n = 17$-18 per matrix type. The type II collagen matrix had the least cell-mediated contraction per DNA.

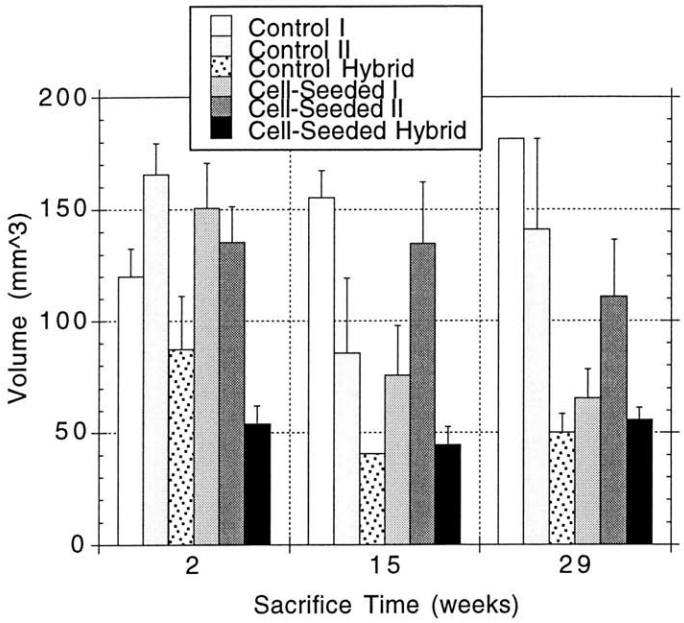

Figure 47. Volume vs. Sacrifice Time

Error bars represent the standard error of the mean. $n = 6$ for the cell-seeded matrices. $n = 1$-3 for the unseeeded control. Volume significantly decreased with time in culture for the seeded matrices.

DNA Content

The DNA content of the seeded matrices, relative to that of the unseeded matrices, decreased at day 29 compared to previous sacrifice days ($p < 0.009$; Bonferroni-Dunn; Figure 48). The only differences in DNA content among the matrix types were between type II and the hybrid at 2 days and between type I and II at 15 days ($p < 0.0163$; Bonferroni-Dunn).

GAG Content

The GAG content of the control matrices, normalized by mass, over time is shown in Figure 49. This parameter for the hybrid matrices was significantly different from the other two matrix types, 4% vs. 6% ($p < 0.0001$; Bonferroni-Dunn). The % mass of GAG did not change significantly with time for the control matrices ($p = 0.5$; ANOVA). The GAG content of the seeded matrices, relative to the content in the unseeded matrices, is shown in Figure 50. The performance of the hybrid matrix with regards to this parameter was significantly different from the other two matrix types only at 29 days ($p \leq 0.0001$; ANOVA). The amount of GAG increased with time for the type I and II matrix types ($p < 0.0015$; ANOVA).

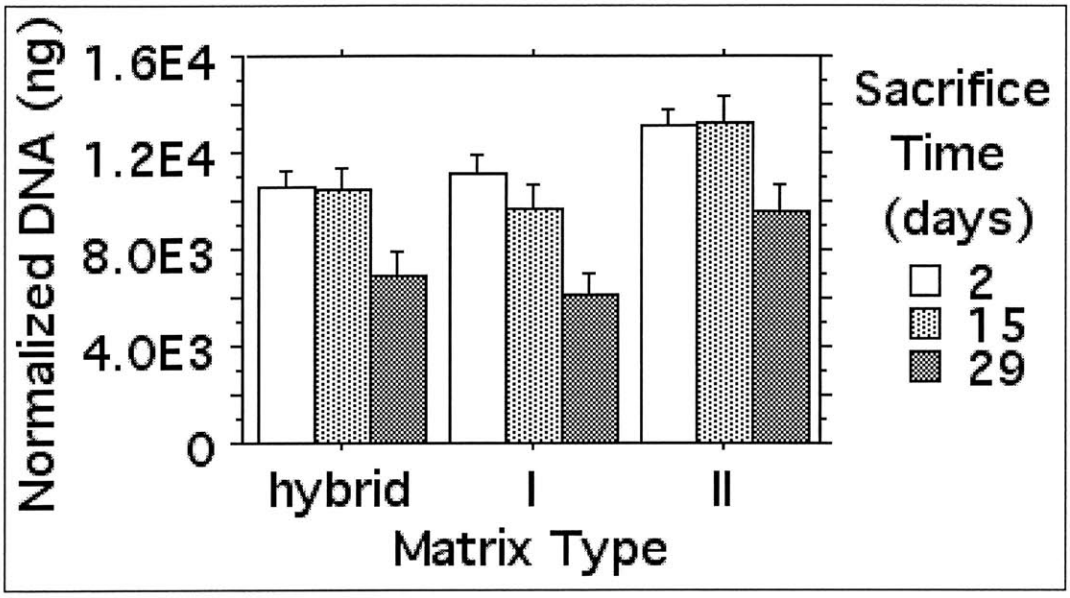

Figure 48. Normalized DNA/Matrix Disc for the Seeded Matrices

Error bars represent the standard error of the mean. n = 17-18 for each matrix type at each time point. The DNA content of the unseeded matrices was subtracted from the DNA of the seeded matrices to achieve the normalization in this plot. The DNA content decreased significantly at day 29. The type II matrices had slightly more DNA.

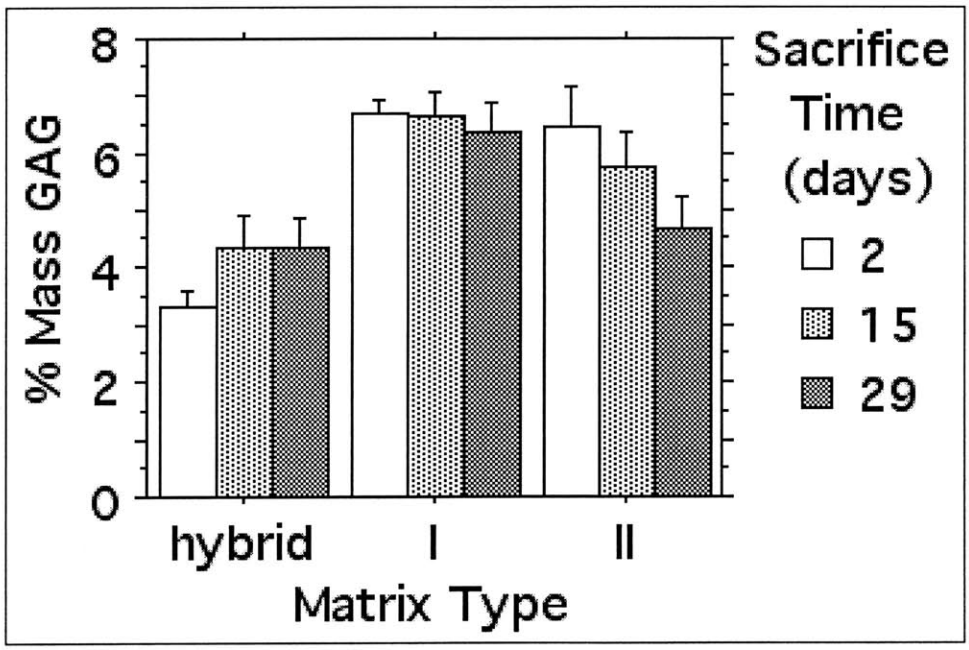

Figure 49. Percentage of Dry Mass that is GAG for the Unseeded Matrices Over Time

Error bars represent the standard error of the mean. n = 7 for each matrix type at each time point. The hybrid matrix had significantly less GAG content. The GAG content did not change significantly with time for the unseeded matrices.

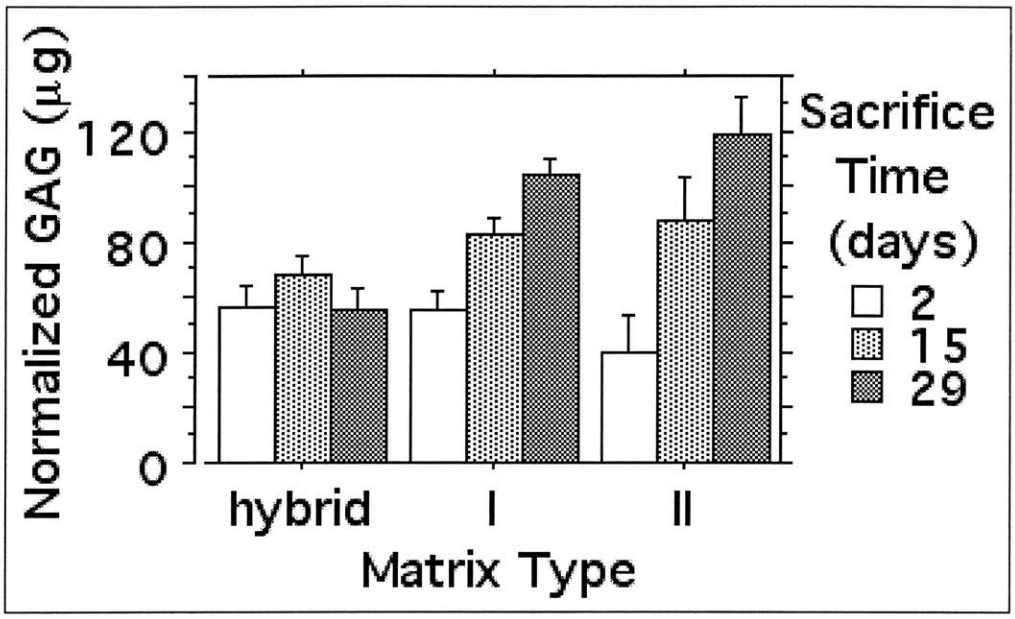

Figure 50. Normalized GAG/Matrix Disc for the Seeded Matrices

Error bars represent the standard error of the mean. n = 17-18 for each matrix type at each time point. The GAG content of the unseeded matrices was subtracted from the GAG in the seeded matrices to achieve the normalization in this plot. The GAG content increased in the type I and II matrices.

Sulfate Incorporation

The incorporated sulfate for the seeded matrices is presented in Figure 51. This parameter was not different between the matrix types at any time point ($p = 0.35$; ANOVA) but did decrease overall with time in culture ($p < 0.0001$; ANOVA).

Proline Incorporation

The incorporated proline for the seeded matrices is presented in Figure 52. This parameter did not change appreciably with time in culture ($p = 0.41$; ANOVA). The type I matrices had significantly more proline incorporation than the type II matrices ($p = 0.008$; ANOVA).

Histology

At 2 days, cells were well distributed throughout the matrix (Figure 53). Although a 1-2 cell layer had formed on the outside of the matrix by this time, a significant number of cells were in the inner portions of the matrix. By 4 weeks (Figure 54), more cells were present inside the matrix, the pores were smaller from contraction, increasing cell layers had formed, and some

new tissue formation could be seen near the edges of the the matrix. No apparent difference was observed between the matrix types. At all time points, a majority of the cells were elongated.

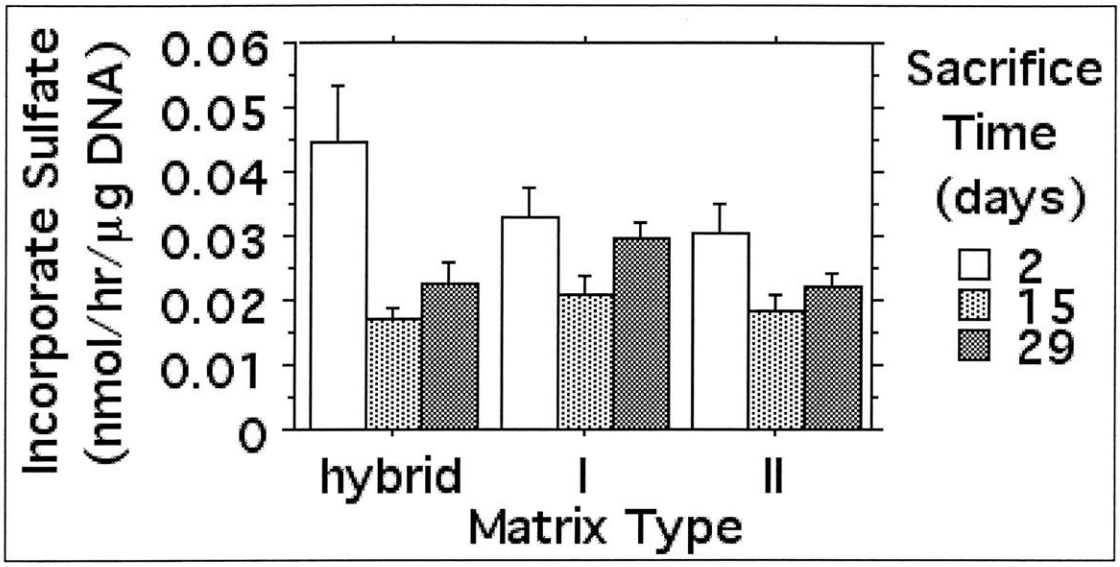

Figure 51. Normalized Incorporated Sulfate/Matrix Disc for the Seeded Matrices

Error bars represent the standard error of the mean. n = 17-18 for each matrix type at each time point. Incorporation increased with time, but no significant difference was observed among the matrix types.

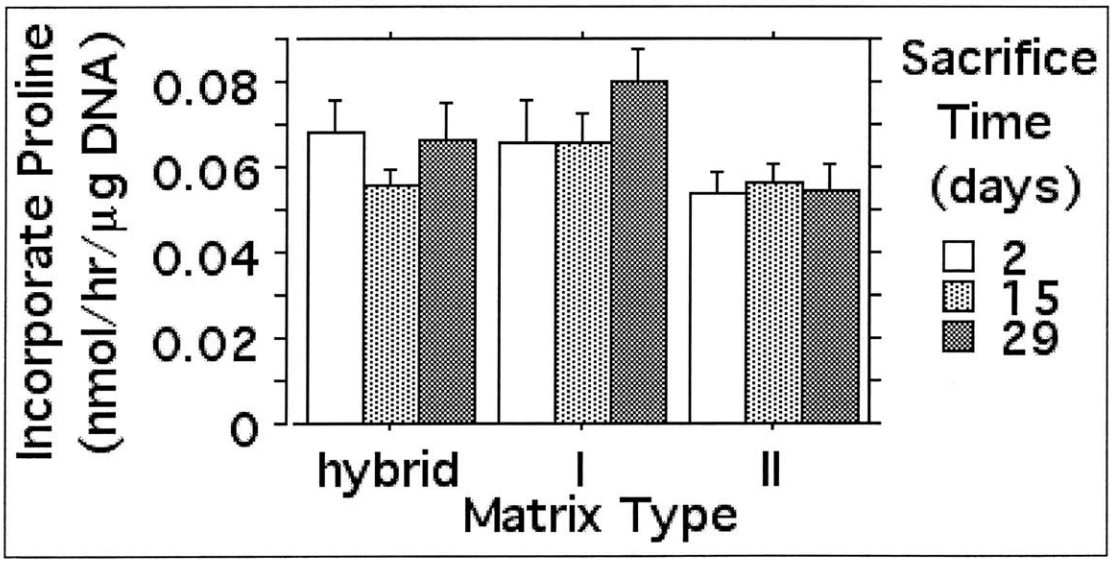

Figure 52. Normalized Incorporated Proline/Matrix Disc for the Seeded Matrices

Error bars represent the standard error of the mean. n = 17-18 for each matrix type at each time point. Incorporation did not change significantly with time in culture.

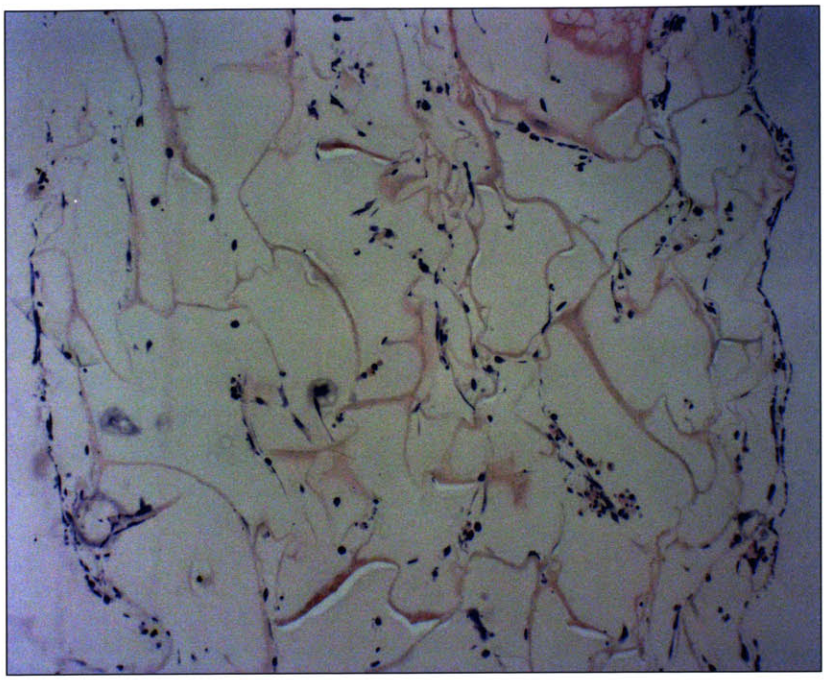

Figure 53. Cell-Seeded Hybrid Matrix at 2 Days

The right side is the edge of the matrix. Note the formation of a 1-2 cell layer on the edge. Cells are well-distributed throughout the inner portions of the matrix.

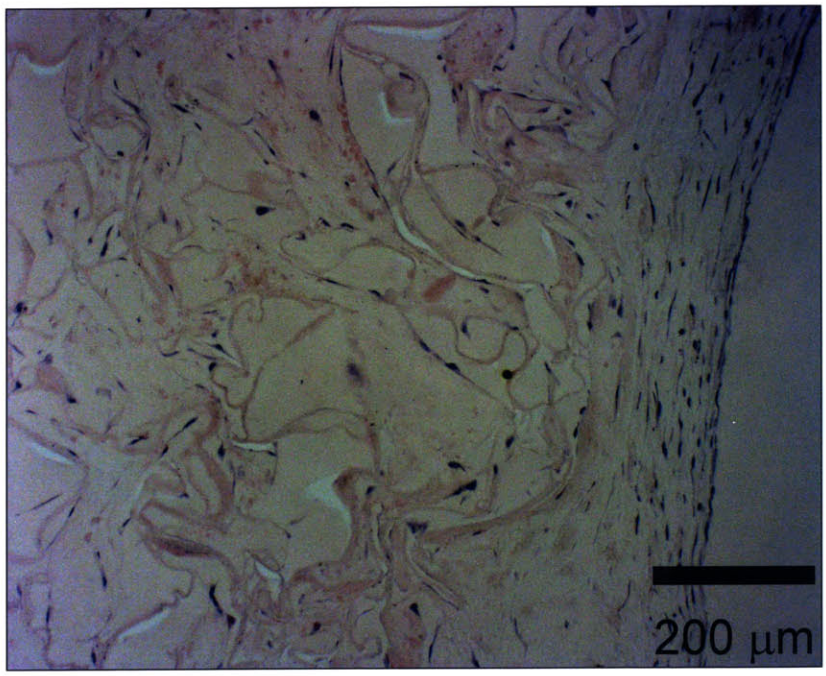

Figure 54. Cell-Seeded Hybrid Matrix at 29 Days

The right side is the edge of the matrix. Increased cell layers have formed on the edge of the matrix. The pores are smaller due to contraction. Some new tissue formation is evident.

Discussion

Tissue Digestion and 2-D Culture

The cell yield from the annulus tissue, 6.6 million cells from 5 lumbar canine discs, at first appears strikingly low. However, Schneider was only able to extract 20 million annulus cells from IVDs from the entire canine spine (200). Melrose et al. (161) tested several digestion protocols for annulus. The authors determined that 90 min. of digestion with 0.2% w/v pronase and 0.01% w/v DNAase followed by overnight digestion with 0.05% w/v bacterial collagenase, and 0.01% w/v DNAase was the most effective. Still, they were only able to average 2.9 ± 1.5 million cells (2.0 ± 0.07 million cells/g tissue) from 6 lumbar ovine discs. Chelberg, et al. (28) used 0.2% pronase and 0.004% DNAase for 60 min., followed by 0.04% bacterial collagenase II and 0.004% DNAase overnight. Their yield was 14 million cells/g of human AF.

The observation that the annulus cells were fibroblast-like in 2-D culture has been reported by other researchers (80, 104, 114, 201). Gruber, et al. also reported that annulus cells in 20% FBS produced a significant amount of matrix but noted that proliferation nearly doubled with this higher serum concentration (80).

Dry Mass

The type I and II seeded matrices increased in mass with time in culture in general. The cells were clearly producing GAG and collagen based on the radiolabel incorporation tests. The amount of GAG in the type I and II matrices did increase with time as well. This extracellular matrix production likely explains the increase in dry mass beyond day 2.

That the control matrices degraded with time in culture is not unexpected. The finding was also seen in Experiment 3. In the present investigation, the loss of dry mass cannot be wholly explained by a decrease in GAG content because the % mass of GAG of the unseeded matrices did not change significantly with time.

Matrix Contraction

The greater contraction of the hybrid matrix initially was observed to occur during hydration prior to EDAC cross-linking. Since the collagen slurries constituting the hybrid were similar to the pure collagen matrix types, the finding is somewhat puzzling. Perhaps the lesser GAG content of the hybrid matrices resulted less cross-linking from DHT and EDAC. This is contradicted by the similar swelling ratios between the matrix types. This initial contraction of the hybrid matrices could have resulted in the seeded cells ultimately experiencing a smaller pore size for this matrix type.

Previous studies have demonstrated that the collagen-GAG matrices do not contract circumferentially (164, 202). Mueller estimated that this was true in 20% of cases (164). Measuring the maximum diameter alone as been tried (164), as well as areal projections (202).

The increasing aspect ratio beyond 1 in the current study confirms previous observations although approximately twice as many matrices had noncircumferential planar contraction. The non-uniform contraction could result from the non-circular pore size of the matrices. As observed in Experiment 1, the pores were often elongated in the horizontal plane and often aligned over sections of the matrix sheets. Cells may have an easier time contracting along the short or long axis of the pores.

In the present investigation, contraction was reported as an effective diameter based on measurements of orthogonal diameters as an indication of strain the matrix may be experiencing. However, the matrix contraction is essentially a volume contraction. For this reason volume was measured as well. The volume contraction showed essentially the same characteristics as the contraction in effective diameter with the exception of the volume of the seeded hybrids at 2 days being unusually low. The lesser thickness of the hybrid matrices may have come into play for the latter.

Contraction of the CG matrices is due to two main areas: matrix related (creep, degradation) and cell-mediated (cell buckling of matrix struts, degradation of the matrix, and matrix production). The unseeded matrices did not exhibit substantial contraction with time, indicating the first main area contributes little in EDAC-cross-linked CG matrices. A majority of the cell-mediated contraction occurred during the first two weeks in culture. The decreased rate of cell-mediated contraction after this time could be due to near maximization of strut buckling of the matrix and the formation of enough new extracellular matrix to hinder additional contraction. EDAC cross-linking definitely decreases the amount of contraction of the CG matrices (132).

That the type II matrices contracted the least over time is interested given that the matrix types had similar swelling ratios. It is possible that even though the swelling ratios of the matrix types were similar the compressive stiffness was not. Lee (134) did show however that swelling ratio was better correlated to cell-mediated contraction than compressive stiffness. The greater wall thickness in the type II matrices could have also affected contraction. Breinan (21) also noted a slightly larger wall thickness in type II matrices. The proprietary nature of the type II Geistlich slurry does not allow for control of all constituents. The slurry may have contained a component that affects cross-linking and is not well measured by swelling ratio. That the cell-mediated contraction of the hybrid matrix was intermediate between the other two collagen types suggests an effect of collagen/slurry type on this parameter. EDAC cross-linking could have affected the collagen types differently in a way also unmeasureable by swelling ratio. However, a previous study with bovine meniscus cells seeded into type I and type II matrices that were similarly cross-linked with UV irradiation (164) also demonstrated greater type I matrix contraction. Thus, it is possible that collagen type did influence the ability of the cells to contract the matrix, with cell-mediated contraction being twice as large in the type I matrix as in the type II. A possible mechanism for this influence may be related to integrin attachment. If annulus cells have more integrins promoting attachment to type I collagen as opposed to type II, cells may have a greater ability to contract the type I matrix.

DNA

Previous researchers (123, 234) have found a DNA concentration of 7-10 pg DNA/cell for mammalian cells. With the initial results for the amount of DNA in the matrices (Figure 48),

the seeding efficiency was 55-75% for the type I and hybrid matrices and 65-95% for the type II matrices. These seeding efficiencies are not dissimilar from those of previous researchers using the drop method for seeding (21, 101). Note that the initial DNA content was measured at 2 days so the actual seeding efficiency may be more or less. It is unclear why the type II matrices retained more cells initially. The greater wall thickness may have been an influence.

Overall, there was not a major difference in the DNA content of the matrices of different collagen types. The decreasing DNA content at 29 days has been observed in previous studies of CG matrix with annulus cells (201) and articular chondrocytes (21) with the drop method of seeding. Lee (132) found an increasing trend of DNA content with articular chondrocytes dynamically seeded into type I CG matrices so perhaps the method of seeding causes a different distribution of cells into the matrix resulting in altered proliferation. The abrupt drop in DNA content from 15 to 29 days could be due to the significant contraction. Cells on the inside of the matrix could have become trapped within the matrix walls and died without sufficient nutrients or cellular communication. Increasing new extracellular matrix may also inhibit the flow of nutrients from the medium.

Biosynthesis

As was determined in Experiment 1, the GAG content of the hybrid was lower than the other two matrix types. The GAG content of the unseeded matrices was very similar to their dry values as reported in Experiment 1. This parameter did change significantly with time in culture. Another researcher showed that unseeded EDAC-cross-linked matrices lost 13% of their total GAG content after 5 days in PBS (181).

That the relative GAG content of the type I and II matrices increased with time indicates GAG production. Sulfate incorporation results showed that this was true. The sulfate incorporation appeared to be inversely related to the GAG content of the matrices. Thus, more GAG was produced earlier during culture time. That the sulfate incorporation rates between the matrix types were not different but more GAG accumulated in the type I and II matrices indicates that GAG produced by the hybrid matrix cells may have been lost to the medium. Note that the average normalized sulfate incorporation rates are slightly higher than those observed for articular chondrocytes seeded into type I "skin protocol" EDAC-cross-linked matrices (134).

The proline incorporation results indicate that collagen production was occurring in all matrix types. Overall, no major differences were observed with this parameter among the matrix types. Articular chondrocytes seeded into type I "skin protocol" EDAC-cross-linked matrices (134) had similar normalized incorporation rates but showed a decrease with time that was not observed here.

Histology

The pipet method of seeding did allow cells to reach the inner portions of the matrix, as evidenced by cell infiltration into those areas at 2 days. A vast majority of the cells in the matrices were elongated. Whether this is a positive finding is unclear. In normal tissue, more than 50% of annulus fibrosus (AF) cells are elongated. In the study of canine annulus cells

seeded into a CG matrices by Schneider, et al. (201), approximately two thirds of the cells were elongated.

Effect of Different Collagen Types on Measured Parameters

This experiment was primarily a study to test the effect of collagen type on proliferative and biosynthetic properties of canine annulus fibrosus cells. Characteristic differences (GAG content, thickness, and initial contraction) in the hybrid matrices make this an imperfect comparison, but some generalizations can be made.

Few differences in performance were observed between the collagen types. The hybrid matrices gained less dry mass than the other two types. Cell mediated contraction was most for type I, least for type II, and in between these two previous for the hybrid. For this parameter, a true effect of collagen type may have been observed. No major differences were seen in DNA content and sulfate incorporation. Cells in the hybrids accumulated less GAG in the matrices. Type I matrices had slightly more proline incorporation. Of the differences that were observed, the magnitudes were not great.

Thus, overall the performance of the different collagen type matrices was similar. Type II collagen matrices allowed for less cell-mediated contraction. The hybrid matrices had slightly less GAG production which could be related to the initial amount of GAG in the matrix as a regular of cell production.

That the performances were similar suggests that proliferative and biosynthetic activity of IVD annulus cells may not be regulated by the collagen composition of the surrounding extracellular matrix (ECM) to a great extent. Since the composition of the annulus contains both type I and II collagen, it is not surprising that both collagen types would equally influence cell function. Perhaps then, in the *in situ* IVD, production of extracellular collagen is influenced not by the composition of the surrounding ECM but rather by the mechanical stress faced by the cell, which changes with location in the annulus as well.

Which CG matrix type should then be used for further investigation? The characteristic differences in the hybrid matrix type make its candidacy for further use uncertain. GAG could be added to the hybrid slurry and the correct pore size achieved if a mechanism was available for freezing the slurry at a lower temperature. With added GAG, perhaps this matrix type would perform better. The type II matrix had the least contraction, which commends it for continued use. However, the type I matrix did not perform that much differently than the type II. Type I CG matrix is easier to manufacture in the general scientific community, and so it is recommended for use by those unable to easily acquire type II slurry.

Tissue Engineering of the AF

The present investigation has positive implications for the IVD annulus tissue engineering. The results show that annulus cells seeded into a CG matrix produce measurable quantities of extracellular matrix within 1 month. With EDAC cross-linking, contraction could be limited to 25% in one month (type II matrix). The next challenge is to find a method of integrating tissue engineering of the annulus with that of the NP, primarily a type II structure. A type II CG matrix could be tested for this reason. Other researchers have already attempted such

a proposition. Siegel, et al. (207) cultured rabbit annulus cells in PGA matrices in bioreactors for 1 month. Then, they removed a 4 mm core and put in nucleus pulposus (NP) cells in a collagen gel in its place and cultured for an additional two weeks. The resulting construct looked well attached at the interface with densely packed cells and local clusters of large cell pockets in the NP area.

Limitations

The seeded annulus cells were cryopreserved P4 chondrocytes. Cryopreserved articular chondrocytes seeded into matrices for tissue engineering have not performed as well in *in vivo* studies compared to passaged, noncryopreserved cells (179). Cells passaged fours times would be expected to have undergone some dedifferentiation. However, Gruber, et al. have shown that there is no statistical difference in IVD annulus cell phenotype after 4 passages in 2-D and 3-D culture (81).

The criteria for maintenance of a cellular phenotype are: expression of tissue-specific proteins and morphology. For annulus fibrosus tissue, it is difficult to assess both of these parameters. Significant numbers of cells are normally round or elongated. In addition, the normal maintenance of several collagen and GAG types within the IVD annulus does not make production of one of these proteins *in vitro* a marker for cellular phenotype. The normal rate of production of these proteins *in vivo* also changes over the animal's lifespan. Thus, even measuring production of several collagens and GAG *in vitro* does not indicate cellular phenotype. Aggrecan (aggregated proteoglycans) distinguishes fibrocartilage from fibrous tissue in addition to some round cells in pericellular matrices. Recent work (190) has examined the feasibility of testing annulus cells *in vitro* for aggrecan production but the process is laborious.

Finally, the present study only examined CG matrices for 29 days. It is entirely possible that *in vitro* culture for a longer period of time would elucidate more differences in performance among the collagen type matrices.

Acknowledgements

This study was supported by the Brigham Orthopedic Foundation, a Veterans Administration Rehabilitation Research and Development Grant (A2737R), and the Harvard/MIT Training Program in Biomaterials (1 T32-DEO7311) (DH). The authors gratefully acknowledge use of the facilities of the Fibers and Polymers Laboratory at MIT under the supervision of Professor Yannas for the fabrication of the collagen-GAG matrices. Dr. Ray Connelly of the New England Medical Center Surgical Research Center is also thanked for providing the canine specimens. Integra Life Sciences supplied the type I collagen. Geistlich Biomaterials provided the type II collagen slurry.

Experiment 5: An *In Vivo* Canine Pilot Study of Cell-Seeded Collagen-GAG Matrices for the Growth of Intervertebral Disc Annulus Tissue

Introduction

The primary goals of the *in vivo* canine pilot study were to demonstrate feasibility of the canine animal model and the efficacy of using a collagen-GAG (CG) matrix implant to facilitate regeneration of the annulus. Such an experiment was never before attempted. With a limited number of subjects, it was sought to explore the outcomes of an untreated annulotomy, implantation of an unseeded matrix, and implantation of a cell-seeded matrix. The last requires at least two surgeries: one to harvest the tissue and one to implant the cell-seeded matrix. Since all animal subjects needed to experience the same surgical conditions, all had two surgeries. Considering that other researchers have shown that different surgical procedures can be performed at at least two different levels of the canine lumber spine (49, 87, 103, 209), one procedure was performed at an upper lumbar disc and one procedure at a lower lumber disc. The two discs operated on were spaced by one or more normal discs. The surgical procedure on the lower lumbar disc was performed two months after the first surgery. Annulotomy defects, as displayed in Figure 55, were 2 mm x 10 mm at the opening and extending 5 mm into the disc. This box defect model of a discectomy has been employed by other researchers (7, 87). Matrix was placed into the defect and adhered to the annulus on the external surface by retaining sutures.

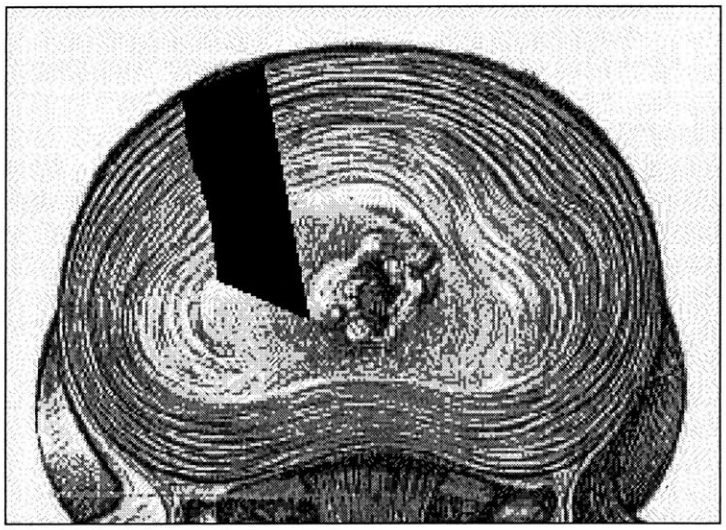

Figure 55. Intervertebral Disc Showing Tissue Removed in an Anterior Annulotomy (in black)

Animal Models of Discectomy/Annulotomy

Rabbits, sheep, pigs, canines, and goats have been most extensively utilized for disc-related research (127) although researchers believe that primates have intervertebral discs (IVDs) and spinal loading that is most similar to a human's. To conduct an animal study of a matrix implant into a discectomy defect, the IVD of the animal needed to be of a sufficient size to be surgically feasible and cost could not be prohibitive. For these reasons, a canine model was selected for the initial animal trials of an annulus matrix implant. A number of canine studies (49, 87, 92, 122, 127, 176, 209, 226) have investigated methods of discectomy that model the human situation. Most (49, 87) chose anterior discectomies versus the normal human posterior discectomy (49, 92, 122, 176, 209) because the surgical approach is much easier in canines. Many have performed different surgical procedures at at least two different levels of the canine lumber spine (49, 87, 103, 127, 176, 209, 226). A sham procedure is sometimes (176) employed as a control. It involves the surgical approach to the disc, touching the disc, and retracting the appropriate spinal nerves, but not making any incision into the disc. The purpose of the sham procedure is to identify what scarring around the disc and nerves may be due to the surgical approach itself.

The Canine Spine

Granted, the canine spine is significantly different than the human spine. The typical dog has 7 cervical, 13 thoracic, 7 lumbar, 3 sacral, and 20 coccygeal vertebrae. 1% of canines have only 6 lumber vertebrae (90). As a quadruped, the spinal loading for a canine is different than that of a human. This can result in different spinal pathology. The annulus is twice as thick on the ventral side as on the dorsal side of the disc in dogs, and annulus degeneration is more common dorsally than ventrally (90). 70% of all clinical cases of herniation in dogs are from T12-L2 (20), whereas humans herniate L4-S1 discs most commonly.

With regard to IVD degeneration is canines, two types of canines exist. Nonchondrodystrophoid dogs generally do not show signs of nuclear degeneration until after 7 years of age (90). From 1-7 years, there is dehydration but the mucoid character of the nucleus pulposus (NP) is preserved. Chondrodystrophoid dogs are generally smaller, dachshunds for instance. Hansen (90) provides a very good description of the changes in discs in dogs with age for both breed groups. Due to worries about degeneration in chondrodystrophoid canines, only nonchondrodystrophoid canines (essentially large dogs) were employed in this study.

Methods

Animals and Surgical Procedure

The West Roxbury VA Animal Care Committee approved this investigation. Three mongrel, nonchondrodystrophoid canines were housed and cared for at the West Roxbury VA Medical Center Animal Research Facility. The canines underwent radiographic assessment prior to any surgeries to rule out spinal contraindications for study treatment. Specifically, the following features would have ruled out participation: reduced disc height, sclerosis of facet joints, sclerosis of end plates, and peripheral osteophytes. None of the canine spines had these features.

Two surgeries were performed on each canine (Table 6). The anterior approach to the spine was selected because of the greater visibility of the IVD and the curvature of the canine spine on this side is similar to that of a human dorsally. The anterior approach has been performed by previous researchers (49, 87). Other researchers have shown that different surgical procedures can be performed at at least two different levels of the canine lumber spine (49, 87, 103, 209). In this experiment, the first surgery was performed at L3-L4 or L2-L3 and the second surgery was at L4-L5 or L5-L6 approximately two months later. The goal of having at least one untouched disc between the two surgeries was not met in one case due to procedural complications.

Table 6. Index of Procedures Performed in Pilot *In Vivo* Canine Study

Canine	Date of Surgery	Site of Surgery	Type of Surgery	Date of Sacrifice
1	10/4/00	L L3-L4	annulotomy	1/24/01
	11/30/00	R L4-L5	annulotomy + implantation of unseeded matrix	
2	1/30/01	L L2-L3	annulotomy	5/30/01
	4/4/01	R L5-L6	annulotomy + implantation of cell-seeded matrix	
3	7/05/01	L L2-L3	annulotomy	10/22/01
	8/30/01	R L4-L5	annulotomy + implantation of cell-seeded matrix	

The sterile surgical procedure was performed as described by Einhaus, et al. (49). Radiographs of the canines were taken intraoperatively to verify the correct disc level. Annulotomy defects, as displayed in Figure 55, were 2 mm x 10 mm at the opening and extending 5 mm into the disc. In general, nucleus pulposus material was not removed. This box defect model of a annulotomy has been employed by other researchers (7, 87). Tissue removed from the first annulotomy procedure was taken for acquisition of cells. The second surgery was performed at a lower level and on the opposite side as the first surgery (to not have to deal with scarring after the first surgery). During the second surgery, matrix (an unseeded in one case and a cell-seeded in two cases) was placed into the defect with a spatula and adhered to the annulus on the external

surface by retaining sutures (3-0 vicryl). The unseeded matrix was wet with sterile saline prior to implantation. Additional x-rays were taken post-operatively and at sacrifice.

The canines were sacrificed by a fatal dose of sodium penthol. The lumbar spine was removed *en bloc* with appropriate photographing of specimens. An x-ray of this spine portion was obtained.

IVD Disc Cells and Matrices

The annulus tissue from the first surgeries was placed into cold, sterile phosphate buffered saline (Dulbecco's PBS; #14190-136, Life Technologies) supplemented with 1% antibiotic-antimycotic solution (Gibco-BRL No. 15240-096, Life Technologies). It was cut into smaller pieces (1-3 mm in length) with a scalpel prior to digestion (Appendix L with modifications as described here). The annulus pieces were placed in trypsin (0.05%)/EDTA (0.53 mM) (#25300-062, Life Technologies) for 1 hour on a shaker in an incubator at 37° C in an atmosphere of 5% CO_2 and 95% humidity. After washing with PBS, the tissue was digested for 2 hours in a solution of DMEM/F12 medium (#11320-033, Life Technologies) supplemented with 1% antibiotic-antimycotic solution, and 0.2 g/L of collagenase (type IA, #C9891, Sigma) on a shaker in an incubator. The cells were washed in cell culture medium and counted (Appendix U). The culture medium consisted of Dulbecco's modified eagle medium/nutrient mixture-F12 (DMEM/F12 medium; #11320-063, Life Technologies, Inc.) supplemented with 1% antibiotic-antimycotic sollution, 0.025 g/L of L-ascorbic acid phosphate (magnesium slat n-hydrate, #D13-12061, Wako Chemicals USA, Inc.), 20% FBS (Austrailian fetal bovine serum; #SH30084.03, Hyclone Laboratories, Inc.), and 1% L-glutamine (#25030-081, Life Technologies, Inc.) (Appendix M). The cells were grown up to passages 2-4.

A type II collagen-GAG matrix commercially prepared from porcine cartilage by Geistlich Biomaterials (Chondrocell; Wolhusen, Switzerland) was employed in this pilot study. These scaffolds had been sterilized by the manufacturer by gamma-irradiation. Macroscopically these matrices contained several layers of different pore sizes when dry. Compared to matrices prepared in the Tissues and Polymers Laboratory at MIT, these type II matrices swell considerably upon hydration. Such commercial matrices have been employed for prior canine studies that examined articular cartilage defects (134). A 5 x 10 x 2 mm dry section of matrix was cut from the type II collagen sheets. It was then cross-linked for 2 hours in an aqueous solution of 1.4 mM 1-ethyl-3-(3-dimethylaminopropyl)carbodiimide (EDAC, Sigma #E7750, Appendix D) hydrochloride and 0.56 mM N-hydroxysuccinimide. These matrices were not treated by DHT.

Each matrix section was seeded with 2 million P2 (dog 2) or P4 (dog 3) annulus cells from the canine in which the matrix was to be implanted 24 hours prior to the second surgery. Generally, at least 2 matrix sections were prepared for each surgery in case one was lost.

Histology

The lumbar spine was fixed in 10% neutral buffered formalin (10% buffered formalin phosphate; SF100-20, Fisher Scientific Co.) for at least 3 weeks. The IVDs of interest (annulotomy, implant level, and untouched control) were then cut (through the adjacent

vertebrae) from the spine and placed in formalin for an additional week. These IVDs and their surrounding bone were decalcified for at least 2 months in 0.1 M EDTA (pH 7.4) (Appendix EE). The disc sections were cut in half sagittally through the defect site and embedded in paraffin with an embedding machine (Tissue-Tek VIP 100, model 4617, Miles Scientific, Mishwaka, IN) (Appendix FF). 7 μm microtomed sections were stained with hematoxylin and eosin (Appendix Q).

The extension of the disc beyond its normal area was assessed. Extension was defined as distance beyond the vertebral bone margins at mid-disc level and was measured using a ruler eyepiece in a Olympus (Vanox-T) light microscope. This was first determined for the control discs and the normal sides of the surgical discs. Then extension was scored by the following system:

0 less than normal
1 within normal range
2 between 0-2 mm beyond normal range
3 greater than 2 mm beyond normal range.

The appearance of the disc tissue was assessed by several different parameters. First, the character of the tissue was scored by the following:

0 no new tissue in defect
1 granulation tissue
2 fibrous tissue
3 disc-like material.

Cells often appeared aligned in a certain direction, similar to lamellae. Thus, the lamellar orientation was characterized with the following scale:

0 no lamellar organization
1 some cells oriented in direction of lamellae
2 lamellar organization of cells at several levels
3 formation of lamellae.

Degeneration of the nucleus pulposus was partially quantified by examining the size and number of clefts in this tissue. The clefts were semi-quantitatively scored by:

0 no clefts
1 a few clefts
2 many small clefts
3 large clefts.

Finally, the formation of blood vessels at the defect site was quantified:

0 no blood vessels
1 a few small blood vessels
2 many small blood vessels
3 large blood vessels.

The cellular properties of the IVD were examined as well. The number of cells in the defect site was scored by the following:

0 no cells
1 fewer cells than normal annulus
2 similar cellularity to normal annulus
3 more cells than normal annulus

The presence of immune cells was also noted:

0 no immune cells

1 a few macrophages
2 many macrophages
3 inflammatory response with many polymorphonuclear cells.

Finally, the amount of grouping of cells in the nucleus pulposus was examined and quantified by the following system:

0 no grouping
1 normal amount compared to control disc
2 more grouping than control disc
3 large amount of grouping.

Results

The surgical procedures were uncomplicated with the exception of the first surgery in the first canine being performed at L3-L4 instead of L2-L3, which caused the surgeries for this canine to be performed at adjacent levels. No canines experienced infections. They were observed to be fully mobile within a few days of surgery. The canines were neurologically intact at all times.

No visible gross abnormalities were present upon exposure of the spine, but scar tissue was evident near the surgical sites. Figure 56 displays the x-ray of the lumbar spine from the third canine. Note the bone sclerosis at the surgical levels. This was in general true for all of the canines, but no osteophytes were observed.

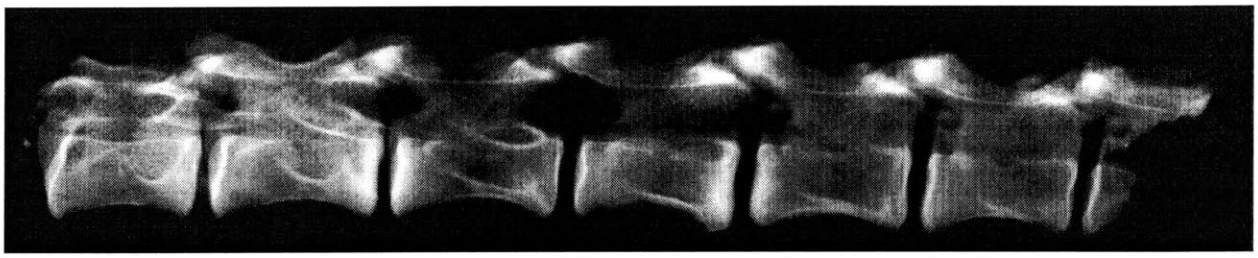

Figure 56. X-Ray of Lumbar Spine Section Removed from an In Vivo Pilot Canine.

Vertebrae L1 through L6 are shown, with L1 being the left-most. Note the sclerosis at L2-L3 (site of annulotomy) and L4-L5 (site of annulotomy + cell-seeded matrix implantation).

Histologically, the control discs and normal sides of surgical discs were found to have an extension beyond the bone margins of 0.2-0.6 mm. The results of the semi-quantitative histological evaluation are shown in Table 7. When comparing results, it is important to keep in mind that the annulotomy only sites were 4 months post-surgery while the implant sites were 2 months post-surgery. Only in one annulotomy case, did disc tissue extend beyond the normal boundary of the disc. In general, the amount of tissue was greater at the implant sites (Figure 57). Cells did appear to be slightly less oriented in the direction of lamellae though. In general, fewer blood vessels were seen in the annulotomy only sites. Occasionally, trapped congealed blood was seen at the implant sites. For the annulotomy only sites, cellularity varied depending on the location in the defect (some areas had no cells). Only for the matrix implant sites was the

cell density consistently greater than that of the normal disc in the entire defect site (Figure 58). Most of the cells in the defect site were elongated, and some were crimped. Occasionally, large nests of cells were observed in the defects implanted with seeded matrices. Macrophages were present around blood vessels in the implant defects. Some of these macrophages were noted to contain hemosiderin. With the limited sample size, it is difficult to compare the unseeded matrix site with the seeded matrix sites. However, the unseeded matrix site was noted to have less tissue filling the inner annulus area than the seeded matrices.

Table 7. Semi-Quantitative Histological Scoring Results for Pilot *In Vivo* Canine Study

Dog, Surgery	Extension	Tissue Formation	Lamellar Orientation	Clefts in NP	Blood Vessels	Cellularity of Defect	Immune Cells	Grouping in NP
1, annulotomy	0	1	2	3	0	3	0	1
2, annulotomy	3	0-1	0		0	0-3	0	1
3, annulotomy	2	2	2	2	3	0-3+	0	1
1, unseeded matrix	1	2	1	3	2	3	1	2
2, seeded matrix	2	1-2	1	1-2	1	3++	1-2	1
3, seeded matrix	2	2	1	3	1	2-3	1	1

Migration of NP material was noted in several cases. For one annulotomy (dog 1), NP tissue extended 3 mm into the annulus defect site. In another annulotomy only (dog 2), a fragment of NP material was found in the area of the disc extending beyond the bone margins. In the case of the unseeded matrix and one seeded matrix (dog 3), NP material was observed in the inner annulus but was contained by the formation of fibrous tissue. For one cell-seeded implant defect (dog 2), fingers of cells were noted to extend to or from the NP in three places. It was unclear if these cells originated in the annulus defect site or the NP.

Other than the observation of very small pieces of foreign material in a few places, no evidence remained of the implanted matrix structure after 2 months. For one annulotomy only case (dog 2), a hypercellular response was noted in adjacent ligament.

Discussion

This investigation is the first time a CG matrix has been implanted into an IVD annulus defect. The pilot *in vivo* study demonstrates the feasibility of the canine animal model for a matrix implant investigation. Two sequential surgeries were performed at different levels via an anterior approach to the spine. Tissue was extracted, cells were grown up in culture, and a cell-seeded matrix was successfully implanted two months later.

While it is difficult to make comparisons with a limited number of specimens, some general observations of healing with the different defects can be made. Once again, it is important to keep in mind that the annulotomy only sites were examined 4 months after surgery

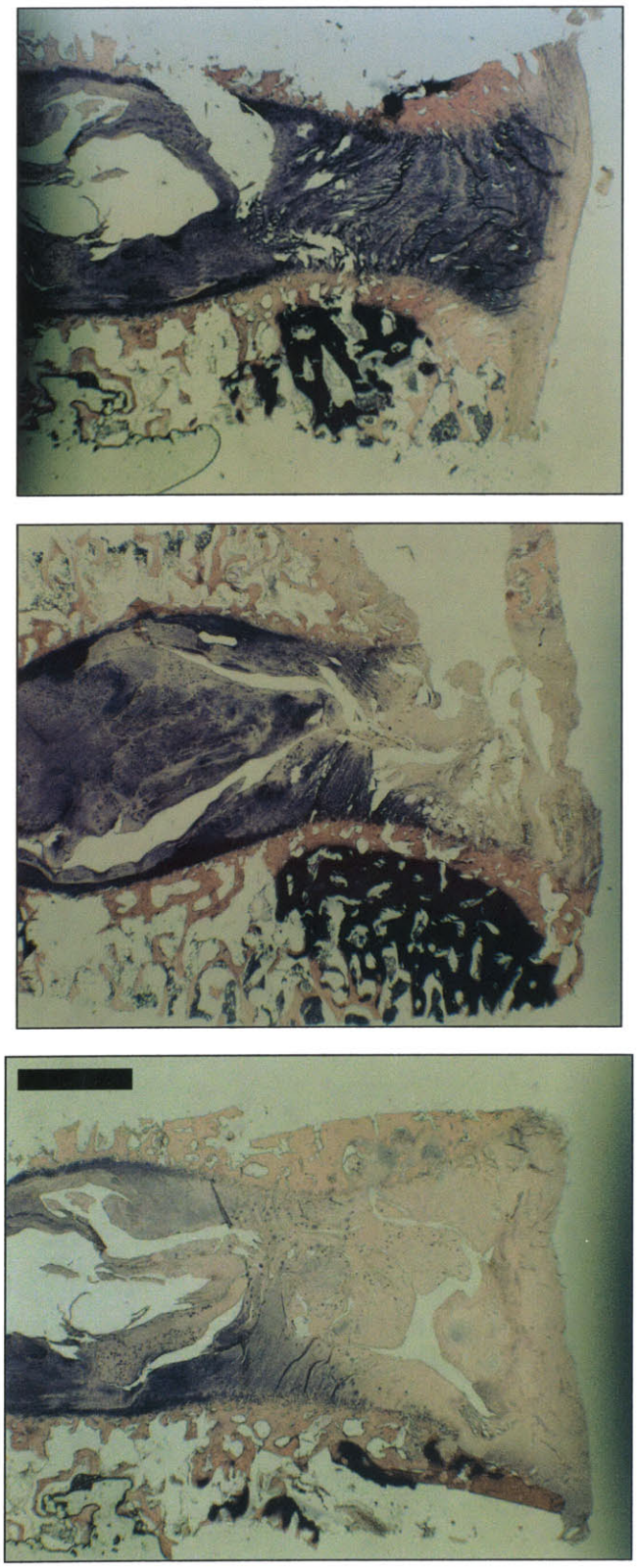

Figure 57. Histological Sections from Dog 1 4 Months after the First Surgery.

Top: L1-L2 control disc. Middle: L3-L4 annulotomy alone disc. Bottom: L4-L5 annulotomy and implantation of unseeded matrix level. Scale bar = 1 mm.

Figure 58. Histological Sections from Dog 3 4 Months after the First Surgery.

Top: L2-L3 annulotomy disc, untouched side. Middle: L2-L3 annulotomy disc, defect side. Bottom: L4-L5 discectomy and implantation of seeded matrix level. Scale bar = 1 mm.

and the implant sites were examined 2 months after surgery. Clearly though, more tissue formed at the implant sites. This could be due to cells (either seeded or migrating in from surrounding tissues) having a scaffold for regrowth. The cells appeared less oriented at the implant sites than at the annulotomy only sites. Here, the fact that the times from surgery were different may have affected the results. The formation of more small blood vessels at the implant sites is interesting from a wound healing perspective. It is often noted that such formation is necessary for new tissue formation. The fact that these small blood vessels were fragile may explain the appearance of trapped congealed blood in the newly formed tissue.

That most of the cells in the defect sites were elongated is not unusual. Normally, 20-60% of annulus cells are elongated in the annulus (94). Cells migrating into or within the defect would also be expected to elongated.

The near complete resorption or disintegration of the matrix after two months was not unexpected. Lee (132) observed matrix present in only 1 of 12 type II CG matrix implanted defects in canine articular cartilage after 15 weeks. Louie (147) found complete resorption after only 12 weeks. The matrix seemed to induce the presence of macrophages. Whether these macrophages were resorbing matrix or were just an artifact of the increased number of blood vessels is unclear.

A limitation of this study was the inability to determine which of the cells in the defect site were from the implantation. Recently, a study using autologous cells in a type I collagen matrix implanted in a sand rat model employed labels of 5-bromo-2'-deoxyuridine and 5-(and 6)-carboxyfluorescein to trace implanted cells (85). After as long as 33 weeks, implanted cells were still present in the defect sites and exhibited an elongated morphology in the annulus region.

In summary, the CG matrix implantation in annulus defects produced a response dissimilar from no implantation at the defect site. Most important were the greater amount of tissue formed and the greater number of blood vessels. These results have positive implications for the tissue engineering of IVD annulus with CG matrices. This regenerative approach may allow for less tissue to be removed from the NP during discectomy procedures in humans because the annulus would have mechanism for regeneration.

Acknowledgements

This study was supported by the Brigham Orthopedic Foundation, Sofamor-Danek Inc., and the Harvard/MIT Training Program in Biomaterials (1 T32-DEO7311) (DH). Geistlich Biomaterials provided the type II collagen matrices. Many thanks to Dr. Hu-Ping Hsu for performing the surgeries.

Conclusion

Intervertebral disc (IVD) degeneration, leading to herniated discs and other major spine conditions, is a significant problem in the U.S. population. The incidence of IVD problems is elevated in the aviation field due to the effects of frequent vibration and high G forces. Spinal pain has also been reported after spaceflight, yet very little is known about the effects of microgravity on the IVDs. Current treatment options for disc-related problems are short-term measures with unfavorable long-term consequences. The current research investigated the engineering of a collagen-glycosaminoglycan (CG) matrix to be used for the growth of IVD annulus fibrosus (AF) tissue. The matrix was used for the growth of disc tissue *in vitro* and potentially as an implant for defects in the annulus.

The five experiments in this thesis were original in many respects. A bioresorbable implant to treat disc implants was never before attempted. The ability of annulus cells to grow into a CG matrix was demonstrated. Culture of IVD cells or tissue in bioreactors had not been done. A hybrid type I and II collagen matrix is novel. Finally, no previous attempt was made to standardize the glycosaminoglycan (GAG) content, pore size, and contractility of CG matrices of different collagen types prior to assessing the selectivity of tissue cells to these matrix types. The methodology and outcomes of the five experiments of this thesis are applicable to the design of CG matrix implants for other tissues.

Suggestions for Future Work

Improving Cross-Linking

Although the 1-ethyl-3-(3-dimethyl aminoproply)carbodiimide (EDAC) cross-linked matrices are much stronger than previous CG matrices used for tissue engineering, they still degrade within 2 months *in vivo*. It may be beneficial to provide a scaffold for a longer period *in vivo*. Increasing time to degradation can be done by increasing cross-linking. Other researchers (181) have found greater cross-linking when alcohol is added to the EDAC protocol. This had been shown to be true for UV cross-linking as well (202). GAG has also been shown to be bonded to collagen by EDAC cross-linking without prior addition of GAG to the matrix (181). A comparison of cross-linking techniques with methods of evaluation including swelling ratio, collagenase resistance, and mechanical testing was performed by Weadock, et al. (227). According to their results, better swelling ratio results can be achieved if DHT for 3 days is performed after EDAC cross-linking. However, it is unclear how the matrix would retain its shape with dry cross-linking after hydration. If it does, it would also be a sterilizing mechanism and a means of not having to perform the EDAC cross-linking immediately prior to seeding. Although the results of the present investigation do not indicate that combining UV and EDAC cross-linking is beneficial, this might not be true if the UV cross-linking was improved. Recently, it has been shown that adding glucose to collagen matrices improves UV cross-linking (174).

Spaceflight Experiment

In Experiment 3, the response of IVD tissue to simulated microgravity was assessed. The results showed that IVD explants could be cultured in a bioreactor. Enclosure of the explants in CG matrices may not be necessary for culture because cells did not migrate out of the explant, but it did improve results. The feasibility of IVD explant culture paves the way for a future spaceflight experiment for IVD tissue. Neither IVD cells or explants of any tissue have ever been flown in space. Culturing an explant instead of just cells alone may be a preferred model to determine the influence of altered environments on a tissue. Explants allow for communication between cells and for the extracellular matrix to be used as a possible cellular metabolite or regulator.

Such an experiment could be performed in the Synthecon bioreactors, which have been used in spaceflight experiments (62), or in new lower shear stress bioreactors being developed for the International Space Station. Given the changes that were observed in Experiment 3, even a short duration (Space Shuttle), flight may provide evidence of changes in the IVD with microgravity. Explant culture allows tissue from larger mammals (canine or bovine) to used instead of rats, and thus closer approximations to human responses can be obtained.

Technically, a bioreactor spaceflight experiment would not be more challenging than previous experiments using live animals. Since differences have been observed among tissue from different subjects, several animals should be used. To acquire tissue, animals should be sacrificed within 2 days of spaceflight. To save precious research space, the explants from the different animals could be pooled. They could be cultured in the bioreactors until flight time, but an acceptable limit should be established for initial ground culture given the difficulty in predicting flight time of the Space Shuttle. Likely this limit is no more than 3-4 days but more ground investigations may be needed to solidify this parameter. If a CG matrix is not employed to surround the matrix, the length of the study should be no longer than 2 weeks based on the results of Experiment 3. Any CG matrix utilized should be EDAC cross-linked. Finally, explants from the same tissue sources should simultaneously be cultured in bioreactors on the ground for comparison.

Modification of CG Matrix

The present investigation explored one parameter of the CG matrix, collagen type. Other matrix parameters, such as pore size and GAG content, may affect the proliferative and biosynthetic abilities of the AF cells. A study should be performed comparing different pore sizes of the same type of matrix similar to work that Breinan (21) conducted for articular chondrocytes seeded into CG matrices. For this case, the GAG content, cross-link density, matrix thickness, and collagen type would need to be held constant. The pore size can be changed by altering the freezing temperature although a lower temperature freeze dryer would need to be used to achieve a pore size smaller than those in the present investigation for a 3 mm-thick matrix. Another study would be modify the GAG content, both in the percent mass and the kind of GAG added. For this case, the pore size, cross-link density, matrix thickness, and collagen type would need to be held constant. The percent mass is easily altered by adding more or less to the slurry. However, altering the GAG content was found to change the pore size of matrices in the present investigation so different freezing temperatures would need to be

employed. The IVD has a significant amount of keratin sulfate so it might be worthwhile to add this in addition to chondroitin sulfate to the slurry. For all of these investigations, culture time longer than 1 month is advised due to the fact that a major difference among the matrix types was not seen in this time period in Experiment 4.

Growth Factors

The use of growth factors could improve the *in vitro* proliferative and biosynthetic rates of cells seeded into CG matrices. The minimal amount of data on the effects of growth factors on IVD culture suggests further investigation is warranted, especially in relation to their effects on culture of isolated cells in matrices and in bioreactors. One study (219) explored the response of canine IVD explants to plasma-derived equine serum, 20% fetal calf serum, insulin-like growth factor-1, epidermal growth factor, and transforming growth factor-β (TGF-β). Annulus tissue responded positively in terms of proliferation and biosynthesis to all of these. Gruber, et al. (80) tested TGF-β 1 of different concentrations on annulus cells grown in agarose on layered cell well plate inserts. An increase in growth and biosynthesis was observed after 4 days but it lessened by 10 days. Saito (194) studied the production of nitric oxide induced by interleukin-1 (IL-1) feeding. Nuclear cells produced more than annular cells. Lee, et al. (137) cultured disc cells with 10 ng/mL of IGF-1, bFGF, TGF-β1, or EGF (all with 0.5% FBS) compared to 10% FBS. The last showed the highest cell proliferation. Siegel, et al. (207) tested rabbit AF and NP cells with 0.1, 1.0, and 10 ng/mL of TGF-β. The cells had a proliferative response but they did not increase matrix production. They concluded that TGF-β1 had the greatest potential for proliferation. Gruber, et al. (82, 83) recently found that 20% FBS, 100 ng/mL PDGF, or 500 ng/mL IGF-1 significantly reduced apoptosis *in vitro*. Lower concentrations of the latter two had no effect on this variable. IL-1α has been found to increase the rate of proteoglycan turnover in annulus and nucleus cells (33). Recombinant human osteogenic protein-1 has been found to increase the proteoglycan and collagen synthesis of disc cells, with nuclear cells having a greater proteoglycan response (217). One problem with choosing *in vitro* growth factors has been the lack of knowledge of how these proteins function *in vivo*. TGF-β has been shown to have a regulatory role in the IVD (220). Use of platelet-derived growth factor (PDGF) and IL-1 in patients has recently begun (231).

Growth factors could also be somehow incorporated into the matrix for cells to take up. Roles for these growth factors would include prevention of contraction, increased matrix production, and increased proliferation. Platelet-derived growth factor (PDGF)-BB has been shown to decrease contractile ability of cells (246).

Gene Therapy

Just as growth factors could be incorporated into the CG matrix, gene vectors might also be placed in the matrices for cells to take up. This might be a mechanism of delivery for treatment of IVD disorders. Gene therapy has been minimally explored in the IVD (130, 140, 156, 162, 245). Lee (134) showed that the CG matrices could be made with plasmid DNA that articular chondrocytes later took up.

Cell Source

Using IVD chondrocytes for future tissue engineering could be problematic from a practical point of view. Surgeons are unlikely to damage another healthy IVD in order to retrieve cells for repair of an IVD at another level. Unless tissue is removed at the time of discectomy, they are also unlikely to retrieve cells from the same disc level due to approach issues. Taking tissue at the time of discectomy and growing the cells in culture for tissue engineering necessitates at least two surgical procedures as was done in the *in vivo* pilot in Experiment 5.

These arguments lead one to look for an alternate source for cells. Chondrocytes from other tissues, like articular cartilage, may be functional for tissue engineering of the IVD although this has never been tested. Here again, retrieval would require damage of an otherwise healthy tissue. Bone marrow stromal cells may be a candidate for tissue engineering of the IVD, especially since methods of retrieving these cells from peripheral blood are improving. The regulators that would transform stromal cells into the IVD phenotype need to be identified.

Canine *In Vivo* Study

A larger canine study is necessary to more definitely assess use of the CG matrices for tissue engineering of the annulus. A proposed investigation is presented here. Three groups of six mongrel, nonchondrodystrophoid canines each would be used in the study, as displayed in Table 8. Group I canines would undergo a sham procedure at a lower lumbar disc and an anterior annulotomy two months later at an upper lumbar disc. Canines in Group II would receive an unseeded matrix implant at annulotomy sites in both a lower and an upper lumber disc. Group III canines would have an annulotomy at an upper lumbar disc. Cells would be harvested from the annulus tissue. These cells would be passaged for expansion. The passaged cells would be seeded into a CG matrix, which would be implanted into an annulotomy site at a lower lumbar disc two months after the first surgery.

Table 8. Canine Groups in the Animal Model

The surgery at the lower lumbar disc would occur 2 months after the first surgery.

Group	Number of Canines	Surgical Condition at Upper Lumbar Disc	Surgical Condition at Lower Lumbar Disc
I	6	sham	annulotomy
II	6	annulotomy/unseeded matrix	annulotomy/unseeded matrix
III	6	annulotomy (annulus harvest)	annulotomy/cell-seeded matrix

Thus at the conclusion of the experiment, the following comparisons could be made: 1) results of untreated annulotomy, annulotomy treated with unseeded matrix, and annulotomy treated with cell-seeded matrix at 2 months; 2) results of sham, untreated annulotomy, and annulotomy treated with unseeded matrix at 4 months; 3) results of annulotomies treated with an unseeded matrix at 2 and 4 months; and 4) results of sham and an untouched normal disc. The

last two must be qualified by the fact that the procedures would be at different levels and spinal biomechanics may affect results. Treatment assessments and comparisons would be based on radiographic studies, neurological studies, gross results at sacrifice (any evidence of herniation), and histological analysis at sacrifice.

It is recommended that the CG matrix employed in this experiment be the GAG-matched, pore-sized matched type II matrix that was 2 hr. EDAC cross-linked for Experiment 4. The dry and contraction properties of this matrix are more well known than those of the commercial type II matrix provided by Geistlich Biomaterials for Experiment 5.

Summary

Five experiments were performed. The *first* component of this thesis involved the manufacture and characterization of the CG matrices used in the other studies. Additionally, type I collagen, type II collagen, and 50/50 type I/II CG matrices were made with nearly equal pore sizes, glycosaminoglycan content, and swelling ratios. *Second*, the capability of IVD tissue to grow into the matrices was assessed by culturing annulus fibrosus explants on top of or between matrices. Cells were able to migrate up to 1 cm from the explant, implying that defects of at least 1 cm could be filled in the IVD annulus. In the *third* experiment, explants and explant-matrix constructs were cultured in NASA-designed, rotating-wall bioreactors designed to simulate microgravity. Static culture served as a control. Explants in simulated microgravity were more hydrated and had greater cellular proliferation. This experiment could also serve as the ground control for a future spaceflight experiment of annulus explants. Additionally, it tested the feasibility of using a UV cross-linked matrix in a more rigorous culture environment. The *fourth* research component studied the effect of collagen composition on the proliferative and biosynthetic responses of annulus cells seeded into CG matrices. Collagen content was varied by using the type I collagen, type II collagen, and 50/50 type I/II CG matrices with matched characteristics mentioned above. Although the results indicated that the type II matrix performed slightly better, no major difference was seen among the different collagen types. The *fifth* investigation was a pilot canine *in vivo* study to assess the capability of the CG matrix constructs to aid in regeneration of annulus fibrosus tissue in surgically-created defects. The results of no treatment were compared with the tissue produced by implanting unseeded and cell-seeded CG matrices. A greater cellular and tissue production response was observed in defects with matrix implantation.

From this research it has been shown that IVD annulus cells can migrate into a CG matrix and that the matrix has potential for improving wound healing in the IVD. Additionally, annulus tissue behaves differently under simulated microgravity conditions.

Footnotes

[1] In this case, the matrix was manufactured by another researcher and EDAC cross-linking and swelling ratio testing were performed on 4 mm-diameter discs instead of the usual 9 mm-diameter.
[2] Results from (134).
[3] Results from (134).
[4] UV cross-linking was chosen because, at the time, it was the strongest cross-linking agent used in the Orthopedic Research Laboratory.
[5] UV cross-linking was chosen because, at the time, it was the strongest cross-linking agent used in the Orthopedic Research Laboratory.
[6] Note that this number was placed on the blocks and slides, but the real number according to the specimen log should be 5462-5463.
[7] Note that this number was placed on the blocks and slides, but the real number should be 5673.

References

1. Ludann Education Services, http://www.ludann.com/1_16/index.html

2. Wheeless' Textbook of Orthopaedics. http://www.medmedia.com/Welcome.html, 1996

3. Bioreactor expands health research. NASA Microgravity Research Division, http://web.mit.edu/afs/athena/org/c/communications/directory/emergency-numbers.html, 1998

4. Abramovitz JN, Neff SR: Lumbar Disc Surgery: Results of the Prospective Lumbar Discectomy Study of the Joint Section on Disorders of the Spine and Peripheral Nerves of the American Association of Neurological Surgeons and the Congress of Neurological Surgeons. *Neurosurgery* 29: 301-308, 1991

5. Adams P, Eyre DR, Muir H: Biochemical Aspects of Development and Ageing of Human Lumbar Intervertebral Discs. *Rheumatology and Rehabilitation* 16: 22-29, 1977

6. Ahlgren BD, Lui W, Herkowitz HN, Panjabi MM, Guiboux J-P: Effect of Anular Repair on the Healing Strength of the Intervertebral Disc: A Sheep Model. *Spine* 25: 2165-2170, 2000

7. Ahlgren BD, Vasavada A, Brower RS, Lydon C, Herkowitz HN, Panjabi MM: Anular Incision Technique on the Strength and Multidirectional Flexibility of the Healing Intervertebral Disc. *Spine* 19: 948-954, 1994

8. Akins RE, Schroedl NE, Gonda SR, Hartzell CR: Neonatal Rat Heart Cells Cultured in Simulated Microgravity. *In Vitro Cell. Dev. Biol.--Animal* 33: 337-343, 1997

9. Ambrosio L, De Santis R, Nicolais L: Composite hydrogels for implants. *Proc. Instn. Mech. Engrs.* 212H: 93-99, 1998

10. Andersson GBJ: Intervertebral Disk Herniation: Epidemiology and Natural History. In: *Low Back Pain: A Scientific and Clinical Overview*, ed by JN Weinstein, SL Gordon, Rosemont, American Academy of Orthopaedic Surgeons, 1996, pp 7-21

11. Andersson GBJ: The Epidemiology of Spinal Disorders. In: *The Adult Spine: Principles and Practice*, ed by JW Frymoyer, TB Ducker, Philadelphia, Lippincott-Raven Publishers, 1997

12. Antoniou J, Steffen T, Nelson F, Winterbottom N, Hollander AP, Poole RA, Aebi M, Alini M: The Human Lumbar Intervertebral Disc: Evidence for Changes in the Biosynthesis and Denaturation of the Extracellular Matrix with Growth, Maturation, Ageing, and Degeneration. *Journal of Clin. Invest.* 98: 996-1003, 1996

13. Baker TL, Goodwin TJ: Three-Dimensional Culture of Bovine Chondrocytes in Rotating-Wall Vessels. *In Vitro Cell. Dev. Biol.--Animal* 33: 358-365, 1997

14. Bao Q-B, McCullen GM, Hingham PA, Dumbleton JH, Yuan HA: The artificial disc: theory, design, and materials. *Biomaterials* 17: 1157-1167, 1996

15. Baumgartner W, Grob D: Instantaneous Axis of Rotation in a Charite Disc Prosthesis. International Society for the Study of the Lumbar Spine, Hawaii, 1999, pp 177A

16. Bayliss MT, Urban JPG, Johnstone B, Holm S: In Vitro Method for Measuring Synthesis Rates in the Intervertebral Disc. *Journal of Orthopedic Research* 4: 10-17, 1986

17. Becker JL, Prewett TL, Spaulding GF, Goodwin TJ: Three-Dimensional Growth and Differentiation of Ovarian Tumor Cell Line in High Aspect Rotating-Wall Vessel: Morphologic and Embryologic Considerations. *Journal of Cellular Biochemistry* 51: 283-289, 1993

18. Ben-fu C, Xue-ming T: Ultrastructural Investigation of Lumbar Intervertebral Disc: Electron Microscope Observation of Normal, Protruding, and Ruptured Discs. *Chinese Medical Journal* 100: 723-730, 1987

19. Boos N, Nerlich AG, Wiest I, von der Mark K, Aebi M: Immunolocalization of type X collagen in human lumbar intervertebral discs during ageing and degeneration. *Histochem. Cell Biol.* 108: 471-480, 1997

20. Bray JP, Burbidge HM: The Canine Intervertebral Disk Part One: Structure and Function. *Journal of the American Animal Hospital Association* 34: 55-63, 1998

21. Breinan HA: Development of a Collagen-Glycosaminoglycan Analog of Extracellular Matrix to Facilitate Articular Cartilage Regeneration. Massachusetts Institute of Technology, 1998

22. Brickley-Parsons D, Glimcher MJ: Is the Chemistry of Collagen in Intervertebral Discs an Expression of Wolff's Law?: A Study of the Human Lumbar Spine. *Spine* 9: 148-163, 1984

23. Buckwalter JA: The fine structure of human intervertebral disc. In: *Symposium on Idiopathic Low Back Pain*, ed by AA White, SL Gordon, St. Louis, C.V. Mosby Company, 1982, pp 108-143

24. Buckwalter JA: Spine Update: Aging and Degeneration of the Human Intervertebral Disc. *Spine* 20: 1307-1314, 1995

25. Burg K, Holder W, Culberson C, Beiler R, Greene K, Loebsack A, Roland W, Eiselt P, Mooney D, Halberstadt C: Comparative study of seeding methods for three-dimensional polymeric scaffolds. *J. Biomed. Mater. Res.* 51: 642-649, 2000

26. Carragee EJ, Han M, Kim D, Yang B: A prospective study of lumbar disc reherniation after limited discectomy for sciatica: Fragment-type and anular defect as predictive factors in lumber disc reherniation. International Society for the Study of the Lumbar Spine, Hawaii, 1999, pp 12

27. Chamberlain LJ: Influence of Implant Parameters on the Mechanisms of Peripheral Nerve Regeneration. Massachusetts Institute of Technology, 1998

28. Chelberg MK, Banks GM, Geiger DF, Oegema TR: Identification of heterogeneous cell populations in normal human intervertebral disc. *J. Anat.* 186: 43-53, 1995

29. Chen CS: Design and analysis of a cell culture system that uses a three-dimensional tissue analog to investigate the role of mechanical forces in connective tissue maintenance. Massachusetts Institute of Technology, 1993

30. Chen CS, Yannas IV, Spector M: Pore strain behavior of collagen-glycosaminoglycan analogues of extracellular matrix. *Biomaterials* 16: 777-783, 1995

31. Chen E: The Effect of Porosity and Crosslinking of a Collagen Based Artificial Skin on Wound Healing. Massachusetts Institute of Technology, Cambridge, 1982

32. Chiba K, Andersson GB, Masuda K, Thonar EJ-MA: Metabolism of the Extracellular Matrix Formed by Intervertebral Disc Cells Cultured in Alginate. *Spine* 22: 2885-2893, 1997

33. Chiba K, Masuda K, Andersson GBJ, Takegami K, Toyama Y, Thonar EJ-MA: Effect of Interleukin-1 alpha on Turnover of Proteoglycan Synthesized by Intervertebral Disc Cells Cultured In Vitro. International Society for the Study of the Lumbar Spine, Hawaii, 1999, pp 179A

34. Chopra V, Dinh TV, Hannigan EV: Three-Dimensional Endothelial-Tumor Epithelial Cell Interactions in Human Cervical Cancers. *In Vitro Cell. Dev. Biol.--Animal* 33: 432-442, 1997

35. Chu CR, Coutts RD, Yoshioka M, Harwood FL, Monosov AZ, Amiel D: Articular cartilage repair using allogenic perichondrocyte-seeded biodegradable porous polylactic acid (PLA): A tissue-engineering study. *Journal of Biomedical Materials Research* 29: 1147-1154, 1995

36. Cinotti G, David T, Postacchini F: Results of Disc Posthesis After a Minimum Follow-Up Period of 2 Years. *Spine* 21: 995-1000, 1996

37. Clejan S, O'Conner KC, Cowger NL, Cheles MK, Haque S, Primavera AC: Effects of Simulated Microgravity on DU 145 Human Prostate Carcinoma Cells. *Biotechnology and Bioengineering* 50: 587-597, 1996

38. Cooper DR, Davidson RJ: The effect of ultraviolet irradiation on soluble collagen. *Biochem. J.* 97: 139-143, 1965

39. Coutts RD, Yoshioka M, Amiel D, Hacker SA, Harwood FL, Monosov A: Cartilage Repair Using a Porous Polylactic Acid Matrix with Allogeneic Perichondrial Cells. 40th Annual Meeting, Orthopaedic Research Society, New Orleans, 1994, pp 240

40. Coventry MB, Ghormley RK, Kernohan JW: The Intervertebral Disc: Its Microscopic Anatomy and Pathology. Part II. Changes in the Intervertebral Disc Concomitant with Age. *JBJS* 27A: 233-247, 1945

41. Crock HV: Isolated lumbar disk resorption as a cause of nerve root canal stenosis. *Clin. Orthop.* 115: 109-115, 1976

42. Davis H: Increasing Rates of Cervical and Lumbar Spine Surgery in the United States, 1979-1990. *Spine* 19: 1117-1124, 1994

43. Davis RA: A long-term outcome analysis of 984 surgically treated herniated lumbar discs. *J. Neurosurg.* 80: 415-421, 1994

44. DePalma AF, Rothman RH: The Intervertebral Disc. W.B. Saunders Company, Philadelphia, 1970

45. Duke PJ, Daane EL, Montufar-Solis D: Studies of Chondrogenesis in Rotating Systems. *Journal of Cellular Biochemistry* 51: 274-282, 1993

46. Dunlop RB, Adams MA, Hutton WC: Disc space narrowing and the lumbar facet joints. *J. Bone Joint Surg. [Br]* 66: 706-710, 1984

47. Duray PH, Hatfill SJ, Pellis NR: Tissue Culture in Microgravity. *Science & Medicine* 46-55, 1997

48. Eckert C, Decker A: Pathological Studies of Intervertebral Discs. *JBJS* 29: 447-454, 1947

49. Einhaus SL, Robertson JT, Dohan FC, Wujek JR, Ahmad S: Reduction of Peridural Fibrosis After Lumbar Laminotomy and Discectomy in Dogs by a Resorbable Gel (ADCON-L). *Spine* 22: 1440-1447, 1997

50. Ellis DL, Yannas IV: Recent advances in tissue synthesis in vivo by use of collagen-glycosaminoglycan copolymers. *Biomaterials* 17: 291-299, 1996

51. Enker P, Steffee A, Mcmillin C, Keppler L, Biscup R, Miller S: Artificial Disc Replacement: Preliminary Report with a 3-Year Minimum Follow-Up. *Spine* 18: 1061-1069, 1993

52. Erringon RJ, Puustjarvi K, White IRF, Roberts S, Urban JPG: Characterisation of cytoplasm-filled processes in cells of the intervertebral disc. *J. Anat.* 192: 369-378, 1998

53. Eyre D, Mooney V, Caterson B, Benya P, Brown M, Buckwalter J, Heinegard D, Modic M, Oegema T, Pearce R, Pope M, Urban J: Intervertebral disk. In: *New Perspectives on Low Back Pain*, ed by JW Frymoyer, SL Gordon, Chicago, IL, Amer. Acad. Orthop. Surgeons, 1989, pp 131-214

54. Eyre DR: Biochemistry of the Intervertebral Disc. *International Review of Connective Tissue Research* 8: 227-291, 1979

55. Fagan AB, Fraser RD, Tahmasebi-Sarvestani A, Vernon-Roberts B, Blumbergs PC, Moore RJ: The Innervation of Annular Tears in the Sheep Lumbar Spine. International Society for the Study of the Lumbar Spine, Hawaii, 1999, pp 140A

56. Fang A, Pierson DL, Mishra SK, Koenig DW, Demain AL: Secondary metabolism in simulated microgravity: beta-lactam production by Streptomyces clavuligerus. *Journal of Industrial Microbiology & Biotechnology* 18: 22-25, 1997

57. Farndale RW, Buttle DJ, Barrett AJ: An improved quantization and discrimination of sulphated glycosaminoglycans by use of dimethylmethylene blue. *Biochem. Biophys. Acta* 883: 173-177, 1986

58. Flynn S: Effects of Gluteraldehyde Crosslinking and Chondroitin-6-Sulfate upon the Mechanical Properties and In Vivo Healing Response of an Artificial Skin. Massachusetts Institute of Technology, Cambridge, 1983

59. Foldes I, Kern M, Szilagyi T, Oganov VS: Histology and histochemistry of intervertebral discs of rats who participated in spaceflight. *Acta Biol. Hung.* 47: 145-156, 1996

60. Freed LE, Grande DA, Lingbin Z, Emmanual J, Marquis JC, Langer R: Joint resurfacing using allograft chondrocytes and synthetic biodegradable polymer scaffolds. *J. Biomed. Mater. Res.* 28: 1994

61. Freed LE, Hollander AP, Martin I, Barry JR, Langer R, Vunjak-Novakovic G: Chondrogenesis in a Cell-Polymer-Bioreactor System. *Experimental Cell Research* 240: 58-65, 1998

62. Freed LE, Langer R, Martin I, Pellis NR, Vunjak-Novakovic G: Tissue engineering of cartilage in space. *Proc. Natl. Acad. Sci. USA* 94: 13885-13890, 1997

63. Freed LE, Vunjak-Novakovic G: Cultivation of Cell-Polymer Tissue Constructs in Simulated Microgravity. *Biotechnology and Bioengineering* 46: 306-313, 1995

64. Freed LE, Vunjak-Novakovic G: Microgravity Tissue Engineering. *In Vitro Cell. Dev. Biol.--Animal* 33: 281-285, 1997

65. Freed LE, Vunjak-Novakovic G: Tissue Culture Bioreactors: Chondrogenesis as a Model System. In: *Principles of Tissue Engineering*, ed by R Lanza, R Langer, W Chick, R.G. Landes Company, 1997

66. Freed LE, Vunjak-Novakovic G, Langer R: Cultivation of Cell-Polymer Cartilage Implants in Bioreactors. *Journal of Cellular Biochemistry* 51: 257-264, 1993

67. Freyman TM: Development of an In Vitro Model of Contraction by Fibroblasts. Massachusetts Institute of Technology, Cambridge, 2001

68. Frick SL, Hanley EN, Meyer RA, Ramp WK, Chapman TM: Lumbar intervertebral disc transfer -- A canine study. *Spine* 19: 1826-1835, 1994

69. Froom P, Margaliot S, Gross M: Low back pain and narrowed disc spaces in fighter pilots. NASA, 1986

70. Frymoyer JW, Hanley E, Howe J, Kuhlmann D, Matteri R: Disc Excision and Spine Fusion in the Management of Lumbar Disc Disease: A Minimum Ten-Year Followup. *Spine* 3: 1-6, 1978

71. Frymoyer JW, Matteri RE, Hanley EN, Kuhlmann D, Howe J: Failed Lumbar Disc Surgery Requiring a Second Operation: A Long-Term Follow-Up Study. *Spine* 3: 7-11, 1978

72. Fullman R: Measurement of Particle Sizes in Opaque Bodies. *Trans. AIME* 197: 447-451, 1953

73. Gibson LJ, Ashby MF: Cellular Solids: Structure and Properties. Cambridge University Press, Cambridge, England, 1997

74. Gomes K, Thomas J, Lowman A, Marcolongo M: The Effect of Dehydration History on Associating Hydrogels for Nucleus Pulposus Replacement. Society for Biomaterials 28th Annual Meeting Transactions, Tampa, FL, 2002, pp 684

75. Goodwin TJ, Jessup JM, Wolf DA: Morphologic Differentiation of Colon Carcinoma Cell Lines HT-29 and HT-29KM in Rotating-Wall Vessels. *In Vitro Cell Dev. Biol.* 28A: 47-60, 1992

76. Goodwin TJ, Prewett TL, Wolf DA, Spaulding GF: Reduced Shear Stress: A Major Component in the Ability of Mammalian Tissues to Form Three-Dimensional Assemblies in Simulated Microgravity. *Journal of Cellular Biochemistry* 51: 301-311, 1993

77. Goodwin TJ, Schroeder WF, Wolf DA, Moyer MP: Rotating-Wall Vessel Coculture of Small Intestine as a Prelude to Tissue Modeling: Aspects of Simulated Microgravity. *P.S.E.B.M.* 202: 181-192, 1993

78. Grabarek Z, Gergely J: Zero-length crosslinking procedure with the use of active esters. *Anal. Biochem.* 185: 131-135, 1990

79. Grande DA, Halberstadt C, Naughton G, Schwartz R, Manji R: Evaluation of Matrix Scaffolds for tissue engineering of articular cartilage grafts. *J. Biomed. Mater. Res.* 34: 211-220, 1997

80. Gruber H, Fisher EC, Desai B, Stasky A, Hoelscher G, Hanley EN: Human Intervertebral Disc Cells from the Annulus: Three-Dimensional Culture in Agarose or Alginate and Responsiveness to TGF-Beta1. *Experimental Cell Research* 235: 13-21, 1997

81. Gruber H, Hanley Jr. E: Human Intervertebral Disc Cells: Differences in Collagen and Proteoglycan Production in Monolayer vs. Three-Dimensional Culture. 45th Annual Meeting of the Orthopaedic Research Society, Anaheim, CA, 1999

82. Gruber H, Norton H, Hanley EJ: Anti-apoptotic effects of IGF-1 and PDGF on human intervertebral disc cells. *Spine* 25: 2153-2157, 2000

83. Gruber HE, Coleman SS, Hanley EN: Anti-apoptotic effects of cytokines on human intervertebral disc cells in vitro. International Society for the Study of the Lumbar Spine, Hawaii, 1999, pp 221B

84. Gruber HE, Hanley EN: Analysis of Aging and Degeneration of the Human Intervertebral Disc: Comparison of Surgical Specimens With Normal Controls. *Spine* 23: 751-757, 1998

85. Gruber HE, Hanley EN: Autologous Disc Cell Implantation in a Small Animal Model. International Society for the Study of the Lumbar Spine 29th Annual Meeting, Cleveland, 2002, pp 25

86. Gruber HE, Stasky AA, Hanley EN, Jr.: Characterization and Phenotypic Stability of Human Disc Cells in Vitro. *Matrix Biology* 16: 285-288, 1997

87. Hampton D, Laros G, McCarron R, Franks D: Healing Potential of the Anulus Fibrosis. *Spine* 14: 398-401, 1989

88. Hanley EN: Surgical Outcomes for Herniated Lumbar Disk. In: *Low Back Pain: A Scientific and Clinical Overview*, ed by JN Weinstein, SL Gordon, Rosemont, American Academy of Orthopaedic Surgeons, 1997, pp 113-123

89. Hanley EN, Shapiro DE: The Development of Low-Back Pain after Excision of a Lumbar Disc. *The Journal of Bone and Joint Surgery* 71-A: 719-721, 1989

90. Hansen H-J: A Pathologic-Anatomical Study on Disc Degeneration in Dog. *Acta Orthopaedica Scandinavica* Suppl. 11: 1-117, 1952

91. Hase H: Ultrastructural study on the nucleus pulposus of the inter-vertebral disc--the behavior of the cells in the nucleus pulposus and their autolytic changes in the monkey. *Nippon Seikeigeka Gakkai Zasshi (Journal of the Japanese Orthopedic Association)* 59: 785-801, 1985

92. Hasegawa T, An HS, Inufusa A, Mikawa Y, Watanabe R: The Effect of Age on Inflammatory Responses and Nerve Root Injuries Following Lumbar Disc Herniation: An Experimental Study in the Canine Model. International Society for the Study of the Lumbar Spine, Hawaii, 1999, pp 230A

93. Hastreiter D, Chao J, Wang Q, Ozuna RM, Spector M: Alpha-Smooth Muscle Actin Expression in Pathological Human Lumbar Disc Nucleus Pulposus In Vivo and In Vitro. *Submitted to JOR.* 2002

94. Hastreiter D, Ozuna RM, Spector M: Regional Variations in Certain Cellular Characteristics in Human Lumbar Intervertebral Discs, Including the Presence of Alpha-Smooth Muscle Actin. *JOR* 19: 597-604, 2001

95. Hatfill SJ, Margolis LB, Duray PH: In Vitro Maintenance of Normal and Pathological Human Salivary Gland Tissue in a NASA-Designed Rotating Wall Vessel Bioreactor. *Cell Vision* 3: 397-401, 1996

96. Heathfield TF, Goudsousian NM, Antoniou J, Aebi M, Alini M: Collagen and Proteoglycan Biosynthesis in Cells Isolated from Intervertebral Disc Tissues of Different Ages. 43rd Annual Meeting, Orthopaedic Research Society, San Francisco, CA, 1997, pp 149

97. Herron LD, Turner J: Patient Selection for Lumbar Laminectomy and Discectomy with a Revised Objective Rating System. *Clinical Orthopaedics and Related Research* 199: 146-152, 1985

98. Holm S, Nachemson A: Cellularity in the Lumbar Intervertebral Disc and Its Relevance to Nutrition. *Orthopaedic Transactions* 7: 457-458, 1983

99. Holm S, Urban J: The intervertebral disc: factors contributing to its nutrition and matrix turnover. In: *Joint Loading*, ed by HJ Helminen, I Kiviranta, M Tammi, e al, Bristol, Wright, 1987, pp 187-226

100. Hoogland T, Steffee AD, Black JD, Greenwald AS: Total Lumbar Intervertebral Disc Replacement: Testing of a New Articulating Spacer in Human Cadaver Spines. 24th Annual ORS, Dallas, 1978, pp 102

101. Hsiao J-Y: Behavior of Human Gingival Fibroblasts in a Collagen-GAG Matrix. Harvard School of Dental Medicine, Boston, 1999

102. Humzah MD, Soames: Human Intervertebral Disc: Structure and Function. *Anat. Res.* 220: 337-356, 1988

103. Hutton WC, Meisel HJ, Akamura T, Minamide A, Ganey T: Autologous Disc Chondrocyte Transplantation for Repair of Acute Disc Herniation. International Society for the Study of the Lumbar Spine 29th Annual Meeting, Cleveland, 2002, pp 26

104. Ichimura K, Tsuji H, Matsui H, Makiyama N: Cell Culture of the Intervertebral Disc of Rats: Factors Influencing Culture, Proteoglycan, Collagen, and Deoxyribonucleic Acid Synthesis. *Journal of Spinal Disorders* 4: 428-436, 1991

105. Ingram M, Techy GB, Saroufeem R, Yazan O, Narayan NS, Goodwin TJ, Spaulding GF: Three-Dimensional Growth Patterns of Various Human Tumor Cell Lines in Simulated Microgravity of a NASA Bioreactor. *In Vitro Cell. Dev. Biol.--Animal* 33: 459-466, 1997

106. Instruments, Hoefer Scientific: Instructions TKO 100 Dedicated Mini Fluorometer. San Francisco

107. Irving H: The Effect of Freeze Drying Temperature on Pore Size in Collagen-GAG Artificial Skin. Massachusetts Institute of Technology, Cambridge, 1986

108. Ishihara H, Warensjo K, Roberts S, Urban JPG: Proteoglycan synthesis in the intervertebral disk nucleus: the role of extracellular osmolality. *Am. J. Physiol. (Cell Physiol.)* 272: C1499-C1506, 1997

109. Ishii T, Tsuji H, Sano A, Katoh Y, Matsui H, Terahata N: Histochemical and Ultrastructural Observations on Brown Degeneration of Human Intervertebral Disc. *Journal of Orthopedic Research* 9: 78-90, 1991

110. Jackson R, Busch S, Cardin A: Glycosaminoglycans: molecular properties, protein interactions, and role in physiological processes. *Physiol. Rev.* 71: 481-539, 1991

111. Jessup JM, Brown D, Fitzgerald W, Ford RD, Nachman A, Goodwin TJ, Spaulding G: Induction of Carcinoembryonic Antigen Expression in a Three-Dimensional Culture System. *In Vitro Cell. Dev. Biol.--Animal* 33: 352-357, 1997

112. Jessup JM, Goodwin TJ, Spaulding G: Prospects for Use of Microgravity-Based Bioreactors to Study Three-Dimensional Host-Tumor Interactions in Human Neoplasia. *Journal of Cellular Biochemistry* 51: 290-300, 1993

113. Johnson EF, Mitchell R, Berryman H, Cardoso S, Ueal O, Patterson D: Secretory Cells in the Nucleus pulposus of the Adult Human Intervertebral Disc: A Preliminary Report. *Acta Anat.* 125: 161-164, 1986

114. Johnson WEB: Personal communication. 1999

115. Johnson WEB, Menage J, Evans EH, Eisenstein SM, Roberts S: Increased Intervertebral Disc Cell Proliferation and Novel Proteoglycan Production: Evidence of Cellular Repair Responses to Degeneratie Tissue Damage? International Society for the Study of the Lumbar Spine, Hawaii, 1999, pp 187A

116. Joplin RJ: The Intervertebral Disc: Embryology, Antomy, Physiology, and Pathology. 591-599, 1934

117. Juliao SF, Dawson JM, Spengler DM, Rand N: Age Related Changes in Apoptotic Rate in the Murine Intervertebral Disc. 45th Annual Meeting of the Orthopaedic Research Society, Anaheim, CA, 1999, pp 1037

118. Kadoya K, Kotani Y, Abumi K, Takada T, Shimamoto N, Shikinami Y, Kadosawa T, Kaneda K: Biomechanical and morphologic evaluation of a three-dimensional fabric sheep artificial intervertebral disc: in vitro and in vivo analysis. *Spine* 26: 1562-1569, 2001

119. Kadoya K, Kotani Y, Kaneda K, Abumi K, Takada T, Shimamoto N, Isayama H, Shikinami Y, Kadosawa T: Static, Viscoelastic, and Fatigue Biomechanical Properties of Sheep Artificial Intervertebral Disc and Their Alternations In Vivo. International Society for the Study of the Lumbar Spine, Hawaii, 1999, pp 189A

120. Katz JN: Lumbar Spine Fusion: Surgical Rates, Costs, and Complications. *Spine* 20: 78S-83S, 1995

121. Keith DK, al. e: Intervertebral disc autografting in a bipedal animal model. *Clin. Orthop.* 337: 13-26, 1993

122. Key JA, Ford LT: Experimental intervertebral disc lesions. *JBJS* 30A: 621-630, 1948

123. Kim Y-J, Sah RL, Doong J-YH, Grodzinsky AJ: Fluorometric Assay of DNA in Cartilage Explants Using Hoechst 33258. *Analytical Biochemistry* 174: 1988

124. Klement BJ, Spooner BS: Utilization of Microgravity Bioreactors for Differentiation of Mammalian Skeletal Tissue. *Journal of Cellular biochemistry* 51: 252-256, 1993

125. Kotani Y, Kaneda K, Abumi K, Takada T, Kadoya K, Kokaji M, Shikinami Y, Kadosawa T: Design and Development of Artificial Intervertebral Disc Prosthesis Consisting of Bioactive Three-Dimensional Fabric. International Society for the Study of the Lumbar Spine, Hawaii, 1999, pp 194A

126. Kotani Y, Kaneda K, Abumi K, Takada T, Kadoya K, Shimamoto N, Matsumoto S, Ebihara H, Kokaji M, Shikinami Y, Kadosawa T: Total Intervertebral Disc Replacement

Using Bioactive Three-Dimensional Fabrics: A Biomechanical and Histologic Study. International Society for the Study of the Lumbar Spine, Hawaii, 1999, pp 195A

127. Krag M: Animal Models for Human Disk Degeneration. In: *Low Back Pain: A Scientific and Clinical Overview*, ed by JN Weinstein, SL Gordon, Rosemont, American Academy of Orthopaedic Surgeons, 1996, pp 479-492

128. Kuettner K, Pauli B, Gall G, Memoli V, Schenk R: Synthesis of cartilage matrix by mammalian chondrocytes in vitro. I. Isolation, culture characteristics, and morphology. *J. Cell Biol.* 93: 743-750, 1982

129. Kumano F, An H, Chiba K, Sampath TK, Thonar EJ-MA, Andersson G: The Effect of Osteogenic Protein-1 on Proteoglycan Replenishment Following Chondroitinase ABC-Induced Chemonucleolysis of the Matrix of Cultured Intervertebral Cells. International Society for the Study of the Lumbar Spine, Hawaii, 1999, pp 25

130. Lattermann C, Oxner W, Xiao X, Li J, Gilbertson L, Kang J: Successful AAV-Vector Mediated Transgene Expression in the Intervertebral Disc in Pre-Immunized Rabbits. 48th Annual Meeting of the ORS, Dallas, TX, 2002, pp 116

131. LeBlanc AD, Evans HJ, Schneider VS, Wendt RE, Hedrick TD: Changes in Intervertebral disc cross-sectional area with bed rest and space flight. *Spine* 19: 812-817, 1994

132. Lee C, Grodzinsky A, Spector M: The Effects of Cross-Linking of Collagen-Glycosaminoglycan Scaffolds on Compressive Stiffness, Chondrocyte-Mediated Contraction, Proliferation and Biosynthesis. *Biomaterials* In press: 2002

133. Lee CK, Langrana NA: Lumbrosacral spine fusion: A biomechanical study. *Spine* 9: 574-581, 1984

134. Lee CR: Behavior of Passaged Chondrocytes in Collagen-Glycosaminoglycan Scaffolds: Effects of Cross-Linking, Mechanical Loading, and Genetic Modification of Scaffold. Massachusetts Institute of Technology, Cambridge, MA, 2002

135. Lee CR, Breinan HA, Nehrer S, Spector M: Articular Cartilage Chondrocytes in Type I and Type II Collagen-GAG Matrices Exhibit Contractile Behavior in Vitro. *Tissue Engineering* 6: 55-565, 2000

136. Lee CR, Spector M: Status of articular cartilage tissue engineering. *Current Opinion in Orthopedics* 9: 88-93, 1998

137. Lee JW, Lee HM, Kim NH: Change of type I and type II collagen biosynthesis by growth factors in cultured cells isolated from rabbit intervertebral disc. International Society for the Study of the Lumbar Spine, Hawaii, 1999, pp 112

138. Lehman T, Spratt KF, Tozz JE, al. e: Long-term follow-up of lower lumbar fusion patients. *Spine* 12: 87-104, 1987

139. Lemaire JP, Skalli W, Lavaste F, Templier A, Mendes F, Diop A, Sauty V, Laloux E: Intervertebral Disc Prosthesis: Results and Prospects for the Year 2000. *Clinical Orthopaedics and Related Research* 337: 64-76, 1997

140. Letmaitre C, Staley W, Williamson B, Ross R, Knight M, Freemont A, Hoyland J: Ex vivo gene transfer by an adenovirus vector to cells isolated from degenerate human intervertebral discs. International Society for the Study of the Lumbar Spine 29th Annual Meeting, Cleveland, 2002, pp 51

141. Lewis ML, Moriarity DM, Campbell PS: Use of Microgravity Bioreactors for Development of an In Vitro Rat Salivary Gland Cell Culture Model. *Journal of Cellular Biochemistry* 51: 265-273, 1993

142. Li S: Response of intervertebral discs to prolonged axial loading and low-frequency vibration. NASA, 1994

143. Lipson SJ, Muir H: Vertebral Osteophyte Formation in Experimental Disc Degeneration: Morphologic and Proteoglycan Changes Over Time. *Arthritis and Rheumatism* 23: 319-324, 1980

144. Lipson SJ, Muir H: Proteoglycans in experimental intervertebral disc degeneration. *Spine* 6: 194-210, 1981

145. Lotz JC, Chin JR, Court C, Colliou O, Liebenberg E: The Association Between Tissue Stress and Cell Death in the Intervertebral Disc. International Society for the Study of the Lumbar Spine, Hawaii, 1999, pp 65

146. Louie L, Schulz-Torres D, Sullivan L, Yannas IV, Spector M: Behavior of fibroblasts cultured in collagen-GAG copolymer matrices. 23rd Annual Meeting of the Society for Biomaterials, New Orleans, 1997, pp 25

147. Louie LK: Effect of a Porous Collagen-Glycosaminoglycan Copolymer on Early Tendon Healing in a Novel Animal Model. Massachusetts Institute of Technology, 1997

148. Louie LK, Yannas IV, Hsu HP, Spector M: Healing of tendon defects implanted with a porous collagen-GAG matrix: Histological evaluation. *Tissue Engineering* 3: 187-195, 1997

149. Luk KDK, Ruan DK, Chow DHK, Leong JCY: Intervertebral Disk Autografting in a Bipedal Animal Model. *Clinical Orthopaedics and Related Research* 337: 13-26, 1997

150. Luk KDK, Ruan DK, Lu DS, Cheung KMC: Fresh Frozen Intervertebral Disc Allografting in a Bipedal Animal Model. International Society for the Study of the Lumbar Spine, Hawaii, 1999, pp 197A

151. Maehara H, Yoshizawa H, Kobayashi S, Yamada S, Suzuki Y: Evidence of Apoptosis in Terminally Differentiated Chondrocytes and Notochordal Cells of the Mice Lumbar Spine: End-Labelling Studies of DNA Fragmentation. International Society for the Study of the Lumbar Spine, Hawaii, 1999, pp 198A

152. Maldonado BA, Bradford DS, Deloria LB, Meglitsch T, Oegema TR: Biosynthesis of Proteoglycans by Isolated Disc Cells Cultured In Vitro. 36th Annual Meeting, Orthopaedic Society, New Orleans, 1990, pp 37

153. Maldonado BA, Oegema TR: Initial characterization of the metabolism of intervertebral disc cells encapsulated in microspheres. *J. Orthop. Res.* 10: 1992, 1992

154. Margolis LB, Fitzgerald W, Glushakova S, Hatfill S, Amichay N, Baibakov B, Zimmerberg J: Lymphocyte Trafficking and HIV Infection of Human Lymphoid Tissue in a Rotating Wall Vessel Bioreactor. *AIDS Research and Human Retroviruses* 13: 1411-1420, 1997

155. Maroudas A, Stockwell RA, Nachemson A, J. U: Factors involved in the nutrition of the human lumbar intervertebral disc: cellularity and diffusion of glucose in vitro. *J. Anat.* 120: 113-130, 1975

156. Matsumoto T, An H, Andersson G, Thonar E, Masuda K: Effect of osteogenic protein-1 (OP-1) on the metabolism of proteoglycan by intervertebral disc cells at different ages. Gene therapy with LMP-1 increases intervertebral disc cell proteoglycan production and changes cell phenotype, Cleveland, 2002, pp 70

157. Matsuzaki H, Wakabayashi K, Ishihara K, Ishikawa H, Ohkawa A: Allografting Intervertebral Discs in Dogs: A Possible Clinical Application. *Spine* 21: 178-183, 1996

158. Maynard JA: The effects of space flight on the composition of the intervertebral disc. *Iowa Orthopedic Journal* 14: 125-133, 1994

159. Meakin J, Redpath T, Hukins D: The effect of partial removal of the nucleus pulposus from the intervertebral disc ont he response of the human annulus fibrosus to compression. *Clinical Biomechanics* 16: 121-128, 2001

160. Meakin J, Reid J, Hukins D: Replacing the nucleus pulposus of the intervertebral disc. *Clinical Biomechanics* 16: 560-565, 2001

161. Melrose J, Smith S, Ghosh P, Taylor TK: Differential Expression of Proteoglycan Epitopes and Growth Chracteristics of Intervertebral Disc Cells Grown in Alginate Bead Culture. *Cells Tissues Organs* 168: 137-146, 2001

162. Moon S, Gilbertson L, Nishida K, Knaub M, Muzzonigro T, Robbins P, Evans C, Kang J: Human intervertebral disc cells are genetically modifiable by adenovirus-mediated gene transfer: implications for the clinical management of intervertebral disc disorders. *Spine* 25: 2573-2579, 2000

163. Motulsky H: The GraphPad Guide to Nonlinear Regression. Graphpad Software, 1996

164. Mueller SM, Schneider TO, Shortkroff s, Breinan HA, Spector M: alpha-smooth muscle actin and contractile behavior of bovine meniscus cells in type I and type II collagen-GAG matrices. *J. Biomed. Mater. Res.* 45: 157-166, 1999

165. Muzic R, Jutan A: leasqr. http://www.mathworks.com/ftp/statv4.shtml

166. Mwale F, Demer CN, Petit A, Termenoff J, Lim V, Fisher J, Zukor D, Huk O, Mikos AG, Roughley P, Antoniou J: Analysis of Poly(Propylene Fumarate-co-Ethylene Glycol) as a Scaffold for Use in Tissue Engineering of the Intervertebral Disc: Retention of Collagen and Progteoglycan. Society for Biomaterials 28th Annual Meeting Transactions, Tampa, FL, 2002

167. Naylor A: The Structure and Function of the Intervertebral Disc. *Orthopaedics* 3: 7-22, 1970

168. Nehrer S, Breinan H, Ashkar S, Shortkroff S, Minas T, Sledge CB, Yannas IV, Spector M: Characteristics of articular chondrocytes seeded in collagen matrices in vitro. *Accepted by Journal of Tissue Engineering* 1998

169. Nehrer S, Breinan HA, Ramappa A, Shortkroff S, Young G, Minas T, Sledge CB, Yannas IV, Spector M: Canine chondrocytes seeded in type I and type II collagen implants investigated in vitro. *J. Biomed. Mater. Res. (Appl. Biomat.)* 38: 95-104, 1997

170. Nerlich AG, Boos N, Wiest I, Aebi M: Immunolocalization of major interstitial collagen types in human lumbar intervertebral discs of various ages. *Virchows Arch.* 432: 67-76, 1998

171. Nerlich AG, Schleicher ED, Boos N: Immunohistologic Markers for Age-Related Changes of Human Lumbar Intervertebral Discs. *Spine* 22: 2781-2795, 1997

172. Nomura T, Mochida J, Okuma M, Nishimura K, Sakabe K: Nucleus pulposus allograft retards intervertebral disc degeneration. *Clinical Orthopaedics & Related Research* 389: 94-101, 2001

173. O'Conner KC, Enmon RM, Dotson RS, Primavera AC, Clejan S: Characterization of Autocrine Growth Factors, Their Receptors and Extracellular Matrix Present in Three-Dimensional Cultures of DU 45 Human Prostate Carcinoma Cells Grown in Simulated Microgravity. *Tissue Engineering* 3: 161-171, 1997

174. Ohan MP, Dunn MG: Evidence for the Generation of Advanced Glycosylated End Products in Glucose-Incorporated Collagen Exposed to Ultraviolet Irradiation. Society for Biomaterials 28th Annual Meeting Transactions, Tampa, FL, 2002

175. Olde Damink LHH, Dijkstra PJ, van Luyn MJA, van Wachem PB, Nieuwenhuis P, Feijen J: Cross-linking of dermal sheep collagen using a water-soluble carbodiimide. *Biomaterials* 17: 765-773, 1996

176. Otani K, Arai I, Mao G-P, Konno S, Olmarker K, Kikuchi S: Experimental Disc Herniation: Evaluation of the Natural Course. *Spine* 22: 2894-2899, 1997

177. Pedrini-Mille A, Maynard JA, Durnova GN, Kaplansky AS, Pedrini VA, Chung CB, Fedler-Troester J: Effects of microgravity on the composition of the intervertebral disk. *J. Appl. Physiol.* 73: 26S-32S, 1992

178. Pellis NR, Goodwin TJ, Risin D, McIntyre BW, Pizzini RP, Cooper D, Baker TL, Spaulding GF: Changes in gravity inhibit lymphocyte locomotion through type I collagen. *In Vitro Cell. Dev. Biol.--Animal* 33: 398-405, 1997

179. Perka C, Sittinger M, Schultz O, Spitzer R-S, Schlenzka D, Burmester GR: Tissue Engineered Cartilage Repair Using Cryopreserved and Noncryopreserved Chondrocytes. *Clinical Orthopaedics and Related Research* 378: 252-254, 2000

180. Phillips FM, Reuben JM: Intervertebral disc degeneration adjacent to inter-transverse lumbar fusion-an experimental model. International Society for the Study of the Lumbar Spine, Hawaii, 1999, pp 64

181. Pieper JS, Oosterhof A, Dijkstra PJ, Veerkamp JH, van Kuppevelt TH: Preparation and characterization of porous crosslinked collagenous matrices containing bioavailable chondroitin sulphate. *Biomaterials* 20: 847-858, 1999

182. Postacchini F, Bellocci M, Ricciardi-Pollini PT, Modesti A: An Ultrastructural Study of Recurrent Disc Herniation: A Preliminary Report. *Spine* 7: 492-497, 1982

183. Prewett TL, Goodwin TJ, Spaulding GF: Three-Dimensional Modeling of T-24 Human Bladder Carcinoma Cell Line: A New Simulated Microgravity Culture Vessel. *J. Tiss. Cult. Meth.* 15: 29-36, 1993

184. Qi WN, Scully SP: Extracellular Collagens Demonstrate a Type Specific Influence on Cytokine Regulation of Articular Chondrocytes. 42nd Annual Meeting, Orthopaedic Research Society, Atlanta, GA, 1996, pp 308

185. Qiu W, Meaney Murray M, Shortkroff S, Lee C, Martin S, Spector M: Outgrowth of chondrocytes from human articular cartilage explants and expression of alpha-smooth muscle actin. *Wound Repair Regen.* 8: 383-391, 2000

186. Rand N, Juliao SF, Dawson JM, Floman Y, Spengler DM: Age Related Changes in Apoptotic Rate in the Intervertebral Disc-A Murine Model for Disc Degeneration. International Society for the Study of the Lumbar Spine, Hawaii, 1999, pp 123

187. Rich D, Johnson E, Grande D: The Use of Periosteal Cell/Polymer Tissue Constructs for the Repair of Articular Cartilage Defects. 40th Annual Meeting, Orthopaedic Research Society, New Orleans, 1994, pp 241

188. Roberts MP: Complications of Lumbar Disc Surgery. In: *Lumbar Disc Disease*, ed by RW Hardy, Jr., New York, Raven Press, Ltd., 1993, pp 161-170

189. Roberts S, Menage J, Duance V, Wotton S, Ayad S: Collagen Types Around the Cells of the Intervertebral Disc and Cartilage End Plate: An Immunolocalization Study. *Spine* 16: 1030-1038, 1991

190. Rong Y, Sumgumaran G, Silbert JE, Spector M: Proteoglycans Synthesized by Canine Intervertebral Disc Cells Grown in a Type I Collagen-Glycosaminoglycan Matrix. *Accepted by: Tissue Engineering* 2002

191. Rosenstein C, Hardy RW, Jr.: Repeat Operations for Lumbar Disc. In: *Lumbar Disc Disease*, ed by RW Hardy, Jr., New York, Raven Press, Ltd., 1993, pp 171-177

192. Ruan D, He Q, Ding Y, Liang G, Hou L, Li J: Frozen intervertebral allografting -- a primary clinical study. Gene therapy with LMP-1 increases intervertebral disc cell proteoglycan production and changes cell phenotype, Cleveland, 2002, pp 168

193. Rydevik B, Holm S: Pathophysiology of the Intervertebral Disc and Adjacent Neural Structures. In: *The Spine*, ed by RH Rothman, FA Simeone, Philadelphia, W.B. Saunder Company, 1992

194. Saito R, Suh J-K, Nishida K, Evans CH, Kang JD: Nitric Oxide Expression by Bovine Intervertebral Disc Cells. 43rd Annual Meeting, Orthopaedic Research Society, San Francisco, 1997, pp 417

195. Sato M, Kikuchi T, Asazuma T, Yamada H, Maeda H, Fujikawa K: Glycosaminoglycan Accumulation in Primary Culture of Rabbit Intervertebral Disc Cells. *Spine* 26: 2653-2660, 2001

196. Satoh K, Konno S, Nishiyama K, Olmarker K, Kikuchi S: The evidence of IgG binding to the lumbar disc herniated tissues. International Society for the Study of the Lumbar Spine, Hawaii, 1999, pp 210A

197. Schiebler ML, Grenier N, Fallon M, Camerino V, Zlatkin M, Kressel HY: Normal and Degenerated Intervertebral Disk: In Vivo and In Vitro MR Imaging with Histopathologic Correlation. *AJR* 157: 93-97, 1991

198. Schmiedberg SK, Chang DH, Frondoza CG, Valdevit ADC, Kostuik JP: Isolation and characterization of metallic wear debris from a dynamic intervertebral disc prosthesis. *Journal of Biomedical Materials Research* 28: 1277-1288, 1994

199. Schneider PG, Oyen R: Surgical replacement of the intervertebral disc. First communication: Replacement of lumbar discs with silicon-rubber. Theoretical and experimental investigations. *Z. Orthop.* 112: 1078-1086, 1974

200. Schneider T: Personal communication. 1997

201. Schneider TO, Mueller SM, Shortkroff S, Spector M: Expression of alpha-Smooth Muscle Actin in Canine Intervertebral Disc Cells In Situ and in Collagen-Glycosaminoglycan Matrices In Vitro. *JOR* 17: 192-199, 1999

202. Schulz-Torres D: Effects of Modulus of Elasticity of Collagen Sponges on Their Cell-Mediated Contraction In Vitro. Massachusetts Institute of Technology, 1998

203. Schwarz RP, Goodwin TJ, Wolf DA: Cell Culture for Three-Dimensional Modeling in Rotating-Wall Vessels: An Application of Simulated Microgravity. *J. Tiss. Cult. Meth.* 14: 51-58, 1992

204. Seitsalo S, Heikki Ö, Keshkimäki I, Rissanen P: Reoperations After Lumbar Disc Surgery-Regional and Interspecialist Variations: A Population-Based Study. International Society for the Study of the Lumbar Spine, Hawaii, 1999, pp 35

205. Setton LA, Baer AE, Wang JY, Guilak F, Kraus VB: Mechanical Properties of Intervertebral Disc Matrix Synthesized in vitro. International Society for the Study of the Lumbar Spine, Hawaii, 1999, pp 212A

206. Shinmei M, Yamagishi M, Kikuchi T, Shimomura Y: Isolation and culture of the cells from Annulus fibrosus and nucleus pulposus of rabbit intervertebral disc. 34th Annual Meeting, Orthopaedic Research Society, Atlanta, GA, 1988, pp 376

207. Siegel JA, Lonner BS, Grande DA, James T: The Effect of Transforming Growth Factor-Beta on Intervertebral Disc Tissue. International Society for the Study of the Lumbar Spine, Hawaii, 1999, pp 213A

208. Smith JW, Walmsley R: Experimental Incision of the Intervertebral Disc. *The Journal of Bone and Joint Surgery* 33B: 612-625, 1951

209. Songer MN, Rauschning W, Carson EW, Pandit SM: Analysis of Peridural Scar Formation and Its Prevention After Lumbar Laminotomy and Discectomy in Dogs. *Spine* 20: 571-580, 1995

210. Spangfort EV: The Lumbar Disc Herniation: A Computer-Aided Analysis of 2,504 Operations. *Acta Orthopaedica Scandinavica (Suppl.)* 142: 1-95, 1973

211. Spaulding GF, Jessup JM, Goodwin TJ: Advances in Cellular Construction. *Journal of Cellular Biochemistry* 51: 249-251, 1993

212. Stone K, Rodkey W, Steadman J, al. e: Future Directions: Collagen-based prostheses for meniscal regeneration. *Clinical Orthopaedics* 252: 129-135, 1990

213. Stone K, Rodkey W, Webber R, McKinney L, Steadman R: Meniscal regneration with copolymeric collagen scaffolds: In vitro and in vivo studies evaluated clinically, histologically, and biochemically. *The American Journal of Sports Medicine* 20: 104-111, 1992

214. Stone KR, Steadman JR, Rodkey WG, Li ST: Regeneration of a meniscal cartilage with use of a collagen scaffold: Analysis of Preliminary Data. *J. Bone Jt. Surg.* 79-A: 1770-1777, 1997

215. Stringer S, Gallagher J: Heparan sulfate. *Int. J. Biochem. Cell. Biol.* 29: 709-714, 1997

216. Sylvest J, Hentzer B, Kobayasi T: Ultrastructure of Prolapsed Disc. *Acta Orthop. Scand.* 48: 32-40, 1977

217. Takegami K, An H, Kumano F, Chiba K, Sampath TK, Andersson G, Thonar EJ-MA: Effect of Recombinant Osteogenic Protein-1 on Proteoglycan and Collagen Synthesis by Rabbit Intervertebral Disc Cells. International Society for the Study of the Lumbar Spine, Hawaii, 1999, pp 200A

218. Taylor VM, Deyo RA, Cherkin DC, al. e: Low back pain hospitalization: Recent United States trends and regional variations. *Spine* 19: 1207-1213, 1994

219. Thompson JP, Oegema TR, Bradford DS: Stimulation of Mature Canine Intervertebral Disc by Growth Factors. *Spine* 16: 253-260, 1991

220. Tolonen J, Gronblad M, Virri J, Seitsalo S, Rytomaa T, Karaharju E: Transforming growth factor beta receptor induction in herniated intervertebral disc tissue: an immunohistochemical study. *European Spine Journal* 10: 172-176, 2001

221. Trout JJ, Buckwalter JA, Moore KC: Ultrastructure of the Human Intervertebral Disc: II. Cells of the Nucleus Pulposus. *The Anatomical Record* 204: 307-314, 1982

222. Underwood EE: Surface Area and Length in Volume. In: *Quantitavie Microscopy*, ed by RT DeHoff, FN Rhines, New York, McGraw-Hill Book Company, 1968

223. Urban JPG, Holm S, Maroudas A: Diffusion of Small Solute into the Intervertebral Disc: As In Vivo Study. *Biorheology* 15: 203-223, 1978

224. Urbaniak JR, Bright DS, Hopkins JE: Replacement of Intervertebral Discs in Chimpanzees by Silicone-Dacron Implants: A Preliminary Report. *J. Biomed. Mater. Res. Symposium* 4: 165-186, 1973

225. Vaughan PA, Malcolm BW, Maistrelli GL: Results of L4-L5 disc excision alone versus disc excision and fusion. *Spine* 13: 690-695, 1988

226. Vuono-Hawkins M, Zimmerman MC, Lee CK, Carter EM, Parsons JR, Langrana NA: Mechanical Evaluation of a Canine Intervertebral Disc Spacer: In Situ and In Vivo Studies. *Journal of Orthopaedic Research* 12: 119-127, 1994

227. Weadock K, Olson RM, Silver FH: Evaluation of Collagen Crosslinking Techniques. *Biomat., Med. Dev., Art. Org.* 11: 293-319, 1984

228. Weadock KS, Miller EJ, Bellincampi LD, Zawadsky JP, Dunn MG: Physical crosslinking of collagen fibers: Comparison of ultraviolet irradiation and dehydrothermal treatment. *Journal of Biomedical Materials Research* 29: 1373-1379, 1995

229. Weadock KS, Miller EJ, Keuffel EL, Dunn MG: Effect of physical cross-linking methods on collagen-fiber durability in proteolytic solutions. *Journal of Biomedical Materials Research* 32: 221-226, 1996

230. Weber H: Lumbar disc herniation: A controlled, prospective study with ten years of observation. *Spine* 8: 131-140, 1993

231. Wehling P: The use of a combination of PDGF and IL1-ra in the treatment of lumbar disc pain: Pathophysiological background, safety and 6 month clinical experience. International Society for the Study of the Lumbar Spine 29th Annual Meeting, Cleveland, 2002, pp 2

232. Weidner N, Rice DT: Intervertebral Disk Material: Criteria for Determining Probable Prolapse. *Human Pathology* 19: 406-410, 1988

233. Weir BKA: Prospective study of 100 lumbosacral discectomies. *J. Neurosurg.* 50: 283-289, 1979

234. West D, Sattar A, Kumar S: A Simplified in Situ Solubilization Procedure for the Determination of DNA and Cell Number in Tissue Cultured Mammlian Cells. *Analytical Biochemistry* 147: 289-295, 1985

235. Wilke H, Kavanagh S, Neller S, Haid C, Claes L: Effect of a prosthetic disc nucleus on the mobility and disc height of the L4-5 intervertebral disc postnucleotomy. *Journal of Neurosurgery* 95: 208-214, 2001

236. Wing PC, Tsang IKY, Susak L, Gagnon F, Gagnon R, Potts JE: Back Pain and Spinal Changes in Microgravity. *Orthopedic Clinics of North America* 22: 255-262, 1991

237. Wong M: Quantification of Pore Size in Collagen-GAG Artificial Skin. Massachusetts Institute of Technology, Cambridge, 1985

238. Yannas I: Biologically active analogues of the extracellular matrix: Artificial skin and nerves. *Angewandte Chemie* 29: 20-35, 1990

239. Yannas IV, Burke JF: Design of an artificial skin. I. Basic design principles. *Journal of Biomedical Materials Research* 14: 65-81, 1980

240. Yannas IV, Burke JF, Gordon PL, Huang C, Rubenstein RH: Design of an artificial skin. II. Control of chemical composition. *J. Biomed. Mater. Res.* 14: 107-131, 1980

241. Yannas IV, Burke JF, Orgill DP, Skrabut EM: Wound Tissue Can Utilize a Polymeric Template to Synthesize a Functional Extension of Skin. *Science* 215: 174-176, 1982

242. Yannas IV, Lee E, Orgill DP, Skrabut EM, Murphy GF: Synthesis and characterization of a model extracellular matrix which induces partial regeneration of adult mammalian skin. *Proc. Nat'l. Acad. Sci. USA* 86: 1989

243. Yannas IV, Orgill DP, Skrabut EM, Burke JF: Skin Regeneration with a Bioreplaceable Polymeric Template. In: *Polymeric Materials and Artificial Organs*, ed by CG Gebelein, 1984, pp 191-197

244. Yannas IV, Tobolsky AV: Cross-linking of gelatin by dehydration. *Nature* 215: 509-510, 1967

245. Yoon S, Park J-S, Kim K-S, Li J, Huton W, Boden S: Gene therapy with LMP-1 increases intervertebral disc cell proteoglycan production and changes cell phenotype. International Society for the Study of the Lumbar Spine 29th Annual Meeting, Cleveland, 2002, pp 53

246. Zaleskas J, Kinner B, Freyman T, Yannas I, Gibson L, Spector M: Growth Factor Regulation of Smooth Muscle Actin Expression and Contraction of Human Articular Chondrocytes and Meniscal Cells in a Collagen-GAG Matrix. *Experimental Cell Research* 270: 21-31, 2001

Appendices

Appendix A. Type I Collagen Matrix Protocol

Slurry Protocol

1. Cool blenders to 4° C (takes at least 30 min.) using directions on the wall. Steps 2-4 and 6 can be done while waiting. Step 1 of the freeze-drying protocol should also be performed if freeze-drying immediately.

2. Prepare 0.05 M acetic acid if unavailable:
17.4 ml glacial acetic acid + enough distilled water to make 6 L = 6 L of 0.05 M acetic acid
Glacial acid is in the cabinet across from the blenders labeled "acids."

3. Fill the blender with 600 ml of 0.05 M acetic acid. One blender gives enough slurry for 3 sections of 1 freeze-dryer tray.

4. Weigh 3.6 g of dry tendon collagen (kept in the refrigerator). Use right scale.

5. Place collagen in the blender and blend on high for 90 min.

6. Mix 0.32 g chondroitin 6-sulfate (in dessicator in the refrigerator) in 120 ml of 0.05 M acetic acid with magnetic stirrer. Use the left scale for weighing.

7. Add 120 ml of chondroitin 6-sulfate solution over 15 min using the peristaltic pump. Make sure the switch is on "reverse."

8. After the addition, blend the mixture for an additional 90 min. on high.

9. Pour out slurry and refrigerate if not freeze-drying immediately. Slurry can be used for up to one month after making. If longer than a week after making, reblend for 15-30 min. Clean the blender with 0.05 M acetic acid.

10. De-gas the slurry with a vacuum flask for 10-30 min. (latter time for the current machine). Clean the vacuum flask afterwards.

Vitreous Freeze-drying Protocol

1. Drain condenser (tube under condenser). Turn on the freeze button and the condenser button.

2. Wait for shelf to cool down to -45° C (at least 1 hour).

3. Clean the freeze-drying tray with 0.05 M acetic acid. Put the amount of slurry into the long trays based on the thickness you desire below. Avoid bubbles as much as possible and try to pop the ones that form.

"*skin protocol*:" Pour the slurry into the tray if using a pan with one section. If using a pan with 3 sections, pipette the slurry into the sections in equal amounts.
"*1/2 thickness*:" Pipette the slurry into the sections of 2 whole trays (6 sections) in equal amounts.
"*double thickness*:" Pour all the slurry into the half width unsectioned tray.
"*cartilage protocol*:" Pipette 180 mL of slurry per section of a tri-partitioned tray.

4. Wait for approximately 1 hour until the slurry is frozen (or more if it doesn't look frozen). (For a half tray it takes about 1.5 hours.)

5. After the slurry is frozen, turn on the vacuum. First, make sure the chamber release button is off. Once vacuum is on, press door shut. Make sure the door is sealed before leaving. Often the door will not seal and the vacuum will never establish itself - this is not good for the vacuum pump!

6. Once the vacuum is below 200 mtorr (0.5-3 hours depending on the ambient conditions and when the freeze-dryer was last serviced), turn the temperature set to 0° C. Leave both freeze and heat buttons on. Turn on heat button if not previously on. Leave overnight or at least 12 hours for sublimation.

7. Set temperature to 20° C and turn off freeze button. (Leave on heat button.)

8. Turn the DHT temperature setting to slightly past 105° C if DHTing immediately.

9. When the freezer is at 20° C, turn off the heat button, vacuum button, and condenser button. Release the chamber. Remember to drain the condenser chamber. After defrosting, the chamber and condenser should be wiped dry with a paper towel. Don't forget to place the plug back in the drain for the next run.

DHT Cross-linking

After freeze-drying, the thickness of the matrix should measured with a micrometer. Then, the matrix should be placed into the DHT oven for dehydrothermal cross-linking for 24 hours. The conditions of the vacuum oven are 1 atm and 105° C. The matrix sheets are placed in aluminum foil with one end open. Additionally, this can be placed in a tape-sealed autoclave bag for added sterilely when you remove the matrix but it is unclear how this affects the cross-linking. Be careful not to crumple the edges of the matrix sheet. After 24 hours, the matrix should be stored in a dessicator prior to use. The instructions for starting the vacuum on the DHT and purging the oven are on it.

Storage

Unless hydrated, all matrix should be stored in a dessicator with blue desiccant.

Appendix B. Type II Matrix Protocol

Based on procedure developed by Lee (134). Uses Chondrocell type II collagen slurry from Geistlich Biomaterials. Slurry should be stored at 4°C.

Cartilage Protocol Developed by Lee (134)

1. Transfer more than desired amount of slurry to 50 ml centrifuge tube.

2. Centrifuge for 5 minutes at 3500 rpm to de-gas slurry.

3. Pipette slurry into 6-well plate wells. 3.5 mL per well is the standard volume for "cartilage protocol" developed by Lee (134). Resulting pore sizes for this volume and few others are listed in Appendix K. Pipette and release some slurry before doing this because it sticks to the inside of the pipette. Tap/bang plate on countertop to evenly distribute slurry. Remove bubbles with a 1 cc syringe and needle.

4. Freeze-dry (freeze with lids on, remove lids before pulling vacuum) and DHT as for type I CG slurry (see Appendix A)..

GAG and Pore-Size Matched Protocol

This protocol will yield a type II matrix with pore size and GAG content similar to the type I "cartilage protocol" matrix.

1. Add 0.0105 g of chondroitin sulfate (CS) per 20 mL of type II slurry. CS is added by mixing in a beaker with a stir bar on the highest stirrer setting for 20 min. This method works better for 20-50 mL amounts. Some congealing of the slurry occurs at higher volume amounts, slower speeds, and longer mixing times. Results could likely be improved if a rotating attachment to the dremel could be found. It is also good to put ice packets around the beaker to keep it cold.

2. Transfer more than desired amount of slurry to 50 ml centrifuge tube.

3. Centrifuge for 5 minutes at 3500 rpm to de-gas slurry. Some of the slurry may separate after this step. Gently pipette the solution until gross mixing occurs.

4. Pipette 4 mL of slurry into each 6-well plate well. (Each well will yield 6-10 9 mm discs.) Pipette and release some slurry before doing this because it sticks to the inside of the pipette. Tap/bang plate on countertop to evenly distribute slurry. Remove bubbles with a 1 cc syringe/needle.

5. Freeze-dry (freeze with lids on, remove lids before pulling vacuum) and DHT as for type I CG slurry (see Appendix A)..

Appendix C. Hybrid Matrix Protocol

This protocol will yield a 50% type I and 50% type II collagen matrix with pore size and GAG content similar to the type I "cartilage protocol" matrix. Uses Chondrocell type II collagen slurry from Geistlich Biomaterials. Slurry should be stored at 4°C.

1. Re-blend the type I slurry for 20-30 min. in the large blenders if it has been refrigerated for a while.

2. Remove the type II slurry jar from the refrigerator 30 min. prior to use to increase its temperature.

3. Add 20 mL of blended type I slurry per 20 mL of type II slurry. Mix in a beaker with a stir bar on the highest stirrer setting for 30 min. This method works better for 40-80 mL amounts. Results could likely be improved if a rotating attachment to the dremel could be found.

4. Transfer more than desired amount of slurry to 50 ml centrifuge tube. Refrigerate the rest.

5. Centrifuge for 5 minutes at 3500 rpm to de-gas slurry.

6. Pipette 4 mL of slurry into each 6-well plate well. (Each well will yield 6-10 9 mm discs.) Pipette and release some slurry before doing this because it sticks to the inside of the pipette. Tap/bang plate on countertop to evenly distribute slurry. Remove bubbles with 1 cc syringe and needle.

7. Freeze-dry (freeze with lids on, remove lids before pulling vacuum) and DHT as for type I CG slurry (see Appendix A)..

Appendix D. 1-ethyl-3-(3-dimethylaminopropyl)carbodiimide (EDAC) Cross-Linking Protocol

Modified from (134). Based on (175).

General:
6 mmol EDAC/g collagen
5:2 ratio EDAC:NHS
Calculations here are based on 3-4 mm thick 9 mm-diameter CG discs with an estimated mass of 0.005 g each. (Note that different diameter matrices or matrices that weigh differently should use different amounts of EDAC and GAG.)
For 48 9 mm discs use 100 mL of 1.44 mM EDAC and 0.56 mM NHS.

Supplies:
EDAC (Sigma #E-7750; store desiccated in the freezer): MW = 191.7 g/mol
N-hydroxysuccinimide (NHS) (Sigma #H-7377; store desiccated): MW = 116 g /mol

Procedure:
1. Take out EDAC and let warm up one hour prior to use (so that moisture doesn't condense inside bottle when opened – EDAC is moisture sensitive).

2. Weigh out amounts of EDAC and NHS. For 100 mL final solution, use 0.276 g EDAC and 0.064 g NHS.

3. Hydrate matrices in half the final volume (i.e.: for 100 ml final volume, hydrate in 50 ml) of sterile, dH_2O (#15295-017, Life Technologies).

4. Dissolve EDAC and NHS in half the volume of dH_2O water (i.e.: for 100 ml final volume, dissolve in 50 ml; make up fresh for each use). Swish gently until dissolved (few seconds). Do not stir solution.

5. Sterile filter (0.45 μm) into sterile container (or directly into container with hydrated matrices).

6. With combined solution, cross-link at room temperature for 2 hours in 50 mL centrifuge tubes on a rocker. (Note that Lee cross-linked in a petri dish and stirred manually every 15 min.)

7. Rinse in sterile PBS. Change to fresh, sterile PBS and place on rocker for another 2 hours to remove residual uncross-linked EDAC.

8. Rinse 2x10 minutes in sterile dH_2O.

9. Store at 4°C for up to one week before use in sterile dH_2O (effects of longer storage unknown). In practice no one has used EDAC cross-linked matrix more than 2 days after cross-linking.

Appendix E. Papain Digestion

Note: Samples should be lyophilized and their mass determined prior to digestion.

1. Prepare stock solutions (unclear how long good for, 3 months maybe):
   0.5 M Monobasic stock: 6.9 g $NaH_2PO_4 \cdot H_2O$ in 100 mL distilled H_2O
   0.5 M Dibasic stock: 13.4 g $Na_2HPO_4 \cdot 7H_2O$ in 100 mL distilled H_2O
   Make sure to select the correct vials for these solutions. Some have different amounts of water complexed.

2. Prepare papain buffer:
   2.46 ml dibasic stock solution
   17.54 ml monobasic stock solution
   80 ml distilled H_2O

3. On day of digestion, complete papain buffer with:
   87.82 mg L-Cysteine HCl (anhydrous; #C1276, Sigma)
   186.12 mg Disodium Ethylenediamenetetraacetate (EDTA) (#S311-3, Fisher Scientific Co.)
   pH to 6.2 with 10M NaOH (latter is made with 4 g of NaOH/10 mL distilled H_2O) (usually 3-5 drops of latter are required)

4. Digestion:
   a. Determine how much papain (Sigma #P3125) is needed based on mass of samples:

$$\text{maximum sample mass in mg} \times \frac{0.125\text{mg papain}}{6.25\text{mg sample}} \times \frac{1\text{mL}}{23\text{mg protein}} = \text{amount of papain per sample in mL}$$

Equation 6

   b. Add this much papain to each sample (works better if added after next step).
   c. Add as much papain buffer so that each sample as 1 mL of fluid added to it. i.e. a + c = 1 mL.
   d. Vortex or mix thoroughly.
   e. Float tubes in covered 65°C bath overnight.
   f. Sometimes there is some residual left in the tubes. Digestion results may be improved if protease digestion protocols are used.

Appendix F. Spectrophotometric Assay for Sulfated Glycosaminoglycans with Dimethylmethylene Blue

Modified from (21). Based on (57).

1. Prepare of the color reagent.
Dissolve 3.04 g of glycine and 2.37g NaCl in 950 mL of distilled water. Adjust the pH to 3.0 by adding NaOH or HCl. Add additional water to reach 1 L. Add 16 mg of dimethylmethylene blue. This solution is good for 3 months and should be kept in a light-protected bottle.

2. Turn on spectrophotometer at 535 nm and stir the color solution 30 min prior to use. (Turn Deuterium off.)

3. Prepare the chondroitin sulfate standards as following:
   a. Prepare chondroitin sulfate stock solution at 1 mg/mL. Make at least 10 mL.
   b. Dispense 3 mL color reagent to each cuvette (4 optical sides; #67.755, Sarstedt) (only touch the tops of the cuvettes with your hands) with pipettor.
   c. Add the following amounts of the cuvettes for the standards.

Standards (µg)	dH_2O (µL)	CS (µL)
0	100	0
2.5	97.5	2.5
5.0	95	5.0
10	90	10
15	85	15
20	80	20
30	70	30
40	60	40

   Mix each cuvette well.
   d. Read absorbance of blank first and "Set Ref" with this sample.
   e. Run the standards. It is often good to plot the standard curve (Figure 59) immediately before analyzing samples just to make sure you have calibrated correctly.

4. Analyze samples.
   a. Prepare cuvettes by adding 3 mL of color reagent to each cuvette.
   b. Vortex the sample. Add a 100 µL aliquot of the digested sample into 3 mL dye solution, mix well, and read it when the reading stabilizes.
   c. If the reading of your sample is off the standard curve, you need to reduce the volume of sample in the cuvette. Make up the difference with dH_2O. For example, try 50 µL sample and 50 µL dH_2O. Make sure to record how much aliquot was used and how much fluid the aliquot was taken from.

Finding the Percent Mass of GAG

1. The mass of the dry sample should have been weighed prior to digestion.

2. Perform the DMB GAG assay.

3. The chondroitin sulfate control data should be plotted as amount of chondroitin sulfate (in μg) vs. absorbance (in nm). These data should be fitted with a linear equation.

4. The above equation should be used to find the amount of chondroitin sulfate (X) in the samples by putting their absorbance into the equation.

5. The % weight of GAG is calculated by:

$$\frac{X}{\text{mass of sample}} x \frac{\text{amount aliquot taken from (in } \mu\text{L)}}{\text{amount of aliquot used in assay (in } \mu\text{L)}} x100\% \qquad \text{Equation 7}$$

For example,

$$\frac{X(\text{in } \mu g)}{\text{mass of sample (in g)}} x0.000001x \frac{1000\ \mu\text{L}}{100\ \mu\text{L}} x100\%$$

6. If you don't want the % mass of GAG just do the above calculation without dividing by mass to get the GAG in μg.

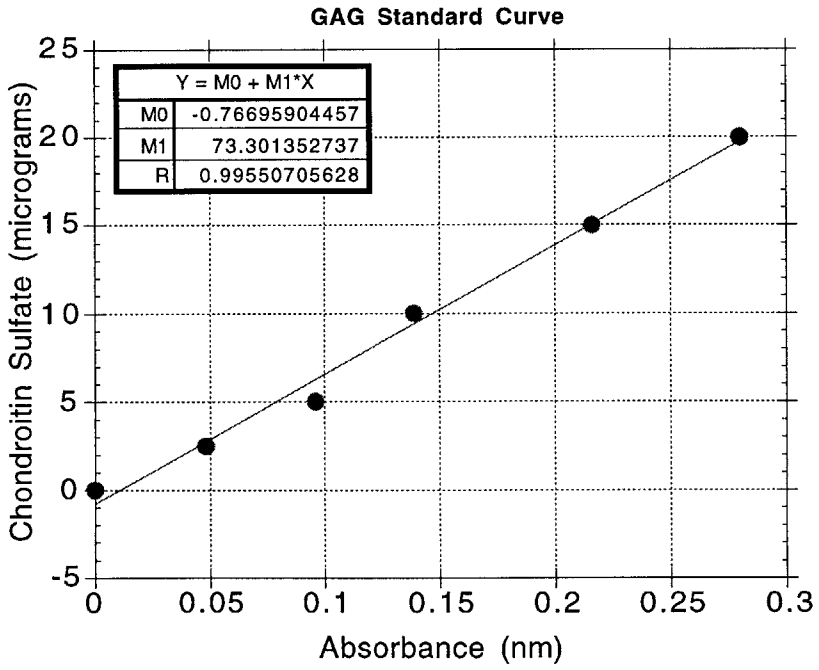

Figure 59. Example GAG Standard Curve

Appendix G. Pore Size Analysis Protocol from JB-4 Sections

Embedding and Sectioning for Pore Analysis

1. Place dry matrix in 100% alcohol overnight at 4°C.

2. Equilibrate for an additional night at 4° C in a solution of 50% ethanol/50% catalyzed JB-4 solution A. (Catalyzation occurs by mixing 9 g of catalyst with 1 L of JB-4 solution A.)

3. Infiltrate in 100% catalyzed JB-4 solution A for 1-4 days at 4° C.

4. Embedding. Combine JB-4 catalyzed solution A:JB-4 solution B at a ratio of 24:1. Mix well and pipette into plastic molds. Place samples face down in plastic molds. Ensure that sample orientation is maintained; you may want to use wooden sticks to maintain orientation and position. Solution begins to harden in approximately 30 minutes. Before hardening is completed (careful- polymerization may progress rapidly once started), place labeled metal embedding blocks in molds. Note: label should be written in standard pencil marking only! Store at 4° C overnight. Pop the blocks from the mold as soon as the next day.

5. Section very slowly at 5 μm on the microtome and then proceed to staining with aniline blue.

Aniline Blue Staining Protocol for JB-4 Sections

Fixation: Formalin

Technique: JB-4 embedded, sectioned at 5 μm

Solutions:
(all %'s are by volume)

Aniline Blue
- 2.5 g aniline blue
- 2 mL glacial acetic acid
- 100 mL distilled water
- Filter before use.

1 % Acetic Acid
- 1 mL acetic acid
- 99 mL distilled water

Staining Procedure:

1. Dip in aniline blue solution for 2-4 min. (generally 2).

2. Place in 1% acetic acid solution for 1 min.

3. Dip 5-10X in 95% alcohol until most of background staining goes away.

4. Dip 5-10X in 100% alcohol.

5. Mount with Cytoseal 60 (Stephems Scientific, Cat. 8310-16, 1-800-831-8099) (4 drops) and coverslip. Try not to get air bubbles.

6. Dry in hood for 1 hour (rather arbitrary). Dry flat for 2 more days (rather arbitrary).

Pore Characterization Parameters (Old Technique Using Old Camera)

Modified from Breinan (21).

Capture Image: (on ORL Microscope computer)

1. Macintosh computer set up:
   - Under the Apple menu, choose Control Panels, then Monitors.
   - choose 32-bit addressing and 24-bit color
   - turn off screen savers

2. Video camera set up
   - Make sure video camera is attached to microscope
   - Arrange sliding eyepiece selector knobs (at level of eyepieces) for TV:
     - Left side slider in "out" position
     - Right side slider in "middle" position
   - Turn Gain and Offset knobs all the way down (counter clockwise)
   - Turn on Hitachi video camera on controller by computer

3) Using the computer to capture the image:
   - Several programs can be used: Scion Image, Ultimage, or Digit
   - Using Scion Image 1.60c to grab video:
     - Adjust light level on microscope so green light on Hitachi is on
     - Choose Start capturing in the Special menu.
     - Turn up gain and offset to get approximate picture on screen.
     - Fine tune image and focus, then click on the image to freeze video.
     - Save image by selecting Save as in the File menu.
     - Use TIFF format. Each image file is about 325K.

Image Clean-Up: (on a faster computer for this and subsequent steps)

1. Open Adobe Photoshop and load image. Save it as the same name with "ed" at the end.

2. Remove any slide artifacts with the eraser.

Make Black and White:

1. Open the "ed" image in NIH Image (or Scion Image on PCs). Save it as the same name with "ed2" at the end.

2. Click on Density Slice in the Options menu. This will highlight the obvious matrix in red, in addition to some extraneous background. Areas that are not red may be manually filled in with the pen, unless of course it is not matrix.

3. Click on Threshold in the Options menu. If a lot of background noise becomes black, go to the palette bar on the left and pull down the threshold level until they disappear.

4. Click on Binary under the Process menu. Click on Make Binary.

5. When all modifications are complete, and you are satisfied with the image, click on Apply LUT in the Process menu. This will provide an image of only black and white (no gray) which will facilitate analysis. Save the image with all the changes.

Pore Analysis:

1. Load the "pore characterization macros" by using Load Macros... under the Special menu. Run Compute Percentage Area [P] under the Special menu. The % value in the little data window is the black percentage of the area, which can be converted to porosity by subtracting it from 100.

2. Select an area of the image with the oval drawing tool. To get a circle, hold the down the shift key at the same time you are using the oval tool. Try to get as much of the image in the selected area as possible.

3. Setting the Scale

Set Scale from the **Analyze** menu. The microscope is calibrated as follows:

Objective magnification	Known Distance (microns)	Pixels
4x	4.13-4.15	1
10x	1.65-1.66	1
20x	0.83	1
40x	0.415-0.417	1
100x	0.166	1

First, change the units to micrometers. In the measured distance box enter 1. In the known distance box, enter the average value from the above table multiplied by 10^{-3}. (This last fixes the fact the program reports the distance values multiplied by 10^{3}.)

4. Run *Linear Intercept* under the **Special** menu. This will produce the pore radii at various angles in the selected area. You must do this before you run the next macro. Run *Plot Intercepts* in the **Special** menu. This will plot the pore radii at the various angle and the calculated best-fit ellipse. Another window will give C0, C1, C2.

Pore Characterization Parameters (New Technique Using New Camera)

Capture Image Using Microscope Camera

1. Follow protocol for Getting Digital Images from Microscope. Use X4 or X10 objective on the microscope, but X4 is better to get more area to analyze.

Photoshop Steps

1. Open Adobe Photoshop and load image. Save it as a jpeg file with the same name with "ed" at the end.

2. Erase bad parts (i.e., garbage that was on the slide). Sometimes it is much easier to erase background staining after step 5.

3. Under the **Adjust** option in the **Image** menu, select **Threshold**. Threshold at 128-135 based on how the image looks, but this could change depending on what light level you selected on the microscope.

4. Under **Mode** option in the **Image** menu, select make **Grayscale**.

5. Under the **Image Size** option in the **Image** menu, change the size so that the height is 480 pixels.

6. Save image.

NIH Image Steps:

1. Open the "ed" image in NIH Image (or Scion Image on PCs).

2. Click on *Threshold* in the **Options** menu. (Yes, you still have to do this even though you did it above.)

3. Click on *Binary* under the **Process** menu. Click on *Make Binary*.

Pore Analysis:

1. Load the "pore characterization macros" by using *Load Macros...* under the **Special** menu. Run *Compute Percentage Area [P]* under the **Special** menu. The % value in the data window is the black percentage of the area, which can be converted to porosity by subtracting it from 100.

2. Select an area of the image with the oval drawing tool. To get a circle, hold the down the shift key at the same time you are using the oval tool. Try to get as much of the image in the selected area as possible. A oval selection can usually do this and results not statistically different from a circle selection.

3. Setting the Scale

Set Scale from the **Analyze** menu. The microscope is calibrated as follows for the X2.5 magnifying objective in the camera and with the image size reduction given above:

Objective magnification		Known Distance (microns)	Pixels
4x	(1 mm = 219.66 pixels)	4.55249	1
10x	(1 mm = 544 pixels)	1.83823	1

First, change the units to micrometers. In the measured distance box enter 1. In the known distance box, enter the average value from the above table *multiplied by* 10^{-3}. (This last fixes the fact the program reports the distance values multiplied by 10^3.)

4. Run *Linear Intercept* under the **Special** menu. This will produce the pore radii at various angles in the selected area. You must do this before you run the next macro. Run *Plot Intercepts* in the **Special** menu. This will plot the pore radii at the various angle and the calculated best-fit ellipse. Another window will give C0, C1, C2.

Calculating Pore Parameters

Transfer the C0, C1, and C2 data to an Excel spreadsheet. It is a very long analysis to get to the major and minor radii of the ellipse (see Hastreiter notebook #III) but the resulting equations are:

$$a = \frac{1}{\sqrt{C_0 + \sqrt{C_1^2 + C_2^2}}} \qquad \text{Equation 8}$$

$$b = \sqrt{\frac{\sqrt{C_1^2 + C_2^2}}{C_0\sqrt{C_1^2 + C_2^2} + C_2^2 - C_1^2}} \qquad \text{Equation 9}$$

$$\text{aspect ratio (AR)} = \max(a,b)/\min(a,b) \qquad \text{Equation 10}$$

$$\text{pore diameter} = 1.5 * 2 * \sqrt{\frac{a^2 + b^2}{2}} \qquad \text{Equation 11}$$

The 1.5 correction factor is necessary because pores are not sectioned through their maximums (72, 73, 222).

Sample Size

Generally, a horizontal (flat) section of matrix and a vertical (side) section of matrix are embedded. The horizontal block is sectioned at mid-thickness because pore size varies with

distance from the freezing pan (large on top, small on the bottom). One slide from each block is stained with aniline blue. 5 images from each slide (10 total) are analyzed for pore parameters and the average is calculated.

Pore Characterization Macros (for NIH Image or ScionImage)

```
macro 'Linear Draw'
{This macro is used for testing different line drawing routines for use
with the macro 'Linear Intercept'}
var
  left,top,width,height,MinDim,nx,ny,i,j,k:integer;
           ThetaStep,NSteps,PI,x1,x2,y1,y2,dy,dx:real;
  Theta,valx,valy,plength,scale,AspectRatio:real;
   IntLength,LineSum:real;
  Intercepts:integer;
   switch,indicator:boolean;
   unit:string;
begin
   GetRoi(left,top,width,height);
   if width=0 then begin
      PutMessage('Selection required.');
      exit;
   end;
   if width<height  then MinDim:=width
      else MinDim:=height;
   PI:=3.141592654;
   GetScale(scale,unit,AspectRatio);
   NSteps:=GetNumber('Enter theta steps between 0 and 90 deg.',3,0);
   ThetaStep:=PI/(2*NSteps);
   for j:=0 to 2*NSteps-1 do begin
      x1:=left;
      y1:=top;
                  Theta:=j*ThetaStep;
     nx:=5*sin(Theta)*width/height;
     ny:=5*abs(cos(Theta));
     for i:=0 to nx do begin
        if Theta=0 then begin
                     x1:=left;
                     x2:=x1+width;
        end  else begin
                     x1:=left+(width*i/(nx+1))+width/(2*(nx+1));
                     x2:=x1+(height*cos(Theta)/sin(Theta));
                  end;
                              y2:=top+height;
                                                  if x2>=left+width then begin
           x2:=left+width;
           y2:=y1+(x2-x1)*sin(Theta)/cos(Theta);
        end  else if x2<left then begin
                               x2:=left;
                              if Theta>PI/2 then y2:=y1+(x2-
x1)*sin(Theta)/cos(Theta);
                            end;
         {plength is the length of the line to be drawn in pixels}
                                                  plength:=sqrt(sqr(x2-
x1)+sqr((y2-y1)/AspectRatio));
```

```
        valx:=x1;
                                                    valy:=y1;
        dx:=(x2-x1)/plength;
        dy:=(y2-y1)/plength;
        switch:=true;
        if plength>=MinDim then begin
                                                    for k:=0 to plength do
              PutPixel(x1+k*dx,y1+k*dy,255);
         end;
     end;
     for i:=1 to ny do begin
        if Theta<=PI/2 then begin
                  x1:=left;
                  x2:=left+width
          end  else begin
                  x1:=left+width;
                  x2:=left;
          end;
        y1:=top+height*i/(ny+1);
        y2:=y1+(width*sin(Theta)/abs(cos(Theta)));
                                                    if y2>top+height then begin
           y2:=top+height;
           x2:=x1+((y2-y1)*cos(Theta)/sin(Theta));
         end;
         {plength is the length of the line to be drawn in pixels}
                                                    plength:=sqrt(sqr(x2-
x1)+sqr((y2-y1)/AspectRatio));
        valx:=x1;
                                                    valy:=y1;
        dx:=(x2-x1)/plength;
        dy:=(y2-y1)/plength;
        switch:=true;
        if plength>=MinDim then begin
                                                    for k:=0 to plength do
              PutPixel(x1+k*dx,y1+k*dy,255);
        end;  {if}
     end;{i}
   end; {j}
end;


macro 'Linear Intercept'
{This macro measures the linear intercept distance over a giver ROI
at intervals of angle}
var
  left,top,width,height,MinDim,nx,ny,i,j,k:integer;
           ThetaStep,NSteps,PI,x1,x2,y1,y2,dy,dx:real;
  Theta,valx,valy,plength,scale,AspectRatio:real;
   IntLength,LineSum,dummy:real;
  Intercepts:integer;
   switch,indicator:boolean;
   unit:string;
begin
   SetOptions('User1;User2');
   GetRoi(left,top,width,height);
   if width=0 then begin
      PutMessage('Selection required.');
      exit;
```

```
   end;
   if width<height  then MinDim:=width
      else MinDim:=height;
   PI:=3.141592654;
   GetScale(scale,unit,AspectRatio);
   NSteps:=18;{GetNumber('Enter # steps between 0 and 90 deg.',3,0);}
   ThetaStep:=PI/(2*NSteps);

{block out next line when doing cumulative measurements}

   SetCounter(2*NSteps);
   SetUser1Label('Theta(rad)');
   SetUser2Label('Lx10^3');
   for j:=0 to 2*NSteps-1 do begin
      LineSum:=0;
      Intercepts:=0;
      x1:=left;
      y1:=top;
                  Theta:=j*ThetaStep;
     nx:=10*sin(Theta)*width/height;
     ny:=10*abs(cos(Theta));
      for i:=0 to nx do begin
        if Theta=0 then begin
                     x1:=left;
                     x2:=x1+width;
        end  else begin
                     x1:=left+(width*i/(nx+1))+width/(2*(nx+1));
                     x2:=x1+(height*cos(Theta)/sin(Theta));
                  end;
                              y2:=top+height;
                                                  if x2>=left+width then begin
           x2:=left+width;
           y2:=y1+(x2-x1)*sin(Theta)/cos(Theta);
        end  else if x2<left then begin
                               x2:=left;
                              if Theta>PI/2 then   y2:=y1+(x2-
x1)*sin(Theta)/cos(Theta);
                            end;
         {plength is the length of the line to be drawn in pixels}
                                                  plength:=sqrt(sqr(x2-
x1)+sqr((y2-y1)/AspectRatio));
        valx:=x1;
                                                  valy:=y1;
        dx:=(x2-x1)/plength;
        dy:=(y2-y1)/plength;
        switch:=true;
        if plength>=MinDim then begin
        LineSum:=LineSum+(plength/scale);
                                                  for k:=0 to plength do begin
              if GetPixel(x1+k*dx,y1+k*dy)>0
                   then indicator:=true
                   else indicator:=false;
              if (switch=true) and (indicator=true) then begin
                  Intercepts:=Intercepts+1;
                  switch:=false;
              end;
              if  (indicator=false) then switch:=true;
           end;
```

```
      end;
     end;
    for i:=1 to ny do begin
        if Theta<=PI/2 then begin
                  x1:=left;
                  x2:=left+width
          end  else begin
                  x1:=left+width;
                  x2:=left;
          end;
        y1:=top+height*i/(ny+1);
        y2:=y1+(width*sin(Theta)/abs(cos(Theta)));
                                                  if y2>top+height then begin
           y2:=top+height;
           x2:=x1+((y2-y1)*cos(Theta)/sin(Theta));
         end;
         {plength is the length of the line to be drawn in pixels}
                                                  plength:=sqrt(sqr(x2-
x1)+sqr((y2-y1)/AspectRatio));
        valx:=x1;
                                                  valy:=y1;
        dx:=(x2-x1)/plength;
        dy:=(y2-y1)/plength;
        switch:=true;
        if plength>=MinDim then begin
        LineSum:=LineSum+(plength/scale);
                                                  for k:=0 to plength do begin
              if GetPixel(x1+k*dx,y1+k*dy)>0
                   then indicator:=true
                   else indicator:=false;
              if (switch=true) and (indicator=true) then begin
                  Intercepts:=Intercepts+1;
                  switch:=false;
              end;
              if  (indicator=false) then switch:=true;
           end;
       end;
     end;{i}
    IntLength:=LineSum/Intercepts;
   dummy:=rUser2[j+1];
    rUser1[j+1]:=180*Theta/PI;

{to do cumulative measurements, type in 'dummy+ before Intlength in the next
line}

    rUser2[j+1]:=IntLength*1000;
   end; {j}
   ShowResults;
end;

macro 'Linear Intercept +'
{This macro measures the linear intercept distance over a giver ROI
at intervals of angle}
var
  left,top,width,height,MinDim,nx,ny,i,j,k:integer;
           ThetaStep,NSteps,PI,x1,x2,y1,y2,dy,dx:real;
  Theta,valx,valy,plength,scale,AspectRatio:real;
   IntLength,LineSum,dummy:real;
```

```
  Intercepts:integer;
   switch,indicator:boolean;
   unit:string;
begin
   SetOptions('User1;User2');
   GetRoi(left,top,width,height);
   if width=0 then begin
      PutMessage('Selection required.');
      exit;
   end;
   if width<height  then MinDim:=width
      else MinDim:=height;
   PI:=3.141592654;
   GetScale(scale,unit,AspectRatio);
   NSteps:=18;{GetNumber('Enter # steps between 0 and 90 deg.',3,0);}
   ThetaStep:=PI/(2*NSteps);

{block out next line when doing cumulative measurements}

   {SetCounter(2*NSteps);}
   SetUser1Label('Theta(rad)');
   SetUser2Label('Lx10^3');
   for j:=0 to 2*NSteps-1 do begin
      LineSum:=0;
      Intercepts:=0;
      x1:=left;
      y1:=top;
                  Theta:=j*ThetaStep;
     nx:=10*sin(Theta)*width/height;
     ny:=10*abs(cos(Theta));
      for i:=0 to nx do begin
        if Theta=0 then begin
                     x1:=left;
                     x2:=x1+width;
        end  else begin
                     x1:=left+(width*i/(nx+1))+width/(2*(nx+1));
                     x2:=x1+(height*cos(Theta)/sin(Theta));
                  end;
                              y2:=top+height;
                                                  if x2>=left+width then begin
           x2:=left+width;
           y2:=y1+(x2-x1)*sin(Theta)/cos(Theta);
        end  else if x2<left then begin
                               x2:=left;
                              if Theta>PI/2 then   y2:=y1+(x2-
x1)*sin(Theta)/cos(Theta);
                            end;
         {plength is the length of the line to be drawn in pixels}
                                                  plength:=sqrt(sqr(x2-
x1)+sqr((y2-y1)/AspectRatio));
        valx:=x1;
                                                  valy:=y1;
        dx:=(x2-x1)/plength;
        dy:=(y2-y1)/plength;
        switch:=true;
        if plength>=MinDim then begin
        LineSum:=LineSum+(plength/scale);
                                                  for k:=0 to plength do begin
```

```
                if GetPixel(x1+k*dx,y1+k*dy)>0
                     then indicator:=true
                     else indicator:=false;
                if (switch=true) and (indicator=true) then begin
                    Intercepts:=Intercepts+1;
                    switch:=false;
                end;
                if  (indicator=false) then switch:=true;
            end;
        end;
      end;
     for i:=1 to ny do begin
         if Theta<=PI/2 then begin
                    x1:=left;
                    x2:=left+width
           end  else begin
                    x1:=left+width;
                    x2:=left;
           end;
         y1:=top+height*i/(ny+1);
         y2:=y1+(width*sin(Theta)/abs(cos(Theta)));
                                                  if y2>top+height then begin
            y2:=top+height;
            x2:=x1+((y2-y1)*cos(Theta)/sin(Theta));
          end;
          {plength is the length of the line to be drawn in pixels}
                                                  plength:=sqrt(sqr(x2-
x1)+sqr((y2-y1)/AspectRatio));
         valx:=x1;
                                                  valy:=y1;
         dx:=(x2-x1)/plength;
         dy:=(y2-y1)/plength;
         switch:=true;
         if plength>=MinDim then begin
         LineSum:=LineSum+(plength/scale);
                                                  for k:=0 to plength do begin
                if GetPixel(x1+k*dx,y1+k*dy)>0
                     then indicator:=true
                     else indicator:=false;
                if (switch=true) and (indicator=true) then begin
                    Intercepts:=Intercepts+1;
                    switch:=false;
                end;
                if  (indicator=false) then switch:=true;
            end;
        end;
      end;{i}
     IntLength:=LineSum/Intercepts;
    dummy:=rUser2[j+1];
     rUser1[j+1]:=180*Theta/PI;

{to do cumulative measurements, type in 'dummy+ before Intlength in the next
line}

     rUser2[j+1]:=dummy+IntLength*1000;
    end; {j}
    ShowResults;
end;
```

```
Macro 'Plot Intercepts'
{This macro plots the linear intercept distance as a function of angle
in cylindrical coordinates
It then finds the best-fit ellipse to a set of linear intercept distance vs.
angle data
using multiple linear regression of the equation Y=C0+C1*X+C2*Z, where
Y=1/L^2 ,  where L is one half  the linear intercept distance at Theta
X=cosine(2*Theta),    Z=sine(2*Theta)
C0=(Mii+Mjj)/2 , C1=(Mii-Mjj)/2 , C2=Mij.
The objective is to solve for M11, Mjj, and Mij
The best-fit ellipse it then plotted on top of the linear intercept
measurements}

var
   left,top,width,height,X0,Y0,X1,Y1,i,n:integer;
   pscale,aspectRatio,dx1,dx2,dy1,dy2,maxdim:real;
   unit:string;
  sumX,sumY,sumZ,sumXZ,sumXY,sumYZ,sumZsqr,sumXsqr:real;
  C0,C1,C2,Mii,Mjj,Mij,Y,X,Z,PI,Theta1,Theta2,L1,L2:real;

begin
  PI:=3.141592654;
 SaveState;
  SetForegroundColor(255);
  SetBackgroundColor(0);
  width:=400;
  height:=400;
  maxdim:=0;
  for i:=1 to rCount do begin
     if rUser2[i]>maxdim then maxdim:=rUser2[i];
  end;
  pscale:=.8*(width+height)/(2*maxdim);
  SetNewSize(width,height);
  MakeNewWindow('Linear Intercepts vs. Theta');
  SetLineWidth(1);
  X0:=(width/2);
  Y0:=(height/2);
  MakeLineROI(0,Y0,width,Y0);
  Fill;
  MakeLineROI(X0,0,X0,height);
  Fill;
   for i:=1 to rCount do begin
     dx1:=pscale*0.5*rUser2[i]*cos(rUser1[i]*PI/180);
     dy1:=pscale*0.5*rUser2[i]*sin(rUser1[i]*PI/180);
     if i<rCount then begin
        dx2:=pscale*0.5*rUser2[i+1]*cos(rUser1[i+1]*PI/180);
        dy2:=pscale*0.5*rUser2[i+1]*sin(rUser1[i+1]*PI/180);
     end else begin
        dx2:=-pscale*0.5*rUser2[1]*cos(rUser1[1]*PI/180);
        dy2:=-pscale*0.5*rUser2[1]*sin(rUser1[1]*PI/180);
     end;
     MoveTo(X0+dx1,Y0+dy1);
     LineTo(X0+dx2,Y0+dy2);
     MoveTo(X0-dx1,Y0-dy1);
     LineTo(X0-dx2,Y0-dy2);
  end;
  n:=rCount;
  sumX:=0;
```

```
  sumY:=0;
  sumZ:=0;
  sumXY:=0;
  sumYZ:=0;
  sumXZ:=0;
  sumZsqr:=0;
  sumXsqr:=0;
  for i:=1 to n do begin
     Y:=1/(sqr(rUser2[i]/2));
     X:=cos(2*PI*rUser1[i]/180);
     Z:=sin(2*PI*rUser1[i]/180);
     sumX:=sumX+X;
     sumY:=sumY+Y;
     sumZ:=sumZ+Z;
     sumXY:=sumXY+(X*Y);
     sumYZ:=sumYZ+(Y*Z);
     sumXZ:=sumXZ+(X*Z);
     sumZsqr:=sumZsqr+sqr(Z);
     sumXsqr:=sumXsqr+sqr(X);
  end;
  C1:=((sumXY*sumZsqr)-(sumXZ*sumYZ))/((sumXsqr*sumZsqr)-sqr(sumXZ));
  C2:=((sumYZ*sumXsqr)-(sumXY*sumXZ))/((sumXsqr*sumZsqr)-sqr(sumXZ));
  C0:=(sumY/n)-C1*(sumX/n)-C2*(sumZ/n);
  for i:=1 to rCount do begin
     Theta1:=rUser1[i]*PI/180;
     if i<rCount then Theta2:=rUser1[i+1]*PI/180
      else Theta2:=rUser1[1]*PI/180;
     L1:=1/sqrt(C0+C1*cos(2*Theta1)+C2*sin(2*Theta1));
     L2:=1/sqrt(C0+C1*cos(2*Theta2)+C2*sin(2*Theta2));
     dx1:=pscale*L1*cos(Theta1);
     dy1:=pscale*L1*sin(Theta1);
     if i<rCount then begin
        dx2:=pscale*L2*cos(Theta2);
        dy2:=pscale*L2*sin(Theta2);
      end else begin
        dx2:=-pscale*L2*cos(Theta2);
        dy2:=-pscale*L2*sin(Theta2);
     end;
     MoveTo(X0+dx1,Y0+dy1);
     LineTo(X0+dx2,Y0+dy2);
     MoveTo(X0-dx1,Y0-dy1);
     LineTo(X0-dx2,Y0-dy2);
  end;
NewTextWindow('Results');
write('C0 = ',C0:8:8);
write('C1 = ',C1:8:8);
write('C2 = ',C2:8:8);
end;


macro 'Count Black and White Pixels [B]';
{
Counts the number of black and white pixels in the current
selection and stores the counts in the User1 and User2 columns.
}
begin
  RequiresVersion(1.44);
  SetUser1Label('Black');
```

```
  SetUser2Label('White');
  Measure;
  rUser1[rCount]:=histogram[255];
  rUser2[rCount]:=histogram[0];
  UpdateResults;
end;


macro 'Compute Percent Black and White';
{
Computes the percentage of back and white pixels in the
current selection. This macro only works with binary images.
}
var
  nPixels,mean,mode,min,max:real;
begin
  RequiresVersion(1.44);
  SetUser1Label('Black');
  SetUser2Label('White');
  Measure;
  GetResults(nPixels,mean,mode,min,max);
  rUser1[rCount]:=histogram[255]/nPixels;
  rUser2[rCount]:=histogram[0]/nPixels;
  UpdateResults;
  if (histogram[0]+histogram[255])<>nPixels
    then PutMessage('This macro requires a binary image.');
end;


macro 'Compute Area Percentage [P]';
{
Computes the percentage of foreground
pixels in the current selection.
}
var
  mean,mode,min,max:real;
  i,lower,upper,fPixels,nPixels,count:integer;
begin
  RequiresVersion(1.50);
  SetUser1Label('%');
  Measure;
  GetResults(nPixels,mean,mode,min,max);
  GetThresholds(lower,upper);
  if (lower=0) and (upper=0) and
     ((histogram[0]+histogram[255])<>nPixels)
     then begin
       PutMessage('This macro requires a binary or thresholded image.');
       exit;
     end;
  if nPixels=0 then begin
  end;
  if (lower=0) and (upper=0) then begin
    if nPixels=0
      then rUser1[rCount]:=0
      else rUser1[rCount]:=(histogram[255]/nPixels)*100;
    UpdateResults;
    exit;
  end;
```

```
  fPixels:=0;
  nPixels:=0;
  for i:=0 to 255 do begin
    count:=histogram[i];
    nPixels:=nPixels+count;
    if (i>=lower) and (i<=upper)
      then fPixels:=fPixels+count;
  end;
  rUser1[rCount]:=(fPixels/nPixels)*100;
  UpdateResults;
end;
```

Appendix H. Getting Digital Images from Microscope

1. Turn on camera via green button on R.

2. Get the SmartCard from the left top drawer. Put the card in the upper slot on the camera's left. The card takes images numbered from 110 down.

3. Switch on the screen.

4. Put the right and left knobs on the microscope to TV settings.

5. Hit the preview button the camera controller. This shows what the actual image recorded will be. Toggle the preview button for fine focusing.

6. Lighten/darken the image with the front turning dial or the back left knob on the microscope.

7. Press expose on the camera controller to take the picture.

8. If something seems odd, check the menu settings of the camera. They should be:
   auto
   SHQ
   1st drive
   100 ISO
   normal
   off
   setup 5s
   SQ 1280 x1024 JPEG
   name reset
   reset yes

The setting visible on the camera controller screen should be SM (can change with the memory button), record auto.

9. Getting the image off of the Smartcard:
   a. Put the card in the flashcard reader.
   b. Open Flash Reader on the computer.
   c. Open DCIM/100olymp.
   d. Images will be number as 1-110. These actually correspond to 110-1 when you were taking the pictures.
   e. Open H drive and put your images there.
   f. Put the Smartcard image files in the recycle bin.

10. Note that there are X2.5 and X3.3 objectives for the camera. Note which is being used.

11. Take images of the ruler slide to get a scale bar for your images.

Appendix I. Unconfined Compressive Stiffness Testing Protocol

Modified from (134). Please see Elliot Frank before doing this. This protocol is rather old because system components have been updated.

General Procedure

1) Specimens: 9-mm diameter disks; hydrated in PBS for 24 hours prior
2) Sequential ramp and hold displacements, corresponding to 1% (4%-10% strain), 2.5% (10-20% strain), or 5% (20-40% strain) strain with stress relaxation occurring over 75 s.
3) Record load and convert to stress
4) Plot stress versus strain and use slope of best-fit line as modulus

Dynastat Set-up

1) Wiring:
   Load cell --> filter
   Filter --> ADC 2 (box below chart recorder)
   Hi-R Displacement (back of Dynastat) --> ADC 3
2) Amplifier Settings:
   Scale 100%
   Zero suppression -0.01 volts
3) Dynastat Servo Settings:
   0 1.0 5.75 5.0 8.3 7.0

Calibration of Dynastat

a) Calibrate load cell
   i) Insert aluminum end of load cell into lower jaw and plug in load cell to filter
   ii) Go to Signals, hit ⇔ (arrows more rounded than this).
   iii) Calibrate by placing 0 g, -1 g, -2 g, -5 g, -10 g, and -50 g masses on the lower platform and hit update. Use tweezers to pick the masses up.
b) Move load cell to upper jaw and insert chamber in lower jaw, tighten small collets, make sure wire on load cell doesn't get caught on anything. Attach plastic plunger to load cell.
c) Push TRIP/RESET button
d) Push CLOSED loop
e) Push PROGRAM OFF
f) Calibrate Displacement
   i) Make sure B is active (also depends on the current set up in the room)
   ii) Set B to COMPRESSION mode (pull knob before turning)
   iii) Put displacement control in Lo-R and read in Hi-R

iv) Push and hold ZERO button, use screwdriver to set to 0.000
v) Push and hold CAL button, use screwdriver to set to 4.945 for right system (5.002 on left system)
vi) Put displacement control in Hi-R and read in Lo-R
vii) Push and hold ZERO button, set to 0.000
viii) Push and hold CAL button, set to 6.692 for right system (5.001 on left system)
ix) Put read in Hi-R (leave control in Hi-R too)

Measuring Matrix Thickness

1. Place PBS in thin-walled small petri dish. Place bottom portion on micrometer (#263M, L.S. Starrett Co.).
2. Place hydrated matrix in petri dish.
3. Adjust level of PBS in petri dish so that it is at the top of the matrix.
4. Slowly lower the micrometer until probe hits water. This is evident when meniscus forms around probe.
5. Record thickness of the matrix specimen after subtracting the thickness of the petri dish. Getting the thickness of the hydrated matrix correct is the key to getting good results.

Placing Matrix in Chamber

a) Set offset under dynssp control menu to 0 (this will be changed later)
b) Push PROGRAM ON on the Dynastat
c) Switch toggle to "transient" (middle) position
d) in DACQSP program control, go to -4 mm
e) Screw down load cell using silver knob at top of testing apparatus until plunger on load cell touches chamber (load cell reading around –29 g) (watch reading on Dynastat).
f) Tighten large collet. Computer reading should be around -1-0 g.
g) Dial knob from 10.0 to 0.0. (The plunger should now be 4 mm above the surface of the chamber.)
h) Set odometer to 999
i) Switch toggle to "Transient" position
j) Change dynproc control offset to 5 mm
k) Set dynproc set-up Hi-R offset to 2x (sample thickness – 4.0)
(ex: Sample thickness = 5.75 mm; 4 mm of thickness is taken from 800 setting in step (e). 5.75-4.0 = 1.75 mm is remaining distance; 2x1.75 = 3.5 → 3.5V should be entered as the offset voltage in the Set-up: Hi-R menu)
l) Read offset voltage of load cell: Set-up: 50 g Load: Read offset
m) Dial scale knob on Dynastat to 10.0
n) Insert matrix, center it as best as possible under plunger
o) Make sure DYN/EXT is on

Computer Set-up

1. Start program *cc.pro* from c:\cyndi directory
2. File menu:
   Open output file under open "file folder symbol"
   Enter sample data (name, description, thickness, area =63.62 mm^2)
   Protocol file should be cc.pro
3. Control menu (set-up ramp, sine, goto commands):
   Waveform: **Ramp/Sine/Goto**
   Acquisition List: **Hi-R, 50g Load**/Hi-R only for Goto
   Iterations: (*whatever is desired*)/1/1
   Iteration hold time: 0
   Ext Scale Setting: **1/0.032/1**
   Offset: Change to 5 mm after matrix in chamber (step 3k)
   Amplitude: (*whatever is desired*)/0/Goto 0
   Control units: **strn/m**
4. Run protocol.
5. To run the next sample, change the matrix in the chamber and start the `cc.pro program at the message "Start here after initial setup ..." 1 @ 0:00` command. Do not close the jaws with a sample inside!

Data Analysis

1. Program output is: Time (s), Displacement (m), Load (g). Each strain setting has a separate output in the file, listed sequentially.
2. Remove any load outliers, like positive deflections from someone hitting the machine for instance.
3. Average the load recorded over the last 30 s for each stress level.
2. Convert these average equilibrium loads to stresses by multiplying by 9.81 m/s^2 and dividing by the area (63.62 mm^2). Convert to Pa.
3. Plot stress versus strain with these results.
4. Apply line fit through data.
5. The slope of the line is the compressive modulus in Pa. If $R^2<0.9$, re-run test.

CC.PRO File

```
# DACQSP Protocol File
program "DACQSP Version 9.8B build 119 (Windows)"
file "C:\Users\Cyndi\Cc.pro"
date "2002/02/07:21:51:37"
protocol begin
(disp,disp:rel) goto 0 m @ 1 mm/s 1 @ 0:00
() message "Initial setup: move to -4mm?" 1 @ 0:00
(disp,disp:rel) goto -4 mm @ 1 mm/s 1 @ 0:00
() message "Close jaws with no sample!" 1 @ 0:00
() message "Start here after initial setup ..." 1 @ 0:00
(disp,disp:rel) goto 4 mm @ 1 mm/s 1 @ 0:00
```

```
() offset disp:rel = 0.008 1 @ 0:00
() offset load = 0 1 @ 0:00
() message "Insert sample!" 1 @ 0:00
(disp:rel) goto 100 % @ 1 mm/s 1 @ 0:00
() offset disp:rel = 0 1 @ 0:00
(disp:rel,load) ramp -4 %/10s/0s s=10/s:0s/0 r=0 max=0 end@90s and hold 1 @ 0:00
(disp:rel,load) ramp -1 %/10s/0s s=10/s:0s/0 r=0 max=0 end@90s and hold 6 @ 0:00
(disp:rel,load) ramp -2.5 %/10s/0s s=10/s:0s/0 r=0 max=0 end@90s and hold 4 @ 0:00
(disp:rel,load) ramp -5 %/10s/0s s=10/s:0s/0 r=0 max=0 end@90s and hold 4 @ 0:00
(disp:rel,load) sine 0 m on=0:00 off=0:00 Ns=256 Nc=2 Nh=4 F=(0) 1 @ 0:00
() message "End of test: hit enter to open jaws!" 1 @ 0:00
(disp,disp:rel) goto 4 mm @ 1 mm/s 1 @ 0:00
end protocol
```

Appendix J. Swelling Ratio Protocol

1. Heat distilled water to 90° C in a beaker on a hot plate. Keep a thermometer in the beaker to adjust the hot plate over time.

2. Place each matrix sample in the water bath for 2 min. in order to denature the collagen and swell it with water. Note that most matrix samples will shrink in size.

3. Water within the pores is expelled by immediately pressing the swollen scaffolds between sheets of filter paper with a 1.0 kg weight placed on top for 20 seconds. Use Whatman #1 (4.25 cm) filter paper which has the same diameter as the 1.0 kg weight (OIML Class M_2; #02-301-5D, Fisher Scientific Co.). The key is to have no water visible on the outer layers of the filter paper after the 20 s. Usually 7 pieces of filter paper on the bottom of the matrix and 4 pieces on top of the matrix fulfills this criteria.

4. Samples are then immediately weighed and the mass recorded as wet mass (WM).

5. Dry samples in the DHT oven overnight at 110° C. It is not necessary to use the vacuum pump but the difference in dry mass is probably minimal.

6. The samples are then weighed and the mass recorded as dry mass (DM).

7. The swelling ratio, defined as the inverse of the volume fraction of dry collagen (V_f), is calculated from the wet and dry weights and the densities of water (ρ_{water} = 1.00 g/cm^3) and collagen (ρ_c=1.32 g/cm^3) as follows:

$$r^* = \frac{1}{V_f} = \frac{\left[\left(DM/\rho_c\right) + \left((WM - DM)/\rho_{water}\right)\right]}{DM/\rho_c} \qquad \text{Equation 12}$$

Modified from (134). Based on (227) and (244).

Matrix #	Date Made	Tray	Shelf	Section	Bad Areas	Type	Volume	Thickness (mm)	% Mass GAG	Pore Diameter (um)	Pore Aspect Ratio	Porosity (%)	Stiffness (Pa)	Manufacturing Notes and Outcome Comments
1						I	regular	2.95 ± 0.44	7.46					made when freezer dryer was not working well
2						I	regular	2.88 ± 0.49	8.28				357 ± 93	made when freezer dryer was not working well, DHT'd + UV cross-linked for 18 hours
3	9/24/98	2	bottom	front	central, front corner	I	regular	4.1 ± 0.38	7.58					
4	9/24/98	2	bottom	middle	central line	I	regular	4.26 ± 0.56	6.85					
5	9/24/98	2	bottom	back	small central edge	I								few bad areas, donated to Alper
6	9/26/98	2	top	front	central side	I	regular	3.53 ± 0.24	7.38					few bad areas
7	9/26/98	2	top	middle	central line	I	regular	4.03 ± 0.65	8.03	245 ± 26	1.67 ± 0.14	90.5 ± 0.9		
8	9/26/98	2	top	back	central	I	regular	3.90 ± 0.57	10.63					
9	10/1/98	4	bottom	front	central front	I								
10	10/1/98	4	bottom	middle	central back	I	regular		6.95	258 ± 64	1.11 ± 0.11	89.6 ± 4.7	266 ± 51	DHT'd + UV cross-linked for 16 hours
11	10/1/98	4	bottom	back	small edge	I	regular	2.8 ± 0.57	8.28	312 ± 48	1.30 ± 0.24	92.1 ± 2.5	272 ± 138	few bad areas
12	10/4/98	2	bottom	front	center, front corner	I	1/2 thickness	2.1 ± 0.49	10.40					
13	10/4/98	2	bottom	middle	central line	I	1/2 thickness	1.60 ± 0.42	10.29					
14	10/4/98	2	bottom	back	front central edge	I	1/2 thickness		8.74					
15	10/4/98	4	top	front	back central, side	I	1/2 thickness		9.51					
16	10/4/98	4	top	middle	central line	I	1/2 thickness	1.68 ± 0.69	11.49	170 ± 127	1.42 ± 0.05	87.3 ± 1.0		
17	10/4/98	4	top	back	central	I	1/2 thickness	2.51 ± 0.24	10.37					
18	2/21/99	2	bottom	back		Chondrocell II	regular							Geistlich new slurry frozen at 20°C
19	2/28/99	2	bottom	back		Chondrocell II	regular	4.63 ± 1.18	0.46 ± 0.20					Geistlich new slurry frozen at 30°C
20	6/12/99	2	top	back	central	Chondrocell II								same protocol as type I except used type II and 1/3 batch size, did not blend well with smaller volume, very thin, pore size looks normal with some large pores
21	6/12/99	4	bottom	middle	central	Chondrocell II								same protocol as type I, added 225-250 mL, pore size was big, matrix very thin
22	6/12/99	4	bottom	back	central	hybrid	236 mL	3.33 ± 0.68						same protocol as type I except 50%/50% type I/II, degassed for 45 min, since more bubbles, thickness on low end, pore size large but may be OK near bad area
23	7/2/99	2	bottom	back	few	hybrid, Chondrocell I	270 mL	3.54 ± 0.82		256 ± 33	1.07 ± 0.07	90.4 ± 2.7		same slurry as 22, rebended and degassed, prefroze the tray, pore size too big overall
24	7/21/99	2	top	back		I	~350 mL							Sigma II, prefroze tray, "Bec" area pore size and thickness looks correct
25	7/23/99	4*centrifuge tube	top			I	90 mL	1.8-2.7						Put in nerve guide freezing bath at -60-70°C; matrix sticky; pore size close but maybe too small; lyophilized for 48 hrs.
26	7/23/99	4*centrifuge tube	top			I	90 mL	1.7-2.6						Put in liquid Nitrogen; pore size too small;matrix cracked; lyophilized for 48 hrs.
27	7/23/99	4*centrifuge tube	top			I	90 mL	2-2.3						Put in liquid Nitrogen and pre-cooled pan; pore size too small;matrix cracked; lyophilized for 48 hrs.
28	7/23/99	4*centrifuge tube	top			I	90 mL	1.8-2.2						Put in nerve guide freezing bath at -70-80°C and pre-cooled pan; matrix sticky; pore size close but maybe too small; lyophilized for 48 hrs.
29	7/31/99	4*centrifuge tube	top			I	22 mL	2.66 ± 0.34						Put in nerve guide freezing bath at -60°C; thinner in middle; has skin
30	7/31/99	4*centrifuge tube	top			I	22 mL	2.47 ± 0.31						Put in nerve guide freezing bath at -50°C; has skin
31	7/31/99	4*centrifuge tube	top			I	22 mL	2.73 ± 0.47						Put in nerve guide freezing bath at -40°C; has slight skin
32	7/31/99	4*centrifuge tube	top			I	22 mL	2.81 ± 0.17						Put in nerve guide freezing bath at -30°C; has slight skin on top
33	8/6/99	4*centrifuge tube	top			I	30 mL	2.69 ± 0.62		232 ± 71	1.08 ± 0.06	88.9 ± 1.7		put in nerve guide freezing bath at -30°C; bottom has small pores; skin on top that can be torn off
34	8/6/99	4*centrifuge tube	top			I	30 mL	3.12 ± 0.56						put in nerve guide freezing bath at -20°C; bottom has somewhat small pores; skin on top
35	9/1/99	4*centrifuge tube	top			I	33 mL	2.71 ± 0.94						put in pre-cooled tube in -25°C freezer, skin on top, very soft, pores look OK
36	9/1/99	4*centrifuge tube	top			I	33 mL							put in tube in -25°C freezer; pore size large, looks like those done in Virtis
37	9/1/99	4*centrifuge tube	top			hybrid	50 mL							put in pre-cooled tube in -25°C freezer; skin on bottom that can be pulled off, pores large
38	9/1/99	4*centrifuge tube	top			hybrid	50 mL							put in tube in -25°C freezer, large pores
39	9/1/99	1/2 tray	bottom			hybrid	406 mL							put in pre-cooled tray in -25°C freezer, does not have uniform thickness, pore size large
40	10/28/99	2	bottom	back		hybrid	241 mL	3.88 ± 1.05						pre-cooled try in freeze dryer, degassed for 40 min.; pore size too big overall
41	10/28/99	4*centrifuge tube	bottom	front		I	45 mL							same slurry as 35; put in pre-cooled tube in -25°C freezer, pores too large
42	10/28/99	4	top	front	middle side	I	regular							
43	10/28/99	4	top	middle	middle central	I	regular	2.55 ± 0.35						
44	10/28/99	4	top	back	large central	I	regular							
45	11/7/99	2	bottom	back		hybrid	245 mL	4.25 ± 0.93						pre-cooled tray, added slurry directly in freeze dryer, degassed for 20 min.; pores too big; bilayer where slurry initially touched frozen pan
46	11/10/99	4*centrifuge tube	top			I	35 mL	3.55 ± 1.37						put in nitrogen freezing bath at -25°C; top pore size larger but bottom OK
47	11/10/99	4*centrifuge tube	top			I	35 mL	3.20 ± 0.57						put in nitrogen freezing bath at -20°C; top pore size larger; had skin on top which could be pulled off
48	11/10/99	4*centrifuge tube	top			I	35 mL	3.10 ± 0.80						put in nitrogen freezing bath at -30°C; pore size good
49	12/2/99	4*centrifuge tube	top			hybrid	40 mL							put in nitrogen freezing bath at -25°C, too thick, pore size appears too small
50	12/2/99	4*centrifuge tube	top			hybrid	40 mL							put in nitrogen freezing bath at -20°C, too thick, pore size appears too small
51	12/2/99	4*centrifuge tube	top			hybrid	40 mL							put in nitrogen freezing bath at -30°C, too thick, pore size appears too small
52		pan				I	regular	3.10 ± 0.14					993 ± 220	made by Rong, cross-linked by DHT for 72 hr, and UV x-link for 18 hours and EDAC for 2 hours
100	10/3/01	2	bottom	back	virtually none	I	180 mL	2.79 ± 0.30	6.30	215 ± 34	1.09 ± 0.11	93.4 ± 1.6		used slurry made by Brendan 2 mo. ago, needed to degas for 20 min. after rebending for 30 min.
101	10/9/01	6-well plate	bottom	back		II, Chondrocell	2.75 mL	2.06 ± 0.29	1.49	113 ± 4	1.17 ± 0.23	85.5 ± 0.3		used Chondrocell slurry (0.7%) batch # 001511
102	10/9/01	6-well plate	bottom	back		II, Chondrocell	3 mL	2.17 ± 0.40	0.92					used Chondrocell slurry (0.7%) batch # 001511
103	10/9/01	6-well plate	bottom	back		II, Chondrocell	3.25 mL	2.35 ± 0.63	2.11					used Chondrocell slurry (0.7%) batch # 001511
104	10/9/01	6-well plate	bottom	back		II, Chondrocell	3.5 mL	2.48 ± 0.52	1.23	125 ± 42	1.10 ± 0.05	88.7 ± 2.0		used Chondrocell slurry (0.7%) batch # 001511
105	10/9/01	6-well plate	bottom	back		II, Chondrocell	3.75 mL	2.60 ± 0.44	1.19					used Chondrocell slurry (0.7%) batch # 001511
106	10/9/01	6-well plate	bottom	back		II, Chondrocell	4 mL	2.91 ± 0.17	1.38					used Chondrocell slurry (0.7%) batch # 001511
107	10/9/01	6-well plate	bottom	back		II, Chondrocell	4.25 mL	2.82 ± 0.32	1.31	126 ± 39	1.01 ± 0.01	88.0 ± 1.7		used Chondrocell slurry (0.7%) batch # 001511
108	10/9/01	6-well plate	bottom	back		II, Chondrocell	4.5 mL	3.10 ± 0.47	1.15	120 ± 25	1.02 ± 0.02	85.8 ± 6.0		used Chondrocell slurry (0.7%) batch # 001511
109	11/30/01	6-well plate	bottom	back		II, Chondrocell	4 mL	2.99 ± 0.38	4.253 ± 0.51	164 ± 45	1.11 ± 0.17	90.9 ± 2.4		added 0.0085 g chondroitin sulfate to 20 mL slurry, mixed with pipette
110	11/30/01	6-well plate	bottom	back		II, Chondrocell	4 mL	2.66 ± 0.64	4.04 ± 0.79					added 0.0043 g chondroitin sulfate to 20 mL slurry, mixed with pipette
111	11/30/01	6-well plate	bottom	back		II, Chondrocell	4 mL	2.57 ± 0.38	2.58 ± 0.38					added 0.0020 g chongroitin sulfate to 20 mL slurry, mixed with pipette
112	11/30/01	6-well plate	bottom	back		II, Chondrocell	4 mL							
113	12/2/01	6-well plate	bottom	back		hybrid,Chondrocell II	4 mL	2.83 ± 0.47	5.38 ± 0.65	243 ± 66	1.16 ± 0.17	91.6 ± 2.2		mixed for 30 min. with stir bar
114	1/8/02	6-well plate	bottom	back		II, Chondrocell	4 mL	2.83 ± 0.28	6.68 ± 0.66					added 0.0088 g CS to 20 mL slurry, stirred for 20 min. with stir bar, froze at -30° C, solvent separation after centrifugation
115	1/8/02	6-well plate	bottom	back		II, Chondrocell	4 mL	2.65 ± 0.45	11.56 ± 0.42	248 ± 89	1.02 ± 0.04	92.1 ± 1.1		added 0.0106 g CS to 20 mL slurry, stirred for 20 min. with stir bar, froze at -30° C, solvent separation after centrifugation
116	1/8/02	6-well plate	bottom	back		II, Chondrocell	4 mL	2.65 ± 0.45						added 0.0085 g CS to 20 mL slurry, stirred by pipetting, froze at -30° C, solvent separation after centrifugation; pore size too large
117	1/8/02	6-well plate	bottom	back		II, Chondrocell	4 mL	2.80 ± 0.22						added 0.0105 g CS to 20 mL slurry, stirred by pipetting, froze at -30° C, solvent separation after centrifugation; pore size too large
118	1/7/02	6-well plate	top	front		hybrid,Chondrocell II	4 mL	2.37 ± 0.24	4.4 ± 0.17					same slurry as matrix 113, restirred for 10 min.
119	1/7/02	6-well plate	top	front		hybrid,Chondrocell II	4 mL	2.83 ± 0.21	6.14 ± 0.03	266 ± 35	1.14 ± 0.14	92.0 ± 1.1		20 mL type I slurry + 20 mL Chondrocell type II slurry + 0.0085 g CS, stirred with stir bar for 30 min.
120	1/7/02	2	bottom	back	central front side	I	180 mL	3.04 ± 0.27	7.89 ± 0.70*	204 ± 37	1.31 ± 0.29	92.1 ± 1.4		pore size seemed large on the back side
121	1/7/02	8.7 cm petri dish	top	front		hybrid,Chondrocell I	23.4 mL	2.66 ± 0.36						20 mL type I slurry + 20 mL Chondrocell type II slurry + 0.0085 g CS, stirred with stir bar for 30 min.; pore size too large except outer ring
122	1/8/02	6-well plate	bottom	back		type II Chondrocell	4 mL	3.11 ± 0.55	6.31 ± 0.07					type II Chondrpll at -35°C with 0.0085 g CS added to 20 mL II slurry, stirred for 20 min. with stir bar; separated with centrifugation
123	1/8/02	6-well plate	bottom	back		type II Chondrocell	4 mL	3.16 ± 0.28	6.44 ± 0.75					type II Chondroll at -35°C with 0.0105 g CS added to 20 mL II slurry, stirred for 20 min. with stir bar; separated with centrifugation
124	1/29/02	1/2 tray	top	front	large central + side	type I	276 mL	3.11 ± 0.38	6.39 ± 0.80	297 ± 58	1.25 ± 0.23	94.7 ± 1.8		from this point on did not DHT in autoclave bag
125	1/29/02	6-well plates	top	front		hybrid,Chondrocell II	4 mL	2.3 ± 0.83	6.17 ± 1.27	285 ± 43	1.08 ± 0.03	93.9 ± 1.2		20 mL type I slurry + 20 mL Chondrocell type II slurry + 0.0105 g CS, stirred with stir bar for 30 min.; pores looked reasonable except for a few areas
126	1/30/02	6-well plates	top	front	a few areas	type II Chondrocell	4 mL	2.71 ± 0.53	4.85 ± 0.05	202 ± 51	1.12 ± 0.14	91.2 ± 2.1		20 mL chondrocell slurry + 0.0105 g CS stirred for 20 min. with stir bar, ice packets around jar
127	1/30/02	6-well plates	top	front	many bad areas	hybrid,Chondrocell II	4 mL	2.31 ± 0.48	3.02 ± 1.24	209 ± 18	1.13 ± 0.08	92.2 ± 1.4		20 mL type I slurry + 20 mL type II slurry (set jar out for 30 min.) stirred for 30 min. with stir bar
128	1/30/02	2	bottom	back	front side central	I	180 mL	2.81 ± 0.48	5.49 ± 0.88					
129	2/10/02	6-well plates	bottom	back	one well bad	type II Chondrocell	4 mL	2.46 ± 0.37	9.56 ± 3.08					20 mL chondrocell slurry + 0.0105 g CS stirred for 20 min. with stir bar, ice packets around jar; first batch with new jar, no separation
130	2/11/02	6-well plates	bottom	back		type II Chondrocell	4 mL	2.92 ± 0.65	8.01 ± 1.12					(20 mL chondrocell slurry + 0.0105 g CS)*2.5*2, 25 min. with stir bar, ice packets around jar; a lot of compressed slurry with this volume and stir time; got 16 wells
131	2/11/02	6-well plates	bottom	back		hybrid,Chondrocell II	4 mL	2.49 ± 0.41	6.88 ± 0.41					(20 mL type I slurry (mixed for 20 min.) + 20 mL type II slurry (set jar out for 30 min.))*2.5*2 stirred for 30 min. with stir bar; got 21 wells

Key:
Regular="skin thickness"
II=Sigma type II
hybrid=50% type I/50% Sigma type II
hybrid, Chondrocell=50% type I/50% Chondrocell II

* Became 7.99 ± 0.38 after 2 hours of EDAC cross-linking.

Appendix L. Annulus Tissue Extraction, Explant Procurement, and Digestion Protocols

Places to Call for Dogs

• NEMC Surgical Research Center
Director: Dr. Ray Connelly
Assistant: Mary Boucher 636-5613 pager: 2563
facility number: 636-5696 Barbara
Directions: 800 Washington St. Enter at main entrance. Take the winding stairs on the left. Take the yellow elevators to the 2nd floor. Go up the stairs to the Pratt Building. Go down the hall. Just past the elevators, go up the stairs on the left to the Ziskind Building. Go through the doors and take a left through Otolaryngology Research to reach Surgical Research.
• Harvard Medical School Animal Facility Dr. Agelene Warner 432-0888
She usually knows who at Harvard will be sacrificing animals.
• Harvard Institutes of Medicine Dr. Contrares 667-0099
• Dr. Michelle Laghy orders dogs for lung harvests 432-2319

Equipment for Harvest

Surgical instruments:
- automatic retractors
- elevators
- deep retractors
- chisel
- hammer
- scalpel handles (#3)
- four towel clamps
- pickups, forceps
- saw case, saw, battery charger, batteries (last needs to be charged but not sterile)

Supplies:
- gauze
- drapes (4)
- iodine scrub brushes
- iodine squeeze bottle
- blades (#10)
- sterile gloves (Dr. Hsu wears 8)
- hats
- booties
- masks
- scrubs
- sterile gowns
- sterile containers (glass jar for entire lumbar spine, centrifuge tubes for discs only)

- 2 bottles of "complete" PBS
- Dulbecco-phosphate buffered saline (D-PBS)
- Antibiotic-antimycotic solution (Gibco-BRL No. 15240-096, Life Technologies) (5 mL/500 mL bottle of PBS)
- cooler with ice

Harvest Instructions

1. Shave the spinal area very close to the skin.
2. Set up sterile instruments on a table.
3. Put on scrubs, sterile gown, and two pairs of sterile gloves.
4. Wash the area--4 Betadine scrubs and brush in one direction.
5. Incise the skin. Hold back the skin with an automatic retractor. Don't touch the skin again.
6. Dissect through the fascial layers. Dissect off the paravertebral muscles.
7. Use the saw or hammer and chisel to cut through the L1 vertebrae, the L6 vertebrae, and the transverse processes.
8. Remove the spine segment with containing 6 vertebrae and five lumbar discs en bloc (Figure 60).
9. A nonsterile person gets the sterile container filled with "complete" PBS and puts in the sample. Often the spinous processes need to be removed to fit the spinal segment in the glass jar with PBS. Seal the container with paraffin and place in the ice-filled cooler.
10. Discard the dog in 2 bags.
11. Grossly clean the blood off the instruments. Perform a more detailed cleaning when back at lab. Reautoclave the instruments for the next use.

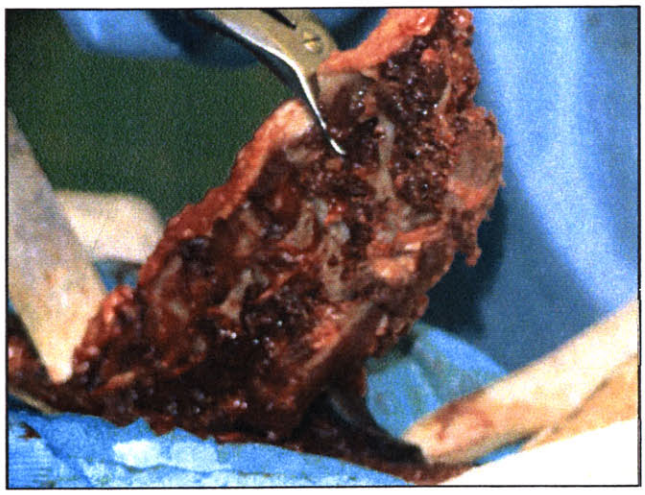

Figure 60. Demonstration of *En Bloc* Removal of a Canine Lumbar Spine

Equipment for Dissection

All instruments, boards, and Petri dishes should have been autoclaved.

- scalpel handles (#4)
- spatulas
- blades (#21 or #22)
- 2 cutting boards
- 3 glass Petri dishes
- forceps (5)
- "complete" PBS
- 5 mm-diameter dermal skin punch (Keyes #33-25)
- hammer
- biohazard bag
- fixative
- specimen cups
- complete medium

Dissection Instructions

1. Sign up for a hood prior to receiving any tissue.
2. Wear a mask. Wash hands and arms and use sterile gloves.
3. Lay down a sterile half-drape.
4. Specimen cups filled with formalin should be prepared ahead of time. Any matrix specimens should be prepared ahead of time.
5. The spinal specimen should be stored in the cooler in the cold room until the area is prepared. Generally, dissection should take place within 4 hours of harvest.
6. All Petri dishes should be filled with 25-50 mL of cold "complete" PBS. Dissect discs off of spine (Figure 61). Place the discs in a glass Petri dish for a minimum of 10 min.
7. Any spine remnants should be placed in a biohazard bag.

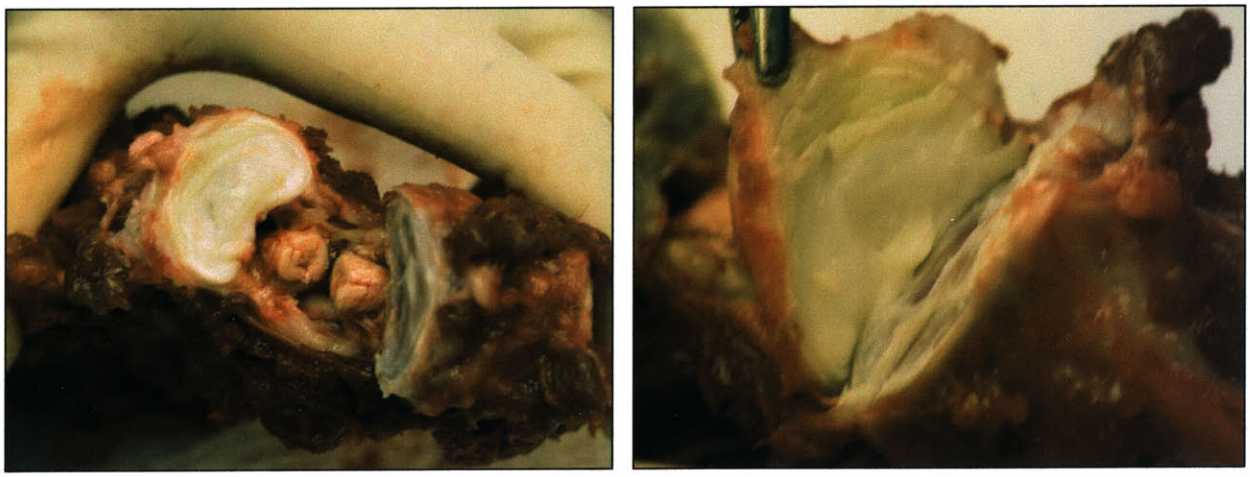

Figure 61. Demonstration of Detaching the Intervertebral Disc as a Whole from the Spine

Left image shows one side of the disc being separated from one adjacent vertebrae and the surrounding spinal structures being cut to open up the space. Right image demonstrates the disc being extracted from the other adjacent vertebrae as a whole.

8. Switch cutting boards, scalpels, and forceps at this point.
9. Dissect the nucleus and ligaments off of the discs. Place the annulus pieces in the 2nd petri dish for 10 min.
10. Here the protocol diverges depending on what you want to do with the tissue.

Explants

11. The annulus tissue should first be bisected along its thickness to make thinner explants, generally 2-3 mm thick. Then use the punch (5 mm-diameter dermal punch), hammer, cutting board, and scalpel to make explants if desired. Remember to fix some tissue for histology.
12. Soak the explants in a third round of Petri dishes for a minimum of 10 min.
13. Place explants in culture dishes or on matrices.
14. Wait 5-10 minutes before adding complete medium for adhesion. Place specimens in animal incubator. Instruments should be cleaned in the following manner.
15. Wipe off any tissue pieces and blood in the hood, discarding the towels in the biohazard bag. Soak the instruments in a 10% bleach solution for 10 min. (Do not leave the instruments in bleach for long because they will rust.) Wash the instruments off with tap water. Soak in a 10% 7X solution for at least 10 min. Wash with distilled water. Place in sealed autoclave bags and autoclave.

Tissue to be Digested

11. Remember to fix some tissue for histology. The annulus remnants are cut into as small pieces as possible, approximately 1 mm^3 is desired.
12. These tissue pieces are spatula'd into the third Petri dish for 10 min. of soaking. They are then ready for digestion.
13. Instruments should be cleaned in the following manner. Wipe off any tissue pieces and blood in the hood, discarding the towels in the biohazard bag. Soak the instruments in a 10% bleach solution for 10 min. (Do not leave the instruments in bleach for long because they will rust.) Wash the instruments off with tap water. Soak in a 10% 7X solution for at least 10 min. Wash with distilled water. Place in sealed autoclave bags and autoclave.

Equipment for Annulus Digestion

- 70 µm nylon cell strainers (sterile)
- specially prepared blue pipette tips (autoclaved)
- Pasteur pipettes (autoclaved)
- micropipette tips with extenders (autoclaved)
- micropipetter
- 4% trypan blue solution
- 50 mL centrifuge tubes
- complete medium
- Collagenase (355 U/mg, type IA; #C9891, Sigma)

- D-PBS
- trypsin (0.05%) + EDTA (0.53 mM) 4Na
- spatulas (autoclaved)
- Antibiotic-antimycotic solution (Gibco-BRL No. 15240-096, Life Technologies)
- DMEM/F12 medium

Annulus Digestion

1. Enzymatic digestion must take place no longer than 4-6 hours following harvest. The tissue and PBS in the Petri dishes are placed in 50 mL centrifuge tubes (try to suction the PBS out of the Petri dishes with non-vacuum pipettes and use the spatula to transfer the pieces to the tube).
2. These are spun for 1-2 min. The PBS in removed and the tissue is rinsed twice more with complete PBS in the same manner.
3. For 5 lumbar discs, 2 50 mL centrifuge tubes are filled with 50 mL of trypsin-EDTA. They should be weighed prior to use and after the tissue is added so that you can determine how much tissue mass was digested. The tissue is then transferred to the trypsin tubes.
4. Once all the pieces are put into the tubes, the tubes are fixed with tape to a shaker in the incubator at 37°C and 5% CO_2. After one hour with young porcine cells and up to two hours with adult canine cells the shaker and the tubes are taken out of the incubator. The tissue should look as if it was glued together, but it must not be in the trypsin longer than two hours even if the changes to the tissue are not obvious.
5. During incubation in the trypsin, the collagenase solution is prepared. 100 mL of solution requires 99 mL of medium, 1 mL of antibiotic solution (Gibco-BRL No. 15240-096, Life Technologies), and 0.2 g of collagenase. The collagenase solution should be stored at 4° C until needed.
6. The trypsin is then sucked out of the tubes carefully with a pipette and the tissue is washed in the tubes with PBS 3 times using the centrifuge.
7. 50 mL of collagenase solution is now added to each tube, and the filled tubes are again fixed to the shaker and put into the incubator for another three hours. (Digestion for longer than this has been tried and is futile.) The solution should now have lost some of its transparency and the visible tissue volume should be reduced to approximately 1/3. One can now assume that the digestion is complete.
8. The whole solution is then filtered through sterile 70 μm cell strainers in new 50 mL centrifuge tubes. (Saving the residual tissue pieces has been tried and is also futile.) The solutions are centrifuged at room temperature for 10 minutes at 1500 rpm.
9. The supernatant is decanted and the pellet is resuspended in 20-25 mL of complete medium. This procedure is repeated twice. At some point, the tubes are combined. 100 μL is removed from the cellular solution for cell counting (Appendix U). After the last centrifugation, the pellet is resuspended at a concentration which suits the desired concentration for culture or freezing.
10. Freezing the cells immediately after digestion often has poor results (i.e. low yield upon thawing). For 75 cm^2 tissue culture flasks, the digested cells should be plated at 2 million cells per flask. Medium should be changed when most of the cells have adhered and only dead cells are floating in the medium. This usually happens after 4-5 days, but cells may need up to 7 days before medium change for adherence. Do not wait longer than this as the dead cells will release mediators which inhibit cell proliferation.

Appendix M. Intervertebral Disc Cell Culture Medium Protocol

Old Protocol

This medium is the same as the new protocol (see below) except for the antibiotics. You add the following together:

- 420 mL DMEM/F12 medium (#11320-033, Life Technologies)
- 10 mL Penicillin (100 U/mL) and Streptomycin (100 µg/mL) (#15070-063, Life Technologies)
- 5 mL Fungizone (2.5 µg/mL; #15295-017, Life Technologies)
- 10 mL L ascorbic acid phosphate (magnesium slat n-hydrate; #D13-12061, Wako Chemicals USA, Inc.) (0.0125 g dissolved in 10 mL DMEM/F12)
- 5 mL L-glutamine (#25030-081, Life Technologies)
- 50 mL fetal bovine serum (Austrailian FBS; #SH30084.03, Hyclone Laboratories) (heat inactivated at 56°C for 30-45 minutes)

New Protocol

General

The following steps should be performed under sterile conditions. These directions are for preparing 500 mL of complete cell culture medium (DMEM/F12, 10-20% FBS, 1% antibiotics, 1% L-glutamine, and 25 µg/ml of ascorbic acid).

Materials

DMEM/F12 medium (#11320-033, Life Technologies)
Heat Inactivated FBS (Austrailian FBS; #SH30084.03, Hyclone Laboratories)
Antibiotic-Antimycotic solution (Gibco-BRL No. 15240-096, Life Technologies)
L-glutamine (#25030-081, Life Technologies)
L ascorbic acid phosphate (magnesium slat n-hydrate; #D13-12061, Wako Chemicals USA, Inc.)
Sterile glass bottle
Pipettes
Pipette Aid
Flame

Methods

1. Thaw all frozen and refrigerated solutions for 30 minutes in a 37° C water bath.

2. Remove 70 or 120 mL (for 10 or 20% FBS medium, respectively) of DMEM/F12 from the 500 mL bottle and place into another sterile container for storage and later use.

3. Add 50 or 100 mL of heat inactivated FBS for 10 or 20% FBS medium, respectively.

4. Add 5 mL of antibiotics.

5. Add 10 mL of ascorbic acid solution.

6. Add 5 mL of L-glutamine.

Complete medium is good for 2 weeks (due to 25% inactivation of ascorbic acid after this time). Do not prepare more medium than you think you will use during that time period.

Heat Inactivation of FBS

1. Turn on the 56°C water bath to warm up.

2. Remove FBS from -20°C freezer (downstairs).

3. Place bottles in 56°C water bath. Once thawed, leave for an additional 30 minutes (60 minutes for 500 ml bottles), shaking every 10 minutes.

Ascorbic Acid Solution

1. Weigh out 0.0125 g of ascorbic acid for every 10 mL of ascorbic acid solution to be prepared. Since you can prepare in advance and store frozen until needed it is easiest to make a larger amount, such as 100 mL.

2. For 100 mL, weigh out 0.125 g ascorbic acid and add 100 mL incomplete DMEM/F12.

3. To sterilize, filter through a 0.45 μm sterile filter.

4. Aliquot into 15 mL tubes in 10 mL aliquots and store in -20°C freezer.

It is VERY IMPORTANT that you label all of your bottles/solutions with your name, date, and description and keep them in your allotted area. If you transfer anything from its original bottle (such as aliquoting trypsin), write the expiration date on the new container.

Appendix N. Media Changing

Materials
Complete Medium
Pipettes
Flame
Vacuum Pipettes
Vacuum setup

Methods
1. Remove the medium from the culture dishes or flasks using the glass vacuum pipettes (use long pipettes for flasks, short pipettes for well plates). Make sure to use a new pipette for each sample from different animals.

2. Replace the media according to the type of culture dish you are using.

75 cm^2 flasks – 15 ml
25 cm^2 flasks – 5 ml
6 well plate – 2-4 ml per well

You can use the same pipette as long as you do not touch the flasks. If you think you might have contaminated it at all, use a new one. Be sure to switch pipettes for samples from different animals.

3. Quickly flame caps and lids before putting them back on to ensure they remain sterile.

4. Amounts can change depending on type of cells and desired culture conditions. If you are changing media for someone and you do not know how much they added, draw up the medium in the flask with a plastic pipette to measure it first.

Appendix O. Protocol for Manual Embedding of Matrix and Matrix Construct Specimens

After rinsing, matrix only specimens should be fixed in formalin for 48 hours. Explant-matrix constructs should be fixed in formalin for at least a week. They will be manually dehydrated prior to embedding in paraffin and JB-4 resin (Polysciences, Inc., Warrington, PA). The process will be such that each matrix will be bisected so that half can be fixed in paraffin and half in JB-4.

1. Samples are gently placed in labeled Tissue Tek cassettes in between 2 blue sponges. Another set of Tissue Tek cassettes is prepared with the same labels.

2. Dehydration. The cassettes are transferred between the following solutions for the designated time periods. All solutions are pre-made in buckets and kept in the flammables cabinet. The longer times in this protocol are for matrix-explant constructs; the shorter times are for matrices only.

Solution	Time
distilled H_20	30 min-1 hour
distilled H_20	30 min-1 hour
50% EtOH	30 min-1 hour
70% EtOH	30 min-1 hour
80% EtOH	30 min-1 hour
95% EtOH	30 min-1 hour
95% EtOH	30 min-1 hour
100% EtOH	30 min-1 hour
100% EtOH	30 min-1 hour
100% EtOH	30 min-1 hour

3. Bisection. The matrix specimens are removed from the cassettes and cut in half with a scalpel to result in two half-circles. One half is then placed in the original cassette and sent for paraffin embedding. The second half is placed in the other cassette with the same label and sent for JB-4 embedding.

4. Paraffin embedding. Cassettes for paraffin (Paraplast Cat. #8889-501006, melting temp 56°C, Oxford Labware, St. Louis, MO) embedding proceed through additional solutions as follows:

Solution	Time	Temp
Histoclear	1 min-2 hour	room temp
paraffin	1 hour	59°C
paraffin	1 hour	59°C

Take care not to touch the cassettes when they have just been in Histoclear (Americlear histology clearing solvent, Baxter Healthcare Corp. #C4200-1, Deerfield, IL) because the solution will eat through gloves. The paraffin baths are located in the paraffin oven.

5. JB-4 embedding. The catalyzed JB-4 A solution is prepared by adding 9 g of catalyst (Polysciences #02618, benzoyl peroxide, 70% wet) to 1000 mL of JB-4 embedding solution A (Polysciences #0226A, Acrylic monomer n-Butoxyethanol). This preparation must be done in a graduated cylinder because the JB-4 A solution bottles only hold 750 mL. The solution is then stirred for approximately 1 hr. until the catalyst dissolves. The catalyzed JB-4 A can be placed back into the JB-4 A bottles as long as they are labeled as "catalyzed."

a. Equilibration. The cassettes are equilibrated overnight in the refrigerator in a solution of 50% ethanol/50% catalyzed JB-4 solution A. Note that JB-4 A is very expensive and the minimal amount of fluid should be used to cover the cassettes.

b. Then, infiltrate in 100% catalyzed JB-4 solution A in a refrigerator for at least 1 day.

c. Final embedding step. Combine JB-4 catalyzed solution A:JB-4 solution B at a ratio of 24 mL:1 mL. Mix well and pipette into plastic molds. Place samples face down in plastic molds. Ensure that sample orientation is maintained. Try to embed the half-disks with the cut surface down. The matrix disks have tendency to float so holding them down with wooden sticks through the metal tops may be necessary. Solution begins to harden in less than 30 minutes. Before the hardening is completed (careful- polymerization may progress rapidly once started), place the pre-made labeled metal embedding blocks in the molds. Note: the label should be written in standard pencil marking only!

Rationale: Placing collagen samples in the paraffin-embedding machine really destroys them. The histological results are much clearer when they are dehydrated and embedded by hand. This process also allows you to divide the sample for paraffin and JB-4 embedding.

Appendix P. Reference List for Histology Samples

Experiment 2: Canine Matrix-Explant Construct Study

Canine #	Disc Level	ORL #	Paraffin	JB-4
1	L1-L2	3915	X	
	L2-L3	3916	X	
	L3-L4	3917	X	
	L4-L5	3918	X	
	L5-L6	3919	X	
2	L1-L2	3925	X	X
	L2-L3	3926	X	X
	L3-L4	3927	X	X
	L4-L5	3928	X	X
	L5-L6	3929	X	X
3	L1-L2	4130	X	X
	L2-L3	4131	X	X
	L3-L4	4132	X	X
	L4-L5	4133	X	X
	L5-L6	4134	X	X
4	L1-L2	4215	X	X
	L2-L3	4216	X	X
	L3-L4	4217	X	X
	L4-L5	4218	X	X
	L5-L6	4219	X	X
5	L1-L2	4364	X	X
	L2-L3	4365	X	X
	L3-L4	4366	X	X
	L4-L5	4367	X	X
	L5-L6	4368	X	X
6	L1-L2	4370	X	X
	L2-L3	4371	X	X
	L3-L4	4372	X	X
	L4-L5	4373	X	X
	L5-L6	4374	X	X

Experiment 3: Bioreactor Matrix Construct Study

Canine #	Disc Level	ORL #	Paraffin	JB-4
7	L1-L2	4418	X	
	L2-L3	4419	X	
	L3-L4	4420	X	
	L4-L5	4421	X	
	L5-L6	4422	X	
8	L2-L3	4607	X	X
	L3-L4	4608	X	X
	L4-L5	4609	X	X
	L5-L6	4610	X	X
	L6-L7	4611	X	X
9	L2-L3	4670	X	X
	L3-L4	4671	X	X
	L4-L5	4672	X	X
	L5-L6	4673	X	X
	L6-L7	4674	X	X
10	L2-L3	4722	X	X
	L3-L4	4723	X	X
	L4-L5	4724	X	X
	L5-L6	4725	X	X
	L6-L7	4726	X	X
12	L2-L3	4798	X	X
	L3-L4	4799	X	X
	L4-L5	4800	X	X
	L5-L6	4801	X	X
	L6-L7	4802	X	X
13	L1-L2	4894	X	X
	L2-L3	4895	X	X
	L3-L4	4896	X	X
	L4-L5	4897	X	X
	L5-L6	4898	X	X

Experiment 4: Medium Type Cell-Seeded Matrix Pilot Study

Human #	Disc Level	ORL #	Paraffin	JB-4
1	L5-S1	4117	X	X

Experiment 4: Collagen Type Seeding Study

Paraffin and JB-4, but not all JB-4 sections oriented correctly.

ORL Lab #	Matrix Type	Study #	Sacrifice Time (days)
5672	I	10	15
5672	I	11	29
5672	I	12	2
5670	I	13	2
5670	I	14	15
5670	I	15	29
5673	I	34	15
5673	I	35	2
5673	I	36	29
5674	I	46	29
5674	I	47	2
5674	I	48	15
5671	I	58	2
5671	I	59	15
5671	I	60	29
5675	I	70	15
5675	I	71	29
5675	I	72	2
5672	II	10	15
5672	II	11	29
5672	II	12	2
5670	II	13	2
5670	II	14	15
5670	II	15	29
5673	II	34	15
5673	II	35	2
5673	II	36	29
5674	II	46	29
5674	II	47	2
5674	II	48	15
5671	II	58	2
5671	II	59	15
5671	II	60	29
5675	II	70	15
5675	II	71	29
5675	II	72	2
5672	hybrid	11	29
5672	hybrid	12	2
5670	hybrid	13	2
5670	hybrid	14	15

5670	hybrid	15	29
5673	hybrid	34	15
5673	hybrid	35	2
5673	hybrid	36	29
5674	hybrid	46	29
5674	hybrid	47	2
5674	hybrid	48	15
5671	hybrid	58	2
5671	hybrid	59	15
5671	hybrid	60	29
5675	hybrid	70	15
5675	hybrid	71	29
5675	hybrid	72	2
control	I	4	2
control	I	9	29
control	I	10	2
control	I	13	15
control	II	1	29
control	II	9	15
control	II	10	2
control	II	15	2
control	II	18	15
control	II	21	29
control	hybrid	1	2
control	hybrid	6	29
control	hybrid	7	29
control	hybrid	10	15
control	hybrid	13	29
control	hybrid	15	2

Experiment 5: *In Vivo* Pilot Study

Dog	ORL #	Date of Surgery	Site of Surgery	Type of Surgery	Date of Sacrifice
1	5094	10/4/00	L L3-L4	annulotomy	1/24/01
	5361	11/30/00	R L4-L5	annulotomy + implantation of unseeded matrix	
2	unknown	1/30/01	L L2-L3	annulotomy	5/30/01
	4922[6]	4/4/01	R L5-L6	annulotomy + implantation of cell-seeded matrix	
3		7/05/01	L L2-L3	annulotomy	10/22/01
	5571[7]	8/30/01	R L4-L5	annulotomy + implantation of cell-seeded matrix	

Appendix Q. Hematoxylin and Eosin (H & E) Staining

For formalin-fixed, paraffin and JB-4 embedded samples. Modified from (21).

Sectioning and Storage

Histological sections are cut on a microtome (Reichert-Jung model 2050 Supercut, Leica Instruments, Nussloch, Germany). The thickness is 7 μm for paraffin sections and 5 μm for JB-4. The sections are placed on glass slides (Fisherbrand Superfrost Plus, Cat. #12-550-15, Fisher Scientific, Pittsburgh, PA). Slides with JB-4 sections are dried on a hot plate at low temperature for 5-30 min., and then stored at room temperature. Paraffin slides are placed in an oven at 50°C to melt off excess paraffin overnight, and then stored at room temperature.

Solutions

HEMATOXYLIN: Filter 200 ml of stock solution into staining dish. Sigma Harris Hematoxylin Solution, Catalog HHS-128, Modified: Hematoxylin, 7.5 g/L; sodium iodate, aluminum and ammonium sulfate, stabilizers and preservative.

ACID ALCOHOL: 200 ml of 70% ethanol (in dH_2O) + 0.5 ml HCl

AMMONIA WATER: 200 ml dH_2O + 5-10 drops ammonium hydroxide, generally 5
pH should be roughly around 10.0 - use pH paper.
Generally this should be mixed up fresh each day.

EOSIN: 100 ml stock solution + 100 ml dH_2O + 1.0 ml glacial acetic acid
Sigma Eosin Y Solution Aqueous, catalog HT110-2-128.

Paraffin Sections

1. DEPARAFFINIZE AND REHYDRATE

Xylene:	2 x 5 min.
100% ethanol:	10-20 dips
100% ethanol:	10-20 dips
95% ethanol:	10-20 dips
80% ethanol:	10-20 dips
70% ethanol:	10-20 dips
dH2O:	10-20 dips

2. Harris hematoxylin, 10 min.

3. Rinse in tap water, approx. 1 min. running or swishing until almost clear

4. Acid alcohol. Dip quickly 5-10 times. 20-30 sec total.

5. Rinse in tap water. Until foaming stops, maybe 30 sec.

6. Ammonia water. Quick dips (5 or so) until blue.

7. Rinse in tap water. About 1 min.

8. Eosin, 45 sec.

9. Rinse in tap water, 2 min.

10. DEHYDRATE

70% ethanol:	10-20 dips
80% ethanol:	10-20 dips
95% ethanol:	10-20 dips
100% ethanol:	10-20 dips
100% ethanol:	10-20 dips
Xylene:	2 x 5 min.

11. Air dry, coverslip with Cytoseal (Cytoseal 60; #18006, Electron Microscopy Sciences).

JB-4 Sections

1. Slides should have been placed on hot plate for 5-30 min. after sectioning.

2. Harris hematoxylin, 1.5-1.75 hours

3. Rinse in tap water, approx. 1 min. running or swishing until almost clear

4. Acid alcohol. Dip very quickly 5-10 times.

5. Rinse in tap water. Until foaming stops, maybe 30 sec.

6. Ammonia water. Quick dips (5 or so) until blue.

7. Rinse in tap water. About 1 min.

8. Eosin, 5 min.

9. Rinse in tap water, 5 min.

10. Air dry, coverslip with Cytoseal.

Appendix R. Protocol for Coating Well Plates with Agarose

1. Agarose coating prevents cells from attaching and growing on the bottom of well plates. This ensures that your explants or constructs will have all medium nutrients solely available to them. Each well of a 6-well plate is to be coated with 2 mL of liquid agarose. Prepare 10-15 mL more agarose than you will need.

2. In a 100 mL glass bottle, place agarose and distilled water. Use 1 g Seaplaque agarose (#50100, BioWhittaker/FMC Bioproducts) per 25 mL water. (Or you can use 1 g of Biorad agarose per 50 mL water.)

3. Autoclave the bottle on the liquid setting in an autoclave bag with the cap untightened.

4. Remove the bottle from the autoclave while it is still hot.

5. Coat the wells with 2 mL of the liquid agarose each. This should be done rather quickly as the agarose will solidify as it cools.

6. Place parafilm around the well plates and put them in the cold room for at least 4 hours. Often it is easiest to do the agarose coating the day before using the plates. Do not use the plates after more than one day in the cold room because the agarose will crack.

7. Warm the plates in the incubator 1-2 hours prior to use.

8. Change agarose-coated well plates every two weeks because the agarose breaks down.

Appendix S. Changing Medium in the Bioreactor

Materials and Equipment:
-autoclaved Pasteur pipettes and sterile 25 mL pipettes
-Wrench (9/16)
-Pliers (green handle)
-sterile field (touch sides with stripes only and unfold like an accordion)
-2 x 20 mL syringes (the one used to add the medium must be a BD brand)
-18 gauge needle
-1 x 50 mL centrifuge tube
-mask
-alcohol wipes

Procedure:
1.) Autoclave the Pasteur pipettes prior to changing medium.
2.) Warm up cell medium for 30 minutes in the hot water bath.
3.) Turn off power of bioreactor (found on the top of the incubator) and immediately remove the vessel from the base (Figure 62). (Do this by placing left hand under the base screw while supporting the vessel, and unscrew the vessel counterclockwise with right hand.)

Figure 62. Removing the Bioreactor from the Rotator Base.

The white base attached to the rotator is held firmly in place while the bioreactor is screwed off the base.

4.) Take the vessel to a sterile environment (biological hood) - wear a mask!
5.) Stand the vessel vertically on its base (valves up), and let the cell/construct aggregates settle to the bottom.
6.) Close any valves that are open (open valves are parallel to the syringe/port, closed valves are perpendicular to it). Note: the valve that will be open is the medium fill port.
7.) Remove syringe (after the valve has been closed) and remove any medium drips using a sterile Pasteur pipette and a vacuum setup (always swipe the pipette through the flame before using it). Clean with alcohol pads. Throw syringe into regular trash.
8.) Remove screw from syringe port (may need pliers) and put it on its side on an alcohol wipe. Remove any medium that is on the syringe port with a Pasteur Pipette. Clean the port with an alcohol swab.
9.) Remove the screw from the medium fill port (the big, rectangular one) and put it on another alcohol wipe (may need wrench - turn counterclockwise). Do not touch the inside of the cap. Remove any medium that is inside the cap and port with a pipette. Wipe the inside of the cap and the port with an alcohol swab.
10.) Remove half of the medium from the vessel via the big, 1/4 inch port (Figure 63). Make sure all of the ports are open. Remove medium using a sterilized Pasteur Pipette (swipe it through the flame first). Aspirate any droplets left behind. Wipe with alcohol swab.

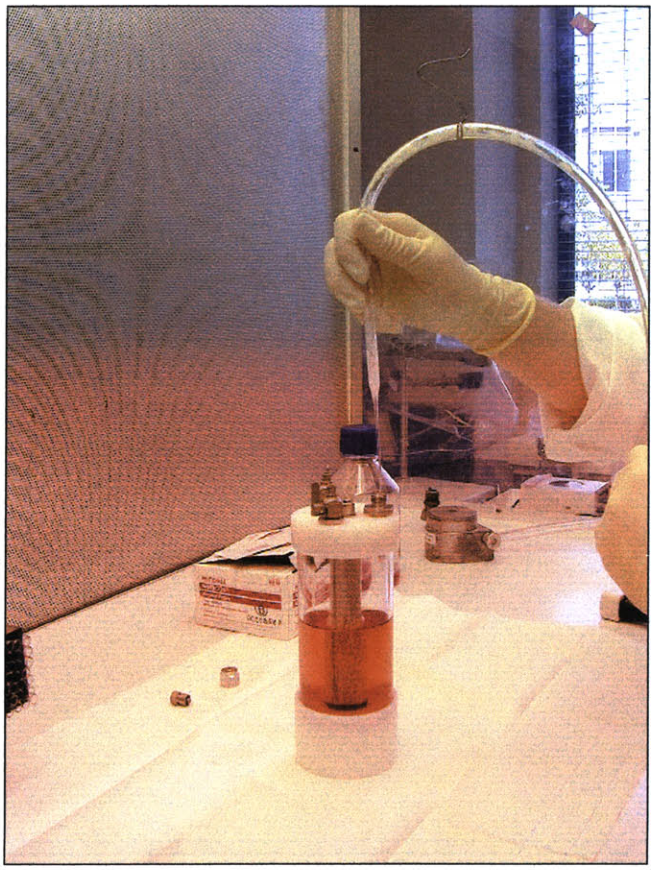

Figure 63. Suctioning Medium from the Bioreactor.

A large glass pipette is carefully inserted into the bioreactor until 50% of the medium is removed. All medium is removed for construct sacrifice days.

11.) Add medium using a 25 mL sterile pipette. Do this SLOWLY and carefully, holding the pipette slightly above the port (Figure 64). Flow the medium down the vessel. Do not disturb the cell/constructs objects. Do not introduce bubbles. Be careful as a bubble will likely form in the port. If any medium is spilled, aspirate it with a pipette/ vacuum and then wipe with an alcohol swab wipe under the screw too). Fill the vessel until you don't see any air space (about 125 mL).

Figure 64. Demonstration of Adding Medium to the Bioreactor

The fill port is used to carefully add medium to the bioreactor.

12.) *Remove air bubbles.* Remove the air from the syringe first. Snap needle on and turn towards you. Carefully remove needle from cap. Fill syringe with 20 mL of medium (best to put medium in a 50 mL centrifuge tube to draw out of). Put the needle cap back on and throw it in the sharp container. Wipe one syringe port with an alcohol pad and attach the full syringe (the syringe should screw into place). Attach syringe to the port by turning counterclockwise. Wipe the other syringe port with an alcohol pad and attach another empty sterile syringe.

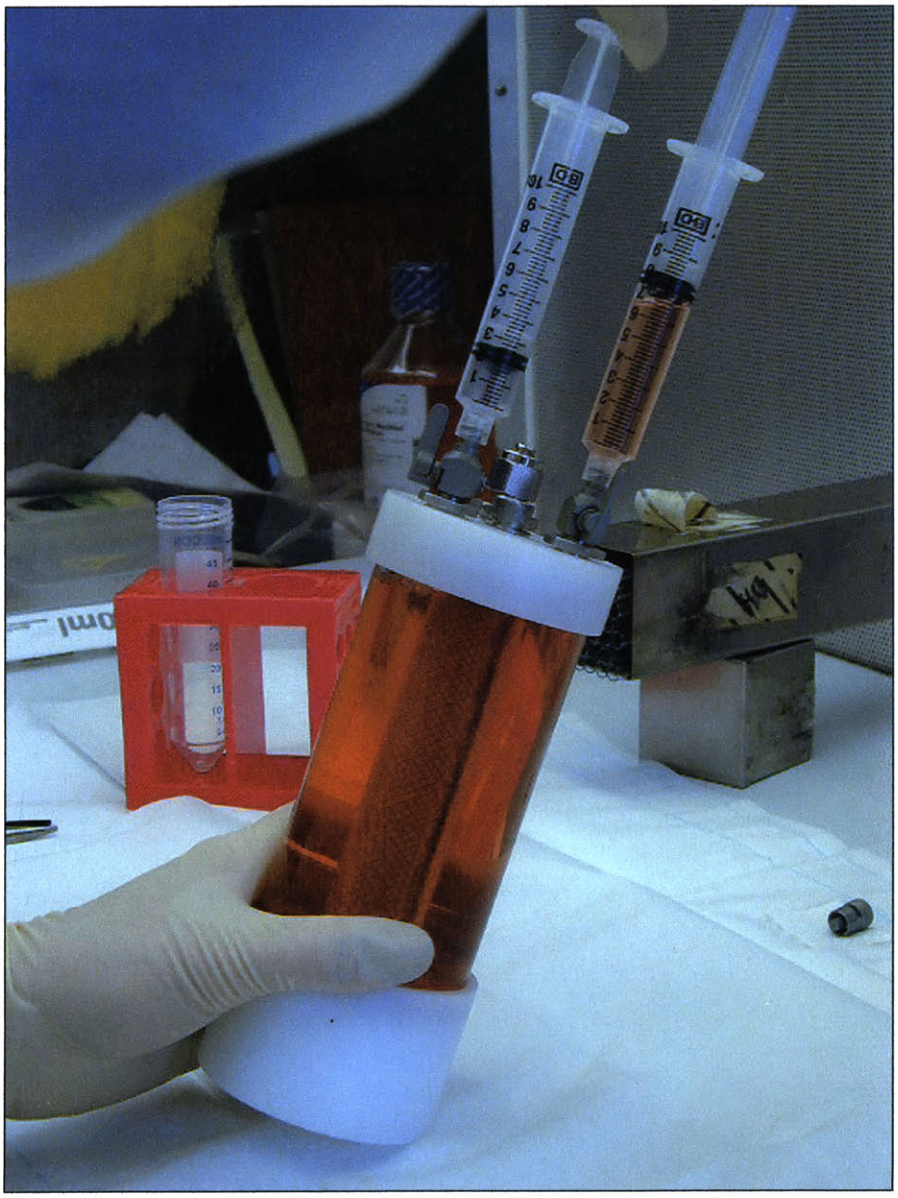

Figure 65. Demonstration of Procedure for Removing Bubbles from Bioreactor

Two syringes are attached to the bioreactor syringe ports. One contains medium. The bioreactor is tipped so that bubbles are centered under the port containing the empty syringe. A small amount of medium is injected into the bioreactor, and then a small volume of air is sucked out.

13.) Pull up slightly on the empty syringe (Figure 65). When you see medium in the empty syringe, gently invert the vessel and tap on the sides to expel air bubbles from under the ports. Maneuver air bubbles under the empty syringe. With both valves open, gently press on the full syringe to replace air bubbles with medium. Generally, you want to do this incrementally and slowly. Remove a few bubbles, add a little medium. Remember it is a closed volume environment. If you remove contents without adding some, you are changing the pressure inside. If more medium is needed, close all ports, remove both syringes, and repeat steps 12 and 13.
14.) When all bubbles are removed, close the syringe valve on the non-medium syringe and only. Pull up on the non-medium syringe while removing it. Discard in the trash. Suction out any medium left in this port. Wipe this port with an alcohol pad and replace the cap.
15.) Leave the medium-filled syringe on with its valve open as the volume/pressure of the medium in the vessel may vary slightly with temperature change.
16.) Attach the vessel to the rotator base and turn on the power. Make sure the syringe isn't hitting the glass or sides of the incubator.

Appendix T. Freezing Drying Protocol for Matrix Samples

Freeze-drying will be performed in the jar chambers by the distilled water source via the following method.

To start:

1. Pull knob on freeze dryer to empty any water in the chamber.
2. Turn on main switch.
3. Wait 10 min. until temperature is -50°C.
4. Turn on vacuum switch.
5. Close any open valves. Put everything on "VENT," and make sure no other valves are open.
6. Wait until pressure is in the green zone, about 5 min. Note that the display may be broken.
7. Attach jar with samples and turn the valve corresponding to the jar to "VAC."
8. Confirm that the temperature goes up.
9. Record operation on record sheet.

To end after overnight freeze-drying:

1. Turn the valve corresponding to the jar 90° to position in between "VAC" and "VENT."
2. Open a different valve to release the pressure.
3. Turn off the vacuum pump.
4. Turn off the main switch.
5. Gradually turn the valve corresponding to the jar to "VENT."
6. Remove the jar.
7. Measure the mass of the matrices the same day.
8. The matrices may be frozen for further use prior to papain digestion, but they will absorb a small amount of water in that environment. Thus, mass measurements will not be accurate after freezing, but assays can still be performed.

Appendix U. Protocol for Cell Counting with a Hemocytometer

Based on (21) and modification by Vickers.

Materials

Complete medium	Pipette Aid	70% ethanol
Trypan Blue	Micropipetters	Calculator
Cell counting slide	Pipette tips	Cell counter

Methods

1. Clean surface of hemocytometer and coverslip with 70% alcohol.

2. The coverslip should rest evenly over the silver counting area.

3. Beginning with a cell pellet, suspend the cells in a known amount of complete medium

4. Collect a 100 µL sample from the cell suspension and put in microcentrifuge tube. Dilute with 100 µL of trypan blue.

5. Mix well, and collect 15 µL of suspension in a micropipette tip.

6. Load the cell suspension into the hemocytometer, allowing it to be drawn under the coverslip by capillary action. Load just enough cell suspension to reach the edges of the silvered surface. Do not overfill as this may change the volume and make the count inaccurate.

7. Place hemocytometer on microscope stage, remove yellow glass filter, and view with standard 10X objective.

8. Count cells in each of the four corner and central squares (clear cells are viable, blue stained cells are dead) (Figure 66). Count cells that lie on the top and left lines but not those on the bottom or right lines of each square in order to avoid counting the same cells twice for adjacent squares. Repeat counts for other counting chamber. When a count of living cells is complete, count the number of dead cells in order to report viability.

9. Calculate total cell number from the following:

$$T = \frac{N_C}{N_S} \times D \times 10^4 \times V \qquad \text{Equation 13}$$

T = Total number of cells in suspension
N_c = Number of cells counted
N_s = Number of squares counted
D = Dilution factor, usually 2
V = Volume of media used to suspend cell pellet

The number 10^4 is the volume correction factor for the hemocytometer: each square is 1x1 mm and the depth is 0.1 mm.

10. Cell viability is calculated by:

$$\left(1-\frac{\#dead}{\#alive}\right)*100\% \qquad \text{Equation 14}$$

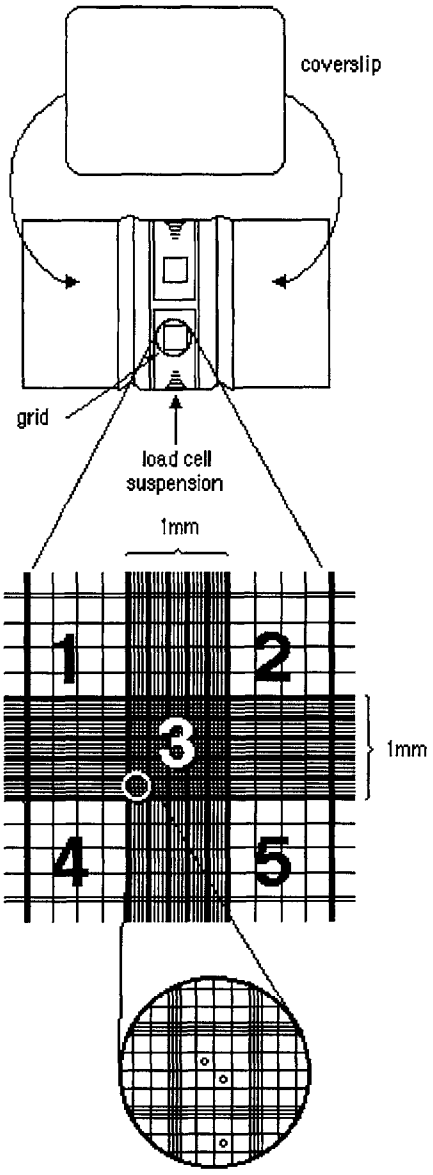

Figure 66. Hemocytometer Counting Diagram

Appendix V. DNA Assay Using Hoechst Dye Protocol

1. Prepare TNE 10x buffer solution: (100 mM TRIS, 10 mM EDTA, 1.0 M NaCl)
   800 ml dH_2O
   3.72 g Disodium Ethylenediamine Tetraacetate (EDTA) ($Na_2C_{10}H_{14}O_8N_2 \cdot 2H_2O$)
   12.1 g TRIS (Gibco #15504-012)
   58.4 g NaCl
   pH to 7.4 with concentrated HCl (approximately 70.5 mL 1 M HCl)
   dH_2O to 1000 ml (approximately 130 ml)
   Store 4°C
   (unclear how long good for, 3 months maybe?)

2. Prepare concentrated Hoechst dye stock solution: (1 mg/ml)
   10 mg Hoechst dye #33258
   10 ml dH_2O
   Store 4°C, shelf life: 6 months
   Protect from light: fluorescent!

3. Prepare the calf thymus DNA (Sigma D-3664) stock solution.
   a. For final DNA concentrations of 10-400 ng/mL: Stock solution of 100 µg/mL. Each dry bottle has 1 mg of DNA. Add 9 mL dH_2O and 1 mL 10X TNE buffer solution. Store at 4°C for up to 6 months.
   b. For final DNA concentrations of 100-2000 ng/mL: Stock solution of 1 mg/mL. Each dry bottle has 1 mg of DNA. Add 1 mL dH_2O. Must be used the day it is made.

3. On day of assay, prepare working solution of dye. There are 2 forms depending on what your final DNA concentration will be.
   a. 90 mL dH_2O filtered through 0.45 µm filter
   b. 10 mL TNE 10x buffer filtered through 0.45 µm
   c1. For final DNA concentrations of 10-400 ng/mL: At latest possible time before working, add 10 µL concentrated Hoechst dye stock solution. Usually, this step is used.
   c2. For final DNA concentrations of 100-2000 ng/mL: At latest possible time before working, add 100 µL concentrated Hoechst dye stock solution.

4. Scale fluorimeter (Hoefer Scientific Instruments TKO 100 Dedicated Mini Fluorometer):
   a. Warm up fluorimeter for 15 minutes.
   b. Add 2 mL of the working dye solution to a cuvette (4 optical sides; #67.755, Sarstedt). Place in fluorometer.
   Start with the "SCALE" knob adjusted to 50% sensitivity. This is approximately 5 clockwise turns of the knob from the fully counter-clockwise position. Adjust the zero knob until the display reads "000."
   c. Prepare standards of calf thymus DNA X 2. Put the following amounts in 2 mL of the working dye solution in cuvettes. Mix well.

I. Final DNA concentrations of 10-400 ng/mL:

Standards (ng)	calf thymus stock solution (μL)	Cuvette Concentration
50 ng	0.5 μL	25 ng/mL
100 ng	1 μL	50 ng/mL
150 ng	1.5 μL	75 ng/mL
200 ng	2 μL	100 ng/mL
300 ng	3 μL	150 ng/mL
400 ng	4 μL	200 ng/mL
500 ng	5 μL	250 ng/mL

II. Final DNA concentrations of 100-2000 ng/mL:

Standards (ng)	calf thymus stock solution (μL)	Cuvette Concentration
500 ng	0.5 μL	250 ng/mL
1000 ng	1 μL	500 ng/mL
1500 ng	1.5 μL	750 ng/mL
2000 ng	2 μL	1000 ng/mL

d. Scale with highest amount of calf thymus DNA standard, typically 250 ng/mL. Put this sample cuvette in. and adjust the "SCALE" knob until the display readout matches the concentration of the standard (i.e., 250).

e. Repeat b and d once or twice until reproducible. Then, run the DNA calf thymus standard curve.

f. It is often good to plot the standard curve (Figure 67) immediately before analyzing samples just to make sure you have calibrated correctly. The slope should always be close to 2.

5. Assay:
   a. Collagen samples must be digested by papain or protease.
   b. Add an aliquot of the sample to the working dye solution in the cuvette for a total volume of 2 mL. For example if you add a 100 μl aliquot of sample to the cuvette, add 1.9 mL final working dye solution to the cuvette. Mix.
   c. Read the fluorescence intensity immediately on the fluorometer
   d. Zero the fluorometer with a blank between samples.

Finding the Percent Mass of DNA

1. The mass of the dry sample should have been weighed prior to digestion.
2. Perform the DNA assay.
3. The calf thymus DNA control data should be plotted as amount of DNA (in ng) vs. fluorescence intensity. These data should be fitted with a linear equation.
4. The above equation should be used to find the amount of DNA (X) in the samples by putting their fluorescence intensity into the equation.
5. The % mass of DNA is calculated by:

$$\frac{X}{\text{mass of sample}} x \frac{\text{amount aliquot taken from (in } \mu\text{L)}}{\text{amount of aliquot used in assay (in } \mu\text{L)}} x100\% \qquad \text{Equation 15}$$

For example,

$$\frac{X(\text{in } ng)}{\text{mass of sample (in g)}} x1x10^{-9} x \frac{1000\ \mu L}{100\ \mu L} x100\%$$

6. If you don't want the % mass of DNA just do the above calculation without dividing by mass to get the DNA in ng.

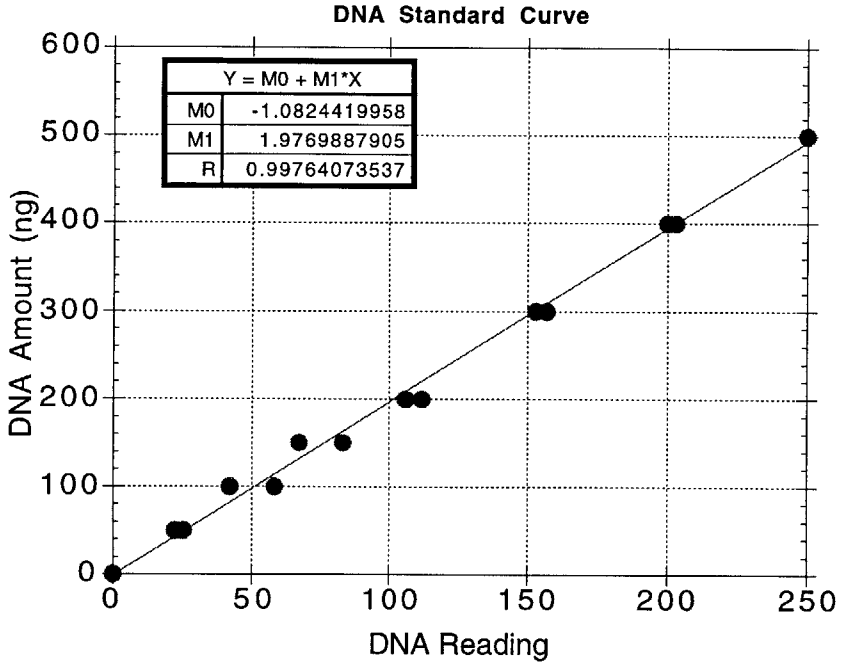

Figure 67. Example DNA Standard Curve

References: (106)

Appendix W. Passaging Cells

Materials
Complete medium
Trypsin
PBS (Phosphate-buffered saline)
Glass and sterile plastic pipettes
Vacuum setup
Centrifuge tubes
Tissue culture flasks

Methods
1. Warm the medium, trypsin, and PBS in 37° C water bath.

2. Remove medium from flasks with vacuum pipette (change pipettes for different animals).

3. Rinse with PBS (enough to cover bottom of flask, ~ 10 ml for 75 cm^2 flask) to removal any residual medium. Trypsin will not detach the cells if it has come into contact with the medium.

4. Remove PBS and add trypsin/EDTA (0.5 ml per well of 6 well plate, 2 ml for 25 cm^2 flask, 5 ml for 75 cm^2 flask).

5. Place in incubator for 5 minutes (unless otherwise instructed).

6. Remove from incubator and tap on the sides of the flask to loosen the cells. Check under microscope to ensure the cells are no longer attached. If they are, return them to the incubator and check each minute until they are unattached.

7. Once the cells are floating, return to the hood and add complete medium to inactivate the trypsin (1.5 mL per well of 6 well plate, 3 mL for 25 cm^2 flask, 10 mL for 75 cm^2 flask).

8. Using a sterile plastic pipette, transfer the medium/trypsin/cell suspension to a centrifuge tube. At this point you can combine the contents of the flasks if they are from the same sample.

9. Balance the tubes and centrifuge at 1500 rpm for 10 minutes.

10. Once you have the cell pellet at the bottom of the tube, draw off the medium with the vacuum pipette (be sure not to suck up the cells!!!).

11. Resuspend and count the cells (Appendix U). While counting, centrifuge the cell suspension a second time to ensure all trypsin has been removed.

12. Decant medium from second centrifugation and resuspend at desired seeding density. Transfer to culture flasks and add complete medium to bring the flasks up to final volume. For 75 cm^2 culture flasks, the passaged annulus cells should be plated at 0.75 x 10^6 cells per flask.

Appendix X. Protocol for Freezing Cells

General
For freezing 6 million cells in each 5 mL cryogenic tube.

Materials
Complete Medium
DMSO (Dimethyl sulfoxide): Autoclaved in light-proof bottle prior to use.
Sterile Filter
Pipettes
Sterile cryogenic tubes

Methods
1. Determine amount of medium needed (1 mL per $2x10^6$ cells) and add it to cells in 50 mL centrifuge tube.

2. Add 10% DMSO (i.e., if there is 15 mL of cell/medium suspension in 50 mL tube, add 1.5 mL of DMSO.)

3. Store in cryogenic tubes (3.3 ml per 5 ml tube).

4. Place in the -20°C freezer for 2-4 hours (longer time in this range is preferable), then transfer to -70°C for storage.

Appendix Y. Pilot Study of Seeding Techniques

Introduction

The best way to seed matrices with cells has not been established. Three methods of seeding of matrices have been documented: static (pipette or drop method), dynamic (agitation, stir flask, spinner flask), and bioreactor. Several previous users of cell-seeded matrices employed the static drop method where the cells are pipetted onto the matrix (21, 101, 202). Other research has determined that dynamic (25) or bioreactor seeding are often preferable to static seeding. Burg, et al. (25) showed that cells seeded and cultured in spinner flasks into polyglycolide matrices had the greatest metabolic activity and cell distribution compared to static seeding and culture in other environments; however, DNA content was not measured in this study.

For this pilot study, the comparison of pipet (drop) seeding was compared to dynamic seeding using a nutator.

Methods

Annulus cells were obtained from digested canine tissue. These cells were passaged four times before seeding into type I CG matrices that were cross-linked by 24 hr. DHT and 16 hr. UV irradiation.

The goal was to seed the 9 mm-diameter CG matrices with 2 million cells each. Seeding was performed by two different means. The first was the pipet method of seeding outlined in Appendix AA. The second procedure was dynamic seeding with a nutator as described by Lee (134). Briefly:

1. The discs were rinsed twice with complete 10% FBS medium (Appendix M).
2. The passaged cells were suspended in medium at a level of 4 million/mL.
3. The cell laden medium and discs were placed in 15 mL centrifuge tubes with 2 discs/mL.
4. These 15 mL centrifuge tubes were placed on a nutator for 1.5-2 hours in an incubator.
5. The discs were transferred to agarose-coated 6-well plates and 1 mL of medium was added to each well.
6. After 24 hours, an additional 2 mL of medium was added to the wells.

The diameter of the matrices was measured with a diameter template placed underneath the well plates at 8 hours, 1 day, 3 days, 1 week, and 2 weeks.

After 24 hours, 4 discs seeded by each method were sacrificed. Another 5 discs seeded by the pipet method were sacrificed after 2 weeks. The discs were rinsed with PBS, frozen, freeze-dried (Appendix T), weighed, and digested in papain (Appendix E). DNA analysis was performed using the Hoechst dye (Appendix V).

Student's t-test was used to compare the groups.

Results

The fluorometer DNA count at 24 hours was 211 ± 27 and 126 ± 5 (mean ± standard deviation) for the pipet and dynamic methods of seeding, respectively ($p = 0.007$; Student's t-test). After 2 weeks, the fluorometer DNA count was 140 ± 7 for the pipet seeded matrices, which was significantly less than at 24 hours ($p = 0.01$; Student's t-test).

The diameters of the matrices are displayed in Figure 68. At 1 and 3 days, the matrices seeded by the pipet method had significantly more contraction ($p < 0.03$; Student's t-test).

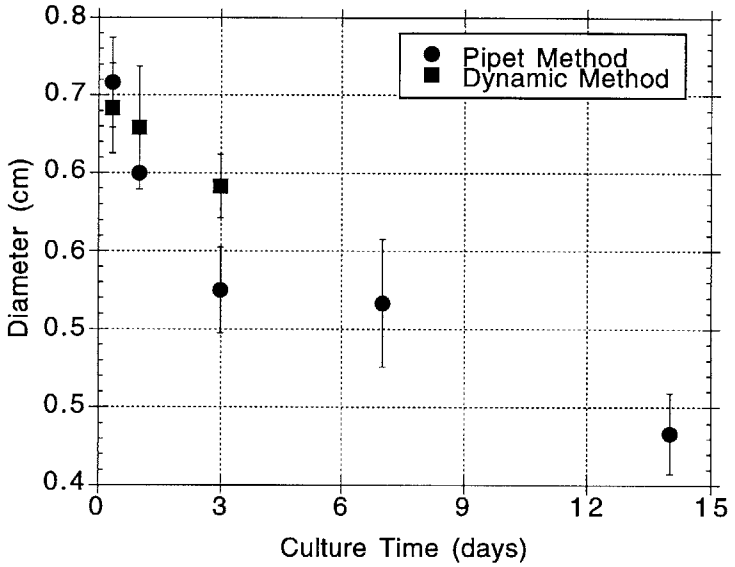

Figure 68. Matrix Disc Diameter vs. Culture Time for the Different Seeding Methods

Error bars represent standard deviations. $n = 6$-12.

Discussion

For the IVD annulus cells seeded at 2 million per 9 mm-diameter disc, the pipet seeding method resulted in nearly 70% more cells in the matrix at 24 hours. Even at 2 weeks after seeding, the DNA count in the pipet seeded matrices was still higher than the dynamically seeded matrices at 24 hours. For this reason, the pipet method of seeding is recommended for this cell density of IVD cells in 9 mm CG discs. The standard deviation of the DNA count was higher with pipet seeding. Interestingly, Lee (134) observed that at this seeding density for articular chondrocytes, the standard deviation was higher with dynamic seeding. Likely, the standard deviation is experimenter dependent.

The pipet seeded matrices contracted more during the first three days of culture. This was likely due to more cells in the matrices. The relationship between number of cells in the matrix and contraction has been well established (202).

Appendix Z. Thawing Cells

Materials
Complete medium
Tissue culture flasks
Aspirating pipettes
Vacuum suction
Flame
Sterile pipettes
Pipette Aid
15 ml tubes

Methods
1. Place cells directly into a 37°C water bath. Agitate gingerly while cells thaw for 40-60 seconds.

2. Slowly add warm medium to the tube until it is full. This insures that the cells thaw into the medium.

3. If not unthawed yet, put the caps back on the tube and gently agitate tube manually.

4. Transfer the cells to a 50 mL tube. Add more warm medium. Wash them clean of medium + DMSO for 10 minutes in the centrifuge.

5. Count the cells, and resuspend at the proper concentration. For 75 cm^2 tissue culture flasks, the thawed annulus cells should be plated at 1 million cells per flask. Cells should be cultured at least 3-4 days before being used for experimentation (or before changing medium, depending on when they attach).

Appendix AA. Cell Seeding Protocol-Pipette Method

1. Matrices are generally pre-wet for 1 hour in PBS if they are not already wet. Do not prewet in medium as the FBS alone can change the diameter of the matrices.

2. The cells are passaged from the flasks. The cells should be suspended at # cells wanted per disc/40 μL for a 9 mm disc. For example, for 2 million cells per 9 mm disc, you want 2 million cells/40 μL, or 50 million cells/1 mL.

3. Under sterile conditions, the pre-wet matrices are dried to some extent on sterile filter paper and placed in 6-well plates coated with 2 mL of agarose (1 g/25 mL Seaplaque agarose autoclaved prior to placement in wells and in cold room for at least 4 hours).

4. 20 μL of the cell suspension is then pipetted onto the surface of all of the matrices. After 10 min., the matrices are flipped over an additional 20 μL of cell suspension is added to this opposite surface.

5. The matrices are placed in an incubator for 2 hours. Then, 0.5 mL of 10% FBS medium is added to each well very slowly and along the sides of the wells.

6. After another 4 hours (6 hours after initial seeding), another 2.5 mL of medium is added to each well.

Appendix BB. Cell-Seeded Matrix Pilot Study with Varying FBS Types

Introduction

Contraction of matrix scaffolds that are to be used for *in vivo* tissue regeneration is a major impediment to successful implant designs. Collagen-glycosaminoglycan (CG) matrices are being engineered *in vitro* for the eventual use in *in vivo* regeneration of cartilage. These matrices have been known to undergo contraction in *in vitro* experiments when they are seeded with cartilage cells. Since control (unseeded) scaffolds also contract, part of the contraction appears to be due to culture in medium alone. Thus, there are at least two components of the contraction: medium-related and cell-mediated.

In vivo, contraction of the CG matrices is detrimental to regeneration because it leads to loss of adhesion to surrounding tissue and a decrease in pore size of the scaffold. In dermal regeneration models it has been shown that delaying contraction will decrease scar formation in favor of regeneration. *In vitro* experimental results have verified that stiffer matrices tend to be less contractable by cells. Thus, a design criteria for the CG matrix is to increase the stiffness so that cell-mediated contraction is minimized.

During *in vitro* culture, contraction is determined by measuring the cross-sectional area of CG matrix discs at various time points. Originally 9 mm in diameter (63.62 mm^2 in cross-sectional area), these discs can shrink to as small as 4 mm in diameter in 6 weeks. Control and cell-seeded matrices are cultured under similar medium conditions to determine cell-mediated contraction. Previously, matrices' resistances to degradation were determined by comparing the percentages of cell-mediated contraction at study end points. However, this does not necessary provide a realistic estimate of how the a matrix's stiffness affects cell-mediated contraction.

In a pilot experiment, control and seeded matrices were cultured in medium containing 10% or 20% fetal bovine serum (FBS) (mediums as described in Experiment 2) for up to six weeks. The reason for using two different types of medium was to determine how or if medium-related contraction is affected by medium constituents. Seeded matrices were initially seeded with 1.5 million human intervertebral disc cells each. Cross-sectional area of the control and seeded matrix discs was measured at 3 hours, 24 hours, and weekly after seeding for up to 6 weeks. Six control and six seeded matrices were sacrificed at 24 hours, 2 weeks, 4 weeks, and 6 weeks for each medium type for subsequent DNA and GAG analysis. Thus, the areal measurement population decreased over time.

The hypothesized model to describe the medium-related contraction (evidenced by the control data) is

$$A_c(t) = a + be^{-t/\tau_1}, \qquad \text{Equation 16}$$

where A_c is the fractional area contraction, a and b are unknown coefficients, and τ_1 is the time constant of medium-related contraction. For cell-seeded matrices, contraction has medium-related and cell-mediated components. The hypothesized equation that describes the fractional areal contraction for cell-seeded matrices is

$$A_{cs}(t) = c + de^{-t/\tau_2} + fe^{-t/\tau_3}, \qquad \text{Equation 17}$$

where c, d, and f are coefficients and τ_2 is the time constant of cell-mediated contraction. Equations 16 and 17 can be fit to the experimental data using nonlinear regression methods to determine the two time constants.

Modeling the contraction data has many benefits. It allows ones to visualize overall trends that may not be apparent by scattered data, such as whether the rate of contraction changes with time. When matrices of increased stiffness are utilized, modeling will allow experimenters to determine the steady-state contraction amount since it may not be reached during a 6-week experiment. Finally, modeling allows for comparison between different sets of contraction data instead of just data endpoints. For the pilot experiment, contraction profiles for control and seeded matrices and the different medium types can be compared.

Methods

Discarded tissue was obtained from a 42 year-old female patient's L5-S1 disc undergoing bilateral L4-L5 and L5-S1 discectomies after 5 months of acute pain (ORL # 4117; Appendix P). Cells were grown out of the explants in 6-well plates. These cells were passaged twice more before seeding by the pipet method (Appendix AA) into type I CG matrices that were cross-linked by 24 hr. DHT and 16 hr. UV irradiation. 64 seeded and 20 control matrices were cultured. DNA and GAG analysis was performed as described in Appendix V and Appendix F, respectively.

Contraction Analysis

The fractional areal contraction was calculated as

$$A_{c \text{ or } cs} = \frac{A - A_0}{A_0}, \qquad \text{Equation 18}$$

where A is the cross-sectional area at the specific time point and A_0 is the cross-sectional area at the initial time point. Two different values for A_0 were explored: the dry area (63.62 mm^2) and the matrix's individual area at 3 hours. Fractional areal contractions for matrices under similar conditions were averaged and a corresponding standard error was determined.

Two nonlinear regression algorithms were used to study the data: the Gauss-Newton and Levenberg-Marquardt algorithms. MATLAB provides a Gauss-Newton algorithm. The Levenberg-Marquardt algorithm was derived from a program written by Muzic and Jutan (165). (All MATLAB scripts can be found at the end of this Appendix.) Models consisting of 2-5 parameters were explored. The 3- and 5-parameter models are given by Equations 16 and 17. The 2- and 4- parameter models are these equations constrained so that they equal zero at time zero:

$$A_c(t) = a - ae^{-t/\tau_1}, \qquad \text{Equation 19}$$

$$A_{cs}(t) = c + de^{-t/\tau_2} - (c+d)e^{-t/\tau_3}. \qquad \text{Equation 20}$$

In addition, it was discovered that there was a linear dependence of the standard error of the fractional areal dependence on time for the controls. Thus, y-weighting was also explored for the control data.

To determine whether increasing the number of model parameters was worthwhile, the F test, AIC criterion, and MDL criterion were employed on the residual sum-of-squares (RSS). Student's t-tests on regression parameters the were used to determine if contraction profiles were different between the control and seeded matrices (comparison 1) and the matrices in 10% and 20% FBS medium (comparison 2). In addition, the overall differences in the profiles for these comparisons were tested by performing an F test on the RSS for the separated data and the RSS for the combined data:

$$F = \frac{\left(RSS_{combined} - RSS_{separate}\right)DF_{separate}}{\left(DF_{combined} - DF_{separate}\right)RSS_{combined}}, \qquad \text{Equation 21}$$

where DF is the degrees of freedom. (Reminder: In regression, DF is the number of data points minus the number of regression parameters.) This method is suggested by Motulsky (163).

Results

The DNA and GAG results are displayed in Figure 69 and Figure 70.

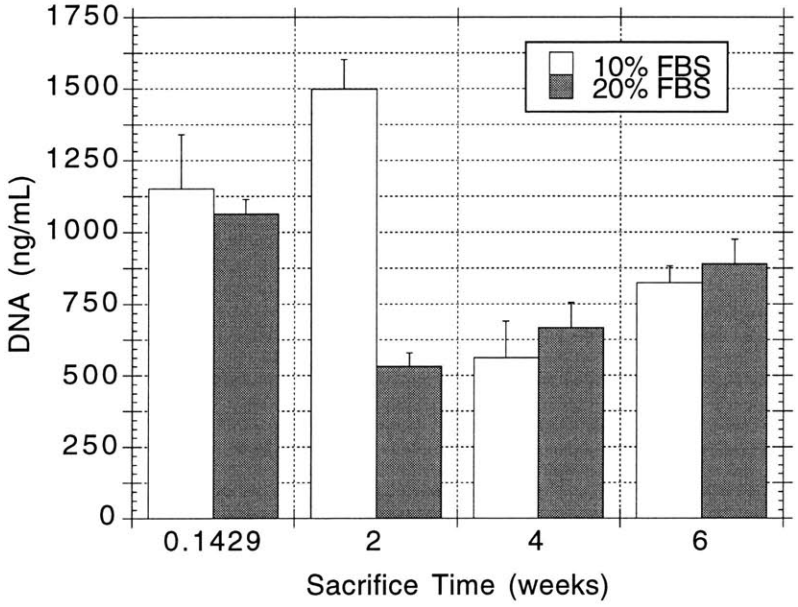

Figure 69. DNA for the Matrices with the Different Medium Types

Error bars represent standard error.

Contraction Analysis

The contraction data from the pilot experiment (using the dry area for A_0) are displayed in Figure 71.

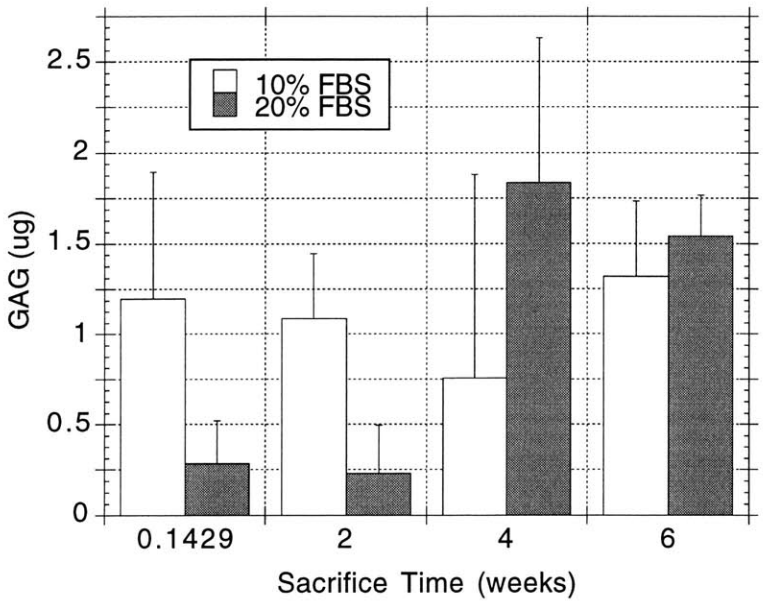

Figure 70. GAG in the Matrices with the Different Medium Types

Error bars represent standard error.

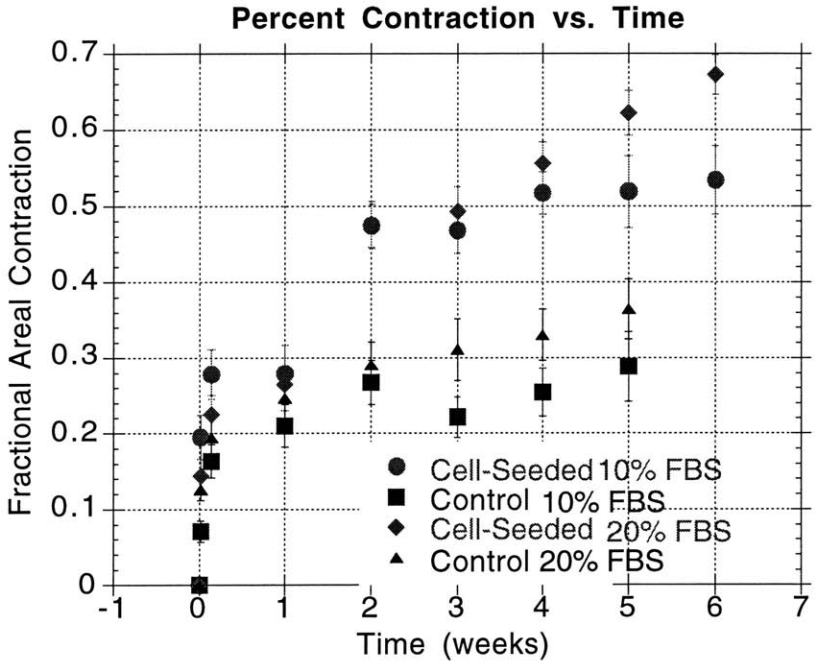

Figure 71. Fractional Areal Contraction vs. Culture Time for the Cell-Seeded Matrix Medium Pilot Study

Error bars represent standard error of the mean. Contraction was normalized by dry area.

After analyzing the plots (not shown here), it was decided that the dry area was a better indicator than the 3-hour cross-sectional area for A_0. In this way, the fractional areal contraction was positive for all data points. Whereas if the 3-hour data was used for normalization, some

data points actually displayed expansion at 1 week compared to 24 hours. Another reason for the dry area choice is that all of the matrices were cut to be 9 mm, but 3-hour diameters varied.

The Gauss-Newton algorithm became inefficient when analyzing the 5-parameter model. Thus, the Levenberg-Marquardt algorithm was employed for all further analyses. Also, the 3- and 5- parameter models of Equations 1 and 2 did not provide for realistic regression since they could fit the curve to a nonzero value at time zero. Therefore, Equations 19 and 20 were used for all subsequent regressions and referred to as the 2- and 4-parameter models, respectively. After studying the initial results, it became clear that the hypothesis that medium-related contraction could be modeled by a single exponential was incorrect. The data for both control and seeded cases appeared to have two phases, one fast and one slow. Consequently, the 2- and 4-parameter models were fit to both the control and seeded data to determine which was better. Y-weighting of the controls had very little effect on the curve fit and the RSS so it was not utilized for the comparisons. An example of the curve fit plots is shown in Figure 72. Visually, it was evident that the 4-parameter model regression fit the data more closely.

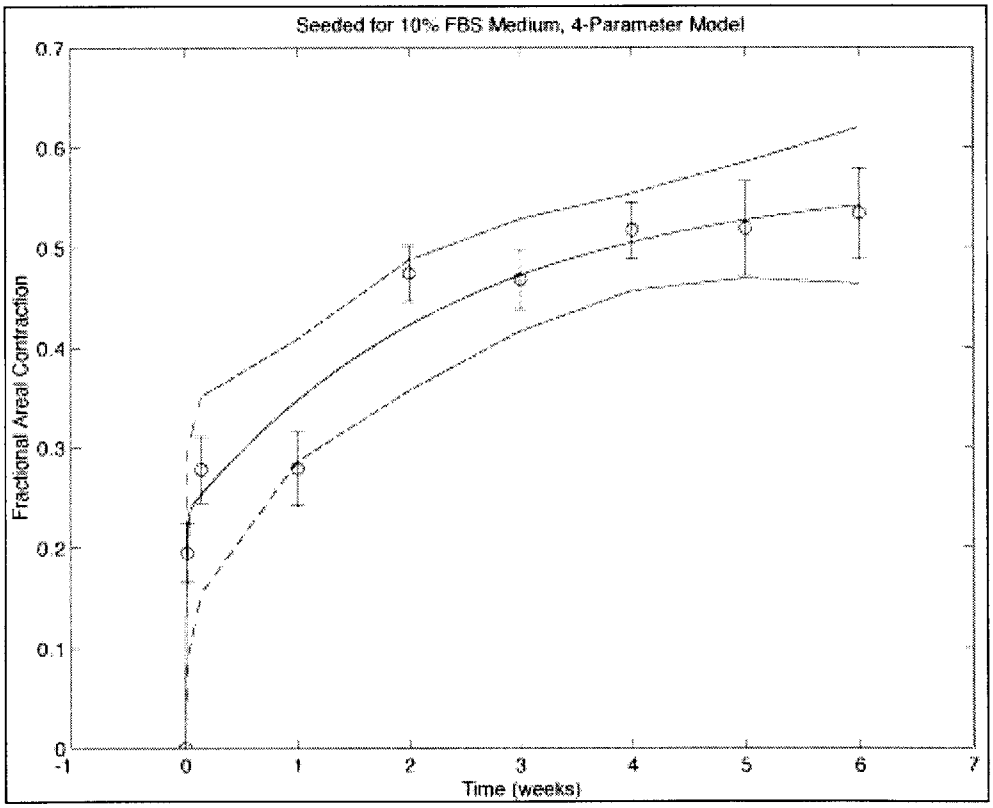

Figure 72. Example Plot of Multiple Exponential Regression of Contraction Data

The data points are the original data used for the regression analysis, displayed with their standard errors of the mean. The solid line is the plot of the fit equation. The dashed lines represent 95% confidence interval lines for the regression line.

Table 9 displays the regression parameters and the goodness-of-fit indicators for all of the data situations. The 95% confidence intervals for some of the regression parameters, especially the time constants, included zero. This suggests that they may not be statistically different than

zero. The statistics comparing the 2- and 4-parameter models are shown in Table 10. Almost invariably, the 4-parameter model is found to fit the data better, indicating that the two additional regression parameters are necessary for all cases. Therefore, statistics for comparisons 1 and 2 use regression characteristics from the 4-parameter models.

Table 9. Regression Parameters and Goodness-of-Fit Indicators for Contraction

Regression parameters are presented with standard errors of the mean.

	Control 10% FBS	Seeded 10% FBS	Control 20% FBS	Seeded 20% FBS
Steady-state constant, 2 parameter (*a*)	0.257 ± 0.014	0.503 ± 0.053	0.319 ± 0.021	0.650 ± 0.080
$1/\tau_1$, 2 parameter (1/weeks)	-7.985 ± 2.833	-1.400 ± 0.812	-8.284 ± 3.637	-0.590 ± 0.225
RSS, 2 parameter	0.0086	0.0805	0.0195	0.0547
R^2, 2 parameter	0.9044	0.8358	0.8581	0.9320
Steady-state constant, 4 parameter (*c*)	0.393 ± 0.285	0.570 ± 0.063	0.434 ± 0.027	0.848 ± 0.173
$1/\tau_2$, 4 parameter (1/weeks)	-26.45 ± 13.03	-96.59 ± 67.36	-60.19 ± 6.56	-77.39 ± 48.58
Exponential constant, 4 parameter (*d*)	-0.176 ± 0.245	-0.234 ± 0.042	-0.190 ± 0.007	-0.189 ± 0.034
$1/\tau_3$, 4 parameter (1/weeks)	-0.138 ± 0.273	-0.410 ± 0.212	-0.240 ± 0.051	-0.215 ± 0.102
RSS, 4 parameter	0.0028	0.0082	0.0002	0.0063
R^2, 4 parameter	0.9668	0.9701	0.9981	0.9855

Table 10. Statistics Comparing the 2- and 4-Parameter Models

* significant at the 0.05 level indicating that the 4-parameter model fits the data better. $^+$criterion indicates that the 4-parameter model fits the data better.

Statistic	Control 10% FBS	Seeded 10% FBS	Control 20% FBS	Seeded 20% FBS
p value for F test of 2 vs. 4	0.0626	0.0033*	0.0000*	0.00045*
AIC, 2 parameter	-19.42	-9.34	-15.73	-11.08
AIC, 4 parameter	-22.41$^+$	-17.64$^+$	-33.68$^+$	-18.80$^+$
MDL, 2 parameter	-19.22	-9.14	-15.53	-10.88
MDL, 4 parameter	-22.01$^+$	-17.21$^+$	-33.28$^+$	-18.41$^+$

The p values for the t-tests performed for comparisons 1 and 2 are presented in Table 11. In general, few comparisons are significant. Table 12 displays the p values for the F tests based on the method suggested by Motulsky (163). No results were significant here.

Table 11. t-Test Statistics for Comparisons 1 and 2

* significant at the 0.05 level

Statistic	τ_2	τ_3	Steady-State Constant (*c*)
p value of t test for control vs. seeded, 10% FBS	0.3307	0.4500	0.5582
p value of t test for control vs. seeded, 20% FBS	0.7330	0.8370	0.0395*
p value of t test for 10% vs. 20% FBS, control	0.0432*	0.7230	0.8899
p value of t test for 10% vs. 20% FBS, seeded	0.8219	0.4271	0.1619

Table 12. F Test Statistics for Comparisons 1 and 2

* significant at the 0.05 level

Comparison	p Value
control vs. seeded, 10% FBS	0.1268
control vs. seeded, 20% FBS	0.1210
10% vs. 20% FBS, control	0.1608
10% vs. 20% FBS, seeded	0.3076

Discussion

From the plots and the statistical results, it is clear that in an exponential model at least two exponentials are necessary.

It is notable that few significant differences were found in comparisons 1 and 2. The differences (inevitably real) between the seeded and control contractions shown in Figure 71 were not found mathematically. Likely, this is partially a result of too few data points. Modeling four parameters based on only nine data points is unlikely to yield significant differences unless the residuals are exceptionally small. Almost paradoxical decreased contraction with time (as seen in the control for 10% FBS medium at week 3) makes small residuals difficult to achieve. A higher rate of data sampling would probably correct some of these inconsistencies and yield more points for regression analysis.

Other factors complicate the analysis. From Figure 71, it appears that more contraction of seeded matrices was achieved at 6 weeks for the 20% FBS medium than the 10% FBS medium. DNA analysis of the same matrices reveals that the seeded matrices in the 20% FBS medium contained more cells than those in the 10% FBS medium. Thus, a dependence of contraction on cell number probably exists as well. Future models (with more data points) might incorporate an additional parameter with the DNA concentration as an input variable.

It should be recognized that areal contraction is not the best indicator of overall contraction. Shrinkage occurs in disc height over time as well.

With regard to the selection of the model type (exponential), this was chosen based on unverified criteria. Many biological phenomena display exponential dependence, and this was the primary reason for the exponential model selection. The data trends in Figure 71 make an exponential model a likely candidate. However, other model types could be employed. A piece-wise linear model with two parts might be envisioned.

The 2-phase contraction data is very interesting. It seems to imply that contraction in the first 24 hours may be just from medium infiltration and initial swelling of matrix fibers. At this time, it is unclear why the control matrix contracts after 24 hours. Perhaps it is based on fluid-influenced degradation of the matrix. It has been suggested that the data could be normalized based on the area at 24 hours. This would result in only slow contraction phase data. A single exponential or univariable linear model may then be appropriate.

The regression values for the steady-state constant (4-parameter model) are alarming. The control matrices will show long-term contraction of approximately 40%. The steady-state constant for the seeded matrices in 20% FBS implied that the matrices will contract 85% over time, twice as much as the controls. In 10% FBS, they would contract only 57%. Several conclusions can be drawn from these results. First, greater matrix stiffness is necessary to stop contraction or *in vivo* implantation will not perform adequately. Second, it appears that 20%

FBS medium is unattractive since it causes more contraction. This last cannot be verified until a DNA (cell number) dependence is added to the model because the increased contraction may just be a result of the greater number of cells.

Conclusion

Control and seeded matrices were placed in two different medium types for up to six weeks. Measurements of cross-sectional area showed that both control and seeded matrices contracted. Seeded matrices contracted more. Nonlinear regression analysis using the Levenberg-Marquardt algorithm revealed that a 4-parameter 2-exponential model fit the data best. However, few significant differences were found between the curves for the control and seeded cases. Most likely, this was caused by too few data points. Future experiments should include areal (or volume) measurements at a greater number of time points. Research should be done to determine if linear models or different normalization standards might model the data better. Finally, future models should probably include a DNA dependence since cell number in the matrices is not constant under varying conditions and might influence contraction.

MATLAB Codes

```
% final project program                    Dawn Hastreiter

% load the data
% data for % from 3 hr.
data3=[0.0000      0.0000      0.0000      0.0000      0.0000
       0.0000      0.0000      0.0000      0.0000;
0.14286  0.11100   0.0130      0.1010      0.0160      0.0930
       0.0200      0.0790      0.0200;
1.0000   0.10600   0.0280      0.1480      0.0200      0.1320
       0.0300      0.1520      0.023000;
2.0000   0.34900   0.0180      0.2140      0.0220      0.3820
       0.0270      0.2020      0.026000;
3.0000   0.39600   0.0220      0.1810      0.0210      0.4210
       0.0320      0.2310      0.033000;
4.0000   0.45100   0.0230      0.2230      0.0270      0.4940
       0.0260      0.2490      0.027000;
5.0000   0.49600   0.0390      0.2490      0.0410      0.5760
       0.0260      0.2590      0.026000;
6.0000   0.51100   0.0370      0.0         0.0         0.6320
       0.0240      0.0         0.0];
time3=data3(:,1);
seedreg3=data3(:,2);
seedregstd3=data3(:,3);
contreg3=data3(1:7,4);
contregstd3=data3(1:7,5);
seedspe3=data3(:,6);
seedspestd3=data3(:,7);
contspe3=data3(1:7,8);
contspestd3=data3(1:7,9);

datadry=[0.0000    0.0000      0.0000      0.0000      0.0000
       0.0000      0.0000      0.0000      0.0000;
0.01785  0.19500   0.0290      0.0710      0.0140      0.1440
       0.0220      0.12600     0.015000;
0.14286  0.27800   0.0330      0.1630      0.0220      0.2250
       0.0250      0.19400     0.025000;
1.0000   0.27900   0.0370      0.2100      0.0280      0.2650
       0.0350      0.24600     0.029000;
2.0000   0.47400   0.0280      0.2670      0.0290      0.4750
       0.0310      0.29000     0.031000;
3.0000   0.46800   0.0300      0.2210      0.0270      0.4930
       0.0320      0.31100     0.041000;
4.0000   0.51700   0.0280      0.2540      0.0320      0.5560
       0.0280      0.33000     0.034000;
5.0000   0.51900   0.0470      0.2880      0.0460      0.6220
       0.0290      0.36400     0.040000;
6.0000   0.53400   0.0450      0.307       0.049       0.67200
       0.0260      0.379       0.044];
timed=datadry(:,1);
seedregd=datadry(:,2);
seedregstdd=datadry(:,3);
contregd=datadry(:,4);
contregstdd=datadry(:,5);
seedsped=datadry(:,6);
seedspestdd=datadry(:,7);
contsped=datadry(:,8);
contspestdd=datadry(:,9);


p01=[.25; -.25; -3]; % for case 1
p02=[.2; -1];  % for case 2
p03=[.2; -4];% case 3
p04=[.25 -.25 -9];          % case 4
p05=[.5765 -.2417 -71.47 -.3797];   % case 5
p06=[.25 -1];               % case 6
p07=[.2606 -.1242 -79.608 -.1233];  % case 7
p08=[.6 -.24 -95 -.35 -.37];        % case 8
p09=[.45 -9];               % case 9

% 10 percent FBS medium using Gauss-Newton method
%[pr3gn,residr3gn,rssr3gn,r2r3gn,cipr3gn,ypr3gn,ciypr3gn]=gn(timed(1:8),
contregd,'exp5',p03)      % case 3
%pause
%[pr4gn,residr4gn,rssr4gn,r2r4gn,cipr4gn,ypr4gn,ciypr4gn]=gn(timed(1:8),
contregd,'exp4',p04)      % case 4
%pause
%[pr5gn,residr5gn,rssr5gn,r2r5gn,cipr5gn,ypr5gn,ciypr5gn]=gn(timed,seedr
egd,'exp6',p05) % case 5
%pause
%[pr6gn,residr6gn,rssr6gn,r2r6gn,cipr6gn,ypr6gn,ciypr6gn]=gn(timed,seedr
egd,'exp5',p06) % case 6
%pause
%[pr7gn,residr7gn,rssr7gn,r2r7gn,cipr7gn,ypr7gn,ciypr7gn]=gn(timed(1:8),
contregd,'exp6',p07)      % case 7
%pause
```

```
% 20 percent FBS medium using Gauss-Newton method
%[ps3gn,resids3gn,rsss3gn,r2s3gn,cips3gn,yps3gn,ciyps3gn]=gn(timed(1:8)
,contsped,'exp5',p03)      % case 3
%pause
%[ps4gn,resids4gn,rsss4gn,r2s4gn,cips4gn,yps4gn,ciyps4gn]=gn(timed(1:8)
,contsped,'exp4',p04)      % case 4
%pause
%[ps5gn,resids5gn,rsss5gn,r2s5gn,cips5gn,yps5gn,ciyps5gn]=gn(timed,seed
sped,'exp6',p05) %case 5
%pause
%[ps6gn,resids6gn,rsss6gn,r2s6gn,cips6gn,yps6gn,ciyps6gn]=gn(timed,seed
sped,'exp5',p06) % case 6
%pause
%[ps7gn,resids7gn,rsss7gn,r2s7gn,cips7gn,yps7gn,ciyps7gn]=gn(timed(1:8)
,contsped,'exp6',p07)      % case 7
%pause


global verbose
verbose=1;
options1=[[0.001; 0.001; 0.001] [.8; .8; .8]]; % for case 1,4
options2 = [[0.001; 0.001] [.8; .8]];     %case 2,3,6
options3=[[0.001; 0.001; 0.001; 0.001] [.8; .8; .8; .8]]; % for case 5,7
% 10 percent FBS medium using Levenberg-Marquardt algorithm
%[fr1lm,pr1lm,kvgr1lm,iterr1lm,corpr1lm,covpr1lm,covrr1lm,residr1lm,rssr
1lm,zr1lm,r2r1lm]=leasqr(time3(1:7),contreg3,p01,'exp1',.0001,100,1,[1;1;1
],'partexp1',options1); %case 1
%pause
%[fr2lm,pr2lm,kvgr2lm,iterr2lm,corpr2lm,covpr2lm,covrr2lm,residr2lm,rssr
2lm,zr2lm,r2r2lm]=leasqr(time3(1:7),contreg3,p02,'exp2',.0001,100,1,[1;1],'
partexp2',options2); % case 2
%pause
[fr3lm,pr3lm,sepr3lm,cipr3lm,cifr3lm,residr3lm,rssr3lm,r2r3lm]=leasqr(tim
ed,contregd,p03,'exp2',.0001,100,1,[1;1],'partexp2',options2,'exp5',contregst
dd); % case 3
title('Control for 10% FBS Medium, 2-Parameter Model')
print -deps case3r
pause
%[fr4lm,pr4lm,sepr4lm,cipr4lm,cifr4lm,residr4lm,rssr4lm,r2r4lm]=leasqr(ti
med(1:8),contregd,p04,'exp1',.0001,100,1,[1;1;1],'partexp1',options1,'exp4',c
ontregstdd); %case 4
%title('Control for 10% Medium, 3-Parameter Model')
%print -dps case4r
%pause
[fr5lm,pr5lm,sepr5lm,cipr5lm,cifr5lm,residr5lm,rssr5lm,r2r5lm]=leasqr(tim
ed,seedregd,p05,'exp3',.0001,100,1,[1;1;1;1],'partexp3',options3,'exp6',seedr
egstdd); %case 5
title('Seeded for 10% FBS Medium, 4-Parameter Model')
print -deps case5r
pause
[fr6lm,pr6lm,sepr6lm,cipr6lm,cifr6lm,residr6lm,rssr6lm,r2r6lm]=leasqr(tim
ed,seedregd,p06,'exp2',.0001,100,1,[1;1],'partexp2',options2,'exp5',seedregst
dd); % case 6
title('Seeded for 10% FBS Medium, 2-Parameter Model')
print -deps case6r
pause
[fr7lm,pr7lm,sepr7lm,cipr7lm,cifr7lm,residr7lm,rssr7lm,r2r7lm]=leasqr(tim
ed,contregd,p07,'exp3',.0001,100,1,[1;1;1;1],'partexp3',options3,'exp6',contre
gstdd); %case 7
title('Control for 10% FBS Medium, 4-Parameter Model')
print -deps case7r
pause
%[fr8lm,pr8lm,kvgr8lm,iterr8lm,corpr8lm,covpr8lm,covrr8lm,residr8lm,rssr
8lm,zr8lm,r2r8lm]=leasqr(time3(1:7),seedreg3(1:7),p08,'exp3',.0001,100,1,[
1;1;1;1;1],'partexp3',options3); %case 8
%pause
%[fr9lm,pr9lm,kvgr9lm,iterr9lm,corpr9lm,covpr9lm,covrr9lm,residr9lm,rssr
9lm,zr9lm,r2r9lm]=leasqr(time3(1:7),seedreg3(1:7),p09,'exp2',.0001,100,1,[
1;1],'partexp2',options2); % case 9
%pause
% weighted control cases
wtr=contregd.^(-.5);
wtr(1)=5;     % because the first data point is 0
[fr10lm,pr10lm,sepr10lm,cipr10lm,cifr10lm,residr10lm,rssr10lm,r2r10lm]=l
easqr(timed,contregd,p03,'exp2',.0001,100,wtr,[1;1],'partexp2',options2,'exp
5',contregstdd); % case 3 with y weighting = case 10
title('Control for 10% FBS Medium, 2-Parameter Model with y Weighting')
print -deps case10r
pause
%[fr11lm,pr11lm,sepr11lm,cipr11lm,cifr11lm,residr11lm,rssr11lm,r2r11lm]
=leasqr(timed(1:8),contregd,p04,'exp1',.0001,100,wtr,[1;1;1],'partexp1',optio
ns1,'exp4',contregstdd); %case 4 with y weighting = case 11
%title('Control for 10 percent FBS Medium, 3-Parameter Model with y
Weighting')
%print -dps case11r
%pause
[fr12lm,pr12lm,sepr12lm,cipr12lm,cifr12lm,residr12lm,rssr12lm,r2r12lm]=l
easqr(timed,contregd,p07,'exp3',.0001,100,wtr,[1;1;1;1],'partexp3',options3,'
exp6',contregstdd); %case 7 with y weighting = case 12
title('Control for 10% FBS Medium, 4-Parameter Model with y Weighting')
print -deps case12r
pause

% 20 percent FBS medium using Levenberg-Marquardt algorithm
%[fs1lm,ps1lm,kvgs1lm,iters1lm,corps1lm,covps1lm,covrs1lm,resids1lm,rs
ss1lm,zs1lm,r2s1lm]=leasqr(time3(1:7),contspe3,p01,'exp1',.0001,100,1,[1;1
;1],'partexp1',options1); %case 1
%pause
%[fs2lm,ps2lm,kvgs2lm,iters2lm,corps2lm,covps2lm,covrs2lm,resids2lm,rs
ss2lm,zs2lm,r2s2lm]=leasqr(time3(1:7),contspe3,p02,'exp2',.0001,100,1,[1;1
],'partexp2',options2); % case 2
%pause
[fs3lm,ps3lm,seps3lm,cips3lm,cifs3lm,resids3lm,rsss3lm,r2s3lm]=leasqr(ti
med,contsped,p03,'exp2',.0001,100,1,[1;1],'partexp2',options2,'exp5',contspe
stdd); % case 3
title('Control for 20% FBS Medium, 2-Parameter Model')
print -deps case3s
pause
%[fs4lm,ps4lm,seps4lm,cips4lm,cifs4lm,resids4lm,rsss4lm,r2s4lm]=leasqr(t
imed(1:8),contsped,p04,'exp1',.0001,100,1,[1;1;1],'partexp1',options1,'exp4',
contspestdd); %case 4
%title('Control for 20% FBS Medium, 3-Parameter Model')
%print -dps case4s
%pause
[fs5lm,ps5lm,seps5lm,cips5lm,cifs5lm,resids5lm,rsss5lm,r2s5lm]=leasqr(ti
med,seedsped,p05,'exp3',.0001,100,1,[1;1;1;1],'partexp3',options3,'exp6',see
dspestdd); %case 5
title('Seeded for 20% FBS Medium, 4-Parameter Model')
print -deps case5s
pause
[fs6lm,ps6lm,seps6lm,cips6lm,cifs6lm,resids6lm,rsss6lm,r2s6lm]=leasqr(ti
med,seedsped,p06,'exp2',.0001,100,1,[1;1],'partexp2',options2,'exp5',seedspe
stdd); % case 6
title('Seeded for 20% FBS Medium, 2-Parameter Model')
print -deps case6s
pause
[fs7lm,ps7lm,seps7lm,cips7lm,cifs7lm,resids7lm,rsss7lm,r2s7lm]=leasqr(ti
med,contsped,p07,'exp3',.0001,100,1,[1;1;1;1],'partexp3',options3,'exp6',con
tspestdd); %case 7
title('Control for 20% FBS Medium, 4-Parameter Model')
print -deps case7s
pause
%[fs8lm,ps8lm,kvgs8lm,iters8lm,corps8lm,covps8lm,covrs8lm,resids8lm,rs
ss8lm,zs8lm,r2s8lm]=leasqr(time3(1:7),seedspe3(1:7),p08,'exp3',.0001,100,
1,[1;1;1;1;1],'partexp3',options3); %case 8
%pause
%[fs9lm,ps9lm,kvgs9lm,iters9lm,corps9lm,covps9lm,covrs9lm,resids9lm,rs
ss9lm,zs9lm,r2s9lm]=leasqr(time3(1:7),seedspe3(1:7),p09,'exp2',.0001,100,
1,[1;1],'partexp2',options2); % case 9
% pause
wts=contsped.^(-.5);
wts(1)=5;     % because the first data point is 0
[fs10lm,ps10lm,seps10lm,cips10lm,cifs10lm,resids10lm,rsss10lm,r2s10lm]
=leasqr(timed,contsped,p03,'exp2',.0001,100,wts,[1;1],'partexp2',options2,'e
xp5',contspestdd); % case 3 with y weighting = case 10
title('Control for 20% FBS Medium, 2-Parameter Model with y Weighting')
print -deps case10s
pause
%[fs11lm,ps11lm,kvgs11lm,iters11lm,corps11lm,covps11lm,covrs11lm,resi
ds11lm,rsss11lm,zs11lm,r2s11lm]=leasqr(timed(1:8),contregd,p04,'exp1',.00
01,100,wts,[1;1;1],'partexp1',options1); %case 4 with y weighting = case 11
%pause
[fs12lm,ps12lm,seps12lm,cips12lm,cifs12lm,resids12lm,rsss12lm,r2s12lm]
=leasqr(timed,contsped,p07,'exp3',.0001,100,wts,[1;1;1;1],'partexp3',options
3,'exp6',contspestdd); %case 7 with y weighting = case 12
title('Control for 20% FBS Medium, 4-Parameter Model with y Weighting')
print -deps case12s
```

```
% statistical tests for significant differences
disp('if p is < 0.05, then the parameters are significantly different')

disp('test if 4 parameters is better than 2 parameters')
disp('by F test')
% by F test; F(p2-p1,n-p2) from Rusling and Kumosinski Eq. 3.15, model 1
must
%                       be a generalization of model 2 (wrong in book)
%                       F = (RSS1-RSS2)/RSS2*(n-p2)/(p2-p1)
disp('If fp < 0.05, then 4 parameters are better.')
disp('10 percent FBS control')
fstatrc=(rssr3lm-rssr7lm)/rssr7lm*(length(contregd)-4)/(4-2)
fp=1-fcdf(fstatrc,4-2,length(contregd)-4)
disp('10 percent FBS seeded')
fstatrs=(rssr6lm-rssr5lm)/rssr5lm*(length(seedregd)-4)/(4-2)
fp=1-fcdf(fstatrs,4-2,length(seedregd)-4)
disp('20 percent FBS control')
fstatsc=(rsss3lm-rsss7lm)/rsss7lm*(length(contsped)-4)/(4-2)
fp=1-fcdf(fstatsc,4-2,length(contsped)-4)
disp('20 percent FBS seeded')
fstatss=(rsss6lm-rsss5lm)/rsss5lm*(length(seedsped)-4)/(4-2)
fp=1-fcdf(fstatss,4-2,length(seedsped)-4)
pause
disp('by AIC and MDL tests')
disp('10 percent FBS control')
aicrc2=length(contregd)/2*log(rssr3lm)+2
aicrc5=length(contregd)/2*log(rssr7lm)+4
mdlrc2=length(contregd)/2*log(rssr3lm)+.5*2*log(length(contregd))
mdlrc5=length(contregd)/2*log(rssr7lm)+.5*4*log(length(contregd))
disp('10 percent FBS seeded')
aicrs2=length(seedregd)/2*log(rssr6lm)+2
aicrs5=length(seedregd)/2*log(rssr5lm)+4
mdlrs2=length(seedregd)/2*log(rssr6lm)+.5*2*log(length(seedregd))
mdlrs5=length(seedregd)/2*log(rssr5lm)+.5*4*log(length(seedregd))
disp('20 percent FBS control')
aicsc2=length(contsped)/2*log(rsss3lm)+2
aicsc5=length(contsped)/2*log(rsss7lm)+4
mdlsc2=length(contsped)/2*log(rsss3lm)+.5*2*log(length(contsped))
mdlsc5=length(contsped)/2*log(rsss7lm)+.5*4*log(length(contsped))
disp('20 percent FBS seeded')
aicss2=length(seedsped)/2*log(rsss6lm)+2
aicss5=length(seedsped)/2*log(rsss5lm)+4
mdlss2=length(seedsped)/2*log(rsss6lm)+.5*2*log(length(seedsped))
mdlss5=length(seedsped)/2*log(rsss5lm)+.5*4*log(length(seedsped))
pause


disp('test if exponents and constant are different between the controls and
seeded')
disp('10 percent FBS medium')
disp('exponent 1')
trexp1=abs((pr5lm(3)-pr7lm(3))/sqrt(sepr5lm(3)^2+sepr7lm(3)^2)) %
Rosner Eq. 8.23
prexp1=(1-tcdf(trexp1,9+9-2*4))*2
disp('exponent 2')
trexp2=abs((pr5lm(4)-pr7lm(4))/sqrt(sepr5lm(4)^2+sepr7lm(4)^2)) %
Rosner Eq. 8.23
prexp2=(1-tcdf(trexp2,9+9-2*4))*2
disp('constant')
trconst=abs((pr5lm(1)-pr7lm(1))/sqrt(sepr5lm(1)^2+sepr7lm(1)^2)) %
Rosner Eq. 8.23
prconst=(1-tcdf(trconst,9+9-2*4))*2
disp('20 percent FBS medium')
disp('exponent 1')
tsexp1=abs((ps5lm(3)-ps7lm(3))/sqrt(seps5lm(3)^2+seps7lm(3)^2)) %
Rosner Eq. 8.23
psexp1=(1-tcdf(tsexp1,9+9-2*4))*2
disp('exponent 2')
tsexp2=abs((ps5lm(4)-ps7lm(4))/sqrt(seps5lm(4)^2+seps7lm(4)^2)) %
Rosner Eq. 8.23
psexp2=(1-tcdf(tsexp2,9+9-2*4))*2
disp('constant')
tsconst=abs((ps5lm(1)-ps7lm(1))/sqrt(seps5lm(1)^2+seps7lm(1)^2)) %
Rosner Eq. 8.23
psconst=(1-tcdf(tsconst,9+9-2*4))*2
pause
disp('try tests that compare overall curve to see if things are different')
% from "The GraphPad Guide to Nonlinear Regression"
disp('If p < 0.05, then the curves are different.')
disp('10 percent FBS')
% combine data sets
xcsr=[timed; timed];
ycsr=[contregd; seedregd];
stdcsr=[contregstdd; seedregstdd];
% leasqr2 simply takes out the confidence interval lines because not
monotonic
[fcsr,pcsr,sepcsr,cipcsr,cifcsr,residcsr,rsscsr,r2csr]=leasqr2(xcsr,ycsr,p05,'ex
p3',.0001,100,1,[1;1;1;1],'partexp3',options3,'exp6',stdcsr);
title('Combined for 10% FBS Medium, 4-Parameter Model')
print -deps csr
rsssep=rssr7lm+rssr5lm;
dfsep=(9+9-4-4);
dfcomb=18-4;
fstat=(rsscsr-rsssep)*dfsep/rsscsr/(dfcomb-dfsep)
fp=1-fcdf(fstat,dfcomb-dfsep,dfsep)
pause
disp('20 percent FBS')
% combine data sets
xcss=[timed; timed];
ycss=[contsped; seedsped];
stdcss=[contspestdd; seedspestdd];
[fcss,pcss,sepcss,cipcss,cifcss,residcss,rsscss,r2css]=leasqr2(xcss,ycss,p05,'e
xp3',.0001,100,1,[1;1;1;1],'partexp3',options3,'exp6',stdcss);
title('Combined for 20% FBS Medium, 4-Parameter Model')
print -deps css
rsssep=rsss7lm+rsss5lm;
fstat=(rsscss-rsssep)*dfsep/rsscss/(dfcomb-dfsep)
fp=1-fcdf(fstat,dfcomb-dfsep,dfsep)
pause


disp('test if 10 percent FBS is different from 20 percent FBS')
disp('controls')
disp('exponent 1')
texp1=abs((ps7lm(3)-pr7lm(3))/sqrt(seps7lm(3)^2+sepr7lm(3)^2)) %
Rosner Eq. 8.23
pexp1=(1-tcdf(texp1,9+9-2*4))*2
disp('exponent 2')
texp2=abs((ps7lm(4)-pr7lm(4))/sqrt(seps7lm(4)^2+sepr7lm(4)^2)) %
Rosner Eq. 8.23
pexp2=(1-tcdf(texp2,9+9-2*4))*2
disp('constant')
tconst=abs((ps7lm(1)-pr7lm(1))/sqrt(seps7lm(1)^2+sepr7lm(1)^2)) %
Rosner Eq. 8.23
pconst=(1-tcdf(tconst,9+9-2*4))*2
disp('seeded')
disp('exponent 1')
texp1=abs((ps5lm(3)-pr5lm(3))/sqrt(seps5lm(3)^2+sepr5lm(3)^2)) %
Rosner Eq. 8.23
pexp1=(1-tcdf(texp1,9+9-2*4))*2
disp('exponent 2')
texp2=abs((ps5lm(4)-pr5lm(4))/sqrt(seps5lm(4)^2+sepr5lm(4)^2)) %
Rosner Eq. 8.23
pexp2=(1-tcdf(texp2,9+9-2*4))*2
disp('constant')
tconst=abs((ps5lm(1)-pr5lm(1))/sqrt(seps5lm(1)^2+sepr5lm(1)^2)) %
Rosner Eq. 8.23
pconst=(1-tcdf(tconst,9+9-2*4))*2
disp('try tests that compare overall curve to see if things are different')
% from "The GraphPad Guide to Nonlinear Regression"
disp('If p < 0.05, then the curves are different.')
disp('control')
% combine data sets
xcsr=[timed; timed];
yrsc=[contregd; contsped];
stdrsc=[contregstdd; contspestdd];
[frsc,prsc,seprsc,ciprsc,cifrsc,residrsc,rssrsc,r2rsc]=leasqr2(xcsr,yrsc,p05,'ex
p3',.0001,100,1,[1;1;1;1],'partexp3',options3,'exp6',stdrsc);
title('Combined for Controls, 4-Parameter Model')
print -deps rsc
rsssep=rssr7lm+rsss7lm;
fstat=(rssrsc-rsssep)*dfsep/rssrsc/(dfcomb-dfsep)
fp=1-fcdf(fstat,dfcomb-dfsep,dfsep)
pause
disp('seeded')
% combine data sets
yrss=[seedregd; seedsped];
stdrss=[seedregstdd; seedspestdd];
```

```
[frss,prss,seprss,ciprss,cifrss,residrss,rssrss,r2rss]=leasqr2(xcsr,yrss,p05,'exp
3',.0001,100,1,[1;1;1;1],'partexp3',options3,'exp6',stdrss);
title('Combined for Seeded, 4-Parameter Model')
print -deps rss
rsssep=rssr5lm+rsss5lm;
fstat=(rssrss-rsssep)*dfsep/rssrss/(dfcomb-dfsep)
fp=1-fcdf(fstat,dfcomb-dfsep,dfsep)
```

gn.m

```
function [p,resid,rss,r2,cip,yp,ciyp]=gn(x,y,model,p0)
% function gn              does nonlinear curve fitting by Gauss-Newton
method and finds
%                          all statistical values, as well as plotting
% p         parameter estimates from nonlinear regression
% resid     residuals
% rss       residual sum-of-squares
% cip       confidence intervals for p
% yp        predicted y values from the regression equation
% ciyp      confidence intervals for yp
% x         inputs
% y         output
% model     function for nonlinear equation
% p0        initial values for p
% j         Jacobian

[p,resid,j]=nlinfit(x,y,model,p0);
rss=sum(resid.^2);
cip=nlparci(p,resid,j);
[yp,ciyp]=nlpredci(model,x,p,resid,j);
ciyp
%nlintool(x,y,model,p0) % plots the predicted line and the cofindence lines
yphigh=yp+ciyp;          % upper confidence for yp
yplow=yp-ciyp;           % lower confidence for yp
plot(x,y,'o',x,yp,'+',x,yphigh,'--',x,yplow,'--');
xlabel('Time (weeks)')
ylabel('Percent Contraction')
% calculate R^2 (ref. = Draper & Smith p. 46)
r=corrcoef(y, yp);
r2=r(1,2).^2;
```

leasqr.m

```
function
[f,p,sep,cip,cif,resid,rss,r2]=leasqr(x,y,pin,func,stol,niter,wt,dp,dfdp,options,
model2,errory)
%function[f,p,kvg,iter,corp,covp,covr,stdresid,Z,r2]=
%              leasqr(x,y,pin,{func,stol,niter,wt,dp,dfdp,options})
%
% Version 3.beta
% Levenberg-Marquardt nonlinear regression of f(x,p) to y(x), where:
% x=vec or mat of indep variables, 1 row/observation: x=[x0 x1....xm]
% y=vec of obs values, same no. of rows as x.
% wt=vec(dim=1 or length(x)) of statistical weights. These should be set
%  to be proportional to (sqrts of var(y))^-1; (That is, the covaraince
%  matrix of the data is assumed to be proportional to diagonal with
diagonal
%  equal to (wt.^2)^-1. The constant of proportionality will be estimated.),
%  default=1.
% pin=vector of initial parameters to be adjusted by leasqr.
% dp=fractional incr of p for numerical partials,default=
.001*ones(size(pin))
%  dp(j)>0 means central differences.
%  dp(j)<0 means one-sided differences.
% Note: dp(j)=0 holds p(j) fixed i.e. leasqr wont change initial guess: pin(j)
% func=name of function in quotes,of the form y=f(x,p)
% dfdp=name of partials M-file in quotes default is prt=dfdp(x,f,p,dp,func)
% stol=scalar tolerances on fractional improvement in ss,default stol=.0001
% niter=scalar max no. of iterations, default = 20
% options=matrix of n rows (same number of rows as pin) containing
%  column 1: desired fractional precision in parameter estimates.
%    Iterations are terminated if change in parameter vector (chg) on two
%    consecutive iterations is less than their corresponding elements
%    in options(:,1). [ie. all(abs(chg*current parm est) < options(:,1))
%     on two consecutive iterations.], default = zeros().
%  column 2: maximum fractional step change in parameter vector.
%    Fractional change in elements of parameter vector is constrained to be
%    at most options(:,2) between sucessive iterations.
%    [ie. abs(chg(i))=abs(min([chg(i) options(i,2)*current param
estimate])).],
%    default = Inf*ones().
% model2=same as func except x and p are switched as input variables,
which
%              is the way MATLAB functions use models
% errory=standard error of the y variables, used for plotting only
%
%       OUTPUT VARIABLES
% f=vec function values computed in function func.
% p=vec trial or final parameters. i.e, the solution.
% kvg=scalar: =1 if convergence, =0 otherwise.
% iter=scalar no. of interations used.
% corp= correlation matrix for parameters
% covp= covariance matrix of the parameters
% covr = diag(covariance matrix of the residuals)
% stdresid= standardized residuals
% rss=residual sum of squares
% Z= matrix that defines confidence region
% r2= coefficient of multiple determination
% sep= standard error of p
% cip = confidence intervals for p
% cif = confidence intervals for the prediced y values
% sef = standard errors for the y values

% {}= optional parameters
% ss=scalar sum of squares=sum-over-i(wt(i)*(y(i)-f(i)))^2.

% All Zero guesses not acceptable
% Richard I. Shrager (301)-496-1122
% Modified by A.Jutan (519)-679-2111
% Modified by Ray Muzic 14-Jul-1992
%     1) add maxstep feature for limiting changes in parameter estimates
%       at each step.
%     2) remove forced columnization of x (x=x(:)) at beginning. x could be
%       a matrix with the ith row of containing values of the
%       independent variables at the ith observation.
%     3) add verbose option
%     4) add optional return arguments covp, stdresid, chi2
%     5) revise estimates of corp, stdev
% Modified by Ray Muzic 11-Oct-1992
%     1) revise estimate of Vy.  remove chi2, add Z as return values
% Modified by Ray Muzic 7-Jan-1994
%     1) Replace ones(x) with a construct that is compatible with versions
%       newer and older than v 4.1.
%     2) Added global declaration of verbose (needed for newer than v4.x)
%     3) Replace return value var, the variance of the residuals with covr,
%       the covariance matrix of the residuals.
%     4) Introduce options as 10th input argument.  Include
%       convergence criteria and maxstep in it.
%     5) Correct calculation of xtx which affects coveraince estimate.
%     6) Eliminate stdev (estimate of standard deviation of parameter
%       estimates) from the return values.  The covp is a much more
%       meaningful expression of precision because it specifies a confidence
%       region in contrast to a confidence interval..  If needed, however,
%       stdev may be calculated as stdev=sqrt(diag(covp)).
%     7) Change the order of the return values to a more logical order.
%     8) Change to more efficent algorithm of Bard for selecting epsL.
%
% Refrences:
% Bard, Nonlinear Parameter Estimation, Academic Press, 1974.
% Draper and Smith, Applied Regression Analysis, John Wiley and Sons,
1981.
%
%set default args

% argument processing
%

plotcmd='plot(x(:,1),y,"o",x(:,1),f,"+"); shg';
if (sscanf(version,'%f') >= 4),
 global verbose
 plotcmd='plot(x(:,1),y,"o",x(:,1),f,"+"); figure(gcf)';
end;

if(exist('verbose')~=1), verbose=1; end;
if (nargin <= 8), dfdp='dfdp'; end;
if (nargin <= 7), dp=.001*(pin*0+1); end; %DT
if (nargin == 6), wt=1.0; end;
if (nargin <= 5), niter=20; end;
```

```
if (nargin == 4), stol=.0001; end;
%

y=y(:); wt=wt(:); pin=pin(:); dp=dp(:); %change all vectors to columns
% check data vectors- same length?
m=length(y); n=length(pin); p=pin;[m1,m2]=size(x);
if m1~=m ,error('input(x)/output(y) data must have same number of rows ')
,end;

if (nargin <= 9),
 options=[zeros(n,1) Inf*ones(n,1)];
 nor = n; noc = 2;
else
 [nor noc]=size(options);
 if (nor ~= n),
  error('options and parameter matrices must have same number of rows'),
 end;
 if (noc ~= 2),
  options=[options(noc,1) Inf*ones(noc,1)];
 end;
end;
pprec=options(:,1);
maxstep=options(:,2);
%
% set up for iterations
%
f=feval(func,x,p); fbest=f; pbest=p;
r=wt.*(y-f);
sbest=r'*r;
nrm=zeros(n,1);
chgprev=Inf*ones(n,1);
kvg=0;
epsLlast=1;
epstab=[.1 1 1e2 1e4 1e6];

% do iterations
%
for iter=1:niter,
 pprev=pbest;
 prt=feval(dfdp,x,fbest,pprev,dp,func);
 r=wt.*(y-fbest);
 sprev=sbest;
 sgoal=(1-stol)*sprev;
 for j=1:n,
  if dp(j)==0,
   nrm(j)=0;
  else
   prt(:,j)=wt.*prt(:,j);
   nrm(j)=prt(:,j)'*prt(:,j);
   if nrm(j)>0,
    nrm(j)=1/sqrt(nrm(j));
   end;
  end
  prt(:,j)=nrm(j)*prt(:,j);
 end;
 [prt,s,v]=svd(prt,0);
 s=diag(s);
 g=prt'*r;
 for jjj=1:length(epstab),
  epsL = max(epsLlast*epstab(jjj),1e-7);
  se=sqrt((s.*s)+epsL);
  gse=g./se;
  chg=((v*gse).*nrm);
%  check the change constraints and apply as necessary
  ochg=chg;
  for iii=1:n,
   if (maxstep(iii)==Inf), break; end;
   chg(iii)=max(chg(iii),-abs(maxstep(iii)*pprev(iii)));
   chg(iii)=min(chg(iii),abs(maxstep(iii)*pprev(iii)));
  end;
  if (verbose & any(ochg ~= chg)),
   disp(['Change in parameter(s): ' ...
     sprintf('%d ',find(ochg ~= chg)) 'were constrained']);
  end;
  aprec=abs(pprec.*pbest);     %---
  if (any(abs(chg) > 0.1*aprec)),%---  % only worth evaluating function if
   p=chg+pprev;                % there is some non-miniscule change
   f=feval(func,x,p);
   r=wt.*(y-f);
   ss=r'*r;
   if ss<sbest,
    pbest=p;
    fbest=f;
    sbest=ss;
   end;
   if ss<=sgoal,
    break;
   end;
  end;                         %---
 end;
 epsLlast = epsL;
 if (verbose),
  eval(plotcmd);
 end;
 if ss<eps,
  break;
 end
 aprec=abs(pprec.*pbest);
%  [aprec chg chgprev]
 if (all(abs(chg) < aprec) & all(abs(chgprev) < aprec)),
  kvg=1;
  if (verbose),
   fprintf('Parameter changes converged to specified precision\n');
  end;
  break;
 else
  chgprev=chg;
 end;
 if ss>sgoal,
  break;
 end;
end;
% set return values
%
p=pbest;
f=fbest;
ss=sbest;
kvg=((sbest>sgoal)|(sbest<=eps)|kvg);
if kvg ~= 1 , disp(' CONVERGENCE NOT ACHIEVED! '), end;

% CALC VARIANCE COV MATRIX AND CORRELATION MATRIX
OF PARAMETERS
% re-evaluate the Jacobian at optimal values
jac=feval(dfdp,x,f,p,dp,func);
msk = dp ~= 0;
n = sum(msk);          % reduce n to equal number of estimated parameters
jac = jac(:, msk);     % use only fitted parameters

%% following section is Ray Muzic's estimate for covariance and
correlation
%% assuming covariance of data is a diagonal matrix proportional to
%% diag(1/wt.^2).
%% cov matrix of data est. from Bard Eq. 7-5-13, and Row 1 Table 5.1

Qinv=diag(wt.*wt);
Q=diag((0*wt+1)./(wt.^2));
%[nrw ncw]=size(wt);
%Q=ones(nrw,ncw)./wt; Q=diag(Q.*Q);
resid=y-f;                     %un-weighted residuals
rss=sum(resid.^2);                                          % residual
sum of squares
covr=resid'*Qinv*resid*Q/(m-n);          %(co)variance of residuals
Vy=1/(1-n/m)*covr;  % Eq. 7-13-22, Bard      %covariance of the data
covr=diag(covr);                       %for compact storage
Z=((m-n)*jac'*Qinv*jac)/(n*resid'*Qinv*resid);
stdresid=resid./sqrt(diag(Vy));

jtgjinv=inv(jac'*Qinv*jac);
covp=jtgjinv*jac'*Qinv*Vy*Qinv*jac*jtgjinv; % Eq. 7-5-13, Bard %cov of
parm est
for k=1:n,
 for j=k:n,
  corp(k,j)=covp(k,j)/sqrt(abs(covp(k,k)*covp(j,j)));
  corp(j,k)=corp(k,j);
 end;
end;

%%% alt. est. of cov. mat. of parm.:(Delforge, Circulation, 82:1494-1504,
1990
%%disp('Alternate estimate of cov. of param. est.')
```

```
%%acovp=resid'*Qinv*resid/(m-n)*jtgjinv

%Calculate R^2 (Ref Draper & Smith p.46)
%
r=corrcoef(y,f);
r2=r(1,2).^2;

% calculate confidence intervals for p
% se is from Draper and Smith P. 528 (their z = jac' here)
% cip is from Rosner P. 462
%sep=(diag(inv(jac*jac')).*rss./(m-n)).^.5          % standard error in p
%cip=[p-tinv(.975,m-n-1).*sep p'+tinv(.975,m-n-1).*sep]% confidence
intervals for p
% I will try it with MATLAB since this is actually easier
cip=nlparci(p,resid,jac);
sep=(p-cip(:,1))./tinv(.975,m-n-1);  % based on Rosner P. 462

% calculate the confidence intervals for the predicted values
[dummy,cifdelta]=nlpredci(model2,x,p,resid,jac);
cif=[f-cifdelta f+cifdelta];                % confidence interval for the
predicted y
sef=cifdelta./tinv(.975,m-n-1); % standard errors in the predicted y from
Rosner P. 463

% if someone has asked for it, let them have it
%
if (verbose),
%  eval(plotcmd);
% plot everything
 errorbar(x(:,1),y,errory,'o');  % plot original data points with errorbars
 xlabel('Time (weeks)')
 ylabel('Fractional Areal Contraction');
 hold on
 xinter=0:.001:6;
 yinter=feval(func,xinter,p);
 plot(xinter,yinter)          % plot fit line
 plot(xinter,interp1(x,cif(:,1),xinter),'r--')  % plot lower confidence interval
 plot(xinter,interp1(x,cif(:,2),xinter),'r--')  % plot upper confidence interval
 ax=axis;
 axis([ax(1) 7 0 ax(4)])
 hold off
 disp(' Least Squares Estimates of Parameters')
 disp(p')
 disp('Standard Errors of the Parameters')
 disp(sep)
 disp('Confidence Intervals for the Parameters')
 disp(cip)
 disp('Predicted y Values')
 disp(f)
 disp('Confidence Intervals for the Predicted y')
 disp(cif)
%  disp(' Correlation matrix of parameters estimated')
%  disp(corp)
%  disp('Covariance matrix of Residuals  ' )
%  disp(covr)
 disp('Residual Sum of Squares')
 disp(rss)
 disp( 'Correlation Coefficient R^2')
 disp(r2)
%  sprintf('95%% conf region: F(0.05)(%.0f,%.0f)>=
delta_pvec'*Z*delta_pvec',n,m-n)
%  Z
end;

% A modified version of Levenberg-Marquardt
% Non-Linear Regression program previously submitted by R.Schrager.
% This version corrects an error in that version and also provides
% an easier to use version with automatic numerical calculation of
% the Jacobian Matrix. In addition, this version calculates statistics
% such as correlation, etc....
%
% Version 3 Notes
% Errors in the original version submitted by Shrager (now called version 1)
% and the improved version of Jutan (now called version 2) have been
corrected.
% Additional features, statisitcal tests, and documentation have also been
% included along with an example of usage.  BEWARE: Some the the input
and
% output arguments were changed from the previous version.
%
%    Ray Muzic    rfm2@ds2.uh.cwru.edu
%    Arthur Jutan  jutan@charon.engga.uwo.ca


leasqr2.m

function
[f,p,sep,cip,cif,resid,rss,r2]=leasqr(x,y,pin,func,stol,niter,wt,dp,dfdp,options,
model2,errory)
%function[f,p,kvg,iter,corp,covp,covr,stdresid,Z,r2]=
%                leasqr(x,y,pin,{func,stol,niter,wt,dp,dfdp,options})
%
% Version 3.beta
% Levenberg-Marquardt nonlinear regression of f(x,p) to y(x), where:
% x=vec or mat of indep variables, 1 row/observation: x=[x0 x1....xm]
% y=vec of obs values, same no. of rows as x.
% wt=vec(dim=1 or length(x)) of statistical weights.  These should be set
%   to be proportional to (sqrts of var(y))^-1; (That is, the covaraince
%   matrix of the data is assumed to be proportional to diagonal with
diagonal
%   equal to (wt.^2)^-1.  The constant of proportionality will be estimated.),
%   default=1.
% pin=vector of initial parameters to be adjusted by leasqr.
% dp=fractional incr of p for numerical partials,default=
.001*ones(size(pin))
%   dp(j)>0 means central differences.
%   dp(j)<0 means one-sided differences.
% Note: dp(j)=0 holds p(j) fixed i.e. leasqr wont change initial guess: pin(j)
% func=name of function in quotes,of the form y=f(x,p)
% dfdp=name of partials M-file in quotes default is prt=dfdp(x,f,p,dp,func)
% stol=scalar tolerances on fractional improvement in ss,default stol=.0001
% niter=scalar max no. of iterations, default = 20
% options=matrix of n rows (same number of rows as pin) containing
%   column 1: desired fractional precision in parameter estimates.
%     Iterations are terminated if change in parameter vector (chg) on two
%     consecutive iterations is less than their corresponding elements
%     in options(:,1).  [ie. all(abs(chg*current parm est) < options(:,1))
%      on two consecutive iterations.], default = zeros().
%   column 2: maximum fractional step change in parameter vector.
%     Fractional change in elements of parameter vector is constrained to be
%     at most options(:,2) between sucessive iterations.
%     [ie. abs(chg(i))=abs(min([chg(i) options(i,2)*current param
estimate])).],
%     default = Inf*ones().
% model2=same as func except x and p are switched as input variables,
which
%               is the way MATLAB functions use models
% errory=standard error of the y variables, used for plotting only
%
%        OUTPUT VARIABLES
% f=vec function values computed in function func.
% p=vec trial or final parameters. i.e, the solution.
% kvg=scalar: =1 if convergence, =0 otherwise.
% iter=scalar no. of interations used.
% corp= correlation matrix for parameters
% covp= covariance matrix of the parameters
% covr = diag(covariance matrix of the residuals)
% stdresid= standardized residuals
% rss=residual sum of squares
% Z= matrix that defines confidence region
% r2= coefficient of multiple determination
% sep= standard error of p
% cip = confidence intervals for p
% cif = confidence intervals for the prediced y values
% sef = standard errors for the y values

%  {}= optional parameters
% ss=scalar sum of squares=sum-over-i(wt(i)*(y(i)-f(i)))^2.

% All Zero guesses not acceptable
% Richard I. Shrager (301)-496-1122
% Modified by A.Jutan (519)-679-2111
% Modified by Ray Muzic 14-Jul-1992
%     1) add maxstep feature for limiting changes in parameter estimates
%       at each step.
%     2) remove forced columnization of x (x=x(:)) at beginning. x could be
%       a matrix with the ith row of containing values of the
%       independent variables at the ith observation.
%     3) add verbose option
%     4) add optional return arguments covp, stdresid, chi2
```

```
%     5) revise estimates of corp, stdev
% Modified by Ray Muzic 11-Oct-1992
%     1) revise estimate of Vy.  remove chi2, add Z as return values
% Modified by Ray Muzic 7-Jan-1994
%     1) Replace ones(x) with a construct that is compatible with versions
%        newer and older than v 4.1.
%     2) Added global declaration of verbose (needed for newer than v4.x)
%     3) Replace return value var, the variance of the residuals with covr,
%        the covariance matrix of the residuals.
%     4) Introduce options as 10th input argument.  Include
%        convergence criteria and maxstep in it.
%     5) Correct calculation of xtx which affects coveraince estimate.
%     6) Eliminate stdev (estimate of standard deviation of parameter
%        estimates) from the return values.  The covp is a much more
%        meaningful expression of precision because it specifies a confidence
%        region in contrast to a confidence interval..  If needed, however,
%        stdev may be calculated as stdev=sqrt(diag(covp)).
%     7) Change the order of the return values to a more logical order.
%     8) Change to more efficent algorithm of Bard for selecting epsL.
%
% Refrences:
% Bard, Nonlinear Parameter Estimation, Academic Press, 1974.
% Draper and Smith, Applied Regression Analysis, John Wiley and Sons,
1981.
%
%set default args

% argument processing
%

plotcmd='plot(x(:,1),y,"o",x(:,1),f,"+"); shg';
if (sscanf(version,'%f') >= 4),
  global verbose
  plotcmd='plot(x(:,1),y,"o",x(:,1),f,"+"); figure(gcf)';
end;

if(exist('verbose')~=1), verbose=1; end;
if (nargin <= 8), dfdp='dfdp'; end;
if (nargin <= 7), dp=.001*(pin*0+1); end; %DT
if (nargin == 6), wt=1.0; end;
if (nargin <= 5), niter=20; end;
if (nargin == 4), stol=.0001; end;
%

y=y(:); wt=wt(:); pin=pin(:); dp=dp(:); %change all vectors to columns
% check data vectors- same length?
m=length(y); n=length(pin); p=pin;[m1,m2]=size(x);
if m1~=m ,error('input(x)/output(y) data must have same number of rows ')
,end;

if (nargin <= 9),
  options=[zeros(n,1) Inf*ones(n,1)];
  nor = n; noc = 2;
else
  [nor noc]=size(options);
  if (nor ~= n),
    error('options and parameter matrices must have same number of rows'),
  end;
  if (noc ~= 2),
    options=[options(noc,1) Inf*ones(noc,1)];
  end;
end;
pprec=options(:,1);
maxstep=options(:,2);
%
% set up for iterations
%
f=feval(func,x,p); fbest=f; pbest=p;
r=wt.*(y-f);
sbest=r'*r;
nrm=zeros(n,1);
chgprev=Inf*ones(n,1);
kvg=0;
epsLlast=1;
epstab=[.1 1 1e2 1e4 1e6];

% do iterations
%
for iter=1:niter,
  pprev=pbest;
  prt=feval(dfdp,x,fbest,pprev,dp,func);
  r=wt.*(y-fbest);
  sprev=sbest;
  sgoal=(1-stol)*sprev;
  for j=1:n,
    if dp(j)==0,
      nrm(j)=0;
    else
      prt(:,j)=wt.*prt(:,j);
      nrm(j)=prt(:,j)'*prt(:,j);
      if nrm(j)>0,
        nrm(j)=1/sqrt(nrm(j));
      end;
    end
    prt(:,j)=nrm(j)*prt(:,j);
  end;
  [prt,s,v]=svd(prt,0);
  s=diag(s);
  g=prt'*r;
  for jjj=1:length(epstab),
    epsL = max(epsLlast*epstab(jjj),1e-7);
    se=sqrt((s.*s)+epsL);
    gse=g./se;
    chg=((v*gse).*nrm);
%   check the change constraints and apply as necessary
    ochg=chg;
    for iii=1:n,
      if (maxstep(iii)==Inf), break; end;
      chg(iii)=max(chg(iii),-abs(maxstep(iii)*pprev(iii)));
      chg(iii)=min(chg(iii),abs(maxstep(iii)*pprev(iii)));
    end;
    if (verbose & any(ochg ~= chg)),
      disp(['Change in parameter(s): ' ...
        sprintf('%d ',find(ochg ~= chg)) 'were constrained']);
    end;
    aprec=abs(pprec.*pbest);      %---
    if (any(abs(chg) > 0.1*aprec)),%---  % only worth evaluating function if
      p=chg+pprev;                       % there is some non-miniscule change
      f=feval(func,x,p);
      r=wt.*(y-f);
      ss=r'*r;
      if ss<sbest,
        pbest=p;
        fbest=f;
        sbest=ss;
      end;
      if ss<=sgoal,
        break;
      end;
    end;                        %---
  end;
  epsLlast = epsL;
  if (verbose),
    eval(plotcmd);
  end;
  if ss<eps,
    break;
  end
  aprec=abs(pprec.*pbest);
%  [aprec chg chgprev]
  if (all(abs(chg) < aprec) & all(abs(chgprev) < aprec)),
    kvg=1;
    if (verbose),
      fprintf('Parameter changes converged to specified precision\n');
    end;
    break;
  else
    chgprev=chg;
  end;
  if ss>sgoal,
    break;
  end;
end;
% set return values
%
p=pbest;
f=fbest;
ss=sbest;
kvg=((sbest>sgoal)|(sbest<=eps)|kvg);
if kvg ~= 1 , disp(' CONVERGENCE NOT ACHIEVED! '), end;
```

```
% CALC VARIANCE COV MATRIX AND CORRELATION MATRIX
OF PARAMETERS
% re-evaluate the Jacobian at optimal values
jac=feval(dfdp,x,f,p,dp,func);
msk = dp ~= 0;
n = sum(msk);          % reduce n to equal number of estimated parameters
jac = jac(:, msk);     % use only fitted parameters

%% following section is Ray Muzic's estimate for covariance and
correlation
%% assuming covariance of data is a diagonal matrix proportional to
%% diag(1/wt.^2).
%% cov matrix of data est. from Bard Eq. 7-5-13, and Row 1 Table 5.1

Qinv=diag(wt.*wt);
Q=diag((0*wt+1)./(wt.^2));
%[nrw ncw]=size(wt);
%Q=ones(nrw,ncw)./wt; Q=diag(Q.*Q);
resid=y-f;                          %un-weighted residuals
rss=sum(resid.^2);                                          % residual
sum of squares
covr=resid'*Qinv*resid*Q/(m-n);              %(co)variance of residuals
Vy=1/(1-n/m)*covr;  % Eq. 7-13-22, Bard       %covariance of the data
covr=diag(covr);                        %for compact storage
Z=((m-n)*jac'*Qinv*jac)/(n*resid'*Qinv*resid);
stdresid=resid./sqrt(diag(Vy));

jtgjinv=inv(jac'*Qinv*jac);
covp=jtgjinv*jac'*Qinv*Vy*Qinv*jac*jtgjinv; % Eq. 7-5-13, Bard %cov of
parm est
for k=1:n,
 for j=k:n,
  corp(k,j)=covp(k,j)/sqrt(abs(covp(k,k)*covp(j,j)));
  corp(j,k)=corp(k,j);
 end;
end;

%%% alt. est. of cov. mat. of parm.:(Delforge, Circulation, 82:1494-1504,
1990
%%disp('Alternate estimate of cov. of param. est.')
%%acovp=resid'*Qinv*resid/(m-n)*jtgjinv

%Calculate R^2 (Ref Draper & Smith p.46)
%
r=corrcoef(y,f);
r2=r(1,2).^2;

% calculate confidence intervals for p
% se is from Draper and Smith P. 528 (their z = jac' here)
% cip is from Rosner P. 462
%sep=(diag(inv(jac*jac')).*rss./(m-n)).^.5          % standard error in p
%cip=[p-tinv(.975,m-n-1).*sep p'+tinv(.975,m-n-1).*sep]% confidence
intervals for p
% I will try it with MATLAB since this is actually easier
cip=nlparci(p,resid,jac);
sep=(p-cip(:,1))./tinv(.975,m-n-1);  % based on Rosner P. 462

% calculate the confidence intervals for the predicted values
[dummy,cifdelta]=nlpredci(model2,x,p,resid,jac);
cif=[f-cifdelta f+cifdelta];                % confidence interval for the
predicted y
sef=cifdelta./tinv(.975,m-n-1); % standard errors in the predicted y from
Rosner P. 463

% if someone has asked for it, let them have it
%
if (verbose),
% eval(plotcmd);
% plot everything
 errorbar(x(:,1),y,errory,'o');  % plot original data points with errorbars
 xlabel('Time (weeks)')
 ylabel('Fractional Areal Contraction');
 hold on
 xinter=0:.001:6;
 yinter=feval(func,xinter,p);
 plot(xinter,yinter)        % plot fit line
 ax=axis;
 axis([ax(1) 7 0 ax(4)])
 hold off
 disp(' Least Squares Estimates of Parameters')
 disp(p')
 disp('Standard Errors of the Parameters')
 disp(sep)
 disp('Confidence Intervals for the Parameters')
 disp(cip)
 disp('Predicted y Values')
 disp(f)
 disp('Confidence Intervals for the Predicted y')
 disp(cif)
% disp(' Correlation matrix of parameters estimated')
% disp(corp)
% disp('Covariance matrix of Residuals  ' )
% disp(covr)
 disp('Residual Sum of Squares')
 disp(rss)
 disp( 'Correlation Coefficient R^2')
 disp(r2)
% sprintf('95%% conf region: F(0.05)(%.0f,%.0f)>=
delta_pvec'*Z*delta_pvec',n,m-n)
% Z
end;

% A modified version of Levenberg-Marquardt
% Non-Linear Regression program previously submitted by R.Schrager.
% This version corrects an error in that version and also provides
% an easier to use version with automatic numerical calculation of
% the Jacobian Matrix. In addition, this version calculates statistics
% such as correlation, etc....
%
% Version 3 Notes
% Errors in the original version submitted by Shrager (now called version 1)
% and the improved version of Jutan (now called version 2) have been
corrected.
% Additional features, statisitcal tests, and documentation have also been
% included along with an example of usage.  BEWARE: Some the the input
and
% output arguments were changed from the previous version.
%
%    Ray Muzic    rfm2@ds2.uh.cwru.edu
%    Arthur Jutan  jutan@charon.engga.uwo.ca
```

exp1.m

```
function y=exp1(x,p)
% y=a+b*exp(c*t)
y=p(1)+p(2).*exp(p(3).*x);
```

exp2.m

```
function y=exp2(x,p)
% y=a-a*exp(b*t)
y=p(1)-p(1).*exp(p(2).*x);
```

exp3.m

```
function y=exp3(x,p)
y=p(1)+p(2).*exp(p(3).*x)-(p(1)+p(2))*exp(p(4)*x);
```

exp4.m

```
function y=exp4(p,x)
% y=a+b*exp(c*t)
y=p(1)+p(2).*exp(p(3).*x);
```

exp5.m

```
function y=exp5(p,x)
% y=a-a*exp(b*t)
y=p(1)-p(1).*exp(p(2).*x);
```

exp6.m

```
function y=exp6(p,x)
y=p(1)+p(2).*exp(p(3).*x)-(p(1)+p(2))*exp(p(4)*x);
```

partexp1.m

```
function y = partexp1(x,f,p,dp,func)
y=[ones(size(x)) exp(p(3)*x) p(2)*x.*exp(p(3)*x)];
```

partexp2.m

```
function y = partexp2(x,f,p,dp,func)
y=[ones(size(x))-exp(p(2)*x) -p(1)*x.*exp(p(2)*x)];
```

partexp3.m

```
function y = partexp3(x,f,p,dp,func)
y=[1-exp(p(4)*x) exp(p(3)*x)-exp(p(4)*x) p(2)*x.*exp(p(3)*x) -
(p(1)+p(2))*x.*exp(p(4)*x)];
```

dfdp.m

```
function prt=dfdp(x,f,p,dp,func)
% numerical partial derivatives (Jacobian) df/dp for use with leasqr
% --------INPUT VARIABLES---------
% x=vec or matrix of indep var(used as arg to func) x=[x0 x1 ....]
% f=func(x,p) vector initialsed by user before each call to dfdp
% p= vec of current parameter values
% dp= fractional increment of p for numerical derivatives
%     dp(j)>0 central differences calculated
%     dp(j)<0 one sided differences calculated
%     dp(j)=0 sets corresponding partials to zero; i.e. holds p(j) fixed
% func=string naming the function (.m) file
%     e.g. to calc Jacobian for funcion expsum
prt=dfdp(x,f,p,dp,'expsum')
%----------OUTPUT VARIABLES-------
% prt= Jacobian Matrix prt(i,j)=df(i)/dp(j)
%===================================
m=length(x);n=length(p);     %dimensions
ps=p; prt=zeros(m,n);del=zeros(n,1);        % initialise Jacobian
to
Zero
for j=1:n
    del(j)=dp(j) .*p(j);    %cal delx=fract(dp)*param value(p)
        if p(j)==0
        del(j)=dp(j);     %if param=0 delx=fraction
        end
    p(j)=ps(j) + del(j);
    if del(j)~=0, f1=feval(func,x,p);
        if dp(j) < 0, prt(:,j)=(f1-f)./del(j);
else
        p(j)=ps(j)- del(j);
        prt(:,j)=(f1-feval(func,x,p))./(2 .*del(j));
        end
    end
    p(j)=ps(j);     %restore p(j)
end
return
```

Appendix CC. Radiolabeling of ^{35}S and ^{3}H Protocol

Modified from (134). Based on (128).

General

1) Label disks during final 24 hrs of culture with ^{35}S and ^{3}H to measure GAG and collagen synthesis, respectively.
2) Wash unincorporated radiolabel.
3) Lyophilize tissue and measure dry weights.
4) Papain or Proteinase K digestion – use digest for GAG content, DNA content, and scintillation counts

Materials Needed

1) Latex gloves (double glove)
2) Tape for labcoat sleeves
3) Aluminum foil to line hood
4) Complete medium (10% FBS, Appendix M)
5) Sterile 15 mL or 50 mL centrifuge tube
6) Pipetman – 20 µL and/or 200 µL
7) Sterile pipette tips – 200 µL capacity
8) Vacuum flask and sterile Pasteur pipettes
9) Radionuclides: tritiated proline (^{3}H) (proline, L-[2,3,4,5-^{3}H]; #NET,483, Perkin Elmer or #TRK534, Amersham Pharmacia Biotech, Inc.) and radioactive sulfate (^{35}S) (#NET041H, Perkin Elmer)
10) PBS
11) Na_2SO_4 (anhydrous sodium sulfate; #S421-1, Fisher Scientific Co.) and L-proline (P-8449, Sigma)
12) Clean spatula/forceps
13) 24 well culture plates
14) Sterile pipettes

Preparation of Radioactive Media

1) Calculate volume of isotope needed:

a. With 1.5 mL media/disc; V=1.5n+2 mL, where n is the number of discs.

b. ^{35}S has a half-life is 87.4 days:

$$volume^{35}S = \frac{R_{cS}V}{C_{vS} \times 2^{-x/87.4}}, \qquad \text{Equation 22}$$

where R_{cS} is the radioactivity concentration you desire for ^{35}S and C_{vS} is the concentration of radioactivity of your sulfate vial. The former (R_{cS}) is usually 10 μCi/mL for 9 mm-diameter CG discs. The latter is often 1000 μCi/mL when you order 1 mCi or 10,000 μCi/mL when you order 10 mCi, but you should check the bottle. x = # days past calibration date on vial.

c. For ^{3}H the half-life is 8-9 years.

$$volume^{3}H = \frac{R_{cH}V}{C_{vH}}, \qquad \text{Equation 23}$$

where R_{cH} is the radioactivity concentration you desire for ^{3}H and C_{vH} is the concentration of radioactivity of your proline vial. The former (R_{cH}) is usually 10 μCi/mL for 9 mm-diameter CG discs. The latter is often 1000 μCi/mL when you order 1 mCi, but you should check the bottle.

2) Wipe hood with 70% EtOH.
3) Line with aluminum foil.
4) Double glove and tape lab coat sleeves.
5) Aliquot calculated volume of warm media into centrifuge tube.
6) Place radionuclide in hood on aluminum foil and loosen cap.
7) Use sterile technique to aliquot calculated volume of ^{35}S.
8) Save 1 mL of this single-labeled media for calibration.
9) Add calculated volume of ^{3}H.
10) Save 1 mL of this double-labeled media for calibration.
11) Remove pipette tips to original wrapper and dispose of in radioactive waste container.
12) Return radionuclides to container and note amount used; return to refrigerator.
13) Rinse Pipetman in cold water.
14) Check Pipetman and hood with Geiger counter.

Labeling of Discs

1) Place 1.5 mL of radiolabeled medium in 24 well plate (#08-772-1, Fisher Scientific Co.) wells. Generally, use the top row only so the bottom rows can be used for washings.
2) Use a forceps to transfer the discs to the radiolabeled wells. Drop them gently. Do not let the forceps touch the radiolabeled medium.
3) Return pipette to paper wrapper and dispose of in radioactive waste container.
4) After 24 hours, radiolabel is complete.

Washing of Discs:

1) Complete PBS with 0.8 mM Na_2SO_4 and 1.0 mM proline.
    a. For 500 mL PBS: 0.057 g Na_2SO_4 and 0.057 g proline.
    b. Recommended to make fresh wash solution each time; can make frozen stock solutions of proline and sulfate and dilute in PBS.
2) Line hood with aluminum foil.
3) Aliquot 1 mL PBS/well in 24 well culture plate. Put this into all the wells below each radiolabeled well in the plate.

4) Place in cold room for 15 minutes.
5) Transfer disks to 3rd row and refrigerate for 15 minutes.
6) Repeat for a total of five washes.
7) Dispose of radiolabeled media in sink and note amount of radioactivity disposed. Optional: Save the medium if you wish to count it.
8) Place each sample in a labeled vial.
9) Optional: Save PBS from last row (1 from each group) to make sure thoroughly washed (radioactive counts ~ background).
10) Lyophilize, measure dry weight, digest... (for DNA, GAG, scintillation counting).

Better results in scintillation counting may be achieved if only 0.5 mL is used for control medium samples that you remove.

Appendix DD. Scintillation Counting of ^{3}H and ^{35}S Radiolabeled Samples

Counting Protocol

1. Combine 100 µL of sample digest or calibrated media with 4 mL of scintillation fluid (ScintiVerse II; Fl-09-0797, Fisher Scientific Co.). Assay samples in duplicate.

2. Spray and wipe off the scintillation vials and holders with staticide (#2005, ACL Staticide). Then, queue them in the machine. The maximum number of samples at once is 230. The first vials go in the tray with 6 at the top. On this tray, turn the dial to 1 (means it counts the tray only once). The rest of the vials go in trays with no number. (Yellow dot on dial means do not count; white dot means count continuously.)

3. Count 1 minute/sample, with ^{3}H counts in channel A and ^{35}S counts in channel B. This is done by pressing the following sequence on the scintillation machine (Packard Tri-Carb 4640; Packard Instrument Co.):

End
Start
Enter 6
Enter
Make sure isotope line says 4
End
Forward and Enable simultaneously

4. After samples are counted, the vials with scintillation fluid and radioactive digest should be dumped into the barrel for liquid scintillation vials.

Calculations

Modified from (134).

The amount of radioactivity, [^{3}H] or [^{35}S], is calculated based on the counts per minute (cpm) from channels A (C_1) and B (C_2) as follows:

$$\begin{pmatrix}[^{3}H]\\ [^{35}S]\end{pmatrix}=\begin{pmatrix}k_{11} & k_{12}\\ k_{21} & k_{22}\end{pmatrix}\begin{pmatrix}C_1\\ C_2\end{pmatrix} \qquad \text{Equation 24}$$

The coefficients k_{11}, k_{12}, k_{21}, and k_{22} are determined from the counts of the media samples taken when adding the isotopes to the media:

From the first media sample (^{35}S only, no ^{3}H) the matrix equation becomes: ([^{35}S] reflects concentration of ^{35}S added to media (i.e., 10 µCi/mL); superscript "S" reflect that counts are from first media sample with ^{35}S only, subscripts denote the channel counted)

$$0 = k_{11}C_1^S + k_{12}C_2^S$$
$$[^{35}S] = k_{21}C_1^S + k_{22}C_2^S \qquad \text{Equation 25}$$

From the second media sample (^{35}S and ^{3}H) the appropriate equations are: ([^{35}S] and [^{3}H] reflect concentrations of ^{35}S and ^{3}H, in µCi/mL, added to media, respectively; superscript "S,H" reflect that counts are from second media sample with both 35S and 3H, subscripts denote the channel counted)

$$[^3H] = k_{11}C_1^{S,H} + k_{12}C_2^{S,H}$$
$$[^{35}S] = k_{21}C_1^{S,H} + k_{22}C_2^{S,H} \qquad \text{Equation 26}$$

Solving these 4 equations for the 4 unknown *k*'s:

$$k_{11} = -k_{12}\frac{C_2^S}{C_1^S} = \frac{[^3H]}{C_1^{S,H} - \dfrac{C_2^{S,H}C_1^S}{C_2^S}}$$

$$k_{12} = \frac{[^3H]}{C_2^{S,H} - \dfrac{C_1^{S,H}C_2^S}{C_1^S}}$$

$$k_{21} = \frac{[^{35}S]\left(C_2^S / C_2^{S,H} - 1\right)}{\left(C_1^{S,H}C_2^S / C_2^{S,H}\right) - C_1^S} \qquad \text{Equation 27}$$

$$k_{22} = \frac{[^{35}S]\left(C_1^{S,H} / C_1^S - 1\right)}{\left(C_1^{S,H}C_2^S / C_1^S\right) - C_2^{S,H}}$$

Note that if you accidentally add the ^{3}H before the ^{35}S, these values change to:

$$k_{11} = \frac{[^3H]\left(C_2^H / C_2^{S,H} - 1\right)}{\left(C_1^{S,H}C_2^H / C_2^{S,H}\right) - C_1^S}$$

$$k_{12} = \frac{[^3H]\left(C_1^{S,H} / C_1^H - 1\right)}{\left(C_1^{S,H}C_2^H / C_1^H\right) - C_2^{S,H}} \qquad \text{Equation 28}$$

$$k_{21} = -k_{22}\frac{C_2^H}{C_1^H} = \frac{[^{35}S]}{C_1^{S,H} - \dfrac{C_2^{S,H}C_1^H}{C_2^H}}$$

$$k_{22} = \frac{[^{35}S]}{C_2^{S,H} - \dfrac{C_1^{S,H}C_2^H}{C_1^H}}$$

Use the sample values of C_1 and C_2 to determine the fraction of the total available

radiolabeled proline and sulfate that was converted into macromolecular form (fraction incorporated).

$$\alpha_{^3H} = \frac{C_1 k_{11} + C_2 k_{12}}{[^3H]}$$
$$\alpha_{^{35}S} = \frac{C_1 k_{21} + C_2 k_{22}}{[^{35}S]} \quad \text{Equation 29}$$

There are 132 nmol/mL cold proline and 358.2 nmol/mL cold sulfate in complete DMEM/F12 media. (Numbers based on manufacture's values for DMEM/F12, the percentage of DMEM/F12 in complete medium--88%, and exclusion of any of these constituents from FBS--has not been measured.) The concentration of cold proline and sulfate far outnumbers the concentration of hot. These calculations assume that the same percent of radiolabeled proline/sulfate and unlabeled proline/sulfate was converted and that the amount of proline/sulfate added in radiolabeled form is insignificant compared to the concentrations of (unlabeled) proline/sulfate in the media. The amount of proline/sulfate incorporated (in nmol) into macromolecular form during the radiolabel period is then determined as follows:

$$\text{proline} = \alpha_{^3H}(132 \text{ nmol/mL})V$$
$$\text{sulfate} = \alpha_{^{35}S}(358.2 \text{ nmol/mL})V' \quad \text{Equation 30}$$

where V is the volume of media fed to the cultures, in milliliters (i.e., 1.5 mL).

The values for the control matrices should be subtracted from the seeded matrices. Then, the incorporation data can be normalized to the time of radiolabel (i.e., 24 hours) and the amount of DNA in the construct to yield the rate of incorporation normalized to cell content (nmol/μg DNA/hr).

Appendix EE. Tissue Decalcification Protocol

Samples containing bone are decalcified in a 15% EDTA decalcifying solution, pH 7.4.

This solution is mixed as follows (makes ≈1800 ml):

- 1570 ml PBS (0.01 M phosphate buffer)
- 44 g NaOH (Fisher Scientific, Cat. #S-318, Fair Lawn, NJ)
- 270 g EDTA (Disodium Ethylenediamine Tetraacetate, Fisher Scientific, Cat. #S311-3, Fair Lawn, NJ)
- ≈ 27 ml concentrated HCl (#A144-500, Fisher Scientific Co.)

Instructions:

1. Make the PBS either with dissolvable tablets (Sigma #P-4417, St. Louis, MO. 1 tablet/200 ml dH2O) or with packets (Sigma #P-3813, 1 packet/L dH2O).

2. Add the NaOH. Dissolve completely. It is difficult to get the EDTA into solution without NaOH.

3. Add the EDTA.

4. pH to 7.4

Appendix FF. Paraffin Embedding with the Tissue Tek Machine

1. Samples should be decalcified and rinsed well of fixative, and placed in plastic tissue cassettes (Tissue Tek unicassettes, #4170 or #4173, Miles, Inc., Elkhart, IN).

2. Dehydration and infiltration.
Tissue specimens were dehydrated and infiltrated by machine (Tissue-Tek VIP 1000, model 4617, Miles Scientific, Mishwaka, IN). Dehydration program #4 was used, with solutions changed automatically as follows:

Solution	Time	Temperature
50% EtOH	1 hour	room temp
70% EtOH	1 hour	room temp
80% EtOH	1 hour	room temp
95% EtOH	1 hour	room temp
95% EtOH	1 hour	room temp
100% EtOH	1 hour	room temp
100% EtOH	1 hour	room temp
100% EtOH	1 hour	room temp
clearing solution	1 hour	room temp
clearing solution	1 hour	room temp
paraffin	1 hour	59°C
paraffin	30 min	59°C
paraffin	30 min	59°C

Clearing solution: Americlear histology clearing solvent, Baxter Healthcare Corp. #C4200-1, Deerfield, IL

Paraffin: Paraplast Cat. #8889-501006, melting temp 56°C, Oxford Labware, St. Louis, MO

3. Embedding. Specimens are embedded with the aid of a Tissue-Tek II paraffin embedding center, model 4603 (Lab-Tek Products, Westmont, IL). The machine provides a molten source of paraffin and cooling plate. Paraffin is placed in stainless steel molds of varying size, the specimen placed in the mold, and the mold placed on a cooling plate. The tissue cassette is placed on the mold and additional paraffin is added to affix the plastic cassette to the mold.